Lab to Field Scale Modeling of Low Temperature Air Injection with Hydrocarbon Solvents for Heavy-Oil Recovery in Naturally Fractured Reservoirs

by

Jose Ramon Mayorquin-Ruiz

A thesis submitted in partial fulfillment of the requirements for the degree of

Doctor of Philosophy

in

Petroleum Engineering

Department of Civil and Environmental Engineering
University of Alberta

Abstract

Alternatives for enhanced oil recovery processes in heavy oil containing deep naturally fractured reservoirs (NFR) are limited due to excessive heat losses when steam is injected. Air injection at high temperature oxidation conditions (in-situ combustion) has been considered as an alternative to aqueous based thermal applications. However, its implementation has serious limitations including poor areal distribution of injected air and poor combustion efficiency due to the heterogeneous nature of these reservoirs as well as the safety risk of unconsumed injected oxygen (O_2) reaching the production wells.

Taking advantage of the low cost and availability of air, one option is to use air at low temperature conditions (low temperature oxidation, LTO) as a pressurizing agent in NFR. Oxygenated compounds are generated at these conditions resulting in oil viscosity increase, reducing fluid mobility. In order to minimize this detrimental effect, a combination of air injection with hydrocarbon solvents can be applied. The objectives of this thesis are to evaluate air injection at LTO conditions in NFR containing heavy oil as a way to improve oil recovery, to clarify the effect of hydrocarbon solvent addition into air on oil recovery and O_2 consumption, and to propose optimal conditions (temperature, air/solvent ratio) and implementation strategies for an efficient use of this suggested method.

Comprehensive laboratory and numerical simulation studies were conducted to achieve these objectives. Static diffusion experiments—simulating cyclic gas injection (huff-and-puff)—were carried out by soaking heavy oil saturated cores into a reactor filled with gas representing a matrix/fracture system. Oil recovery and O_2 consumption were the main parameters assessed and an extensive set of variables including rock type, temperature, fracture volume, solvent type,

matrix size, gas injection sequences, and soaking times were studied. From experimental studies, the following conclusions were made:

1. Gas sequence design affects oil recovery,

2. O_2 consumption in air cycles is higher after the core is soaked into butane rather than propane,

3. It is beneficial to soak cores in air+C_3 mixture rather than pure air or solvent; i.e., lower O_2 concentration in produced gas, less solvent usage, higher and faster oil recovery compared to alternate injection of air and C_3.

Then, core scale numerical simulation models were created for modeling lab experiments for a sensitivity analysis on Air/C_3 ratio and matrix size. The results show that the process is extremely sensitive to matrix size and optimization of air injection (assisted by hydrocarbon solvents) can be achieved based on the minimized hydrocarbon solvent for a given matrix size. Additionally, a sensitivity analysis was performed using an up-scaled numerical model to the field scale containing meter-scale matrix blocks. It was observed that oil production mechanisms acting in a matrix block surrounded by gas filling the fractures are predominantly gas-oil gravity drainage, effective diffusion, and voidage replacement of oil by gas.

Finally, a numerical simulation sector model of a hypothetical NFR was created and several air-gas injection sequences were analyzed. It was concluded that injection of air (LTO conditions) and propane represents an alternative for heavy oil recovery from NFRs at the field scale, and an optimum production time/soaking time ratio can be obtained for given gas injection sequences (type of gas and injection/soaking durations), temperature, and block sizes.

This thesis is dedicated to

Elena, my endless love

and

Jose and Antonio, my inspiration

Acknowledgements

First of all I would like to thank my supervisor Dr. Tayfun Babadagli for his generosity with time and knowledge. Thanks for your guidance and support through my PhD studies.

Also my gratitude to Dr. Fernando Rodríguez de la Garza for his mentorship; thanks for sharing your expertise and advice.

I am grateful to committee members Dr. Ergun Kuru, Dr. Huazhou Li, Dr. Hongbo Zeng, Dr. Vivek Bindiganavile, and Dr. Simón López Ramírez for agreeing to participate in my examination and for their feedback.

My deepest appreciation to PEMEX Exploración y Producción for giving me the opportunity to study a PhD as well as Conacyt-Sener-Hidrocarburos Fund for providing the financial support. Thanks to México.

This research was financially supported by Dr. Tayfun Babadagli's NSERC Industrial Research in Unconventional Oil Recovery (industrial partners are CNRL, SUNCOR, Touchstone Exploration, Sherritt Oil, PEMEX, Statoil, Husky Energy, Saudi Aramco and APEX Eng.) and NSERC Discovery Grant (No: RES0011227). CMG also provided the software that was intensively used in this research. I gratefully acknowledge these supports. Thanks to Canada.

It was an honor being part of the Enhanced Oil and Gas Recovery and Reservoir Characterization Research Group. Thanks to all former and current members (colleagues, technicians and assistant) of this group. Thanks for sharing their culture and history.   I want to extend my gratitude to Héctor Leyva-Gomez and his family for sharing great moments with me and my family during these years. Thank you for being wonderful friends. I would also like to thank Francisco Javier Argüelles-Vivas for walking together in this journey - we made it.

I got a lot of support from many people from different departments in Pemex Exploración y Producción, Conacyt, Banobras and I thank them a lot.

And now, last but not the least, I would like to thank my wife Elena for her support in this amazing odyssey that was not an easy one. Thanks for all your love and sacrifice, thanks for

being here with me; I will always love you. Thanks to my two sons José and Antonio for filling my heart with love and hopes, thanks for your smile, you are the reason to live.

Thanks God for blessing me, my wife and my sons. Thanks for allowing me share these new experiences with them.

TABLE OF CONTENTS

LIST OF TABLES

LIST OF FIGURES

Chapter 1: Introduction

1.1 Introduction

Presented in this dissertation is a study of air injection at low temperature oxidation (LTO) conditions mixed with solvents for heavy oil recovery in naturally fractured reservoirs (NFR). The motivation is based on the fact that there has been an interest in the use of air injection for heavy oil recovery in deep NFRs due to the inherent benefits of air, such as unlimited availability and low cost.

A significant amount of crude oil reserves worldwide is in the form of heavy oil and much of these reserves are contained in naturally fractured reservoirs. A considerable portion of oil reserves could be trapped in the matrix if a dual porosity system exists (Nelson 2001). Such systems are composed of fracture network and rock matrix. The fracture network essentially provides the reservoir-flow channels, and the hydrocarbons are contained in both parts of the system (Cinco-Ley 1996).

Enhanced oil recovery (EOR) methods such as gas and water injection, various miscible processes, chemical injection, and thermal processes for heavy oil recovery are equally applicable in NFRs under favourable conditions (Saidi 1987). However, when dealing with deep and oil-wet fractured reservoirs, options are limited and the economics of the project become a serious concern.

Steam based thermal methods may not be applicable in deep NFRs due to the severe heat loss problem and the heterogeneous structure of the reservoir. The latter could limit in-situ combustion (ISC) applications (Alvarado and Manrique 2010).

In short, enhanced oil recovery methods are quite limited for deep naturally fractured heavy oil reservoirs. Additionally, EOR in offshore fields is constrained not only by reservoir lithology but also by surface facilities and environmental regulations (Alvarado and Manrique 2010). Therefore, its offshore applicability is limited compared to onshore fields, and pressure maintenance by gas and water injection turned out to be one of the limited EOR possibilities in such fields (Alvarado and Manrique 2010). However, their ultimate recovery targets are not as high as desired, which demands the development of new enhanced oil recovery projects.

Air can be an economically attractive process in deep heavy oil containing NFRs, especially for the offshore ones. It is usually desired at high temperature oxidation (HTO) conditions, namely in-situ combustion (ISC). This method has two main concerns: (1) quick progress of high temperature front due to fractured nature without effectively heating the matrix and (2) the possibility of unreacted oxygen reaching the production wells due to heterogeneous structure. An option is to use air at lower temperatures (low temperature oxidation, LTO). Experimental and numerical simulation studies related to the LTO process in homogeneous light oil reservoirs can be found in literature. However, to our knowledge, no study has been reported on the implementation possibilities and how to overcome the disadvantages of the LTO process in heavy oil containing NFRs.

To improve the efficiency of the method and prevent viscosity increase due to reactions between air and heavy oil at low temperatures, hydrocarbon solvent can be used. In this research, various forms of air injection at relatively low temperatures are analyzed such as pure air, pure nitrogen, air/solvent (propane, butane). In air/solvent cases, a mixture of air and solvent is injected jointly or in the form of solvent/air/solvent cycles. The operational form suggested and analyzed is cyclic injection of air with hydrocarbon gases (huff-and-puff). Complete consumption of oxygen in-situ is needed and special attention is given to determine the conditions to achieve this.

The above described analyses are based on experimental and numerical simulation studies. Benefits of injection of LTO air/solvent were addressed as well as the minimum required conditions for the air injection to be successful.

1.2 Literature review

Air injection studies in light oils: LTO conditions

Based on experimental and numerical simulation (homogeneous reservoir) studies, Ren et al. (2002) concluded that when air is injected into a light-oil reservoir, the reactions between the oil and oxygen may be restricted to LTO, depending on the properties of the oil and the injected air flux. The oxygen is consumed by spontaneous LTO reactions producing a "flue gas" comprising 10 to 14% CO_2 and nitrogen. LTO of light oils produces carbon oxides and water as the final products of the reactions, and there is little, if any, change in oil viscosity. Greaves (2004) also

reported that in light oil air injection (LOAI), the main recovery is due to the flue gas, which is generated in-situ by oxidation reactions with crude oil.

Air injection studies in light-medium oils NFR: HTO conditions (ISC)

A very limited number of experimental and numerical simulation studies reported in the literature exist relating to air injection in NFR at HTO conditions (ISC). Sakthikumar and Berson (2001) stated that it is important to predict oxygen movement in the reservoir in case of incomplete combustion and this implies the need for careful reservoir characterization. Rodriguez and Christopher (2004) presented details about an ongoing project that aims to investigate the feasibility of injecting air in the Cardenas field (a naturally fractured carbonate reservoir) through an experimental, theoretical, and numerical simulation work. Lacroix et al. (2004), based on compositional thermal simulations, showed that gas diffusion and thermodynamic transfers are the major physical mechanisms controlling the global kinetics of matrix-fracture transfers and the resulting oxidation of oil in this type of reservoir. Later, Stokka et al. (2005) presented the results of reservoir modeling in a fractured light oil reservoir. Using mechanistic 2-D simulation runs, they showed the importance of diffusion and gravity segregation for the oil production rate. They also found through laboratory experiments on light oil-saturated cores that the stripping of light oil components is greater than the swelling of the oil and also that the diffusion of air into a reservoir sample has a significant impact on recovery.

Air injection studies in heavy oils NFR: HTO conditions (ISC)

A limited number of experimental studies are found in the literature regarding air injection into heavy oil containing fractured rock samples. Shulte and De Vries (1985) published experimental observations about the ISC process in NFR reservoirs containing heavy oil, which showed that the burning process is governed by the diffusion of oxygen from the fractures into the matrix. The main oil-production mechanisms were observed to be thermal expansion and evaporation with subsequent condensation of the oil from the matrix. Their numerical simulation model showed that O_2 breakthrough may occur when air-injection rate exceeds a critical value predominantly determined by fracture spacing.

Based on numerical simulation runs on the naturally fractured heavy oil model, Tabasinejad et al. (2006) concluded that the preferential passage of air through the fractures exists and the combustion front in the fracture moves faster than in the matrix. Fatemi et al. (2008) studied ISC in a fractured reservoir using a thermal simulator and reported that the air injection rate should be optimized for a specific system in order to minimize the air breakthrough. More recently, Fadaei et al. (2010) performed a simulation of the ISC process in a fractured system at core and matrix-block scales and observed that ISC in the fractured system is strongly dependent on the oxygen diffusion coefficient, while the matrix permeability plays an important role in oil production. They also found that oil production is governed mainly by oil drainage because of gravity force, which is enhanced by viscosity reduction. Fadaei et al. (2011) based on ISC experiment using an entire consolidated core with adjacent fracture, showed that with normal air (21% oxygen) the propagation condition does not change significantly when changing the fracture permeability or the air-injection rate. In all these cases, after a successful ignition, a high-temperature ISC front did not propagate through the system. However, the ISC front propagated through the porous medium using enriched air containing 60% oxygen. This shows that oxygen flux from the fracture to the matrix is one of the important parameters for the propagation of ISC in a fractured core.

Field air injection projects and pilot tests: HTO conditions (ISC)

Commercial ISC projects worldwide in heavy oil are reported by Turta et al. (2007), which are mostly implemented in sand or sandstones reservoirs. Belgrave and Chhina (2006) presented information about commercially (or technically) successful air injection (ISC) projects in non-fractured reservoirs. Few field experiences (pilot tests) regarding air injection at HTO conditions in fractured reservoirs are found in the literature but none have been reported successful or commercially attractive. Craig and Parrish (1974) summarized the information obtained from COFCAW (combination of forward combustion and water flooding) pilot tests. They reported that in two of the pilot tests in different reservoirs (30 and 40.6 °API), fractures yield poor combustion efficiency and a poor areal distribution of the injection fluid. Alvarez et al. (2008) presented a literature review of field experiences in heavy-oil reservoirs, including several pilot tests carried out in the Grosmont unit in Canada during the 1970s and 80s. The Grosmont formation consists of vuggy porosity and is heavily karsted. Spontaneous ignition occurred

during each of the combustion pilots after injecting air, but it was difficult to control the combustion front in each case. Pilot tests of air injection at LTO conditions in heavy oil are not found in the literature.

Air injection studies in heavy oils NFR: LTO conditions

Two main concerns limit the application of the air injection HTO process in NFR heavy-oil reservoirs: (1) high temperature front that could eventually reach the producing wells (becoming more risky in offshore fields), and (2) possibility of producing unreacted oxygen at production wells due to reservoir heterogeneities. No detailed analyses of these two problems have been reported in literature and this constitutes the main objective of this thesis work.

1.3   Statement of the problem and objectives

Air injection in light and medium oil has been implemented and analyzed for decades in non-fractured reservoirs in two modes: low temperature oxidation (LTO) and high temperature oxidation (HTO). In addition, few laboratory studies on in-situ combustion in naturally fractured heavy oil reservoirs have been documented. Experimental studies are needed in the LTO mode for fractured heavy oil reservoirs in order to understand different aspects of the oil production mechanisms involved with this oxidation mode.

When air injection is considered an EOR process in naturally fractured heavy oil reservoirs, it is commonly thought to be a thermal EOR process, referring to air injection at high temperature oxidation conditions, namely in-situ combustion (ISC). However, frontal heat displacement may not be possible in NFRs even if the combustion conditions are met. Therefore, the question is whether air at LTO conditions can be injected relying only on oxidation reactions with fracture oil and oil in the matrix after air is diffused into it.

Drawbacks in the use of air at LTO could explain its lack of use in heavy oil reservoirs. For example, air is not an inert gas (reactive gas); oxygen addition reactions occur when oxygen contacts hydrocarbons from which oxygenated compounds, such as asphaltenes, are generated, increasing the oil viscosity. However, important benefits are usually disregarded such as the unlimited availability of air and less cost compared to other fluids (nitrogen, CH_4), the use of

existing gas injection facilities, pressure maintenance, and the substitution for gas produced from the gas cap. Hence, if one can consume all the oxygen through reactions with oil in the fracture system and transfer it into the matrix, this process may be a success. At this point, it is important to make sure that the negative outcome of the reaction of air (oxygen) with oil (viscosity increase through polymerization) is minimized. Thus, determining under what condition this is overcome and what is the minimal temperature to avoid this is required. In other words, determining how to minimize the drawbacks of the air injection LTO and what conditions are required in order to obtain a successful application, and under what condition air injection LTO is not beneficial at all is also needed.

These questions are answered in this research based on the condition that oxygen needs to be completely consumed in the reservoir so that it does not reach the producer well unconsumed. The proposed approach in this research is to together inject air and solvents in the reservoir considering the effect of solvents in the reduction of oil viscosity. The analysis of this option is based on the realization of laboratory -static- experiments and numerical simulation studies over a wide range of air/solvent mixture concentrations.

The main objectives of this research can be summarized as follows:

1. To evaluate air injection at LTO in naturally fractured heavy oil as a way to accelerate and/or increase oil recovery.

2. To identify the conditions (temperature, air/solvent ratio) at which higher/faster oil recovery is obtained.

3. To describe the oil production mechanisms involved in air/solvent injection in naturally fractured heavy oil reservoirs.

4. To clarify the effect of hydrocarbon solvent addition into air on the recovery of oil and consumption of air.

1.4 Solution methodology

The methodology to be used in the study of the injection of air LTO and solvents is based on laboratory experiments and numerical simulations at laboratory and field scales.

Experimental studies in the laboratory

Laboratory experiments are conducted at static conditions wherein a heavy oil-saturated sandstone/carbonate core is soaked into a specific gas (nitrogen, air, solvent, air/solvent mixture, oxygen-enriched air) in a stainless steel reactor at a certain temperature and pressure. Then, the pressure change is observed giving an indication of the gas diffusion into the rock matrix saturated with oil as an adapted technique for non-thermal recovery of heavy oils by solvent injection. Propane and butane are the hydrocarbon solvents to be tested as an addition to air.

The reactor is located inside an oven and heated at a constant temperature. Three different temperatures are tested. Gas is allowed to diffuse into the oil at static conditions for a certain time (soaking time); i.e. no fluid flow occurs into or out of the reactor after the reactor is gas-filled. Gas pressure and oven temperature are recorded by means of a data acquisition system connected to a personal computer. Once the scheduled soaking time is reached, the gas in the reactor is released and a gas chromatographic analysis is conducted. The produced oil volume is measured at the end of the experiment as well as its properties: density, viscosity, asphaltenes content, and refractive index. The total amount of asphaltenes in oil is closely related to the refractive index of the crude oil itself (Wattana et al. 2003). Oil properties are also measured before the experiment.

In certain cases, once the experiment is finished (after releasing the gas and measuring produced oil properties), which is called "cycle," a second cycle is started filling the reactor with the same gas, at the same pressure and temperature for a certain -soaking- time. This is done to gain insight into a cyclical (huff-and-puff) injection of gas into NFRs, which seems more favourable than continuous injection due to the controllability of the gas movement. A schematic of the workflow and setup are shown in **Figure 1-1** and **Figure 1-2**, respectively.
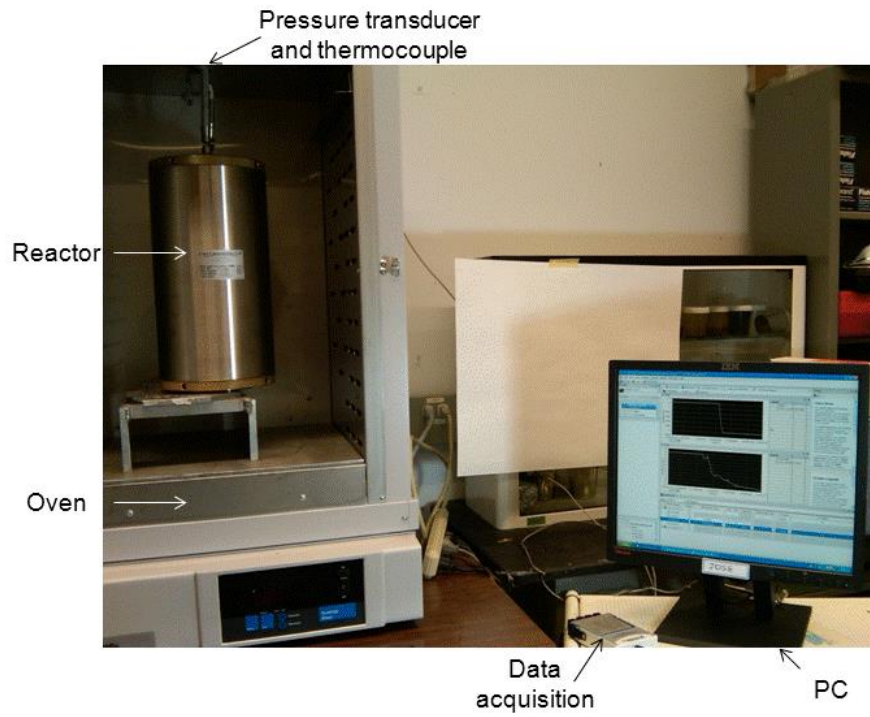
Figure 1-1 Experimental setup.
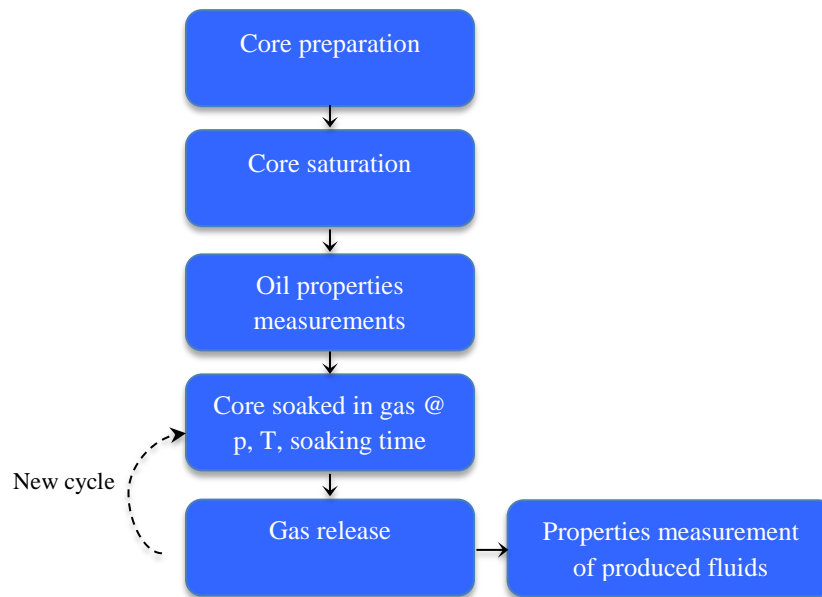
Figure 1-2 Workflow for static experiments.

A wide spectrum of gas concentrations (pure gas and gas mixture) is tested to analyze the effect of oxygen in the oil recovery and its properties. All experiments are conducted with core in a vertical position with one exception (at horizontal position to analyze the effect of gravity).

Numerical simulation studies

Numerical simulation models are created at two different scales: core and field. CMG WINPROP and CMG STARS software packages are used for the generation of PVT and numerical simulation models, respectively.

The numerical simulation model at core scale is created based on the experimental setup and a two-step process is to be followed: (1) matching process and (2) sensitivity analysis. The matching process is done using experimental measurements (gas pressure, produce oil volume) and adjusting core permeability and diffusion coefficients. Once the numerical simulation model is validated by the matching process, sensitivity runs are performed to analyze the effect of the ratio of air-solvent mixture and matrix size. Then, an upscaling study is conducted using the numerical simulation model based on different matrix block sizes.

The numerical simulation model at field scale is created for a sector model of a hypothetical NFR in which different gas injection sequences are analyzed. The modeling of kinetic reactions, particularly LTO reactions, is based on oxygenated compounds generated during LTO reactions (Gutierrez et al. 2009). **Figure 1-3** shows an overview of the solution methodology.
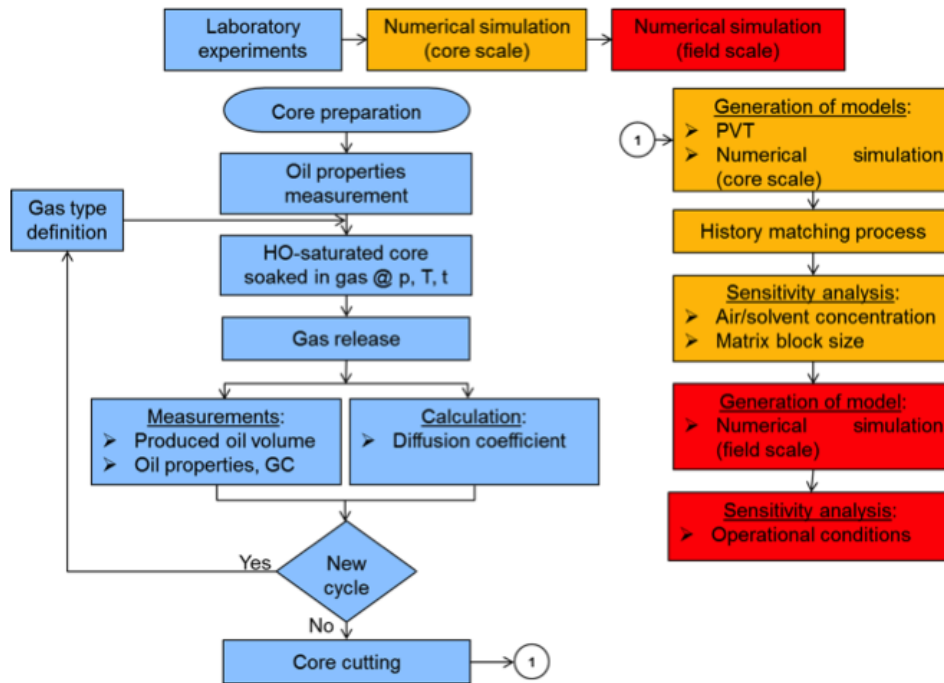
Figure 1-3 Overview of the solution methodology.

1.5 Outline

This is a paper-based thesis. Four papers presented at conferences and/or published in (or submitted to) journals comprise the four chapters of this thesis. Each chapter has its own abstract, introduction, conclusions, and references. In addition to a short introductory chapter (Chapter 1), a chapter summarizing the contributions is included at the end of the thesis.

In Chapter 2, results of laboratory static diffusion experiments are provided giving a detailed explanation of the experimental setup, instrumentation, and type fluid properties measurements conducted. Laboratory tests performed by soaking heavy-oil-saturated cores into air/solvent filled reactors to determine the critical parameters on recovery are analyzed. This lab work is extended in Chapter 3 and a set of variables including rock type, temperature, fracture volume, solvent type, matrix size, gas injection sequences, and soaking times are studied through static diffusion experiments.

In Chapter 4, numerical simulation studies at cores scale are reported. The aim of these models is to history match the static diffusion experiments and to conduct sensitivity analysis to

air/solvent ratio and matrix size. At the end, an upscaling approach based on the matrix size is presented.

In Chapter 5, a numerical simulation sector model of a hypothetical NFR is created and several air/gas injection sequences are analyzed to determine an optimum production time/soaking time ratio.

Chapter 6 summarizes the contributions of this dissertation to the literature and industry. Chapter 7 includes all references reviewed in each chapter.

References

Alvarado, V. and Manrique, E. 2010. *Enhanced Oil Recovery. Field Planning and Development Strategies*. Gulf Professional Publishing.

Alvarez, J.M., Sawatzky, R.P., Forster, L.M. et al. 2008. Alberta's Bitumen Carbonate Reservoirs—Moving Forward with Advanced R&D. Presented at the World Heavy Oil Congress, Edmonton, Alberta, Canada, 10 – 12 March. Paper 2008-467.

Belgrave, J.D.M. and Chhina, H.S. 2006. Air Injection: Timely and Widely Applicable! Presented at 1st World Heavy Oil Conference. Paper 2006-432.

Chandras Das, S. A Study of Oxidation Reaction Kinetics during Air Injection Process. Master of Engineer Science Thesis, the University of Adelaide. April, 2009.

Cinco-Ley, H. 1996. Well test Analysis for Naturally Fractured Reservoirs. *J Pet Technol* **48** (01): 51 – 54. SPE-31162-JPT. http://dx.doi.org/10.2118/31162-JPT.

Craig, F.F., Jr. and Parrish, D. R. 1974. A Multipilot Evaluation of the COFCAW Process. *J Pet Technol* **26** (06): 659–666. SPE-3778-PA. http://dx.doi.org/10.2118/3778-PA.

Fadaei, H., Debenest, G., Kamp, A. M. et al. 2010. How the in-Situ Combustion Process Works in a Fractured System: 2D Core- and Block-Scale Simulation. *SPE Res Eval & Eng* **13** (01):

118–130. SPE-117645-PA. http://dx.doi.org/10.2118/117645-PA.

Faddaei, H., Castanier, L.M., Kamp, A.M. et al. 2011. Experimental and Numerical Analysis of In-situ Combustion in a Fractured Core. *SPE J* **16** (02): 358 – 373. SPE-141117-PA. http://dx.doi.org/10.2118/141117-PA.

Fatemi, S.M., Kharrat, R. and Vossoughi, S. 2008. Feasibility Study of In-Situ Combustion (ISC) in a 2-D Laboratory-Scale Fractured System Using a Thermal Simulator. Presented at the World Heavy Oil Congress 2008, Edmonton, 10 – 12 March. Paper 2008-449.

Greaves, M. 2004. Air Injection-Improved Oil Recovery Strategy for the UK Continental Shelf. Business Briefing: Exploration and Production. The Oil & Gas Review. pp. 118-121.

Gutierrez, D., Moore, R.G., Mehta, S A. et al. 2009. The Challenge of Predicting Field Performance of Air Injection Projects Based on Laboratory and Numerical Modelling. *J Can Pet Technol* **48** (04): 23 – 34, PETSOC-09-04-23-DA. http://dx.doi.org/10.2118/09-04-23-DA.

Lacroix, S., Delaplace, P., Bourbiaux, B. et al. 2004. Simulation of Air Injection in Light-Oil Fractured Reservoirs: Setting-Up a Predictive Dual Porosity Model. Presented at the SPE Annual Technical Conference and Exhibition, Houston, 26–29 September. SPE-89931-MS. http://dx.doi.org/10.2118/89931-MS.

Nelson, R.A. 2001. *Geologic Analysis of Naturally Fractured Reservoirs*. 2nd Edition, Gulf Professional Publishing. Houston, Texas.

Ren, S.R., Greaves, M., and Rathbone, R.R. 2002. Air Injection LTO Process: An IOR Technique for Light-Oil Reservoirs. *SPE J* **7** (01): 90–99. SPE-57005-PA. http://dx.doi.org/10.2118/57005-PA.

Rodriguez, F. and Christopher, C. A. 2004. Overview of Air Injection Potential for Pemex. Presented at AAPG International Conference, Cancun, Mexico, 24–27 October. Paper 89612.

Saidi, A.M. 1987. Reservoir Engineering of Fractured Reservoirs (Fundamental and Practical Aspects). Total Edition Presse, Paris.

Sakthikumar, S. and Berson, F. 2001. Air Injection into Light and Medium-Heavy Oil, Carbonate Reservoirs. Paper presented at Exitep. Mexico.

Shulte, W.M. and de Vries, A.S. 1985. In-Situ Combustion in Naturally Fractured Heavy Oil Reservoirs. *SPE J* **25** (01): 67–77. SPE-10723-PA. http://dx.doi.org/10.2118/10723-PA.

Stokka, S., Oesthus, A., and Frangeul, J. 2005. Evaluation of Air Injection as an IOR Method for the Giant Ekofisk Chalk Field. Presented at the SPE International Improved Oil Recovery Conference, Kuala Lumpur, 5–6 December. SPE-97481-MS. http://dx.doi.org/10.2118/97481-MS.

Tabasinejad, F., Karrat, R., and Vossoughi, S. 2006. Feasibility Study of In-Situ Combustion in Naturally Fractured Heavy Oil Reservoirs. Presented at the International Oil Conference and Exhibition in Mexico, Cancun, 31 August – 2 September. SPE-103969-MS. http://dx.doi.org/10.2118/103969-MS.

Turta, A.T., Chattopadhyay, S.K., Bhattacharya, R. N., et al. 2007. Current Status of Commercial In Situ Combustion Projects Worldwide. *J Can Pet Technol* **46** (11): 8–14. PETSOC-07-11-GE. http://dx.doi.org/10.2118/07-11-GE.

Wattana, P., Wojciechowski, D.J., Bolaños, G. et al. 2003. Study of Asphaltene Precipitation Using Refractive Index Measurement. *Petroleum Science and Technology* **21** (3–4): 591–613. http://dx.doi.org/10.1081/lft-120018541.

Zhang, Y., Hyndman, C.L., and Maini, B. 1998. Measurement of Gas Diffusivity in Heavy Oils. Paper presented at the 49th Annual Technical Meeting of The Petroleum Society, Calgary. 8–10 June. Paper 98-63.

Chapter 2 : Low-Temperature Air/Solvent Injection for Heavy-Oil Recovery in Naturally Fractured Reservoirs

2.1 Summary

Limited studies on oil recovery from naturally fractured reservoirs using low-temperature air injection show that the process is strongly dependent on oxygen (O_2)-diffusion coefficient and matrix permeability, both of which are typically low. A new approach (i.e., the addition of hydrocarbon solvent gases into air) is expected to improve the diffusivity of the gas mixture and to accelerate the oxidation. To study this new idea, called low-temperature air/solvent injection, laboratory tests were performed by soaking heavy-oil-saturated cores in air/solvent filled reactors to determine the critical parameters on recovery. Laboratory tests were complemented by conducting experiments using air at different O_2 concentrations: zero (i.e., nitrogen), 21.0 mol% (air), and 37.3 mol% (O_2-enriched air).

For safety reasons, it is imperative that enough time be given for air diffusion before the injected air breaks through a highly permeable fracture network. This implies that the huff 'n' puff type of injection is a plausible option as opposed to the continuous injection of air. A high recovery factor was obtained by soaking a single matrix in an air/solvent chamber at static conditions rather than with air only. The period of pressure stabilization was faster for the air/solvent mixture than in 100% solvent. The asphaltene content was lower in the air/solvent case than in the 100%-air injection case. Instead of pure air, injection of an air/solvent mixture yields a better recovery with less asphaltene. This is expected to reduce the cost of the process compared with pure-solvent injection. At low temperatures (75°C), O_2 consumption in the matrix oil was low, while at high temperatures, the O_2 was partially (150°C) or totally (200°C in the presence of propane) diffused and consumed in the matrix.

2.2 Introduction

A limited number of laboratory experiments and numerical simulation studies reported in the literature related to air injection in naturally fractured reservoirs (NFRs) were oriented to combustion [high-temperature oxidation (HTO)] in medium and light oil. Rodriguez and Christopher (2004) presented details about an ongoing project that intends to investigate the feasibility of injecting air in the Cárdenas field—a naturally fractured light-oil carbonate reservoir—through an experimental, theoretical, and numerical-simulation work. Chávez and

González (2013) presented more details of the Cárdenas field project. Efforts were also made on the numerical simulation of air injection in a light oil fractured reservoir. Lacroix et al. (2004), on the basis of compositional thermal simulations, showed that gas diffusion and thermodynamic transfers are the major physical mechanisms controlling the global kinetics of matrix/fracture transfer and the resulting oxidation of oil. Later, Stokka et al. (2005) presented the results of reservoir modelling in a fractured light-oil reservoir. Their results from mechanistic simulation runs for a 2D model showed the importance of diffusion and gravity segregation for the oil-production rate. Through laboratory experiments on fractured light-oil containing cores, they also discovered that the stripping of light-oil components is greater than the swelling of the oil and that the diffusion of air into a reservoir sample has a significant impact on recovery.

More recently, Fadaei et al. (2010) performed a simulation of an in-situ-combustion (ISC) process in a fractured system at core and matrix-block scales and observed that ISC in the fractured system was strongly dependent on the oxygen (O_2) –diffusion coefficient, while the matrix permeability played an important role in oil production. They also found that oil production is governed mainly by oil drainage because of gravity force, which is enhanced by viscosity reduction. On the other hand, note that viscosity will likely increase with air injection, especially at low temperatures, typically occurring in most heavy-oil reservoirs.

A few experimental studies were found in the literature regarding air injection into heavy-oil-containing fractured rock samples. Schulte and de Vries (1985) published experimental results on the ISC process in heavy-oil-containing NFRs, which showed that the burning process was governed by the diffusion of O_2 from the fractures into the matrix. The main oil-production mechanisms were observed to be thermal expansion and evaporation with subsequent condensation of the oil from the matrix. On the basis of a semi-2D numerical-simulation exercise, they also found that O_2 breakthrough was observed when the air-injection rate exceeded a critical value, predominantly determined by the fracture spacing.

Few field experiences (pilot tests) regarding air injection at HTO conditions in fractured reservoirs were found in the literature, but none were reported to be successful or commercially attractive. Craig and Parrish (1974) summarized the information obtained in the evaluation of a combination of forward combustion and waterflooding pilot tests. In two of the pilot tests at

different reservoirs (30 and 40.6 °API), they observed that fractures can yield poor combustion efficiency and that a poor areal distribution of the injection fluid was possibly caused by a fracture. Alvarez et al. (2008) presented a literature review of field experiences in heavy-oil reservoirs, including several air-injection-pilot tests carried out in the Grosmont unit in Canada (having vuggy porosity and heavily karsted) during the 1970s and 1980s. Spontaneous ignition occurred during each of the combustion pilots after injecting air, but it was difficult to control the combustion front in each case.

Air injection in light and medium oil has been implemented and analyzed for decades in non-fractured reservoirs in two modes: low-temperature oxidation (LTO) and HTO. In addition, a few laboratory studies on in-situ combustion in naturally fractured heavy-oil reservoirs were documented. More experimental studies are needed in the LTO mode for fractured heavy-oil reservoirs in order to understand different aspects of the mechanics of the process [e.g., the effect of oil composition, fracture characteristics (dimension, spacing), matrix/fracture interaction, process sustainability, and air/oil ratio]. The reactions that take place in the LTO mode (typically O_2 addition) and the impact of those on oil production need to be clarified experimentally. A first attempt on this was made by Mayorquin-Ruiz and Babadagli (2012a). The present paper constitutes an extended version of this paper with more experiments and detailed analysis.

Additionally, it is critical to understand the effect of LTO air injection on sweep efficiency at the reservoir scale by modelling the appropriate mechanisms, which also requires laboratory-scale identification of matrix/fracture interaction while the fracture system is filled with air. Considering that air diffusion into the oil saturated matrix is low and hydrocarbon gases are expensive, testing the mixture of these two to improve the recovery and to reduce the risk involved because of unconsumed O_2 is required.

Two main concerns limit the application of ISC process in naturally fractured heavy-oil reservoirs: (1) The high-temperature front that could eventually reach the producing wells (becoming more serious in offshore fields) and (2) the possibility of producing unreacted O_2 at production wells because of heterogeneity. On the basis of these facts, low-temperature air/solvent injection in heavy-oil NFRs was proposed as an alternative to HTO air injection (combustion) and was analyzed experimentally in this work.

2.3 Statement of the problem

For heavy-oil-containing deep and naturally-fractured reservoirs, not many enhanced-oil-recovery options exist. Inert gas injection could be useful to generate gravity drainage between matrix and fracture for thick reservoirs (Limón-Hernandez et al. 1999; Rodriguez et al. 2001, 2004; Cruz et al. 2009). However, this is expensive and because of a low mass-diffusion capability of the commonly used gases [typically nitrogen (N_2)] into matrix oil, there is no additional effect on top of enhanced gravity drainage. Replacement of inert gases with others could be an option, and air is the least expensive one to serve as a pressurizing agent. However, several issues are critical when air is injected into fractured reservoirs:

- Air performs a task similar to that performed by N_2 in terms of pressure supply by filling the fracture network.

- Oxygen (O_2) in the air must be consumed to prevent its arrival into the production well because of safety reasons. Because the HTO (in-situ combustion) reactions would not occur easily (and/or undesirable) because of the heterogeneous nature of the reservoir, the only method to consume the O_2 is its diffusion into matrix.

- In this case, if temperature is high enough, oxidation reactions may generate extra oil recovery. At lower temperatures, the opposite may occur and oil viscosity may increase because of a polymerization reaction. Hence, temperature is a critical factor in this process.

As observed, air diffusing into matrix is the essential part of air injection. If this diffusion takes place while pressurizing the reservoir and creating drainage of matrix oil by filling the fracture network, air can substitute for N_2. The first task is to investigate these conditions. The second task is to facilitate the air diffused into matrix. If proper conditions are provided during LTO, air may result in viscosity reduction above a certain temperature range (Gutierrez et al. 2009). Thus, the following questions should be asked:

1. One has to get air diffused into matrix oil to prevent the breakthrough of heated O_2. Also, the air diffused into matrix should not start any polymerization that causes an increase in

oil viscosity. What is the minimal reservoir temperature that satisfies these two important requirements for a successful air injection?

2. Because temperature may not be as high because of technical limitations and cost (heating deep reservoirs may not be practical), can we add a hydrocarbon solvent to prevent or minimize viscosification of matrix oil and obtain additional recovery from the matrix?

3. What are the application conditions (i.e., optimal temperature, solvent addition, sequence of injection cycles, proper soaking time) at a given temperature for full consumption of air into matrix by diffusion?

This study intends to answer these questions by applying an extensive experimental study.

2.4 Experimental work

A total of 10 experiments were conducted, eight of which were at low temperature (75 °C) and two of which were at high temperatures (150 and 200 °C) with gas pressure at approximately 200 psi. All of the experiments were performed with heavy-oil- saturated sandstone cores in vertical orientation. In a low-temperature experiment using nitrogen (N_2), the core was oriented horizontally to analyze the effect of gravity drainage on oil production. Fluid and core properties are shown in **Table 2-1**. In all cases, a heavy-oil-saturated sandstone core was soaked in the gas contained in a stainless-steel reactor. The cores were placed inside a stainless-steel reactor where the core represented the matrix and the free volume surrounding the core represented the fracture. A similar setup was used by Riazi et al. (1994). Gas was allowed to diffuse into the matrix oil at static conditions for a certain period. This period represented a cycle and once the reactor was filled out, there was no flow in or out. Oil expelled from the core during this period was collected at the inside bottom of the reactor and measured at the end of the cycle. The reactor was heated inside an oven at constant temperature. Reactor pressure and oven temperature were recorded by means of a pressure transducer and thermocouple, respectively, connected to an automatic data-acquisition system. At the end of the pre-set period (cycle), the gas in the reactor was released and then analyzed using either a gas detector or gas chromatography. Oil properties (e.g., density, viscosity, and asphaltene content) were measured before and after each cycle. Also, oil refractive-index measurements were performed to

determine the amount of asphaltene content in the oil qualitatively before and after the experiment. A second or third cycle was run, filling the reactor again with the same or different gas and repeating the process explained previously.

Table 2-1 Fluid and core properties for each experiment.

Experiment	Core				Crude-Oil Properties at Atmospheric Pressure					
	Porosity (%)	Length (in.)	Diameter (in.)	Pore volume (cm^3)	Density (°API)	Asphaltene Content (wt%)	Temperature (°C)	Density at Temperature (g/cm^3)	Viscosity at Temperature (cp)	Refractive Index at Temperature
1	19.0	6.022	1.972	57.3	10.8	28.0	75	0.9586	758.4	1.54513
2	16.5	6.000	1.978	49.9	11.6	22.5	150	0.9099	24.4	1.51722
3	15.5	5.760	1.977	44.9	12.5	26.0	75	0.9432	548.8	1.54339
4	14.6	5.495	1.979	40.4	10.9	20.4	75	0.9553	501.1	1.54366
5	16.4	5.811	1.979	48.0	12.5	34.5	200	0.8623	4.7	1.48699
6	17.0	6.054	1.978	51.8	12.5	34.5	75	0.9469	174.3	1.53443
7	18.2	6.033	1.980	55.4	12.5	30.8	75	0.9468	217.9	1.54706
8	18.5	5.701	1.979	53.3	12.3	27.2	75	0.9479	246.0	1.53673
9	17.4	6.010	1.978	52.8	12.1	29.3	75	0.9495	291.5	1.53792
10	17.7	5.843	1.976	52.1	12.1	29.3	75	0.9490	290.9	1.53767

A wide spectrum of pure gases and gas mixtures was tested in order to analyze the effect of oxygen (O$_2$)/solvent mixture on oil recovery and oil properties (**Table 2-2**). Gases used at low-temperature (75 °C) experiments were (a) N$_2$, (b) air, (c) O$_2$-enriched air, (d) propane (C$_3$), (e) air/C$_3$ mixture, (f) C$_3$ (Cycle 1) and air (Cycles 2 and 3), and (g) air (Cycles 1 and 3) and C$_3$ (Cycle 2). Gases used at high-temperature (150 and 200 °C) experiments were (h) air and (i) a mixture of air and C$_3$.

Table 2-2 Experimental operating conditions.

Experiment	Cycle	Gas	Temperature (°C)	Maximum Pressure (psia)	Soaking Time (days)
1	1	Air	75	281.6	8.1
1	2	Air	75	277.8	22.1
2	1	Air	150	320	8.4
2	2	Air	150	320	21.2
3	1	C_3	75	200	9.4
4	1	C_3 (53.1 mol%) + Air (46.9 mol%)	75	197.7	8.6
5	1	C_3 (51.5 mol%) + Air (48.5 mol%)	200	281.1	8.1
5	2	C_3 (51.5 mol%) + Air (48.5 mol%)	200	283.8	8.2
6	1	N_2	75	252.4	8.0
6	2	N_2	75	256.2	8.1
7	1	N_2 (62.7 mol%) + O_2 (37.3 mol%)	75	244.3	7.1
7	2	N_2 (62.7 mol%) + O_2 (37.3 mol%)	75	243.5	8.0
8	1	N_2 (horizontal core)	75	249.5	8.1
8	2	N_2 (horizontal core)	75	244.5	8.5
9	1	C_3	75	195.6	4.5
9	2	Air	75	202.6	4.2
9	3	Air	75	176.5	3.9
10	1	Air	75	209.3	4.1
10	2	C_3	75	187.1	4.0
10	3	Air	75	187.4	4.0

2.4.1 Setup and equipment

Core Preparation

Cores were cut from a Berea-outcrop- sandstone block (approximately 18% porosity and 200-md permeability) and dried in an oven at 140 °C. Then, the cores were saturated with gas-free (dead) heavy oil under vacuum at 80 °C.

Oil Properties

Oil properties were measured before and after each cycle. Dead-heavy-oil density was measured with a Rudolph Research Density Meter DDM2910 at atmospheric pressure from 25 to 90 °C. At the end of some experiments, produced-oil samples were heated at low temperatures for a few minutes to release the dissolved gas so that the oil density could be properly measured. The oil viscosity was measured at atmospheric pressure from 25 to 90 °C using a Brookfield Viscometer (model LVDV- II+P CP and spindle number CPE-51) connected to a water bath that heated the oil sample. All heavy-oil samples showed a Newtonian behaviour before and after experiments.

Asphaltene-Content Measurements

The asphaltene content in oil samples was measured using the following procedure:

- The oil sample (approximately 1 mg in weight) was put in a flask and mixed with 40 mL of heptane (approximately 40 times by weight).

- The flask containing the oil/heptane mixture was then kept in a dark cabinet for 3 to 4 days. During this period, the flask was shaken from time to time.

- The mixture was filtered with a previously weighed 11-μm filter paper.

- The filter paper containing the asphaltene/heptane mixture was put into an oven at 80 ℃ for approximately 1 day. After this, the dry filter paper was weighed.

- The asphaltene content (wt%) was then calculated by dividing the weight of asphaltene left on the filter paper by the oil-sample weight and multiplying by 100.

Asphaltene content was measured in two oil samples of similar characteristics, and a difference of approximately 5 wt% was found between them; this value was considered a measure of dispersion.

Asphaltene precipitation may occur when the equilibrium of the stabilizing forces has been perturbed (Sheu and Mullins 1995). Further analysis (e.g., numerical simulation) is required to analyze if asphaltene deposition occurred in the core and to evaluate its impact on oil recovery.

Oil Refractive-Index (RI) Measurements

Analysis of asphaltene-content measurements was complemented with oil RI measurements. Wattana et al. (2003) noted that the total amount of asphaltene found in a particular oil is closely related to the RI of the crude oil itself. They showed that the RI of a crude oil increased with the content of asphaltenes in the crude oil. Similar observations were made by Pathak et al. (2010). In the present work, oil RI measurements were used to identify the presence of asphaltene content in the crude-oil samples qualitatively.

The oil RI was measured using a Rudolph Research J257 Automatic Refractometer at atmospheric pressure from 25 to 70℃. The values of oil RI at higher temperatures were not obtained directly because of instrument temperature limitation; those were extrapolated on the basis of their well-defined linear trends.

Thermal Analysis

Oil thermal analysis was performed using thermogravimetric-analysis (TGA) and differential-scanning-calorimetry (DSC) methods to identify the ranges of temperature at which different reactions occur. In both TGA and DSC, air was used as an oxidizing agent. In oil samples of Experiments 1 and 2, the thermal analysis was conducted at two different heating rates, 10 and 15ºC/min.

Heavy-Oil-Saturated Core Soaked in a Gas-Filled Reactor

A 6-in.-length, 2-in.-diameter core was put in a funnel attached to a beaker to collect the expelled oil from matrix. The core, funnel, and beaker were placed into a 10-in.-length, 6.2-in.-diameter stainless-steel reactor, which in turn was introduced into an oven.

A pressure transducer was connected to the top of reactor to record reactor pressure. On the other hand, a thermocouple was introduced into the oven in order to monitor the oven temperature. Both the pressure transducer and thermocouple were connected to a data-acquisition system controlled by a personal computer (**Figure 2-1**). A gas tank was connected to the top of the reactor by means of a hose to fill it with specific gas [nitrogen, air, oxygen (O_2) -enriched air, propane (C_3), and an air/C_3 mixture].
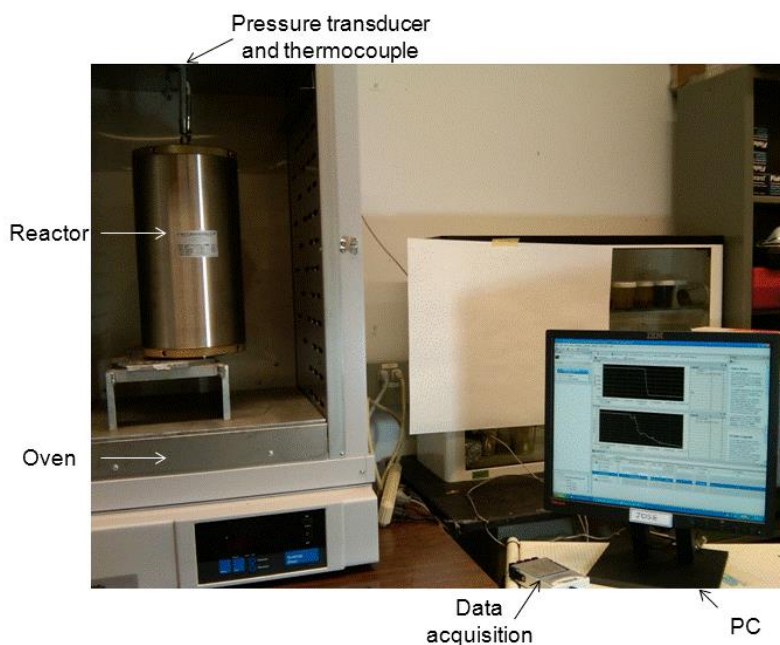
Figure 2-1 Experimental setup.

Gas Chromatography

The composition of the gas samples collected at the end of each cycle was analyzed using a Lumidor MicroMax Pro Gas Detector [to measure peak concentrations of only four components: O_2, carbon monoxide, hydrogen sulfide (H_2S), and methane (C_1)], an Agilent Technologies 7090A Gas Chromatography System (not calibrated to detect H_2S), or a SRI 8610C gas chromatograph. In some experiments, carbon dioxide is not reported because the instrument was not tuned for it.

2.4.2 Experimental results

In this section, the results of 10 experiments are presented—the experiment number corresponds to the chronological order in which experiments were performed. Experimental results are discussed in a different sequential order, starting with pure-nitrogen (N_2) experiments followed by increased oxygen (O_2) concentration/gas mixtures experiments. Then, pure-solvent-experiment results are discussed, followed by solvent/air/gas-mixture experiments. Eight of the 10 experiments were conducted at 75°C and two at higher temperatures (150 and 200°C). In most of

the experiments, two cycles were tested; one or three cycles were tested in some experiments. **Table 2-3** shows a summary of experimental results: oil-recovery factor (RF) per cycle (not cumulative); asphaltene content after experimentation; and gas chromatography. **Figure 2-2** and **Figure 2-3** show oil RF and asphaltene-content plots, respectively. **Figure 2-4** is a reactor pressure plot for experiments at 75ºC.

Table 2-3 Experimental results.

	1			2			3	4	5			6		
	Cycle 1	Cycle 2	Total	Cycle 1	Cycle 2	Total	Cycle 1	Cycle 1	Cycle 1	Cycle 2	Total	Cycle 1	Cycle 2	Total
R. F. (%)	9.0	9.9	18.9	23.3	26.5	49.8	30.9	28.0	36.0	4.7	40.6	19.9	3.3	23.2
Asphaltene content (weight %)	48.5	38.2		33.3	25.1	---	20.7	25.0	42.3	43.7		29.5		
Temperature (°C)	75			150			75	75	200			75		
ρ_o @ temperature (gr/cm³)				0.9041			0.9545	0.9581	0.8636			0.9499		
μ_o @ temperature (cp)		622.9		24.2			514.6	882.3	5.4			286.3	315.7	
RI @ temperature		1.5477		1.5135			1.5407	1.5416	1.4897			1.5373		
Gas chromatography (mol %) — C_1	0.000	48.000	---	12.000	0.012	---	0.000	0.007	0.556	0.624				
C_2	Not measured		---	Not measured	0.000	---	0.001	0.000	0.074	0.066				
C_3			---		2.851	---	98.907	29.365	36.369	36.844		0.083	0.102	
C_4			---		0.010	---	0.032	0.109	0.183	0.211		0.012	0.028	
C_5			---		0.004	---	0.002	0.000	6.608	7.539		1.903	0.118	
C_6			---		0.004	---	0.000	0.000	0.020	0.014				
O_2	20.700	20.700	---	18.200	13.051	---	0.156	13.535	0.824	0.620		1.180	1.025	
N_2	Not measured		---	Not measured	72.605	---	0.901	56.984	50.820	47.217		96.822	98.561	
CO_2			---		10.651	---	0.004	0.000	2.747	3.193				
CO	0.020	0.069	---	0.180	0.818	---	0.000	0.000	1.287	1.013			0.165	
H_2S	0.000	0.000	---	0.0002	0.000	---	0.000	0.000	0.511	2.659				

		7			8			9				10			
		Cycle 1	Cycle 2	Total	Cycle 1	Cycle 2	Total	Cycle 1	Cycle 2	Cycle 3	Total	Cycle 1	Cycle 2	Cycle 3	Total
R. F. (%)		19.0	4.6	23.6	22.4	1.5	23.9	29.5	0.0	0.0	29.5	17.0	14.1	0.0	31.1
Asphaltene content (weight %)		29.2	38.4		28.7			40.5				33.5	45.8		
Temperature (°C)		75			75			75				75			
ρ_o @ temperature (gr/cm^3)					0.9511			0.9499				0.9520	0.9556		
μ_o @ temperature (cp)		1010.9	1694.9		341.6			366.8				700.9	624.8		
RI @ temperature					1.5380			1.5376				1.5401	1.5403		
Gas chromatography (mol %)	C_1												0.007		
	C_2														
	C_3				9.373			92.690	0.352	0.009		0.003	88.540	0.334	
	C_4	0.000	0.002		3.210			0.155		0.000		0.006	0.224	0.002	
	C_5	0.021	0.032			0.019				0.017				0.016	
	C_6					0.001								0.116	
	O_2	33.505	33.851		1.129	1.342		1.198	19.037	19.184		19.091	1.757	18.842	
	N_2	66.473	66.115		86.288	98.638		5.958	80.611	80.790		80.900	9.473	80.690	
	CO_2														
	CO														
	H_2S														

In this paper, the term "total oil RF" refers to the summation of oil RF obtained in Cycles 1 and 2. The oil RF corresponds to the oil volume collected at the bottom of the reactor at the end of a cycle, divided by the initial oil volume in the core. Oil-production mechanisms are suggested and discussed on the basis of experimental results. It is not the objective of this work to discuss the quantitative contribution of each of the oil-production mechanisms. Detailed numerical-simulation studies of some of the laboratory results reported in this work are reported by Mayorquin- Ruiz and Babadagli (2012b).

Oil-thermal-expansion mechanism is expected to occur in all of the experiments, and its contribution to the total oil RF is assumed to be similar for experiments performed at 75ºC. Clearly, the contribution of this oil-production mechanism to the total oil RF is expected to be higher in experiments at 150 and 200ºC. Oil distribution in cores is shown in Appendix B.
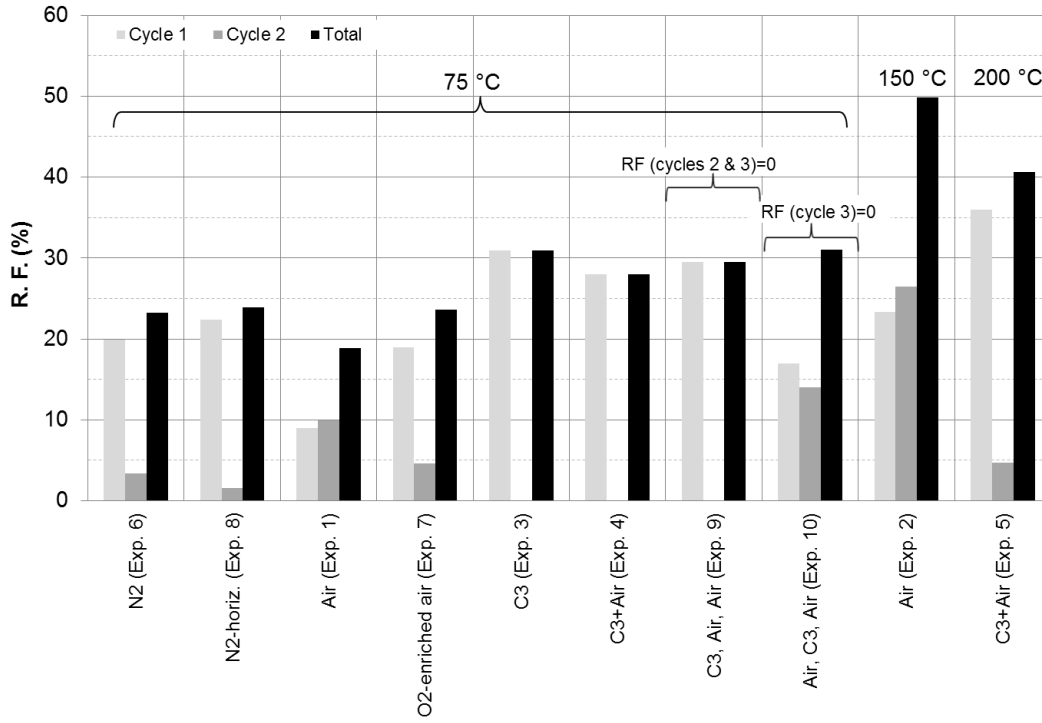
Figure 2-2 Oil RF for experiments.
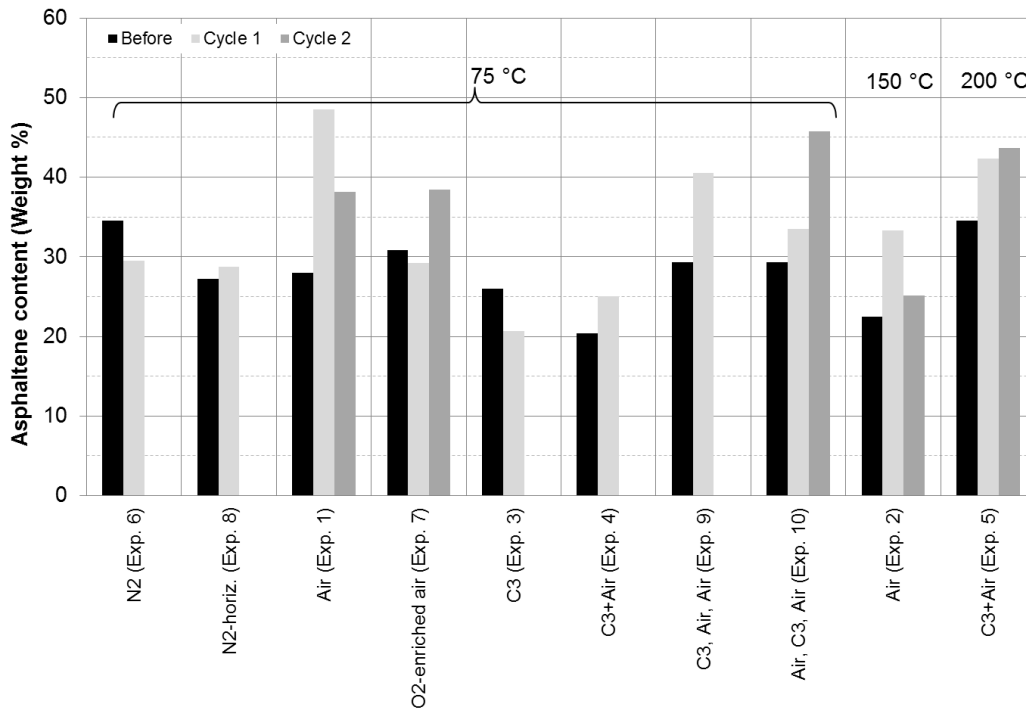
Figure 2-3 Asphaltene content in oil before and after cycles for experiments.

Experiments with Air Mixtures (Different N_2/O_2 Concentrations) at 75ºC: Experiments 6, 8, 1, and 7

Experiment 6: Heavy-Oil-Saturated Vertical Core Soaked in N_2 at 75ºC—Two Cycles

The oil RF obtained was 19.9 and 3.3% in Cycles 1 and 2, respectively (Table 2-3); total oil RF is 23.2%. Table 2-1 and Table 2-3 show that oil viscosity at 75 ºC increased 64% (from 174 to 286 cp) in Cycle 1; oil viscosity in Cycle 2 remained practically unchanged with regard to Cycle 1 oil viscosity. As for the oil density, it can be observed that there was a negligible increase (from 0.9468 to 0.9498 gr/cm^3) at 75 ºC in Cycle 1. The Cycle 2 produced oil volume was not significant enough for measuring other oil properties. In terms of asphaltene content for produced oil in Cycle 1, two opposite behaviours were observed depending on the method (quantitative or qualitative) used for the estimation of asphaltene content. On the basis of the quantitative method, a decrease was observed from 34.5 wt% (before Cycle 1) to 29.5 wt% (after Cycle 1) (i.e., 14.5% reduction); while oil refractive index (RI) (a qualitative method) showed an increase from 1.53443 to 1.53727, which also meant an increase in asphaltene content. Conclusions related to asphaltene content will be established together with the results of Experiment 8, where N_2 at 75 ºC was used with the core at horizontal orientation.
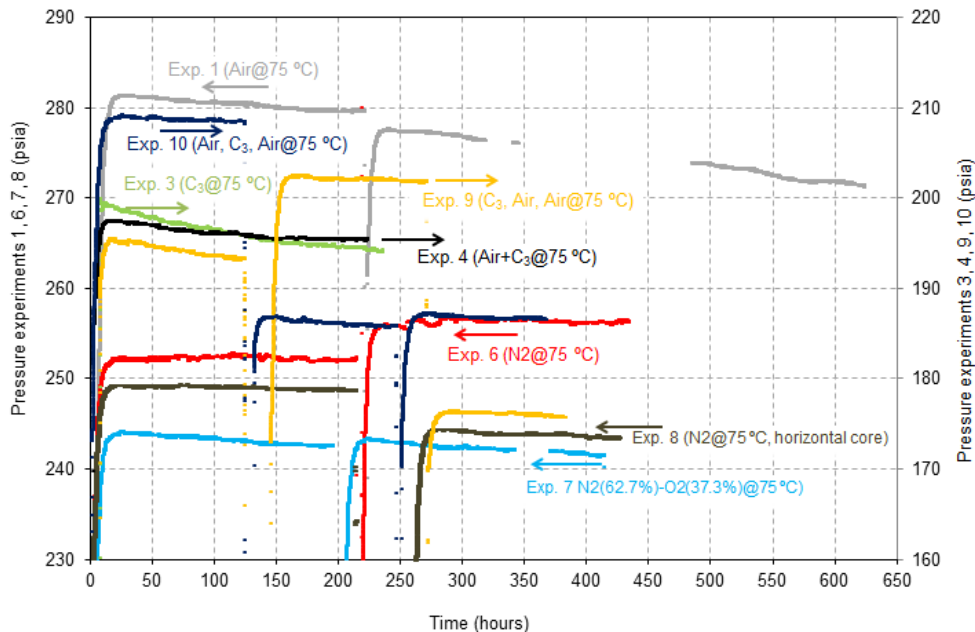
Figure 2-4 Reactor pressure measurements for experiments at 75ºC.

On the basis of the gas chromatography (**Figure 2-5**) of the released gas in Cycles 1 and 2, it can be observed that the gas mixtures consisted mainly of N_2 (more than 90 mol%). Additionally, a small concentration of light hydrocarbon components was detected in Cycle 1 [2 mol% of C_5 and some traces of propane (C_3) and C_4]. In Cycle 2, traces of C_3, C_4, and C_5 were detected, along with traces of carbon monoxide (CO). The presence of CO in the gas mixture is explained by the incomplete combustion of carbons; O_2 presence is explained by the presence of air in the reactor before filling it with N_2. Carbon oxides presence can also be associated to final products of low-temperature-oxidation (LTO) reactions, as also observed by Ren et al. (2002) for light oils. In all experiments, air at atmospheric-pressure conditions (reactor was not at vacuum) existed before filling the reactor with the corresponding gas mixture.
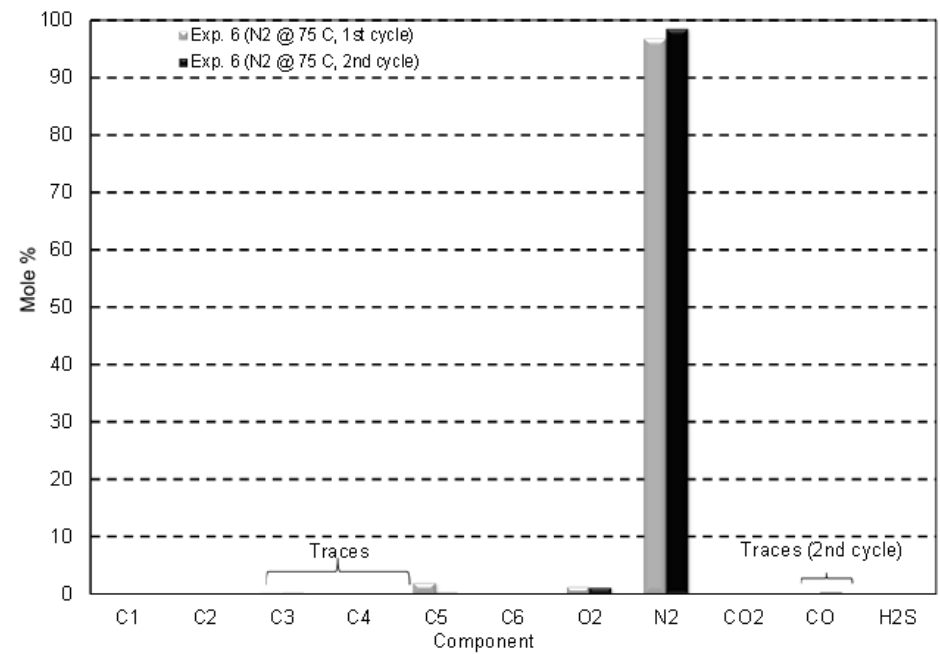
Figure 2-5 Released-gas chromatography. Experiment 6 (N_2 at 75 ºC, vertical core).

During the release of gas mixture in Cycle 1, the concentration of methane (C_1), CO, O_2, and hydrogen sulfide (H_2S) was monitored and it was observed that concentration of the component of the lightest molecular weight (C_1) was high at the beginning and then reduced after some time. On the other hand, the concentration of components of heavier molecular weight (CO and O_2) was initially low and then increased with time. Finally, there was a lag in the increase of the concentration of components of the heaviest molecular weight (O_2) compared with that of CO, having lower molecular weight than O_2. The same situation occurred during the release of gas in

Cycle 2. In regard to the recorded reactor pressure (Figure 2-4), it was observed that it remained practically constant along the experiment.

Experiment 8: Heavy-Oil-Saturated Horizontal Core Soaked in N_2 at 75ºC—Two Cycles

Total oil RF was 23.9% (RF in Cycles 1 and 2 was 22.4 and 1.5%, respectively, as shown in Table 2-3). Oil viscosity at 75 ºC increased approximately 39% in Cycle 1 from 246 to 342 cp (Table 2-1 and Table 2-3). Produced oil volume in Cycle 2 was not enough to measure its properties. Regarding the oil density at 75ºC (Table 2-1 and Table 2-3), a negligible increase of approximately 0.3% was calculated for Cycle 1 (from 0.9479 to 0.9511 g/cm^3). On the other hand, the asphaltene content in produced oil during Cycle 1 showed an increase in both quantitative and qualitative methods. The quantitative method showed an increase from 27.2 to 28.7 wt% (i.e., 5.5%), while oil RI showed an increase from 1.53673 to 1.53801.

On the other hand, the composition of the released gas (**Figure 2-6**) showed a high concentration of N_2 (more than 80%) in both Cycles 1 and 2. C_3 and C_4 were detected in Cycle 1, while traces of C_5 and C_6 were detected in Cycle 2. O_2 was detected in both cycles because of the existing air in the reactor before filling it with N_2. The recorded reactor pressure remained practically constant throughout the experiment (Figure 2-4).
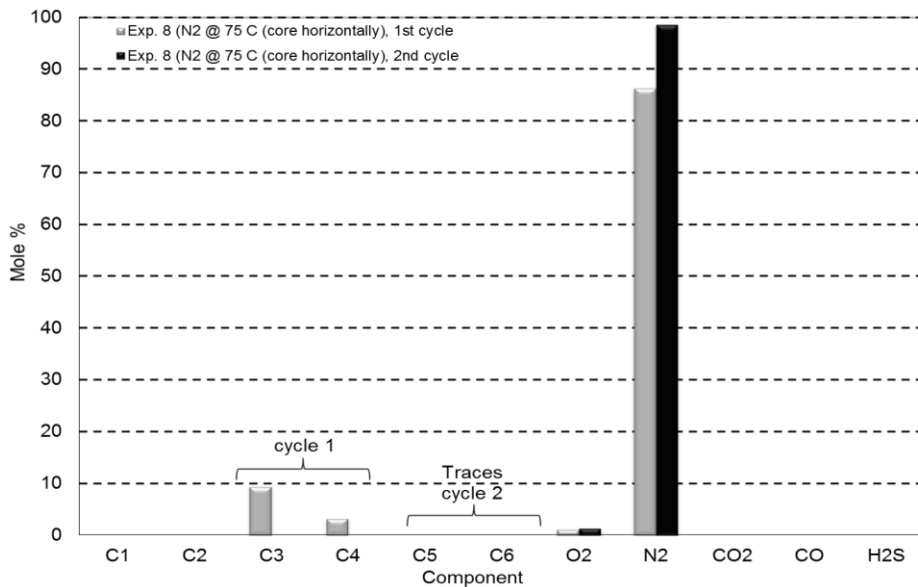
Figure 2-6 Released-gas chromatography. Experiment 8 (N_2 at 75 ºC, horizontal core).

Discussion of Experiments 6 and 8

Similar conditions existed in Experiments 6 and 8; similar reactor pressure, temperature, and inert gas (N_2) were used for soaking the heavy-oil-saturated core. Core length and diameter and rock permeability were also similar. Therefore, both samples had a similar area/volume ratio (approximately 0.8% higher in core used for Experiment 8). The two main differences between Experiments 6 and 8 were core orientation and oil viscosity before experimentation (41% higher oil viscosity in Experiment 8 compared with Experiment 6).

Despite differences in core orientation and initial oil viscosity, the total oil RF was practically the same in both experiments, with only 3% difference observed between them. This difference can be attributed to heterogeneities observed in cores. On the basis of the visual inspection for oil distribution inside the core of Experiment 6, it was observed that gravity drainage and effective diffusion took place. In Experiment 8, on the other hand, effective diffusion was observed to be a more important oil-production mechanism compared with gravity drainage. Oil distribution at the end of the experiments developed a type of cone-shaped oil distribution similar to that occurring in oil recovery by gravity drainage in matrix blocks, as sketched by Yanze and Clemens (2011).

Gas-pressure decay (**Figure 2-4)** was observed in both experiments. The gas pressure declined gradually with time as the gas molecules diffused into the oil phase. The rate of pressure decay was the lowest in these two experiments compared with the rest of the experiments. Also, pressure drop in the two cycles was the smallest, implying the lowest diffusion of all experiments. In fact, previous experience showed that N_2 diffusion capability into oil is much lower than that of the other gases used in this study. On the other hand, on the basis of the gas chromatographic results of the released gas in Experiment 8 (Figure 2-6), it was noted that a certain concentration of light hydrocarbon components diffused from the oil phase into the gas phase, which confirms that an effective diffusion process took place in the oil-recovery process. A higher concentration of light hydrocarbon components in the gas phase was detected in Experiment 8 compared with Experiment 6.

Although a different experimental setup and procedure were used, Guo et al. (2009) observed that the rate of N_2 diffusion in oil was the slowest among different gas/oil systems and the

pressure drawdown for that N_2/oil system was the smallest. On the other hand, Islas-Juarez et al. (2004) found a gas-pressure drop in an experiment at static conditions using a hexane/N_2 system. They observed an increasing N_2 mass concentration in the liquid phase with time at different depths; although not reported, an increasing hexane concentration in the gas phase would be expected. These two groups of researchers focused on a diffusive process, and gravity drainage was excluded from their physical model.

Convection in "annular fracture" gas is considered negligible on the basis that no temperature gradient was imposed at the reactor; oven temperature was kept constant. This was confirmed experimentally with the gas-chromatography results showing that heavier hydrocarbon components in the gas phase were at the bottom of the reactor, while lighter ones were at top.

An increase in the oil RI at the end Cycle 1 of Experiments 6 and 8 implies an increase in the asphaltene content occurred after the oil was in contact with N_2. Asphaltene-content measurements also showed an increase in produced oil obtained after Cycle 1 of Experiment 8 (only 5.5%), which was consistent with an increase in the oil RI. The opposite was observed in Cycle 1 (produced oil) of Experiment 6 (i.e. an increase in oil RI was measured, while the measured asphaltene content decreased 14.5%). The difference is not critically high, but it is also difficult to reach a firm conclusion on whether a mechanism is involved or not. The asphaltene content before experimentation in Experiments 6 and 8 was 34.5 and 27.2 wt%, respectively. But slightly higher oil RI was measured before Experiment 8, compared with that of Experiment 6. One major difference between these two experiments in this case is the situation of the core. This might affect the asphaltene deposition in the core and thereby the asphaltene content of the produced oil. It is worth mentioning that Jamaluddin et al. (2002) indicated that N_2 aggravated asphaltene instability in reservoir fluids.

Oil viscosity showed an important increase in Cycle 1 of 64 and 39% for Experiments 6 and 8, respectively. This oil-viscosity increase could be related in some degree to an increase of asphaltene content, as also observed by Luo and Gu (2007), and also to the extraction of lighter components from matrix oil to fracture gas because of effective diffusion, which has already been discussed. Presence of O_2 in the gas mixture could have had an impact on hydrocarbon

oxidation and asphaltene precipitation, but because of the small O_2 concentration, it would not be expected to be a major impact.

Experiment 1: Heavy-Oil-Saturated Core Soaked in Air at 75 C—Two Cycles

In this experiment, pure air was used. Hence, the O_2 concentration was increased from zero (as in the previous two experiments) to 21 mol%, with the rest being N_2. Oil thermal analysis [thermogravimetric analysis (TGA) and differential scanning calorimetry (DSC)] was completed before the experiment (Appendix A), and four reactions were identified (Mayorquin-Ruiz and Babadagli 2012a):

1. LTO reaction and distillation occurring in the temperature range of 25 to 280ºC. This range is characterized by the absence of exothermic peaks (on the basis of the DSC signal, no heat is generated in the oil sample at low-O_2 partial pressure). In the LTO reactions, O_2-addition reactions occur. Addition reactions are those in which atoms or groups of atoms are added to a molecule and no part of the original molecule is lost. There is simply a net gain of the reagent atoms in the product molecule (Whitfield 1966). According to Rodriguez and Christopher (2004), O_2-addition reactions do not yield as much heat as bond scission.

2. Low-temperature-combustion (LTC) reactions are observed at approximately 280 to 380ºC. LTC was also observed by Razzaghi et al. (2008) in a similar temperature range.

3. High-temperature-combustion (HTC) reactions occur from 380 to 510ºC. This is observed clearly in the DSC signal by the appearance of several exothermic peaks.

4. A second HTC is shown from 510ºC to approximately 800ºC. On the basis of thermal analysis results and temperature of Experiment 1, it can be concluded that LTO reaction and distillation occurred during the experiment. No heat would be generated at these conditions.

The oil RF obtained in each cycle is 9.0 and 9.9% in Cycles 1 and 2, respectively (Table 2-3). Total oil RF is 18.9%. It is important to note that the duration of Cycle 2 is 22.1 days, which is approximately three times longer than in Cycle 1 (8.1 days) (Table 2-2). Oil viscosity at 75ºC

(Table 2-1 and Table 2-3) was reduced in Cycle 2 from 758 to 623 cp (18% reduction). The asphaltene content increased 73% from 28.0 to 48.5 wt% in Cycle 1 and also increased 36% from 28.0 to 38.2 wt% (Table 2-3). Oil RI for Cycle 2 oil also showed an increment from 1.54512 to 1.54771, which is consistent with the increase in asphaltene content. The produced oil properties from Cycle 1 and density of oil from Cycle 2 were not measured because the produced-oil volume was not enough for a healthy measurement.

A detailed chromatographic analysis was not performed because TCD-FID was not available. However, a gas detector showed a minimum peak of 20.7 mol% O_2 concentration in the released-gas mixture (**Figure 2-7**) when O_2 concentration in the air was approximately 20.9%. It can also be observed that CO was also present in the released-gas mixture in both cycles.
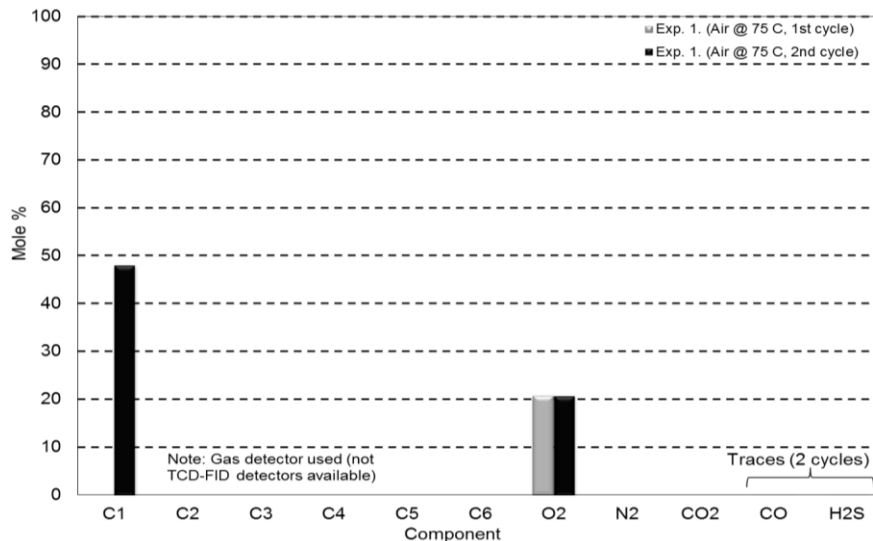
Figure 2-7 Released-gas chromatography. Experiment 1 (air at 75ºC).

On the other hand, reactor pressure declined gradually with time (Figure 2-4) faster than in Experiments 6 and 8 where N_2 was used. It can also be observed that pressure did not stabilize in both cycles and kept decreasing steadily, even when a longer period of time was spent on Cycle 2. This is because of the diffusion/reaction of O_2 with matrix oil; in Experiments 6 and 8, a slow diffusion of N_2 into matrix oil was inferred on the basis of pressure. A visual inspection of the cores cut through after the experiment showed that the center of the matrix was not completely swept.

Discussion on Experiment 1

A total of 18.9% oil RF was obtained when N_2 was used (Experiment 6, Cycle 1), and this value is only 9% when 21 mol% of O_2 is added (Experiment 1, Cycle 1). This difference can be explained by three reasons: (1) in Experiment 1, the oil viscosity (758 cp) at 75ºC was higher than that of Experiment 6 (174 cp) at same temperature; (2) LTO reactions that occurred at temperatures below 350ºC produced some complex components with high viscosity (Fadaei et al. 2010; Kapadia et al. 2013); and (3) higher asphaltene content was obtained in Experiment 1 associated to the LTO (Lakatos et al. 1998), and some of that could have been deposited in the core which in turn could have reduced the core permeability (Leyva and Babadagli 2011).

According to Gutierrez et al. (2009), two reaction modes for oil and O_2 are (1) bond-scission reactions and (2) O_2-addition reactions. They stated that both reactions occur simultaneously, but one dominates the other, and also that O_2-addition reactions are dominant at temperatures below 300 ºC, while bond-scission reaction starts dominating above 350ºC. Additionally, O_2-addition reactions tend to produce oxygenated species (e.g., aldehydes, alcohols, ketones, acids, and hydroperoxides) (Gutierrez et al. 2009; Bashkirov et al. 1965; Vaughan and Rust 1955), which then tend to react and polymerize with each other, forming asphaltenes (Gutierrez et al. 2009).

Evidence shows that Experiment 1 was in the range of LTO reactions where O_2-addition reactions occur, which explains the increase in the asphaltene content. This asphaltene-content increase, however, was not reflected in the oil-viscosity increase at 75ºC, and, in fact, the opposite occurred. On the basis of oil-viscosity measurements at different temperatures, it was observed that the oil-viscosity (Cycle 2) trend goes across the trend of the viscosity of the oil before the experiment. This behavior is not expected and can be explained by the presence of the air trapped in the oil sample during the oil-viscosity measurements. In fact, fluctuations in the viscosity-reading values were observed during measurements. Hence, the viscosity measurements of Cycle 2 oil should not been considered representative. On the other hand, both refractive index and asphaltene-content measurements of Cycle 2 oil samples showed an increment, as expected.

On the basis of gas chromatography, it was confirmed that an LTO reaction occurred in Experiment 1. CO was present, which indicates an incomplete combustion (Brady et al. 2000).

36

CO also means that O_2 was consumed partially, although that consumption was minimal because a high O_2 concentration existed in the released gas of both cycles.

A visual inspection of the cores cut through after the experiment showed that a type of cone-shaped oil distribution was formed in the upper middle portion, meaning that gravity drainage and diffusion played a role in the expulsion of matrix oil to the fracture. Comparing the pressure decay (Figure 2-4) of Experiment 1 with that of Experiment 6, it can be observed that there is a faster pressure-decay rate in the former. Also, it shows a higher drawdown, which is related to the O_2 uptake.

Experiment 7: Heavy-Oil-Saturated Core Soaked in O_2-Enriched Air at 75ºC—Two Cycles

Experiment 7 was carried out to analyze the oil-production behavior when O_2-enriched air was used. As such, the O_2 concentration was increased from 21 to 37.3 mol%, while N_2 concentration was reduced from 79 mol% to 62.7 mol%. Total oil RF was 23.6%. The breakdown of the RF in Cycles 1 and 2 was 19.0 and 4.6%, respectively (Table 2-3). Oil viscosity (Table 2-1 and Table 2-3) increased in Cycles 1 and 2 compared with oil viscosity before experimentation (from 218 to 1,011 cp in Cycle 1 and from 218 to 1,695 cp in Cycle 2). The asphaltene content (Table 2-3) in Cycle 1 reduced from 30.8 to 29.2 wt%, while in Cycle 2 it increased from 30.8 to 38.4%. Produced-oil volume from Cycles 1 and 2 was not enough to measure density and RI in a healthy manner. It was only possible to measure the oil properties before experimentation.

Gas chromatography (**Figure 2-8**) showed that only traces of light hydrocarbons were detected. On the other hand, N_2 and O_2 concentrations were unchanged practically in both cycles. A gradual decay in pressure was also observed (Figure 2-4).
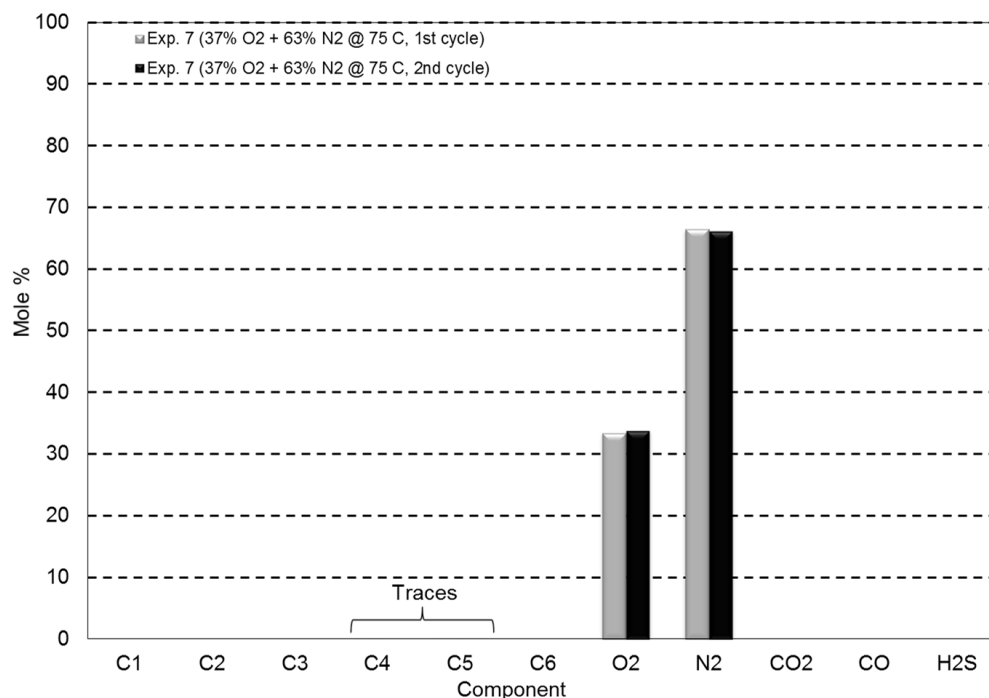
Figure 2-8 Released-gas chromatography. Experiment 7 (O_2-enriched air at 75ºC).

Discussion of Experiment 7

Similarities were found between Experiments 6 and 7 (N_2). For example, total oil RF and RF in each of the cycles, along with oil viscosity (174 cp in Experiment 6 and 218 cp in Experiment 7) and asphaltene content (34.5 wt% for Experiment 6 and 30.8 wt% for Experiment 7) before the experiments, were alike. Additionally, the asphaltene-content values in the oil of Cycle 1 of those two experiments were close to each other. Finally, the gas composition was also similar in the sense that traces of light components were detected. All these similarities could indicate that the same oil-production mechanisms were acting similarly in both experiments. In other words, using O_2-enriched air was the same as using pure N_2.

Another explanation for the similarities in the RFs might be the method by which the reactor was filled with the gas mixture during the O_2-enriched-air case. First, the reactor was filled with N_2 at a certain pressure, and after that, O_2 was added to the reactor. Hence, N_2 was in contact with the matrix oil first, which means that O_2 did not come into contact with the "fresh" matrix oil. This can be confirmed using numerical simulations and is an ongoing investigation.

Experiments with Air/C₃ Mixtures (Different C₃/Air Concentration) at 75ºC: Experiments 3 and 4

Previous Experiments (6, 8, 1, and 7) showed how different O_2 concentrations in air impact oil recovery. The next two experiments were run to understand how different concentrations of C_3/air mixtures (Experiments 3 and 4) will change oil recovery.

Experiment 3: Heavy-Oil-Saturated Core Soaked in C₃ at 75ºC—One Cycle

The RF obtained from this experiment (only one cycle) was 30.9% (Table 2-3). The oil viscosity at 75 ºC (Table 2-1 and Table 2-3) at the end of the experiment showed a slight decrease from 549 to 515 cp (approximately 6%). The oil density showed a negligible increase of 1.2%. Even if a clear trend in oil densities were obtained, it was observed experimentally that above 75 ºC, the measurements were not performed because density-meter readings did not stabilize because of the presence of gas in the oil samples. The asphaltene content (Figure 2-3) decreased from 26.0 to 20.7wt%, while the oil RI (Table 2-1 and Table 2-3) also decreased from 1.54338 to 1.54071, showing consistency.

Gas chromatography (**Figure 2-9**) showed that the main component in the gas phase is C_3. Traces of light components were detected (C_1, C_2, C_4, and C_5), along with small concentrations of O_2 and N_2. The presence of these last two components is caused by a small amount of air trapped in the reactor before it was filled with C_3. The pressure decay (Figure 2-4) of the C_3 experiment is the fastest of all experiments, indicating the strongest diffusion into matrix oil.

Discussion of Experiment 3

On the basis of the presence of light components in the released gas, it is clear that effective diffusion played a role in the oil-production mechanism. Light components came out of the oil, and solvent diffused into the oil, which can be the explanation to the slight reduction in oil viscosity. This is qualitatively supported by the oil distribution observed in the core at the end of the experiment through the absence of the characteristic cone-shaped oil distribution. Although an effective diffusion occurred in all directions, it was higher in the vertical sides of the core because it represents a larger area in contact with C_3 compared with that of the top and bottom parts. On the other hand, a reduction in the asphaltene content was observed through quantitative

measurement of asphaltene content and oil RI readings. This implies asphaltene precipitation and deposition in the core.
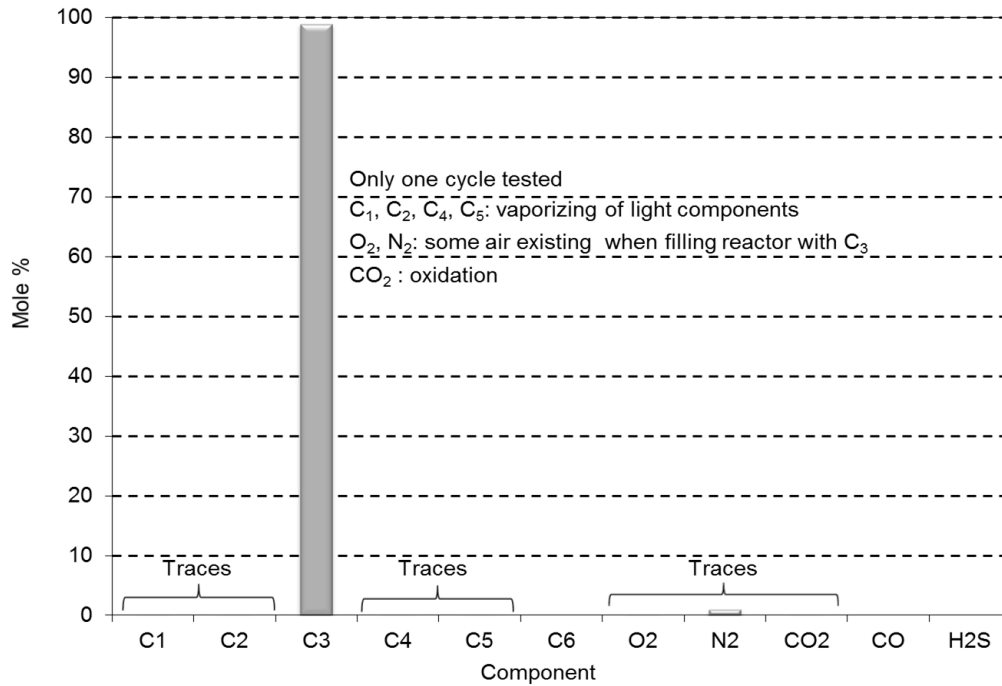
Figure 2-9 Released-gas chromatography. Experiment 3 (C_3 at 75ºC).

Even if it is of small magnitude, the reduction in oil viscosity results in an improvement in the expulsion of matrix oil to the fracture. RF obtained in Experiment 3 is rather similar compared with that obtained in Experiment 10 (to be discussed later), which was the highest RF of the experiments performed at 75 ºC. It is also interesting to note that the RF we obtained from pure-C_3 injection is consistent with that obtained by Pathak et al. (2010) with a similar rock, crude oil, and solvent, along with pressure and temperature conditions.

Experiment 4: Heavy-Oil-Saturated Core Soaked in a Mixture of C_3 (53.1 mol%) and Air (46.9 mol%) at 75ºC—One Cycle

In this experiment, air was mixed with C_3 to reduce its amount (and cost) and only one cycle was conducted. The RF (Figure 2-2) obtained at the end was 28.0%. Oil properties changed in Cycle 1 [e.g., oil viscosity (Table 2-1 and Table 2-3) increased from 501 to 882 cp (76% increase); oil density increased 0.3%, from 0.9553 to 0.9581 g/cm3; oil RI decreased from 1.54365 to 1.54155; while the asphaltene content increased from 20.4 to 25.0 wt%]. Higher concentrations of N_2, C_3,

and O_2, and traces of light hydrocarbon components were observed (**Figure 2-10**). A ratio of 19.2% O_2/80.8% N_2 was observed in the released-gas mixture. On the other hand, the C_3 concentration in the released-gas mixture was 29.3%. Also observed in this experiment was that gas pressure declined gradually with time (Figure 2-4).
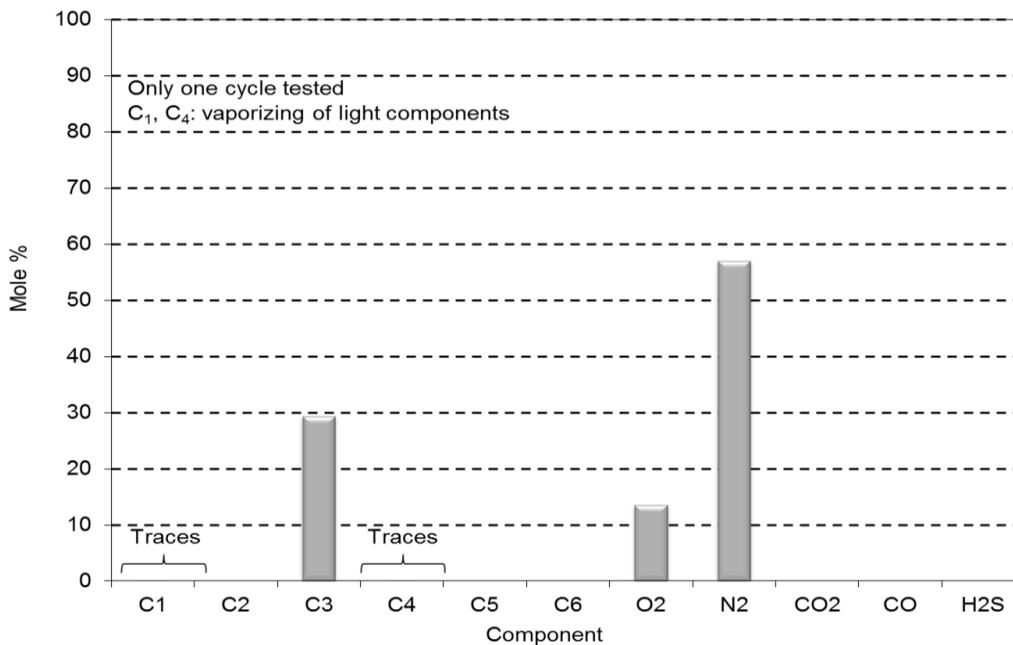
Figure 2-10 Released-gas chromatography. Experiment 4 (C_3/air mixture at 75ºC).

Discussion of Experiment 4

Oil properties from Experiments 4 and 3 are similar, and this enabled us to make a comparative analysis. However, it is important to note that Experiment 4 was 0.8 days shorter than Experiment 3. The RF in Experiments 4 and 3 was 28.0 and 30.9%, respectively, and this slight difference can be attributed to the time difference in these two experiments. Also, a high increase (76%) in oil viscosity was obtained in Experiment 4, but it remained unchanged practically in the case of Experiment 3, which could be related to the asphaltene precipitation caused by the oxidation of oil. However, the increase in the asphaltene content was reduced dramatically when compared with the air-only case (Experiment 1). Instead, oil RI showed a decrease in the asphaltene content, qualitatively.

Gas chromatography (Figure 2-10) indicated that effective diffusion played a role in the oil production, on the basis of the reduction of C_3 concentration, which is confirmed visually in the core longitudinal area.

Experiments with Air and C_3 in Different Cycles at 75ºC: Experiments 9 and 10

In Experiment 4, a mixture of C_3 and air was tested for a single cycle. In Experiments 9 and 10, three cycles were conducted, but in each cycle the same gases were injected alone rather than in a mixture. The first trial (Experiment 9) was injecting C_3 first to dilute the oil through its much stronger diffusion and mix-in capability before injecting air. In the second trial (Experiment 10), air was injected first. Then, C_3 was applied to reduce viscosity, which was increased (as expected) by oxidation (polymerization reactions are possible at this temperature).

Experiment 9: Heavy-Oil-Saturated Core Soaked in C_3/Air/Air at 75 ºC—Three Cycles

Three cycles were tested with different gases: C_3 (Cycle 1), air (Cycle 2), and air (Cycle 3). The duration of each cycle was approximately 4 days. Total oil RF was 29.5% (Table 2-3), which came mostly from Cycle 1 (i.e., only a trace amount of oil was produced in Cycles 2 and 3). Oil viscosity (Table 2-1 and Table 2-3) increased 26% from 291 to 367 cp. Oil density and oil RI remained practically unchanged. The asphaltene content increased from 29.3 to 40.5 wt% (Table 2-3).

Gas chromatography (**Figure 2-11**) showed that the main component was C_3 (92.7 mol%) in Cycle 1, and small amounts of C_4, N_2, and O_2 were also detected. These last two components came from the air existing in the reactor before C_3 injection. The components of the released gas in Cycle 2 were mainly N_2 and O_2, with a small concentration of C_3. In Cycle 3, besides N_2 and O_2, traces of C_3, C_4, and C_5 were detected. Gas-pressure decay (Figure 2-4) was also observed in the three cycles.
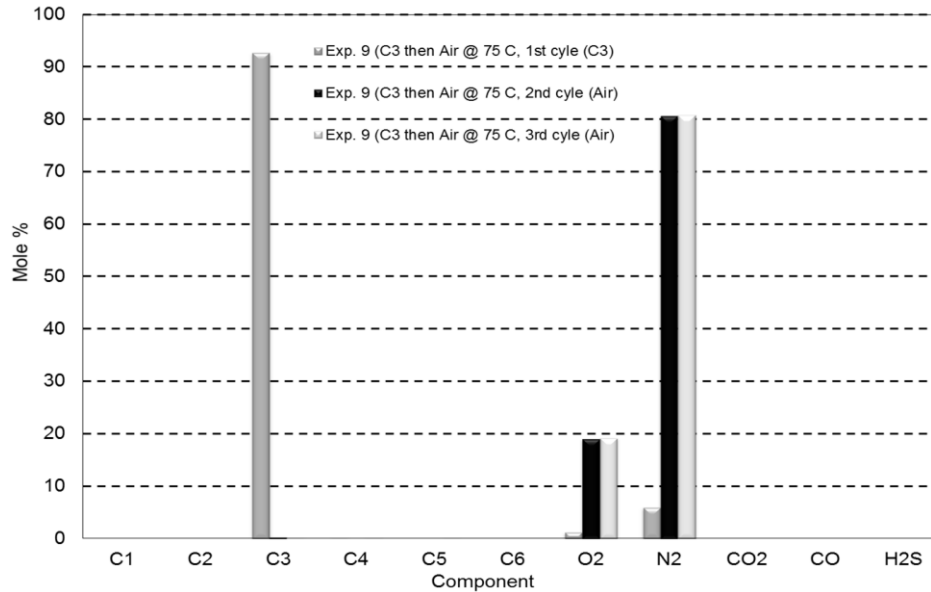
Figure 2-11 Released-gas chromatography. Experiment 9 (C_3/air/air at 75ºC).

Discussion of Experiment 9

The oil RFs in identical experiments (i.e., Experiment 3 and the first cycle of Experiment 9) are similar (30.9 and 29.5%, respectively), even if the durations of the cycles were substantially different (4.5 days for Experiment 9 and 9.4 days for Experiment 3). This validates the performance of C_3 and also indicates that much shorter soaking times are needed to reach the ultimate recovery by C_3. The oil viscosities of the two experiments before experimentation were not critically different. Oil viscosity increased 26% in Experiment 9 because of an increase in asphaltene content.

It is obvious that C_3 produced all recoverable oil for given pressure and temperature conditions through its high diffusion capability and gravity drainage caused by a reduction in viscosity. Air was unable to diffuse and react with the remaining thicker oil, to generate additional recovery in Cycles 2 and 3. More analysis is required to understand whether polymerization of the C_3/heavy-oil mixture left in the core occurs, which could block the pores to the fluid flow. It is interesting to observe that the rate of gas-pressure decay in Cycles 2 and 3, where air was used, is not as great as that of Experiment 1 (air). This implies that oil in the matrix after the C_3 phase did not allow air to diffuse into it at given pressure and temperature conditions.

Experiment 10: Heavy-Oil-Saturated Core Soaked in Air/C₃/Air at 75ºC—Three Cycles

Three cycles were tested with different gases: air (Cycle 1), C_3 (Cycle 2), and air (Cycle 3). The duration of each cycle was approximately 4 days. The RFs (Table 2-3) were 17.0, 14.1, and 0.0% for Cycles 1, 2, and 3, respectively, yielding a total of 31.1%. The oil viscosity in Cycles 1 and 2 (Table 2-1 and Table 2-3) increased from 291 to 701 cp, and from 291 to 625 cp, respectively. The oil density of Cycles 1 and 2 showed a slight increment (0.9490 to 0.9520 g/cm3, and from 0.9490 to 0.9556 g/cm^3, respectively). Oil RI also increased from 1.53767 to 1.54010 (Cycle 1), and from 1.53767 to 1.54025 (Cycle 2).

Asphaltene content (Figure 2-3) changed in both cycles from 29.3 to 33.5 wt% (Cycle 1) and from 29.3 to 45.8 wt% (Cycle 2).

Cycle 1 released-gas chromatography (**Figure 2-12**) showed that N_2 and O_2 are the main components and that trace amounts of light hydrocarbon components were also detected. Released gas in Cycle 2 showed a high concentration of C_3 and some amount of O_2 and N_2. In Cycle 3, N_2 and O_2 are the main components of the released gas; some traces of light hydrocarbon components were detected.

Figure 2-12 Released-gas chromatography. Experiment 10 (air/C₃/air at 75ºC).

Discussion of Experiment 10

The total RF in this experiment is similar to the other experiments in which C_3 is involved (Experiments 3 and 9) with different injection schemes at 75ºC. Air injection after the C_3 cycle did not produce any oil in Experiments 9 and 10. However, starting with air and continuing the process with C_3 yielded a similar recovery to pure-C_3 injection as a single phase. Hence, the combination of air and C_3 should be considered in practice as an economic option by also testing the time required to reach the ultimate recovery (approximately 30% in our laboratory conditions at 75ºC). Also, the asphaltene content of Experiment 10 increased in Cycles 1 and 2, as expected. Gas chromatography, however, did not show any CO or carbon dioxide (CO_2), which is an indication of no oxidation reaction during air injections.

Experiments with Air/C_3 Mixtures (Different C_3/Air Concentration) at High Temperatures (150 and 200ºC): Experiments 2 and 5. To observe the effect of temperature on the process, air and air/C_3-mixture experiments were repeated at higher temperatures: 150ºC using air only (Experiment 2) and 200ºC, using an air/C_3 mixture (Experiment 5). Gas-pressure measurements for experiments at high temperatures are shown in **Figure 2-13**.
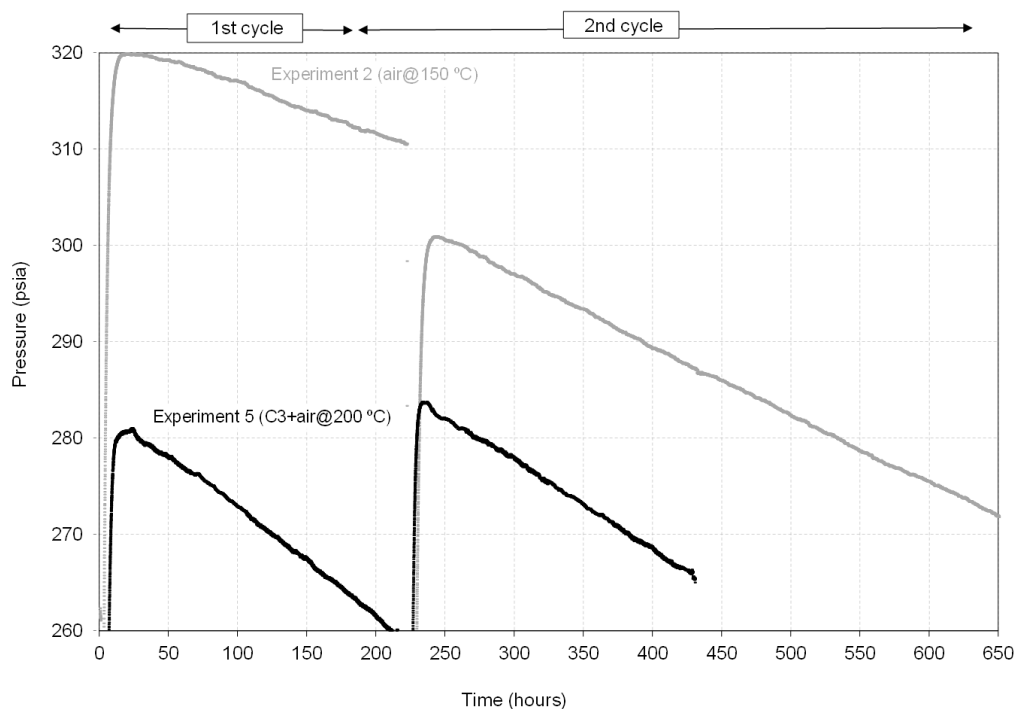
Figure 2-13 Reactor pressure measurements for experiments at 150 and 200ºC.

Experiment 2: Heavy-Oil-Saturated Core Soaked in Air at 150 ºC—Two Cycles

Before the experiment, thermal analysis was performed on the oil used. TGA and DSC signals behave almost the same as in Experiment 1 (Appendix A). Hence, the same comments apply to Experiment 2. On the basis of the results of thermal analysis and the temperature of Experiment 2 (150 ºC), it could be concluded that only an LTO reaction and distillation will occur during the experiment and no heat would be generated at this condition.

The RFs obtained in each of the two cycles were 23.3 and 26.5%, in Cycles 1 and 2, respectively (Table 2-3). The total oil RF was 49.8%. Duration of Cycles 1 and 2 (Table 2-2) were 8.4 and 21.2 days, respectively. The oil viscosity for Cycle 1 at 150ºC (Table 2-1 and Table 2-3) remained unchanged practically, but oil density negligibly decreased from 0.9099 to 0.9041 g/cm^3. Oil RI also showed a decrease from 1.51722 to 1.51350. On the other hand, the asphaltene content increased in two cycles from 22.5 to 33.3 wt% (Cycle 1) and from 22.5 to 25.1 wt%. The oil density and oil viscosity of Cycle 2 were not measured because the produced-oil volume was not great enough to measure.

The compositional analysis of the released gas in Cycle 1 (**Figure 2-14**) showed C_1 and traces of CO and H_2S. The O_2 concentration obtained in this cycle was 18.2 mol%. It is worthwhile to note that a gas detector was used that allowed for the detection of only four components: O_2, CO, C_1, and H_2S; no TCD-FID detectors were available for a more detailed analysis. Detectors were available to gauge released gas in Cycle 2. In the analysis of the gas produced in Cycle 2, even a lower concentration of O_2 was detected (13.0 mol%) with considerable concentration of N_2, C_3, CO_2, and CO. As in the previous experiments, the gas pressure (Figure 2-13) decreased at a much higher rate. The highest drawdown of all 10 experiments was observed in this experiment.

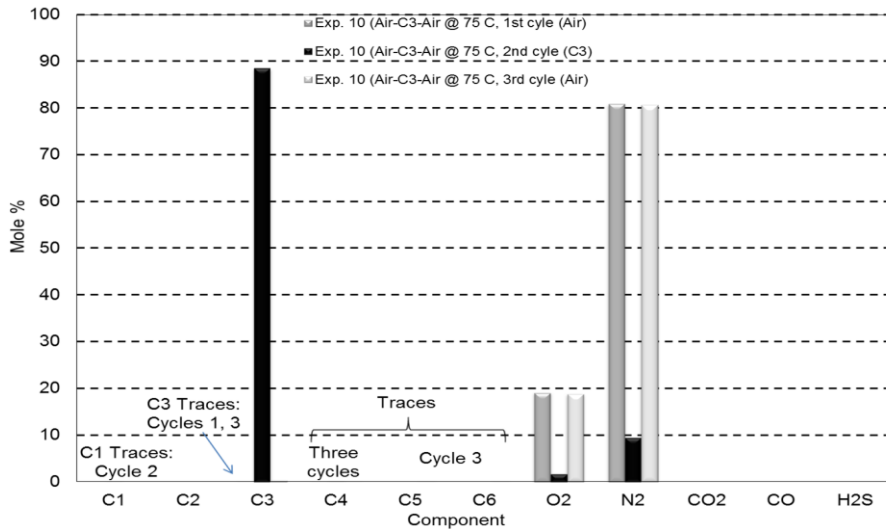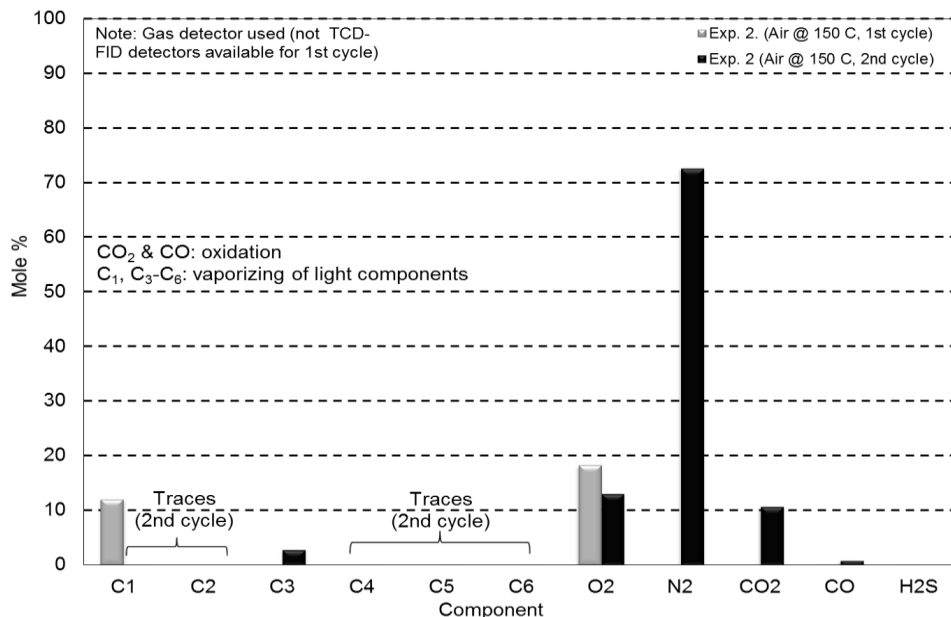**Figure 2-14 Released-gas chromatography. Experiment 2 (air at 150ºC).**

Discussion of Experiment 2

The total oil RF in this experiment represented the maximum RF of all experiments conducted at low and high temperatures. This is caused by increased temperature (higher oil thermal expansion and augmented gravity drainage) and also the longer duration of Cycle 2. Despite an increase in the asphaltene content because of the high temperature, the oil viscosity was not affected (Luo and Gu 2007 also reported a similar observation).

O_2 was partially consumed (from 20.9 to 13.0 mol%) at 150 ºC and because of a high concentration of CO_2 and CO, is likely that some heat was generated. Gas-pressure decay was much faster than that of Experiment 1 (air at 75 ºC) because of the combined effect of effective diffusion and consumption of O_2.

Experiment 5: Heavy-Oil-Saturated Core Soaked in Air/C₃ Mixture at 200 ºC—Two Cycles

No thermal analysis was available for this oil, but on the basis of previous thermal analysis (Experiments 1 and 2) results, we expect that similar reactions would occur for this oil in a wide range of temperatures.

Total oil RF (Figure 2-2) was 40.6%. Cycles 1 and 2 yielded 36.0 and 4.7% RFs, respectively (Table 2-3). The oil properties in Cycle 1 remained unchanged practically. Oil viscosity (Table 2-1 and Table 2-3) slightly increased from 4.7 to 5.4 cp (15% increase), and oil density showed an increment from 0.8623 to 0.8636 g/cm3 (0.2% increase). The oil RI increased from 1.48699 to 1.48974, and the asphaltene content (Figure 2-3) changed in both cycles from 34.5 to 42.3 wt% (Cycle 1) and from 34.5 to 43.7 wt% (Cycle 2). It can be observed that a correlation exists between oil RI and asphaltene content.

The composition of released gas (**Figure 2-15**) showed the same components in both cycles: considerable amounts of N_2 and C_3, along with C_5, CO_2, and traces of C_1, C_2, C_4, C_6, O_2, CO, and H_2S. On the other hand, a high rate of gas-pressure decay was observed in this experiment, which is the highest of all 10 experiments. The second-highest drawdown was also observed compared with the other experiments.
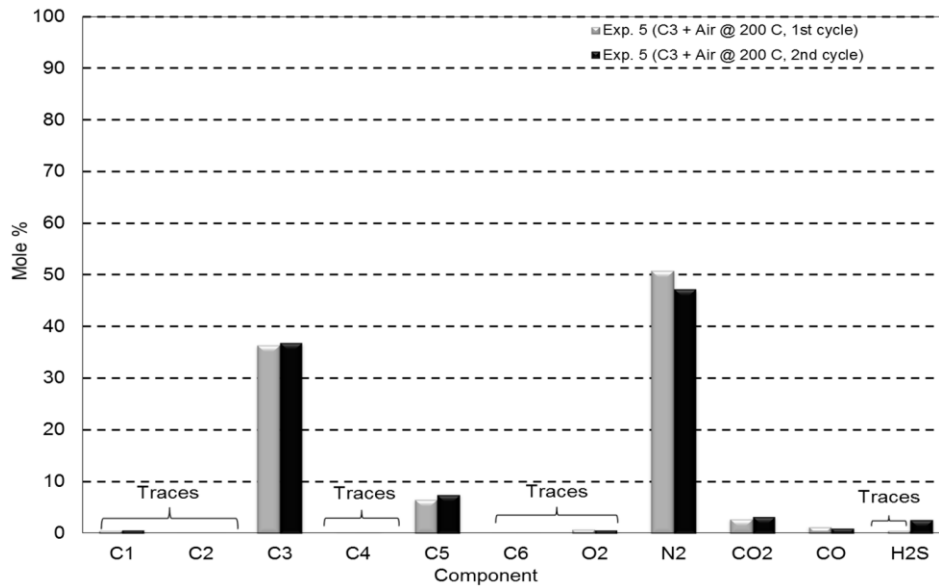
Figure 2-15 Released-gas chromatography. Experiment 5 (air/C_3 mixture at 200ºC).

Discussion of Experiment 5

The total RF in this experiment represented the second-highest RF of all of the experiments carried out at low and high temperatures. The total RF at a higher temperature (Experiment 5) is lower than that of a lower temperature (Experiment 2), despite lowered viscosity (because of temperature effects) and use of a solvent. Even though experimental design for Experiments 5

and 2 makes their results not comparable directly, we can speculate that the lower RF in Experiment 5 compared with that of Experiment 2 could be explained by two reasons: (1) recovery increases when the temperature is near the saturation temperature of the solvent and decreases when temperature is increased even further (Pathak et al. 2011); and (2) it is likely that the products generated in LTO (e.g., asphaltenes) were deposited in the core, blocking the pores to the fluid flow. On the other hand, in addition to LTO reactions, bond-scission reactions could have occurred because it could be confirmed by the presence of carbon oxides (CO and CO_2) in the released gas of both cycles.

Final Discussion and Overall Evaluation of the Observations

On the basis of the experimental results, it was shown that O_2 was unconsumed practically and instead, an increase in asphaltene content occurred because of the products associated with LTO reactions. In fact, oil thermal analysis demonstrated that LTO and distillation occurred at 75 ºC. Additionally, when the RFs of the experiments using only air were compared with that of the air/C_3 mixture, a better RF was observed of this last case, along with less of an increase in the asphaltene content. However, lack of O_2 uptake was an issue.

On the other hand, experiments at higher temperatures showed that O_2 was consumed partially (150ºC) or totally (200ºC). Thermal analysis indicated that the temperatures at which the experiments were performed fell into the LTO region, which caused an increase in the asphaltene content. However, partial bond-scission reactions also occurred, as indicated by the presence of carbon oxides in the released gas; carbon oxides can also be associated with final products of LTO reactions. It was also observed that at higher temperatures, the gas-pressure decay was much faster than in the cases at lower temperatures. This is an indication of O_2 consumption, also accelerated by reduced viscosity of oil caused by higher temperatures.

In all experiments, during the heating process of the reactor, the gas pressure increased. Once the temperature was stabilized, the gas pressure reached a maximum value and then started to decline gradually. This gas-pressure decay was not only related to the effective diffusion of gas molecules into the oil-filled pore volume, but also to the O_2 consumption in the matrix oil. It was found, in general, that at a certain gas-pressure-decay rate, the oil recovery was greater in first cycles than in second cycles. This means that the effective diffusion is more critical in the first

cycles because a greater concentration gradient exists between fracture-gas composition and matrix-oil composition.

On the basis of the experimental data, it was possible to infer that oil-production mechanisms involved in the experiments were oil thermal expansion, effective diffusion, and gravity drainage. It was observed that the degree of participation of these mechanisms was a function of the type of gas existing in the fracture, along with the pressure and temperature. The results showed that the use of the air/C_3 mixture provides promising results in terms of RF and asphaltene content. It is obvious that the reduction in the use of solvents will improve project economics. The use of C_3 mixed with air could be beneficial under certain conditions of pressure, temperature, and concentration, and they were reported in this paper.

Finally, it should be emphasized that thermal expansion is a critically important mechanism at higher temperatures. However, one may be able to distinguish this implicitly by reviewing the RFs given in Table 2-2 and Figure 2-3. Any difference in the RFs of the same-temperature experiments is because of other mechanisms [mainly the diffusion of gas into the matrix and its reactions with oil (e.g., oxidation)]. That is the reason that base-case experiments (Experiments 1, 2, and 6) are provided for comparison purposes.

2.5 Conclusions

The experiments showed encouraging results at 75ºC, where a heavy-oil-saturated core was immersed in an air/propane (C_3) gas mixture rather than pure air; a certain amount of C_3 added to air may yield a highly attractive recovery. This means that an optimum C_3/air ratio should be investigated. However, an important issue prevails at 75ºC; high oxygen (O_2) concentration is present in the gas mixture at the end of the experiments. From the pressure data, one may observe that C_3 diffusion into oil is the fastest, while the rate of nitrogen diffusion is the slowest; the air (or O_2) diffusion falls in between these two cases.

High temperatures (150 and 200ºC) showed a more promising condition compared with 75 ºC because of the high O_2 consumption; it is possible that carbon oxides are related not only to final products of low-temperature oxidation reactions, but even to exothermic conditions that might have occurred because of an increased O_2 partial pressure. At these elevated temperatures, the

50

impact of oxygenated compounds is minor and the recovery factors for both pure-air and air/C_3-gas mixture are similar. However, for this gas mixture, the operating conditions near C_3-saturation temperature show better results.

Critical parameters in oil recovery are soaking time, operation conditions (pressure and temperature), and fluid-injection sequence. The effects of these parameters on oil recovery are clarified to a greater extent, and the margins of the optimal conditions are defined. Further efforts can be made toward the optimization of the methodology (air/C_3 injection) for different matrix sizes and fracture volumes (i.e., reservoir properties).

2.6 Nomenclature

C_1 = methane, CH_4

C_2 = ethane, C_2H_6

C_3 = propane, C_3H_8

C_4 = butane, C_4H_{10}

C_5 = pentane, C_5H_{12}

C_6 = hexane, C_6H_{14}

μ_o = oil viscosity, cp

ϕ = porosity, fraction

References

Alvarez, J. M., Sawatzky, R. P., Forster, L. M. et al. 2008. Alberta's Bitumen Carbonate Reservoirs—Moving Forward with Advanced R&D. Presented at the World Heavy Oil Congress, Edmonton, Alberta, Canada, 10–12 March. Paper 2008-467.

Bashkirov, A. N., Kamzolkin, V. V., Sokova, K. M. et al. 1965. The Mechanism of the Liquid-Phase Oxidation of Paraffinic Hydrocarbons. In The Oxidation of Hydrocarbons in the Liquid

Phase, first edition. ed. Emanuel N.M. 183–193. New York: Elsevier. http://dx.doi.org/10.1016/B978-0-08-010491-1.50018-5.

Brady, J. E., Russell, J. W., and Holum, J. R. 2000. *Chemistry: Matter and Its Changes*, third edition. New York: John Wiley & Sons, Inc.

Chávez, E. and González, J. A. 2013. Implantación de la Prueba Tecnológica de Inyección de Aire en Cárdenas JSK. Presented at Congreso Mexicano del Petróleo, Cancún-Riviera Maya, México, 5–8 June.

Craig, F. F., Jr. and Parrish, D. R. 1974. A Multipilot Evaluation of the COFCAW Process. *J Pet Technol* **26** (06): 659–666. SPE-3778-PA. http://dx.doi.org/10.2118/3778-PA.

Cruz, L., Sheridan, J., Aguirre, E. et al. 2009. Relative Contribution to Fluid Flow from Natural Fractures in the Cantarell Field, Mexico. Presented at the Latin American and Caribbean Petroleum Engineering Conference, Cartagena de Indias, Colombia, 31 May–3 June. SPE-122182-MS. http://dx.doi.org/10.2118/122182-MS.

Fadaei, H., Debenest, G., Kamp, A. M. et al. 2010. How the in-Situ Combustion Process Works in a Fractured System: 2D Core- and Block-Scale Simulation. *SPE Res Eval & Eng* **13** (01): 118–130. SPE-117645-PA. http://dx.doi.org/10.2118/117645-PA.

Guo, P., Wang, Z., Shen, P. et al. 2009. Molecular Diffusion Coefficients of the Multicomponent Gas-Crude Oil Systems under High Temperature and Pressure. *Ind Eng Chem Res* **48** (19): 9023–9027. http://dx.doi.org/10.1021/ie801671u.

Gutierrez, D., Skoreyko, F., Moore, R. G. et al. 2009. The Challenge of Predicting Field Performance of Air Injection Projects Based on Laboratory and Numerical Modelling. *J Can Pet Technol* **48** (04): 23–34. PETSOC-09-04-23-DA. http://dx.doi.org/10.2118/09-04-23-DA.

Islas-Juárez, R., Samaniego V, F., Luna, E. et al. 2004. Experimental Study of Effective Diffusion in Porous Media. Presented at the SPE International Petroleum Conference in Mexico, Puebla, Mexico, 8–9 November. SPE-92196-MS. http://dx.doi.org/10.2118/92196-MS.

Jamaluddin, A. K. M., Joshi, N., Iwere, F. et al. 2002. An Investigation of Asphaltene Instability under Nitrogen Injection. Presented at the SPE International Petroleum Conference and Exhibition in Mexico, Villahermosa, Mexico, 10–12 February. SPE-74393-MS. http://dx.doi.org/10.2118/74393-MS.

Kapadia, P., Gates, I. D., Mahinpey, N. et al. 2013. Kinetic Models for Low Temperature Oxidation Subranges Based on Reaction Products. Presented at the SPE Heavy Oil Conference—Canada, Calgary, 11–13 June. SPE-165527-MS. http://dx.doi.org/10.2118/165527-MS.

Lacroix, S., Delaplace, P., Bourbiaux, B. et al. 2004. Simulation of Air Injection in Light-Oil Fractured Reservoirs: Setting-up a Predictive Dual Porosity Model. Presented at the SPE Annual Technical Conference and Exhibition, Houston, 26–29 September. SPE-89931-MS. http://dx.doi.org/10.2118/89931-MS.

Lakatos, I., Lakatos-Szabo, J., Bauer, K. et al. 1998. Potential Application of Oxygen-Containing Gases in Heavy Oil Bearing Reservoirs. Presented at the European Petroleum Conference, The Hague, 20–22 October. SPE-50647-MS. http://dx.doi.org/10.2118/50647-MS.

Leyva, H. and Babadagli, T. 2011. Optimal Application Conditions for Heavy-Oil/Bitumen Recovery by Solvent Injection at Elevated Temperatures. Presented at the SPE Heavy Oil Conference and Exhibition, Kuwait City, Kuwait, 12–14 December. SPE-150315-MS. http://dx.doi.org/10.2118/150315-MS.

Limón-Hernández, T., De-la-Fuente, G., Garza-Ponce, G. et al. 1999. Overview of the Cantarell Field Development Program. Presented at the Offshore Technology Conference, Houston, 3–6 May. OTC-10860-MS. http://dx.doi.org/10.4043/10860-MS.

Luo, P. and Gu, Y. 2007. Effects of Asphaltene Content on the Heavy Oil Viscosity at Different Temperatures. Fuel 86 (7–8): 1069–1078. http://dx.doi.org/10.1016/j.fuel.2006.10.017.

Mayorquin-Ruiz, J. R. and Babadagli, T. 2012a. Can Injection of Low Temperature Air-Solvent (LTASI) Be a Solution for Heavy Oil Recovery in Deep Naturally Fractured Reservoirs? Presented at the SPE EOR Conference at Oil and Gas West Asia, Muscat, Oman, 16–18 April. SPE-153997-MS. http://dx.doi.org/10.2118/153997-MS.

Mayorquin-Ruiz, J. R. and Babadagli, T. 2012b. Optimal Design of Low Temperature Air Injection for Efficient Recovery of Heavy Oil in Deep Naturally Fractured Reservoirs: Experimental and Numerical Approach. Presented at the SPE Heavy Oil Conference Canada, Calgary, 12–14 June. SPE-149896-MS. http://dx.doi.org/10.2118/149896-MS.

Pathak, V. 2011. Heavy Oil and Bitumen Recovery by Hot Solvent Injection: An Experimental and Computational Investigation. Presented at the SPE International Student Paper Contest at SPE Annual Technical Conference and Exhibition, Denver, 30 October–November 2. SPE-152374-STU. http://dx.doi.org/10.2118/152374-STU.

Pathak, V., Babadagli, T., and Edmunds, N. R. 2010. Hot Solvent Injection for Heavy Oil/Bitumen Recovery: An Experimental Investigation. Presented at the Canadian Unconventional Resources and International Petroleum Conference, Calgary, 19–21 October. SPE-137440-MS. http://dx.doi.org/10.2118/137440-MS.

Razzaghi, S., Kharrat, R., and Vossoughi, S. 2008. Design of in Situ Combustion Process by Using Experimental Data. Presented at the World Heavy Oil Congress, Edmonton, Alberta, Canada, 10–12 March.

Ren, S. R., Greaves, M., and Rathbone, R. R. 2002. Air Injection LTO to Process: An IOR Technique for Light-Oil Reservoirs. *SPE J* **7** (01): 90–99. SPE-57005-PA. http://dx.doi.org/10.2118/57005-PA.

Riazi, M. R., Whitson, C. H., and da Silva, F. 1994. Modelling of Diffusional Mass Transfer in Naturally Fractured Reservoirs. *J Pet Sci Eng* **10** (3): 239–253. http://dx.doi.org/10.1016/0920-4105(94)90084-1.

Rodriguez, F. and Christopher, C. A. 2004. Overview of Air Injection Potential for Pemex. Presented at the AAPG International Conference, Cancún, México, 24–27 October. Paper #89612.

Rodríguez, F., Ortega, G., Sánchez, J. L. et al. 2001. Reservoir Management Issues in the Cantarell Nitrogen Injection Project. Presented at the Offshore Technology Conference, Houston, 30 April–3 May. OTC-13178-MS. http://dx.doi.org/10.4043/13178-MS.

Rodriguez, F., Sanchez, J. L., and Galindo-Nava, A. 2004. Mechanisms and Main Parameters Affecting Nitrogen Distribution in the Gas Cap of the Supergiant Akal Reservoir in the Cantarell Complex. Presented at the SPE Annual Technical Conference and Exhibition, Houston, 26–29 September. SPE-90288-MS. http://dx.doi.org/10.2118/90288-MS.

Schulte, W. M. and de Vries, A. S. 1985. In-Situ Combustion in Naturally Fractured Heavy Oil Reservoirs. *Society of Petroleum Engineers Journal* **25** (01): 67–77. SPE-10723-PA. http://dx.doi.org/10.2118/10723-PA.

Sheu, E. Y. and Mullins, O. C. 1995. Asphaltenes: Fundamentals and Applications, first edition. New York: Springer. http://dx.doi.org/10.1007/978-1-4757-9293-5.

Stokka, S., Oesthus, A., and Frangeul, J. 2005. Evaluation of Air Injection as an Ior Method for the Giant Ekofisk Chalk Field. Presented at the SPE International Improved Oil Recovery Conference, Kuala Lumpur, 5–6 December. SPE-97481-MS. http://dx.doi.org/10.2118/97481-MS.

Vaughan, W. E. and Rust, F. F. 1995. Low Temperature Oxidation of Paraffin Hydrocarbons: Oxidation of Paraffin Wax. *In The Chemistry of Petroleum Hydrocarbons*, first edition. ed. Brooks B.T. and Boord C.E. and Kurtz J. S. S. Jr., et al., Vol. II. 309–323. New York: Reinhold Publishing Corporation.

Wattana, P., Wojciechowski, D. J., Bolaños, G. et al. 2003. Study of Asphaltene Precipitation Using Refractive Index Measurement. Petroleum Science and Technology 21 (3–4): 591–613. http://dx.doi.org/10.1081/lft-120018541.

Whitfield, R. C. 1966. *A Guide to Understanding Basic Organic Reactions*, first edition. London: Concepts in Chemistry, Longmans.

Yanze, Y. and Clemens, T. 2011. The Role of Diffusion for Non-Miscible Gas Injection in a Fractured Reservoir. Presented at the SPE EUROPEC/EAGE Annual Conference and Exhibition, Vienna, Austria, 23–26 May. SPE-142724-MS. http://dx.doi.org/10.2118/142724-MS.

Appendix A. Thermal analysis of the oil used in experiments 1 and 2

Figure 2-16 shows the results of thermogravimetric analysis (TGA) conducted in oil samples of experiment 1 at two heating rates: 10 and 15 °C/min.
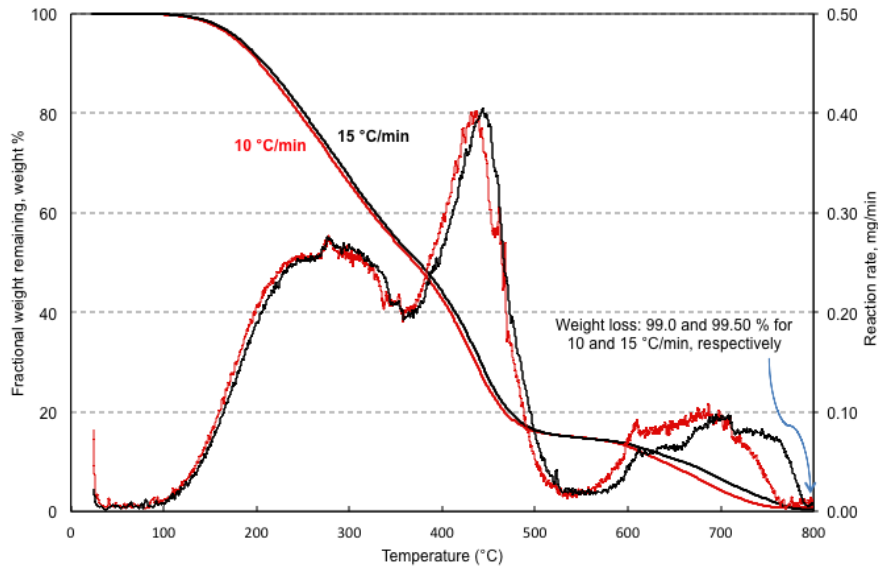
Figure 2-16 TGA for crude oil sample before experiment 1 (air @ 75 °C).

Figure 2-17 show the results of differential-scanning-calorimetry (DSC) conducted in oil sample of experiments 1 at two heating rates: 10 and 15 °C/min.
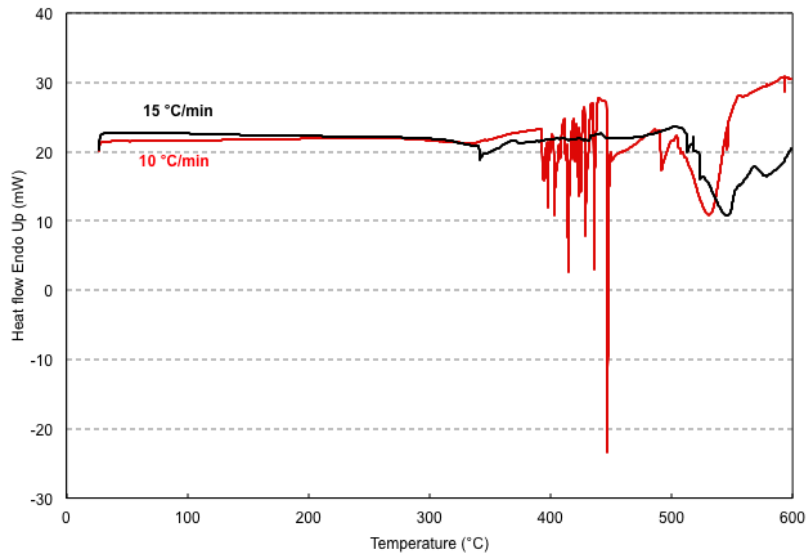
Figure 2-17 DSC for crude oil sample before experiment 1 (air @ 75 °C).

56

Figure **2-18** shows the results of thermogravimetric analysis (TGA) conducted in oil samples of experiment 2 at two heating rates: 10 and 15 °C/min.
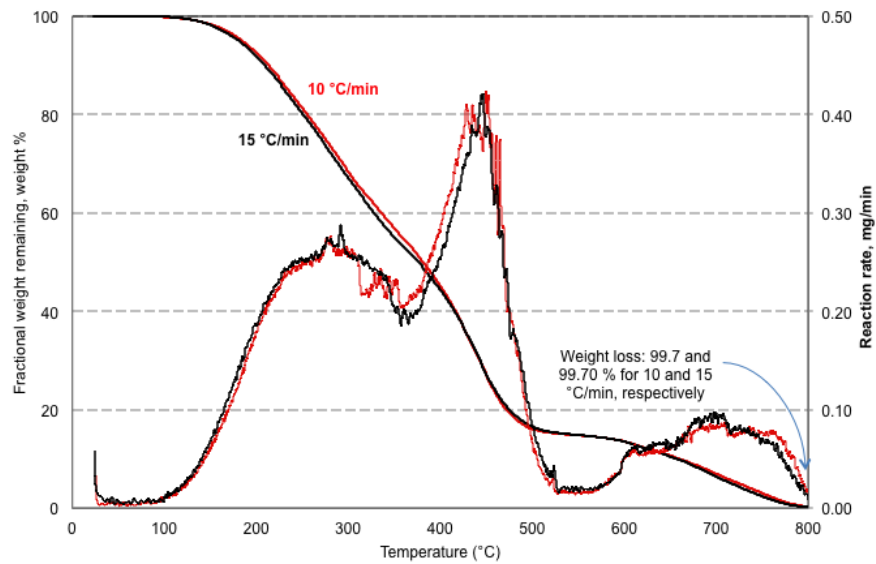
Figure 2-18 TGA for crude oil sample before experiment 2 (air @ 150°C).

Figure **2-19** shows the results of differential-scanning-calorimetry (DSC) conducted in oil sample of experiments 2 at two heating rates: 10 and 15 °C/min.
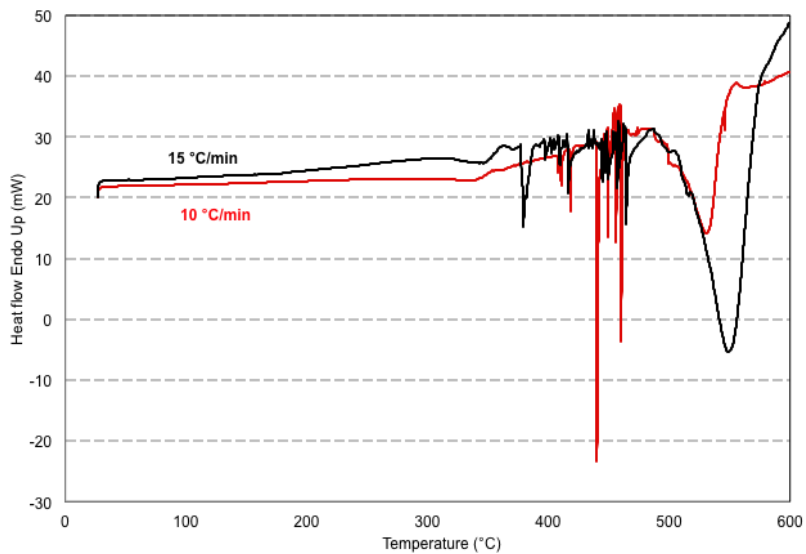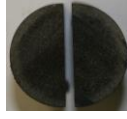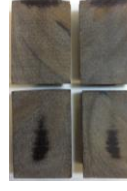
Figure 2-19 DSC for crude oil sample before experiment 2 (air @ 150°C).

Appendix B. Photos from cores after experimentation

Figure 2-20 Cores after experimentation.

Experiment	Photo	Experiment	Photo
1		6	
2		7	
3		8	
4		9	
5		10	

Chapter 3 : Low Temperature Air Injection with Solvents in Heavy-Oil Containing Naturally Fractured Reservoirs: Effects of Matrix/Fracture Properties and Temperature on Recovery

This version was submitted to a journal for review.

3.1 Summary

Implementation of in-situ combustion process in fractured reservoirs might be risky due to quick breakthrough of unconsumed oxygen to the producers. Recently, we proposed low temperature air-solvent injection (LTASI) as an alternative process to overcome this problem (SPE 149896 and 174542). This process involved oxygen addition reactions (low temperature oxidation) rather than bond scission reactions (in-situ combustion). Because increase in matrix oil viscosity is the drawback associated with oxygen addition reactions, reduction of it by adding hydrocarbon solvent into the air injected can be a solution. Determination of optimal application conditions of this kind of expensive and risky process is critically important.

Based on promising results, we conducted new static experiments of air and hydrocarbon solvent injection at low temperature oxidation conditions. Vertically situated sandstone and limestone samples were exposed to air+propane (or butane) mixture under static conditions mimicking huff-and-puff (cyclic injection) type injection. The main purpose was to determine the effect of change in matrix size as well as different matrix/fracture volume ratios on matrix oil recovery. This is important because this method is proposed as a cyclic injection application and the cyclic times are determined by the volume of the fractures, which are to be filled with injected air/propane and the diffusion rate of these gases into matrix.

During the experiments, the gas was injected in the annular space representing a fracture surrounding a heavy oil saturated core at certain pressure and temperature for a certain (soaking) time period. The produced gas and liquid oil were tested in different cycles using a gas chromatograph. The effect of fracture volume, matrix size, and application temperature on the produced fluid composition was clarified.

An extensive experimental schedule for static diffusion experiments was accomplished in which the effect of some variables in the oil recovery and oxygen consumption was analyzed. The variables evaluated include rock type (sandstone, limestone), temperature (75, 150, 200°C), fracture volume, solvent type (C_3, C_4), matrix size (2-in diameter, 6-in length; 3.2-in diameter, 9-in length), and injection sequences (Air/C_3/Air, C_3/Air/C_3, etc.). A total of 21 experiments were carried out for a comparative analysis and optimal application conditions yielding maximized oil recovery and maximized oxygen consumption through oxidation reactions in the matrix were

determined. These optimal conditions will provide minimized risk due to early breakthrough of unconsumed oxygen and maximized profit, which is needed due to the high cost of propane.

3.2 Introduction

Although it is not a wide-spread application, field implementation of air injection at high temperature oxidation conditions, namely in-situ combustion (ISC), has been successful in heavy oil recovery from non-fractured reservoirs. As one of the longest running cases, the Suplacu de Barcau field (a heavy oil reservoir of unconsolidated sands) is an example of air injection history over 50 years (Ruiz 2013). Field implementation of this kind of enhanced oil recovery (EOR) process in naturally fractured reservoirs is problematic due to its heterogeneous nature. Poor areal distribution of injected fluid and poor combustion efficiency due to fractures are common problems as reported by Craig and Parrish (1974) based on the evaluation of pilot tests. Difficulty controlling the combustion front is another challenge. Alvarez et al. (2008) reported this type of problem through a review of air injection pilot tests conducted in a heavy vuggy porosity and heavily karsted formation.

A limited number of laboratory studies on ISC process in heavy oil fractured medium (matrix+fractures) have been published. Schulte and de Vries (1985) reported that oxygen diffusion into matrix governed the burning process. Stokka et al. (2005) reported lab results in cores saturated with light oil and observed that air diffusion has a significant impact on recovery. Numerical simulation studies addressing air injection at high temperature oxidation conditions are also available in the literature. Lacroix et al. (2004) demonstrated that gas diffusion into matrix and thermodynamic processes mainly control the global kinetics and the oil oxidation. Stokka et al. (2005) numerically showed the importance of diffusion and gravity segregation for the oil production rate.

Air injection at low temperature oxidation (LTO) conditions has also been addressed. Greaves et al. (2000) investigated the air injection LTO process experimentally using crushed reservoir cores and sandpacks saturated with light oil and showed that significant oil recovery could be obtained under the low rate LTO conditions. Lakatos et al. (1998) determined the consequences of the low temperature oxidation experimentally. They observed asphaltene formation in the crude at LTO conditions. Lee and Noureldin (1989) reported that the presence of water modified

the destructive effect of LTO and both acidity and viscosity of the LTO product decreases when water is present.

Recently, Mayorquin and Babadagli (2015) reported on laboratory tests where a heavy-oil saturated core was soaked into air/propane gas mixture yields a better recovery than using only air. More promising results were also observed at high temperatures (150 and 200°C) than at low temperature (75°C), especially from an oxygen consumption point of view. Mayorquin and Babadagli (2012) created a numerical simulation model of air diffusion into a single matrix and obtained diffusion coefficients through matching lab results. They also performed a sensitivity study for different matrix properties and composition of injected gas. Mayorquin et al. (2015) modeled the injection of air at LTO conditions in a hypothetical fractured heavy oil reservoir and showed the benefits of solvent when injected alternate to air. They concluded that an optimum production time/soaking time ratio exists for different gas sequences, temperatures, and block sizes. All these efforts indicate that air diffusion into matrix is critically important in the oil recovery and oxygen consumption. This is controlled by matrix properties (lithology, size, and permeability), fracture volume filled with injected gas, cycle (soaking) periods, and temperature. Hence, additional experimental studies are needed for better comprehension of the injection of solvent and air at low temperature oxidation conditions.

3.3 Statement of the problem

EOR alternatives for commercial exploitation of heavy oil containing fractured reservoirs are limited (especially beyond certain depth). Air injection is an economical option for such reservoirs but it only serves as a cheap pressurizing agent, which may generate a pressure difference between fracture and matrix to drain matrix oil. While this slow process occurs, air is transferred into matrix and oxygenated compounds are generated. Transfer of air into matrix is desired to drain matrix oil and consume the oxygen for safety reasons. However, once oxygen is in contact with oil in the matrix the viscosity of oil increases at low temperatures due to polymerization effect. In order to minimize this negative effect, solvents can be co-injected with air. The solvent reduces not only the viscosity of matrix oil but also the viscosity of the oxygenated compounds. Minimization of solvent requirement for this process is essential due to its high cost.

On the other hand, air injection at high temperature oxidation conditions could be problematic not because of the thermal process itself but because of reservoir heterogeneities (low and high permeability channels), which are characteristics of naturally fractured reservoirs. To overcome these technical difficulties (uncontrollable heat front), low temperature oxidation (LTO) conditions are desired and the process can be applied in the form of cyclic (huff-and-puff) injection. Critical issues emerge for this alternative solution as listed below:

- What is the reservoir temperature at which the injected O_2 could be consumed to the safe levels without creating a large extent of polymerization for particular heavy oil characteristics?

- Could solvent injection be helpful for obtaining additional oil from the matrix and for minimizing the oil viscosity increase related to the generation of oxygenated compounds?

- What are the proper application conditions (amount of injected solvent, soaking time duration, co-injection of air/solvent, alternate air/solvent injection, etc.) at given reservoir conditions for safe limits of oxygen consumption in the matrix?

To answer these questions, a set of experiments were programmed and the results are presented in this research. The main focus is to generate a "single matrix-single fracture" condition with variable characteristics of these two media. In a sense, this study complements the previous attempt presented by Mayorquin and Babadagli (2015), which was limited to fixed matrix and fracture size (volume).

3.4 Experimental procedure

A core saturated with heavy-oil sample was placed into a reactor and the space between the core (matrix) and the reactor wall represented an annular fracture (a simple form of dual porosity media). After introducing a given amount of gas (air, propane or both) into the model, the reactor was left for a soaking period at a certain pressure-temperature. As no fluid was injected (or produced) continuously, the experiments can be categorized as "static". Once the designed soaking time is reached, the gas was collected first for gas chromatography analysis. Then, the oil accumulated at the reactor bottom was removed and analyzed (density, viscosity, refractive

index and asphaltene measurements). This process was repeated several times depending on the nature of the experiments and each of these "cycles" represents the cycles in a huff-and-puff process.

The oil recovery was measured by weighting the core before and after the cycles. Initial oil density was considered in corresponding calculations for volume conversion. Operational parameters (gas pressure and oven temperature) were recorded continuously throughout the experiment using pressure transducer and thermocouples.

A comprehensive experimental schedule was designed to analyze the effect of multi-variables on oil recovery and oxygen consumption. These variable parameters include rock type (sandstone, limestone), temperature (75, 150, 200°C), fracture volume, solvent type (C_3, C_4), cylindrical core size (2-in diameter, 6-in length; 3.2-in diameter, 9-in length), and gas sequences (Air/C_3/Air, C_3/Air/C_3, etc.). A total of 21 experiments were conducted. As experiments in this work complement those reported by Mayorquin and Babadagli (2015), the numeration of our experiments is an extension of their numeration experiments (our experiments newly presented in this paper begin with 11). Oil and core properties and experimental operational conditions are given in **Table 3-1 and Table 3-2**, respectively. Rock types used in laboratory studies were sandstone (experiments 11-22, 25-27, 30, 31) and limestone (experiments 23, 24, 28, 29).

Table 3-1 Experimental fluid and core properties.

| Experiment | Core | | | | Crude-Oil Properties at Atmospheric Pressure | | | | | |
	Porosity (%)	Length (in.)	Diameter (in.)	Pore volume (cm³)	Density (°API)	Asphaltene Content (wt%)	Temperature (°C)	Density at Temperature (g/cm³)	Viscosity at Temperature (cp)	Refractive Index at Temperature
11	17.2	6.020	1.984	52.3	10.5	39.6	75	0.9594	820.1	1.55385
12	17.2	6.020	1.984	52.3	10.5	39.6	75	0.9594	820.1	1.55385
13	16.1	6.022	1.984	49.0	10.5	39.6	75	0.9594	820.1	1.55385
14	16.5	6.023	1.984	50.2	10.5	39.6	75	0.9594	820.1	1.55385
17	18.2	6.021	1.984	55.4	9.5		75	0.9674	1422.0	1.55832
18	18.2	6.015	1.983	55.5	9.5		200	0.8849	10.4	1.50957
19	18.2	6.019	1.985	55.7	9.5		200	0.8849	10.4	1.50957
20	17.3	6.016	1.982	52.2	8.5		150	0.9238	41.5	1.53504
21	17.2	6.086	1.985	52.7	8.5		150	0.9238	41.5	1.53504
22	18.2	5.891	1.983	54.3	8.5		150	0.9238	41.5	1.53504
23	18.9	5.906	1.982	56.3	8.0		150	0.9291	48.8	1.53695
24	18.6	5.920	1.982	55.6	8.0		75	0.9786	1579.3	1.56545
25	20.4	5.920	1.989	61.4	8.0		150	0.9291	48.8	1.53695
26	18.8	5.723	1.988	54.9	8.0		150	0.9291	48.8	1.53695
27	16.4	8.825	3.257	197.7	6.8	27.7	150	0.9452	77.2	1.54403
28	16.2	6.038	1.986	49.6	8.9		150	0.9305	42.3	1.53680
29	17.1	5.963	1.988	51.8	8.9		75	0.9785	3484.3	1.56530
30	16.4	8.938	3.260	212.1	8.1	27.2	150	0.9388	77.0	1.54218
31	19.0	9.000	3.253	233.4	11.2		150	0.9182	83.3	1.54259
32	15.3	5.898	1.997	46.4	8.4	27.2	150	0.9319	64.6	1.54319
33	15.4	5.643	1.994	44.3	8.4	27.2	150	0.9319	64.6	1.54319

Table 3-2 Experimental operational conditions.

Experiment	Cycle	Gas	Temperature (°C)	Maximum Pressure (psia)	Soaking Time (days)
11	1	Air	75	232.8	4.2
11	2	Air	75	229.8	4.0
11	3	Air	75	230.2	3.9
12	1	Air	75	221.0	1.5
12	2	Air	75	212.4	3.1
12	3	C_3	75	194.0	5.2
13	1	Air	75	202.1	4.5
13	2	C_3	75	179.1	4.2
13	3	Air	75	200.7	4.8
14	1	C_3	75	218.9	4.2
14	2	Air	75	203.1	4.7
14	3	C_3	75	189.7	4.4
17	1	C_3	75	408.5	4.0

17	2	Air	75	286.6	3.8
17	3	C_3	75	415.6	4.2
18	1	C_3	200	279.9	4.6
18	2	Air	200	251.6	3.6
18	3	C_3	200	269.9	4.1
19	1	Air	200	262.2	3.5
19	2	C_3	200	255.1	3.7
19	3	Air	200	251.2	10.8
20	1	Air	150	188.0	3.5
21	1	Air	150	198.5	4.0
21	2	C_3	150	189.0	2.9
21	3	Air	150	168.3	4.2
22	1	C_3	150	201.9	3.6
22	2	Air	150	164.2	4.1
22	3	C_3	150	191.4	4.0
23	1	C_3	150	187.2	4.6
23	2	Air	150	160.2	4.0
23	3	C_3	150	160.1	4.2
24	1	C_3	75	196.8	4.1
24	2	Air	75	194.7	4.0
24	3	C_3	75	176.4	4.7
25	1	Air	150	215.4	4.4
25	2	C_4	150	190.6	4.1
25	3	Air	150	166.2	4.4
26	1	C_4	150	163.5	4.4
26	2	Air	150	167.1	4.2
26	3	C_4	150	168.4	4.2
27	1	Air	150	185.9	6.5
27	2	C_3	150	192.6	4.4
27	3	Air	150	201.0	4.3
27	4	C_3	150	197.9	4.3
27	5	Air	150	192.3	4.2
27	6	C_3	150	189.9	5.2
28	1	Air	150	200.7	4.4
28	2	C_3	150	187.5	4.5
28	3	Air	150	182.1	5.2
29	1	Air	75	213.2	4.1
29	2	C_3	75	179.6	4.2
29	3	Air	75	192.8	4.2
30	1	C_3	150	179.1	4.2
30	2	Air	150	208.5	4.0
30	3	C_3	150	191.1	4.1
30	4	Air	150	196.3	4.5
30	5	C_3	150	194.8	12.0
31	1	C_3 (18.0 mol%)/Air (82.0 mol%)	150	210.8	4.0
31	2	C_3 (6.5 mol%)/Air (93.5 mol%)	150	204.3	4.2
31	3	C_3 (10.1 mol%)/Air (89.9 mol%)	150	205.3	4.1
32	1	C_3 (29.2 mol%)/Air (70.8 mol%)	150	163.4	4.0
32	2	C_3 (21.4 mol%)/Air (78.6 mol%)	150	192.2	4.5
32	3	C_3 (20.0 mol%)/Air (80.0 mol%)	150	195.4	4.4
33	1	C_3 (22.9 mol%)/Air (77.1 mol%)	150	201.1	4.0
33	2	C_3 (13.1 mol%)/Air (86.9 mol%)	150	183.5	4.5
33	3	C_3 (11.1 mol%)/Air (88.9 mol%)	150	182.5	3.8

3.4.1 Setup and equipment

Setup (**Figure 3-1**) as well as lab procedures and instruments used for conducting experimental studies and fluid properties measurements are shown in Mayorquin and Babadagli (2015). The main difference with this earlier work is that they conducted experiments using a fixed core size-fracture volume/total volume (V_f/V_T) ratio. In this work, experiments were conducted using the same setup as well as another one designed for variable matrix and fracture sizes/volumes (**Figure 3-2**). A solid stainless steel block within the reactor was used to reduce the fracture volume to obtain a small V_f/V_T ratio. The volumes for different V_f/V_T ratios are shown in **Table 3-3**. Small core size dimensions were 2-in-diameter and 6-in-length, while the large core size dimensions were 3.25-in diameter and 9-in-length. The dimensions of the reactor were 6.23-in-diameter and 10-in-length.
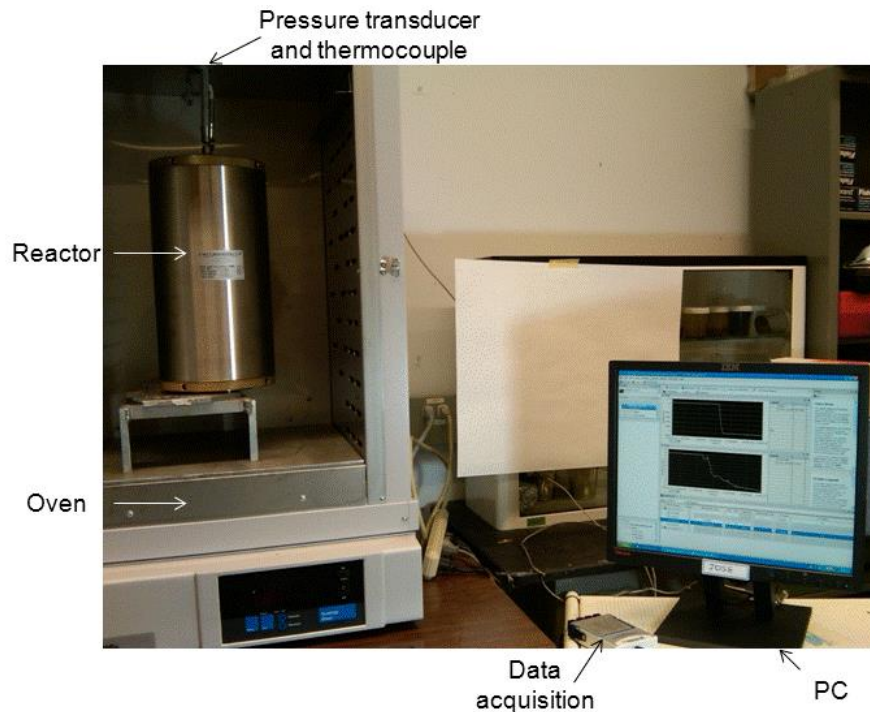
Figure 3-1 Experimental setup (from Mayorquin-Ruiz and Babadagli 2015).
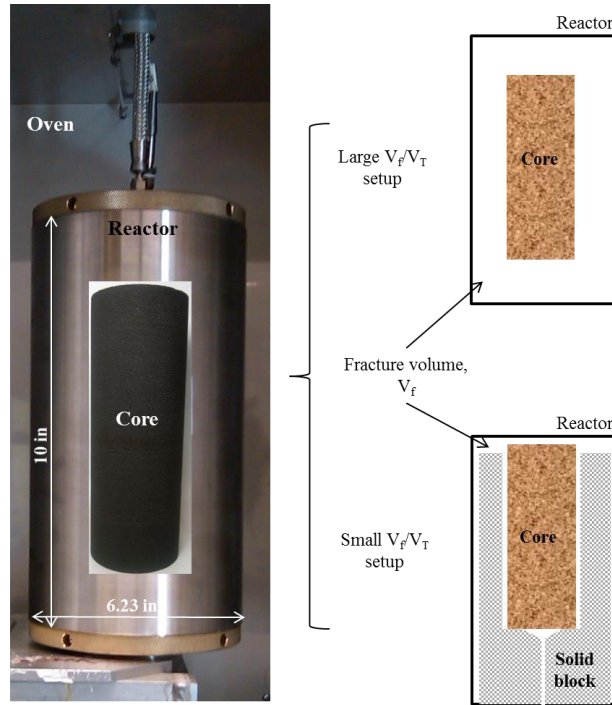
Figure 3-2 Reactor configurations for two different V_f/V_T ratios.

Table 3-3 Core and reactor volumes for different setups.

Setup	Experiments	Reactor void volume, V_T (cm^3)	Core (matrix) bulk volume, V_m (cm^3)	Fracture volume, V_f (cm^3)	V_f/V_T ratio
Small core size, small V_f/V_T ratio	11,12,13,14,20,21,22,23, 24,25,26,28,29, 32, 33	1288	308.7	979.3	0.76
Small core size, large V_f/V_T ratio	17,18,19	5000	308.7	4691.3	0.94
Large core size, small V_f/V_T ratio	27,30,31	5000	1223.49	3776.51	0.76

3.4.2 Experimental results

Experimental results (recovery factors) obtained for all experiments are shown in **Table 3-4**, oil properties and gas chromatography of produced fluids are shown in Appendix A. Oil recovery factors (RF) are provided for each cycle and the total cumulative RF is shown in the "Total"

column. The graphical presentations of the results are provided as the plots of RF and -generated- gas composition (**Figure 3-3** to **Figure 3-11**). In these plots, gas sequences are labeled as Gas 1/Gas 2/Gas 3, etc., in which Gas 1 is the gas type (Air, C_3, C_4, or Air+C_3 mixture) used in Cycle 1, Gas 2 is the gas type used in Cycle 2, and so on. For instance, Air/C_3/Air means that air was used in Cycle 1, C_3 (propane) was used in Cycle 2, and air was used in Cycle 3.

Table 3-4 Experimental results.

Experiment	Cycle	Gas	Temperature (°C)	R. F. per cycle	Total R. F.
11	1	Air	75	7.5	11.7
	2	Air	75	3.3	
	3	Air	75	1.0	
12	1	Air	75	6.2	22.9
	2	Air	75	6.9	
	3	C_3	75	9.9	
13	1	Air	75	1.6	10.5
	2	C_3	75	8.8	
	3	Air	75	0.0	
14	1	C_3	75	16.0	21.8
	2	Air	75	0.2	
	3	C_3	75	5.6	
17	1	C_3	75	57.6	66.4
	2	Air	75	0.0	
	3	C_3	75	8.8	
18	1	C_3	200	26.9	29.4
	2	Air	200	1.3	
	3	C_3	200	1.3	
19	1	Air	200	26.0	37.5
	2	C_3	200	7.0	
	3	Air	200	4.5	
20	1	Air	150	12.4	12.4
21	1	Air	150	8.5	14.1
	2	C_3	150	2.1	
	3	Air	150	3.6	
22	1	C_3	150	26.3	26.3
	2	Air	150	0.0	
	3	C_3	150	0.0	
23	1	C_3	150	24.7	24.7
	2	Air	150	0.0	
	3	C_3	150	0.0	
24	1	C_3	75	13.0	15.8
	2	Air	75	0.0	
	3	C_3	75	2.8	
25	1	Air	150	33.0	36.4
	2	C_4	150	2.9	
	3	Air	150	0.5	
26	1	C_4	150	29.5	29.5
	2	Air	150	0.0	
	3	C_4	150	0.0	
27	1	Air	150	2.3	19.6
	2	C_3	150	11.8	
	3	Air	150	3.2	

	4	C_3	150	2.3	
	5	Air	150	0.0	
	6	C_3	150	0.0	
28	1	Air	150	6.2	8.0
	2	C_3	150	1.8	
	3	Air	150	0.0	
29	1	Air	75	0.0	9.2
	2	C_3	75	8.2	
	3	Air	75	1.0	
30	1	C_3	150	16.4	18.7
	2	Air	150	2.4	
	3	C_3	150	0.0	
	4	Air	150	0.0	
	5	C_3	150	0.0	
31	1	C_3 (18.0 mol%)/Air (82.0 mol%)	150	13.0	23.4
	2	C_3 (6.5 mol%)/Air (93.5 mol%)	150	6.3	
	3	C_3 (10.1 mol%)/Air (89.9 mol%)	150	4.0	
32	1	C_3 (29.2 mol%)/Air (70.8 mol%)	150	19.2	34.4
	2	C_3 (21.4 mol%)/Air (78.6 mol%)	150	10.7	
	3	C_3 (20.0 mol%)/Air (80.0 mol%)	150	4.5	
33	1	C_3 (22.9 mol%)/Air (77.1 mol%)	150	15.0	26.6
	2	C_3 (13.1 mol%)/Air (86.9 mol%)	150	7.8	
	3	C_3 (11.1 mol%)/Air (88.9 mol%)	150	3.8	

Oil recovery results are shown in stacked column plots in which each individual column represents the oil recovery for a particular cycle. The column color represents the type of gas used in that particular cycle: blue (air), green (C_3, propane), orange (C_4, butane), blue and green color gradient (Air+C_3 mixture). In the same stacked column plots, the initial oil viscosity is plotted in the secondary logarithmic y-axis as dots.

To present the composition of the generated gas (mainly to indicate oxygen consumption), another plot type was used. This is a N_2/O_2 ratio vs. CO_2 concentration line plot based on the composition of gas mixture remaining in the reactor (annular fracture) at the end of cycles. As a reference, the N_2/O_2 ratio and CO_2 concentration in the air at the original (atmospheric) conditions is around 3.7 and 0.04%, respectively. An increase in these values means that O_2 was diffused into matrix and chemically reacted (consumed) with oil. Oil distribution in cores is shown in Appendix A.

The rest of the section contains presentation and analysis of the results for each critical parameter; i.e., matrix and fracture properties, solvent type, and application conditions.

Fracture Volume Effect

Naturally fractured reservoirs generally have a large variability in matrix block size or fracture spacing and hence fracture volume (or fracture porosity). This is a critical issue in the application of the proposed method as in each cycle, one has to fill the fracture volume with the gas and consume it through matrix diffusion during the soaking period. Therefore, the amount of the gas injected and cycle time are critically controlled by the fracture volume. In order to assess the effect of fracture porosity (or V_f/V_T ratio in Table 3-3) on RF and O_2 consumption, different injection sequences were conducted on small V_f/V_T and large V_f/V_T ratios (where V_f is the fracture volume and V_T the reactor void volume). Note that these ratios were determined for sake of representing a wide range of matrix and fracture volume for a lab scale experimental analysis.

The following five gas injection sequences were compared (four of which were conducted at 75 °C and one at 150°C) keeping the other conditions the same in all cases (rock type [sandstone], core size [6-in-length, 2-in-diameter], and solvent type -C_3):

Air/Air/C_3 at 75 °C: Experiment 12 (Small V_f/V_T ratio)

Air/C_3/Air at 75 °C: Experiment 10 (Large V_f/V_T ratio) vs. Experiment 13 (Small V_f/V_T ratio)

C_3/Air/C_3 at 75 °C: Experiment 17 (Large V_f/V_T ratio) vs. Experiment 14 (Small V_f/V_T ratio)

Air/Air at 150 °C: Experiment 2 (Large V_f/V_T ratio) vs. Experiment 20 (Small V_f/V_T ratio)

C_3/C_3/C_3 at 75 °C: Experiment 3 (Large V_f/V_T ratio)

C_3/Air/C_3 at 200 °C: Experiment 18 (Large V_f/V_T ratio)

The following observations can be made from the experimental results (**Figure 3-3**). Note that oil recovery and gas chromatography results of Exp. 2, 3, and 10 were taken from Mayorquin and Babadagli (2015) for comparison purposes.
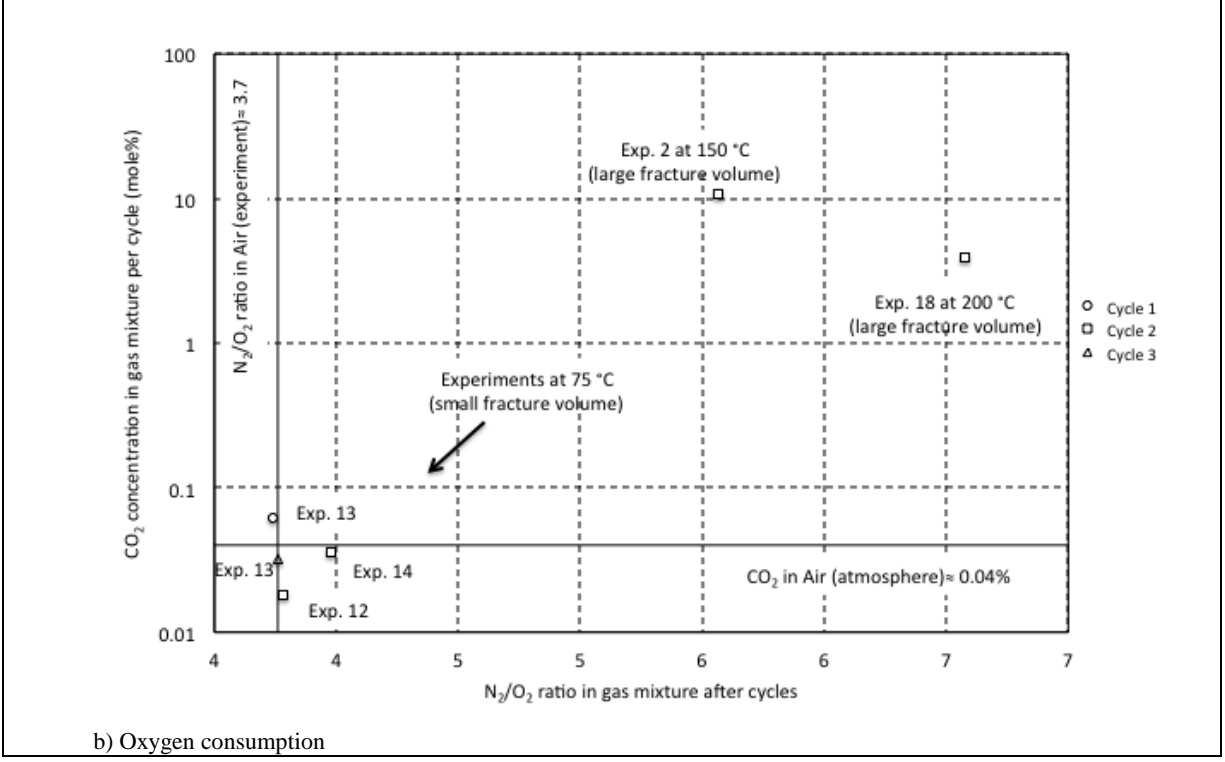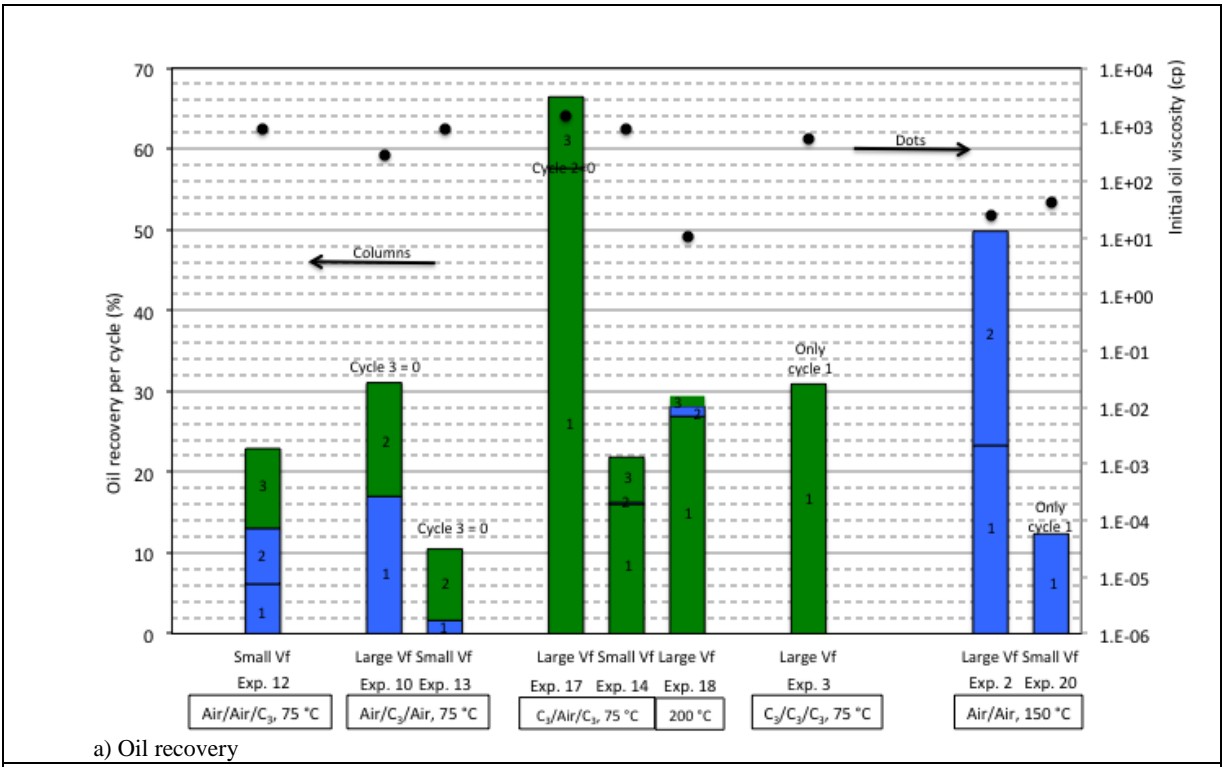
a) Oil recovery

b) Oxygen consumption

Figure 3-3 Experimental results. Effect of large and small V_f/V_T ratios.

1. Experiments 3 and 12 were not compared with a different V_f/V_T ratio cases because of experimental failures but their oil recoveries are included in Figure 3-3 for comparative purposes.

2. In general, higher oil recovery (Figure 3-3a) was obtained in Large V_f/V_T ratio experiments compared to Small V_f/V_T ratio experiments, except for the Air/Air/C_3 sequence. In the case (Air/Air/C_3) with Large V_f/V_T ratio, high amount of air polymerized the oil after diffusing into the matrix and resulted in no recovery even after two cycles. The succeeding C_3 injection yielded lower recovery compared to the case of Small V_f/V_T ratio.

3. Initial oil viscosity (before experimentation at corresponding experiment temperature) was slightly different for the same gas sequence experiments (due to saturation process under vacuum). In this regard, it is interesting to compare results of gas sequences C_3/Air/C_3 at 75ºC and Air/Air at 150ºC.

    In the first gas sequence (C_3/Air/C_3), the oil viscosity was higher in Exp. 17 (1422 cp) than Exp. 14 (820.1 cp) but both experiments had similar duration. Then, lower oil recovery would be expected in Exp. 17. An opposite behavior can be explained by the -larger- amount of C_3 available to diffuse into matrix oil being higher in the Large V_f/V_T ratio than in the Small V_f/V_T ratio. Another interesting fact is that no oil recovery existed in Cycle 2 of Exp. 17 when air was used due to an increased fluid viscosity related to oxygenated compounds formation. In Cycle 3, an increase in oil recovery was observed due to the fact that C_3 diffused into matrix oil+oxygenated compounds mixture reducing its viscosity enhancing gravity drainage.

    In the second gas sequence at a higher temperature (Air/Air at 150ºC), Exp. 2 and 20 had similar initial oil viscosities, 24.4 and 41.5 cp, respectively. In Exp. 2, a higher volume of oxygen was available to diffuse/oxidize matrix oil than in Exp. 20, which means that oxygenated compounds would have had a higher detrimental effect in oil viscosity and hence in oil recovery. However, this situation does not occur because by the high temperature at which those two experiments were conducted (150 ºC). Hence, the effect of oxygenated compounds in oil viscosity at high temperature was not as critical as in the case of 75ºC cases. Based on the thermal analysis, high temperature oxidation (HTO) reactions

are not present at 150ºC (Mayorquin and Babadagli 2015). O_2 consumption occurred in Exp. 2 as noticed by the O_2 concentration in Cycle 2 of 13.1 mol % and CO_2 concentration of 10.7 mol % (Table 3 in Mayorquin and Babadagli 2015). No gas chromatography was available for Exp. 20 because of gas leaking.

4.   For Small V_f/V_T ratio experiments conducted at 75ºC, the gas injection sequence starting with C_3 gave a higher oil recovery than experiments starting with air. For example, comparing Exp. 12, 13, and 14, having the same initial oil viscosity (820.1 cp), it was observed that oil recovery in Cycle 1 (C_3) of Exp. 14 was 16%, while the oil recovery in Cycle 1 (air) of Exps. 12 and 13 was 6.2 and 1.6%, respectively. Differences can be explained by two reasons: (1) In a relatively high oil viscosity and relatively low temperature, propane diffuses into matrix oil reducing its viscosity enhancing gravity drainage, and (2) air is consumed in the matrix oil generating oxygenated compounds creating the opposite effect (oil viscosity increase).

5.   There was only one experiment conducted at 200ºC (Exp. 18) with a Large V_f/V_T ratio. It can be observed that a high oil recovery was obtained in Cycle 1 being the highest value compared to the Cycle 1 cases with C_3 of other experiments (except for Exp. 3, which lasted almost twice the time due to low oil viscosity-enhanced gravity drainage). Also, the highest O_2 consumption was obtained for Exp. 18 due to a high temperature (Figure 3-3b). Unlike Exp. 17 at 75ºC, in Exp. 18 at 200ºC, certain amount of oil recovery was observed in Cycle 2 (air) implying that that increased fluid viscosity related to oxygenated compounds is less critical at high temperature (200ºC).

6.   Mayorquin and Babadagli (2015) reported results of an experiment conducted in sandstone rock at 200ºC using Air+C_3 gas mixture at Large V_f/V_T ratio (Exp. 5 in their work; total oil recovery is 40.6%). In this work, two experiments on the same rock type and temperature are reported with different gas sequences: C_3/Air/C_3 (Exp. 18) and Air/C_3/Air (Exp. 19) with the same initial oil viscosity (Table 3-1). It was observed that total oil recovery in Air/C_3/Air (37.5%) sequence is higher than C_3/Air/C_3 (29.4%). It is interesting to observe that Cycle 1 oil recovery is practically the same (26.9% in Exp. 18; 26.0% in Exp. 19), which means that solvent effect in oil viscosity reduction does not play an important role in

oil production mechanism at those temperature conditions (200ºC), at least at early times and temperature-related low-oil viscosity gravity drainage seems to be the main factor in Cycle 1.

In Cycle 2, a noticeable difference in oil recovery occurred depending on the type of gas used in Cycle 1. When air was used after C_3 (Exp. 18), a lower oil recovery was obtained than when using C_3 after air (Exp. 19). The low oil recovery in Cycle 2 of Exp. 18 could be explained by the oxidation of a less heavy liquid (aided by C_3 diffusion in heavy oil), developing a more viscous fluid in the matrix oil delaying the oil recovery. Also, air was in contact with more residual matrix oil due to replacement mechanism of oil by gas in the core. On the other hand, in Cycle 2 of Exp. 19 propane diffused into the existing oxygenated oil lowering its viscosity and improving oil recovery (compared to that of Cycle 2 of Exp. 18). Also note that, inside the matrix, C_3 contacts more oil+oxygenated compounds mixture because it replaces the produced oil.

In Cycle 3, Exp. 19 showed a relatively high oil recovery, which can be explained by its longer duration (10.8 days) compared to duration of Cycle 3 in Exp. 18 (4.1 days).

In general, after Cycle 1 (Cycle 2 and later), higher oil recovery was obtained when C_3 was used after air (i.e., Air/C_3) than when air was used after C_3 (i.e., C_3/Air). Based on experimental results at 75 and 150ºC, one may conclude that gas sequence design as well as cycle duration play a role in the total oil recovery. On the other hand, it was also observed that the higher the V_f/V_T ratio, the higher the oil recovery.

Temperature Effect

Two extreme temperature cases (75 and 150°C) are compared in **Figure 3-4**, which typically correspond to temperatures of reservoirs located at depth range of 1500-5000 m. Other conditions remain unchanged, such as type of rock (sandstone), core size (6-in.-length, 2-in.-diameter), solvent (C_3), and fracture volume (Low V_f/V_T ratio). Experiments that are compared are as follows:

Air/C$_3$/Air: Experiment 13 (75°C) vs.   Experiment 21 (150°C)

C$_3$/Air/C$_3$:   Experiment 14 (75°C) vs.   Experiment 22 (150°C)

Results of Exp. 20, which consisted of only one Cycle (Air at 150°C), are included to compare with Cycle 1 of Exp. 21.
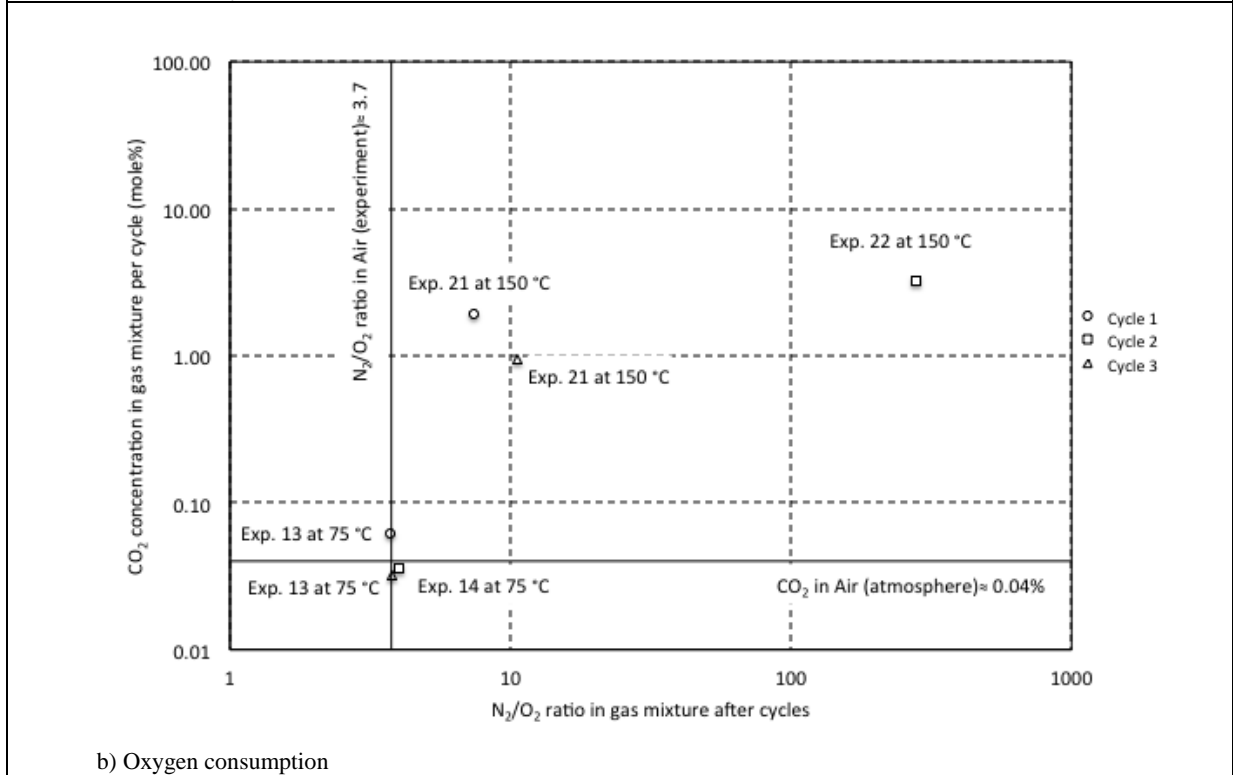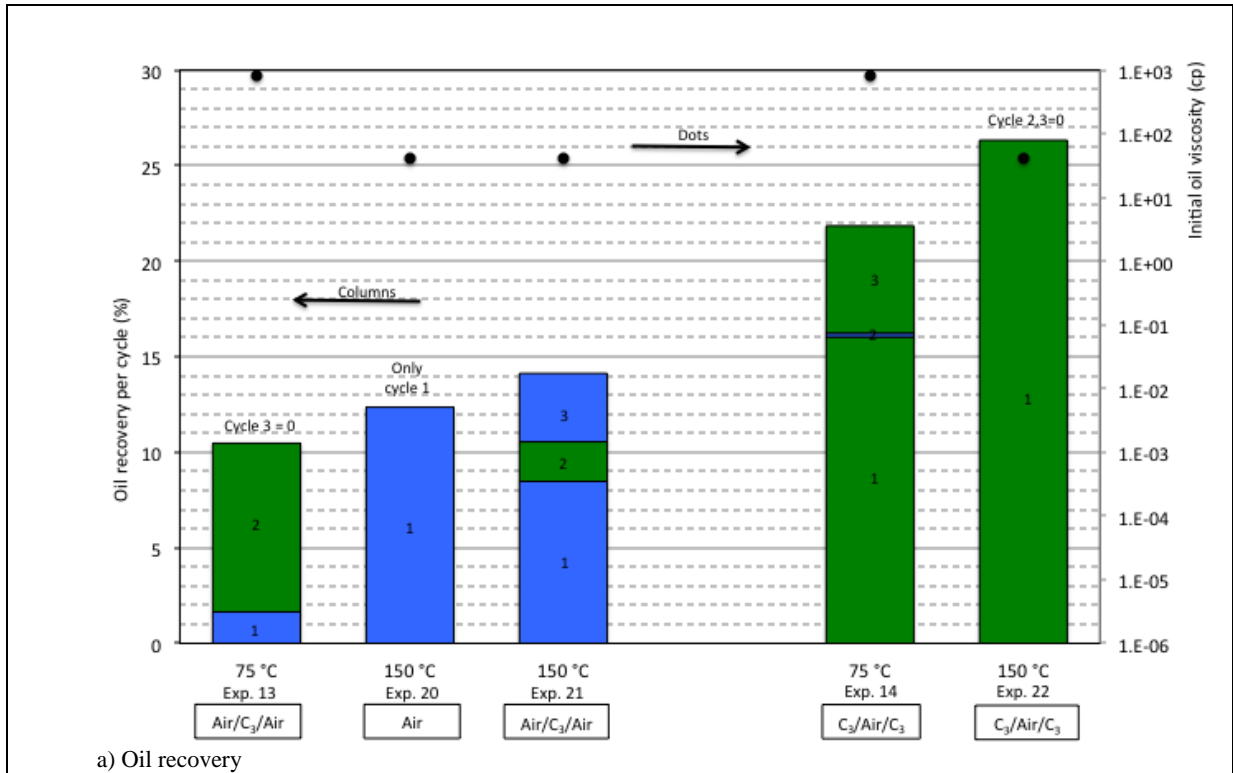
a) Oil recovery

b) Oxygen consumption

Figure 3-4 Experimental results. Effect of low and high temperatures.

Discussion on experimental results at 75°C (Exp. 13 and 14)

As shown in Figure 3-4a, solvent (C_3) is required in order for the matrix oil to drain out from the core, and is more effective when used in Cycle 1. When air is used, oxygen consumption (Figure 3-4b) occurs at very low levels; i.e., the N_2/O_2 ratio and CO_2 concentration are comparable to atmospheric air. It is evident that, in Cycle 3, C_3 diffuses into matrix fluids (mixture of oil and oxygenated compounds generated in Cycle 1) and reduces its viscosity allowing its expulsion from the core.

Combined with the previous observation, it can be concluded that C_3 is needed when temperature is 75°C (high oil viscosity) in order to reduce the matrix oil viscosity, which is more effective to use it in Cycle 1. Oxygen is practically unconsumed at 75°C regardless of the gas sequence, and thus air acts only as pressurizing agent at this temperature if injected after C_3.

Discussion on experimental results at 150°C (Exp. 21 and 22)

In general oil recovery (Figure 3-4a) is higher in experiments conducted at 150 °C than those at 75°C regardless of the gas sequence. The low initial oil viscosity at 150°C explains the main reason behind the higher oil recovery (there is a difference of almost one order of magnitude between initial oil viscosity in 150°C and 75°C experiments).

It is also evident that oxygen consumption is more important at 150°C, which is explained by a sharp increase of one or two orders of magnitude in both the N_2/O_2 ratio (O_2 concentration reduces) and the CO_2 concentration. CO was also observed (Appendix A) in the gas mixture in cycles where air was used.

Gas sequence also matters in oil recovery at 150°C. A higher oil recovery was obtained when using C_3 in Cycle 1 of Exp. 22, which is explained by a higher C_3 mass transfer from fracture gas into matrix oil reducing its viscosity and thus improving the gravity drainage mechanism. In the experiments at 150°C, it is more evident that O_2 consumption is higher (higher N_2/O_2 ratio) in air cycles preceded by C_3 cycles.

Note that only one cycle was conducted (only air) in Exp. 20. This cycle is comparable with Cycle 1 of Exp. 21 as the same conditions were prevailed. The differences were used as a measure of experimental error (or to test the repeatability) as shown in Appendix B.

Rock Type Effect

Experiments were conducted using two different types of cores having different lithology and permeability; sandstone and limestone. The cores were cut from the same outcrop rock blocks and used only once. The experiments were run under similar conditions: core size (6-in.-length, 2-in.-diameter), solvent (C_3), and fracture volume (Low V_f/V_T ratio). Two gas sequences were compared at two temperatures (75ºC and 150ºC):

Experiments at 75ºC:

Air/C_3/Air: Experiment 13 (Sandstone)   vs.   Experiment 29 (Limestone)

C_3/Air/C_3:   Experiment 14 (Sandstone)   vs.   Experiment 24 (Limestone)

Experiments at 150ºC:

Air/C_3/Air: Experiment 21 (Sandstone)   vs.   Experiment 28 (Limestone)

C_3/Air/C_3:   Experiment 22 (Sandstone)   vs.   Experiment 23 (Limestone)

Discussion on experimental results at 75 °C

Figure 3-5 shows the results of experiments conducted on sandstone and limestone cores at 75ºC. Oil recovery was lower in limestone cores than sandstone cores regardless the gas sequence, which can be explained by lower permeability of the limestone than sandstone. Initial oil viscosity in the limestone cores was slightly higher than in sandstone cores but this is not expected to be as critical as the permeability effect (this is confirmed below in comparison between experiments at 150°C).

80
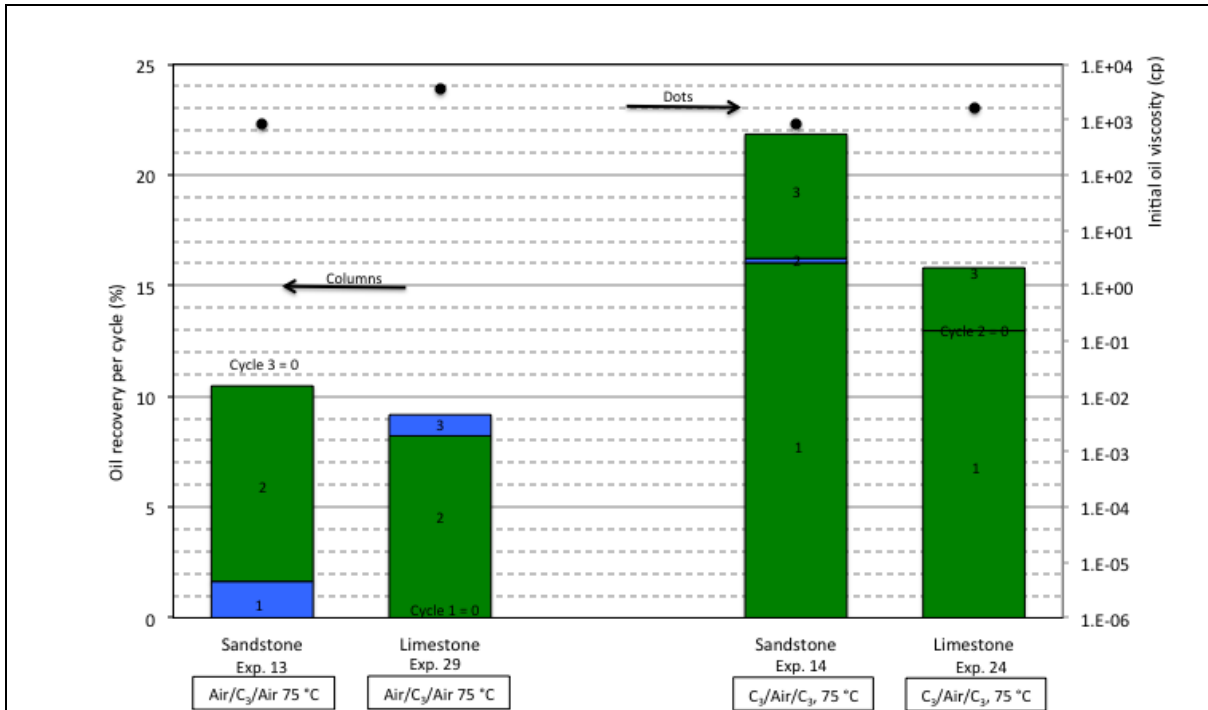
a) Oil recovery
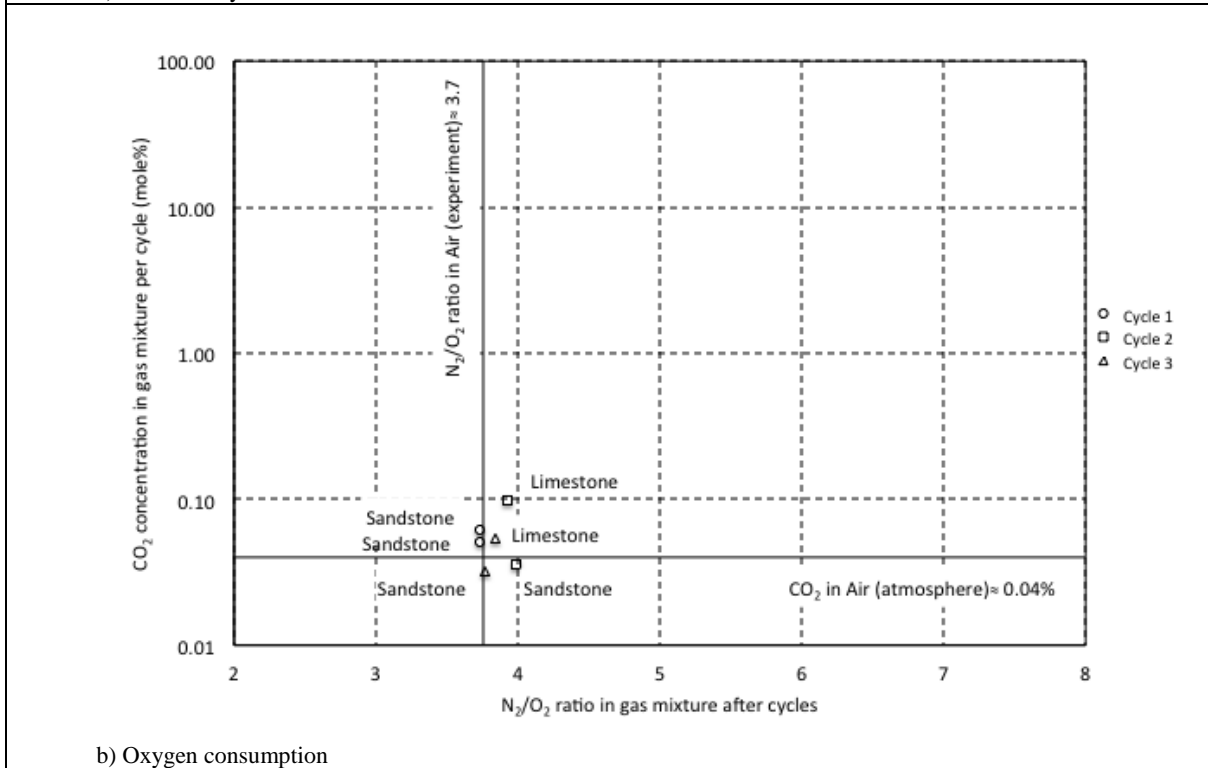
b) Oxygen consumption

Figure 3-5 Experimental results. Effect of rock type at 75ºC.

In regards to O_2 consumption (Figure 3-5b), it can be observed that N_2/O_2 ratio as well as CO_2 concentration were near the atmospheric air conditions, meaning that O_2 consumption was limited in both rock type experiments. However, it is clear that a certain level of liquid hydrocarbon oxidation existed based on two facts. Firstly, CO concentration in the gas mixture of Cycle 2 in Exp. 24 was 117 ppm (CO concentration in atmospheric air is around 0.1 ppm). Carbon oxides are expected to be final products of LTO reactions for light oils (Ren et al. 2002). Secondly, viscosity of oil recovered in Cycle 2 of Exp. 29 was 7123.6 cp, which was higher than initial oil viscosity (3484.3 cp).

Discussion on experimental results at 150°C

Figure 3-6 shows the results of experiments conducted on sandstone and limestone cores at 150ºC. Oil recovery in experiments at 150ºC was higher than those at 75ºC due to a lower oil viscosity, as expected. Also, oil recovery was lower in the limestone cores than sandstone cores regardless of the gas sequence in experiments at 150°C, which can be attributed to the lower permeability of limestone rock. Initial oil viscosity was practically the same in both cases.

a) Oil recovery

b) Oxygen consumption

Figure 3-6 Experimental results. Effect of rock type at 150ºC.
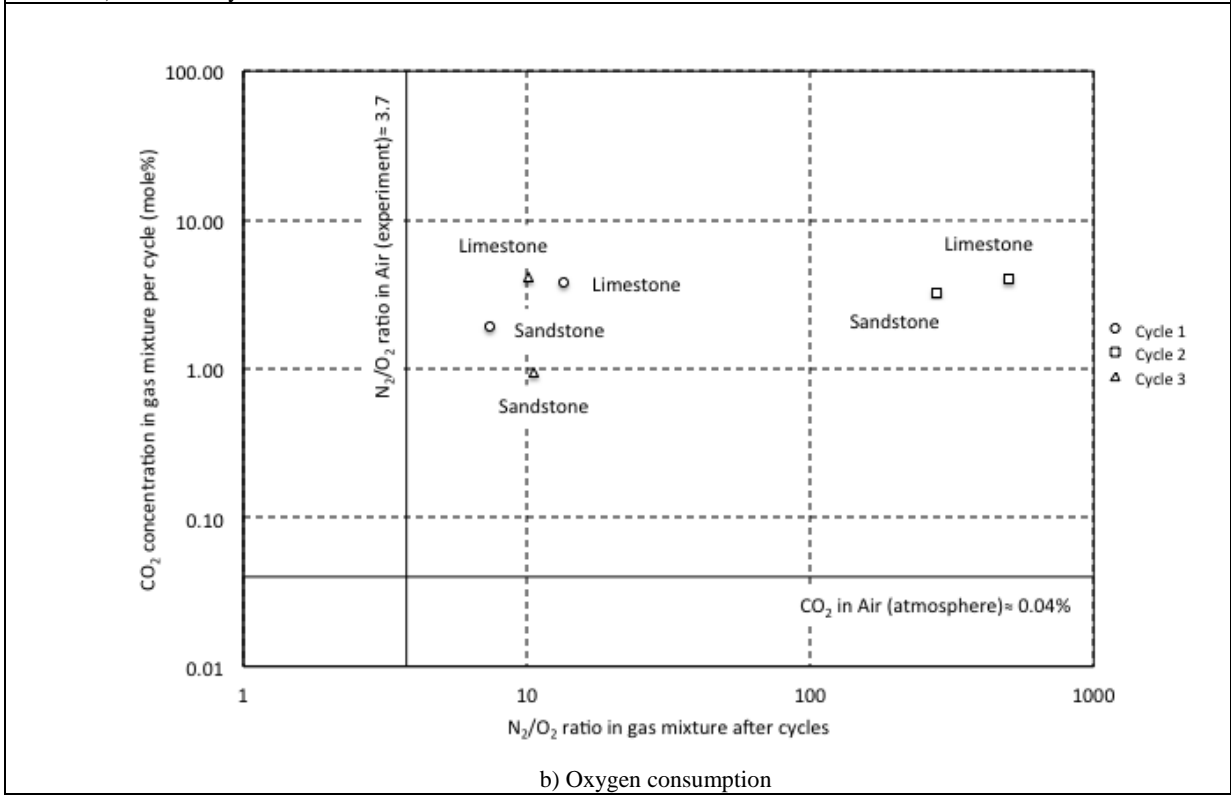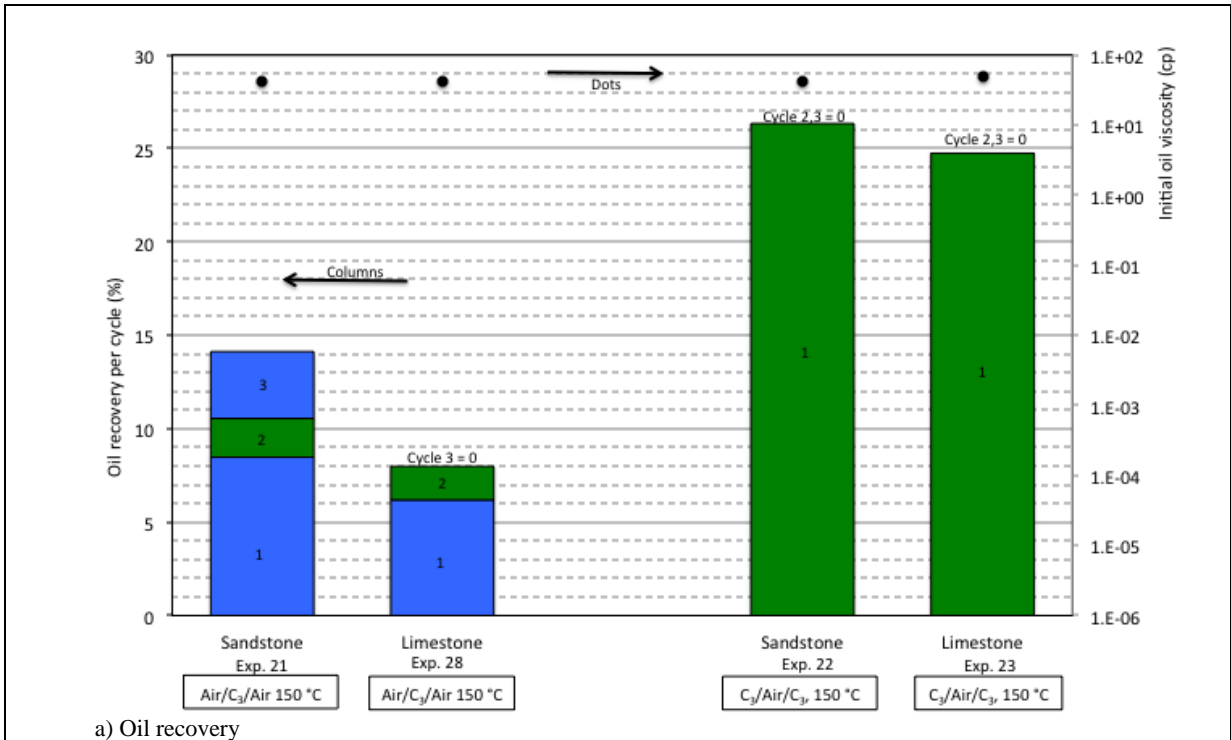
On the other hand, the high values of N_2/O_2 ratio and CO_2 concentration in produced gas suggest that a critical amount of O_2 was consumed. In the case of Air/C_3/Air sequence (Exp. 21 and 28) (Figure 3-6b), considerable reduction in O_2 concentration in Cycles 1 was observed (11.6 and 6.6 mol% for sandstone and limestone cores, respectively as shown in Appendix A). Also, high concentration of carbon oxides was present in Cycles 1 and 3. CO concentrations were not less than 1496 ppm, which was the instrument maximum detection value (MicroMax Gas Pro Gas Detector). An increase in oil viscosity was observed in produced oil of Cycle 1 of Exp. 28 (Air/C_3/Air) from 42.3 cp (initial oil viscosity) to 246.1 cp, which confirms the generation of oxygenated compounds.

In the case of C_3/Air/C_3 sequence (Exp. 22 and 23) (Figure 3-6b), an almost complete O_2 consumption in Cycle 2 was observed. Note that the cores were initially soaked into C_3 (Cycle 1), which means that O_2 consumed more efficiently in a lighter liquid oil-C_3 mixture, which was also confirmed in the Cycle 3 of Air/C_3/Air sequence (Exp. 21).

From 150 ℃ experiment cases, one may reach the following conclusions: (1) higher oil recovery is obtained for a C_3/Air/C_3 sequence, however no oil was expelled from cores in Cycles 2 and 3 (in Cycle 2 oil viscosity increased; in Cycle 3 propane did not have an effect on oil viscosity reduction), (2) a high O_2 consumption was observed in two gas sequences (Air/C_3/Air and C_3/Air/C_3), which might be higher at longer duration of cycles, and (3) the highest O_2 consumption was obtained when O_2 contacts C_3/heavy oil liquid mixture instead of heavy oil.

Based in our lab experimental conditions at core scale, it was difficult to account for the effect of mineralogy in oil recovery or its effect on LTO reactions. However, Drici and Vossoughi (1985) found that low-temperature oxidations are strongly affected by surface area, which is higher in Berea sandstone rocks than Indiana limestone rocks due to a higher presence of fine (high surface area) clays (Churcher et al. 1991). Also, Faure and Landais (2000) reported that, in the presence of illite (clay), oxygen-bearing compounds are formed during the oxidation of a mixture of *n*-alkanes. On the contrary, with calcite and without addition of mineral phase, the extract does not contain any oxidation products. Kok (2009) investigated the effect of limestone and sandstone on the combustion of light crude oils by means of thermal analysis techniques and

found that the crude oil+sandstone mixture had lower activation energy than crude oil+limestone mixture in the LTO region.

According to Churcher et al. (1991), Indiana limestone is made up predominantly of the mineral calcite (99%) with a small amount of quartz (1%); also trace amounts of illite and kaolinite. Berea sandstone is made up of sand grains (quartz 85 to 90%; feldspar (3 to 6%) cemented by quartz, dolomite (1 to 2%), clays (6 to 8%), and traces amounts of iron sulphides. Similarly, Berea Sandstone Petroleum Cores website inform that two main components of their Berea sandstone are mainly silica (93.13%) and alumina (3.86%).

Solvent Type Effect

Two gas sequences were conducted using two different solvents: C_3 and C_4. Comparable experiments were run under similar conditions of core size (6-in.-length, 2-in.-diameter), fracture volume (Low V_f/V_T ratio), rock type (sandstone cores), and temperature (150°C). **Figure 3-7** shows the results of corresponding cases. The analyzed gas sequences are:

Air/C_3/Air: Experiment 21 (C_3)   vs.   Experiment 25 (C_4)

C_3/Air/ C_3:   Experiment 22 (C_3)   vs.   Experiment 26 (C_4)

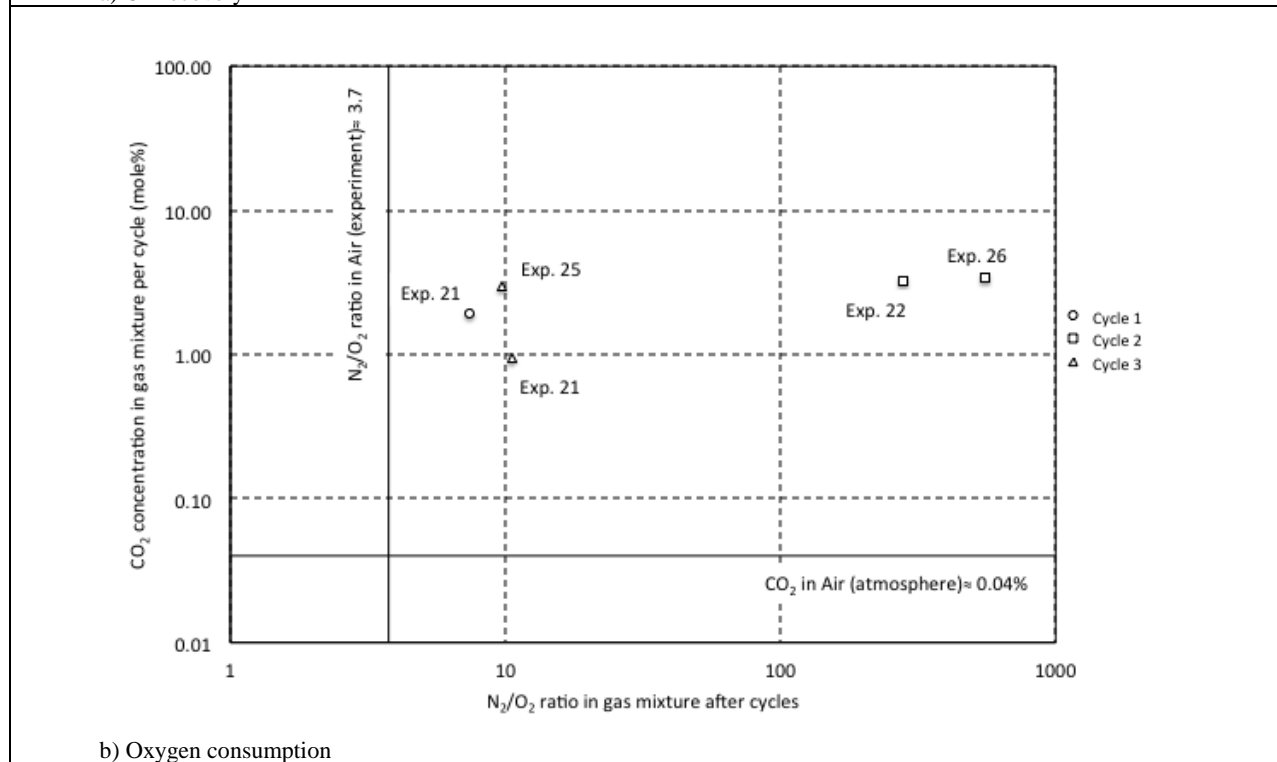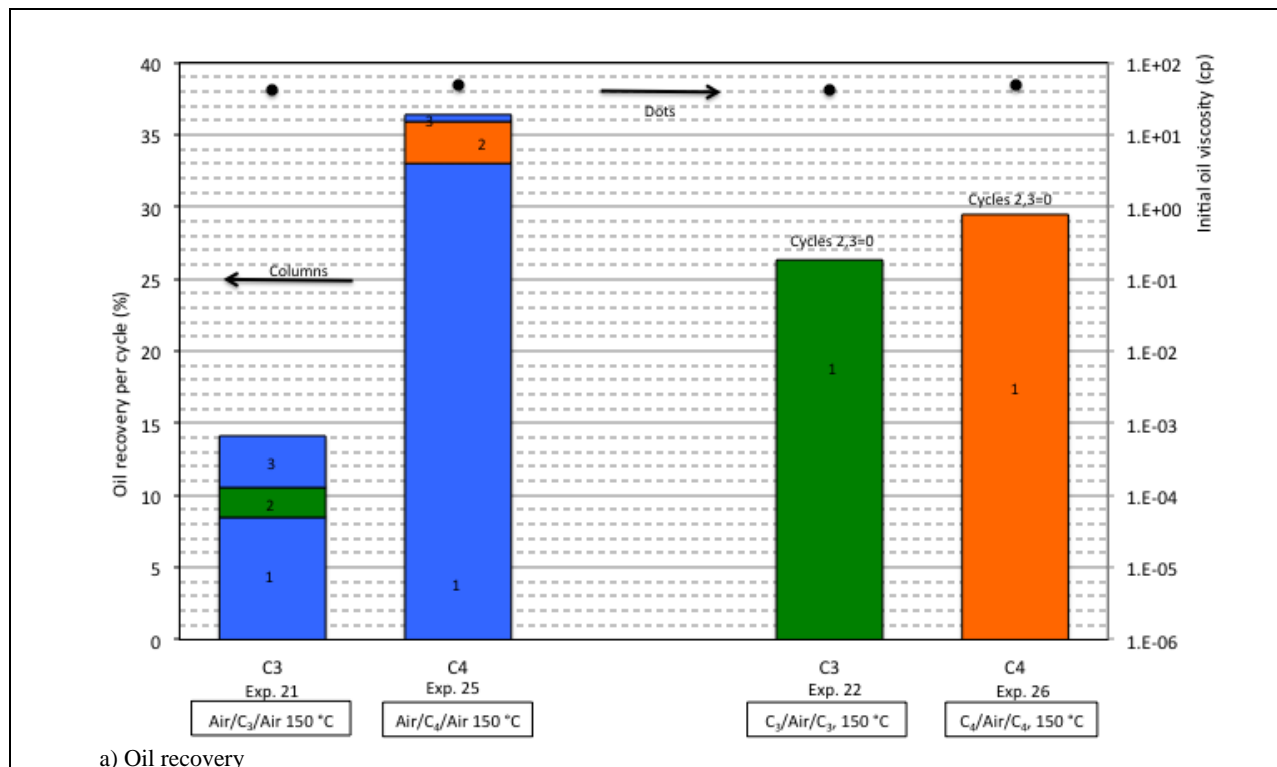a) Oil recovery

b) Oxygen consumption

Figure 3-7 Experimental results. Effect of solvent type.

Comparison of Exp. 21 and 25 may not be straightforward because oil recovery for Cycle 1 (Air) in Exp. 25 was quite high (even higher than that of Cycles 1 of Exp. 22 and 26 where C_4 was used). However, Cycles 2 of Exps. 21 and 25 yielded a higher oil recovery with C_4 compared to C_3. The same observation applies to Exp. 22 and 26; i.e. a higher oil recovery was obtained using C_4 than C_3 in Cycles 1 and 3.

Experiments 22 and 26 have similar initial oil viscosity. Recovery factor in Cycles 1 of Exp. 26 (using C_4) was higher than Exp. 22 (using C_3). The dilution of C_4 in heavy oil was stronger than C_3, which means a less viscous oil/solvent mixture was attained improving the conditions for oil expulsion by means of gravity drainage. As previously mentioned, in the comparison of other variables, there was no oil recovery in Cycles 2 and 3. In Cycle 2, oil viscosity increase inhibited the oil flow out of matrix and air acted only as a pressurizing agent. In Cycle 3, the solvents (C_3 and C_4) were not capable of reducing the fluid viscosity at low values for the fluid to flow at those conditions (oil residual saturation, soaking time).

Additionally, a high O_2 consumption (Figure 3-7b) was obtained in any experiment regardless of the solvent or gas sequence due to the high temperature (150°C). However, a higher O_2 consumption was reached in Cycle 2 (Air, Exp. 26) after the core was soaked in C_4 gas because the more diluted oil/C_4 mixture that remained in the core after Cycle 1 (C_4), the higher the oxidation.

Core Size Effect

Two gas sequences experiments were conducted using two different block sizes: Short core (2 in.-diameter, 6-in.-length) and Long core (3.25-in.-diameter, 9-in.-length). These experiments were run under similar conditions of fracture volume (Low V_f/V_T ratio), rock type (sandstone), temperature (150°C), and solvent (C_3). **Figure 3-8** shows results of the corresponding cases. The analyzed gas sequences are:

Air/C_3/Air: Experiment 21 (Short core)   vs.   Experiment 27 (Long core)

C_3/Air/ C_3:   Experiment 22 (Short core)   vs.   Experiment 30 (Long core)
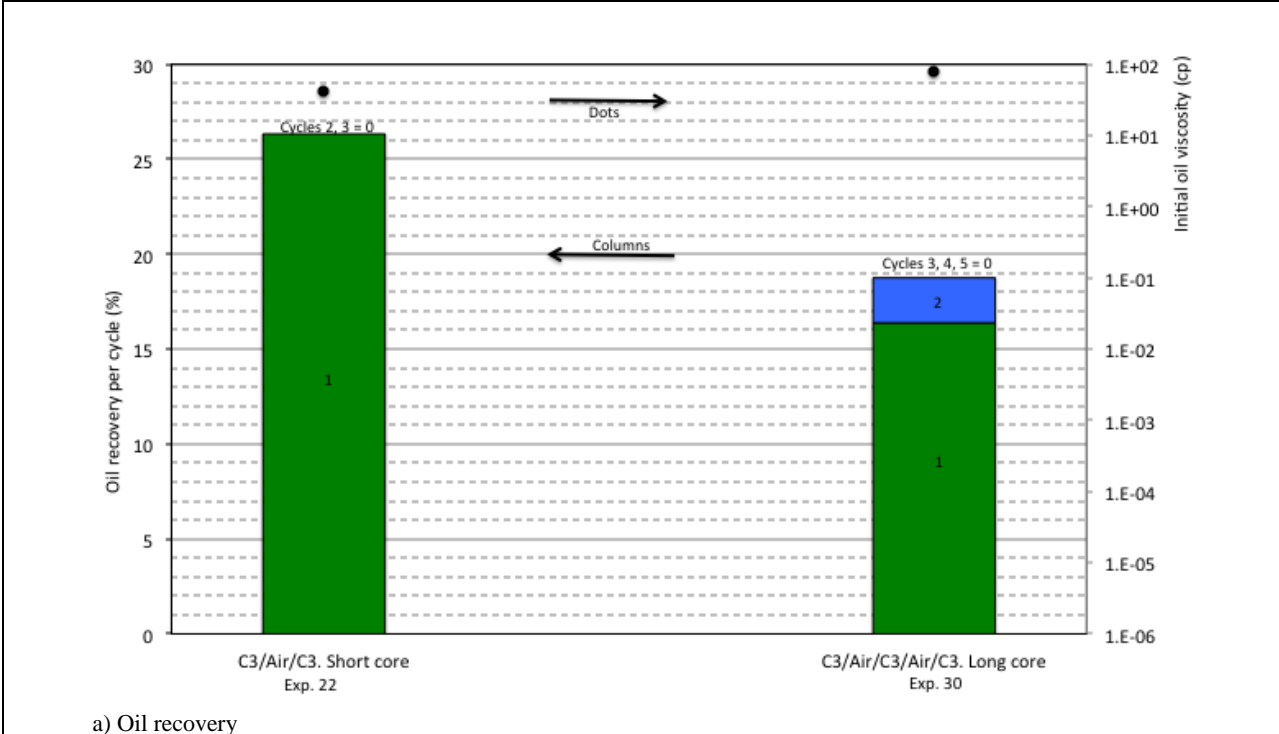
a) Oil recovery
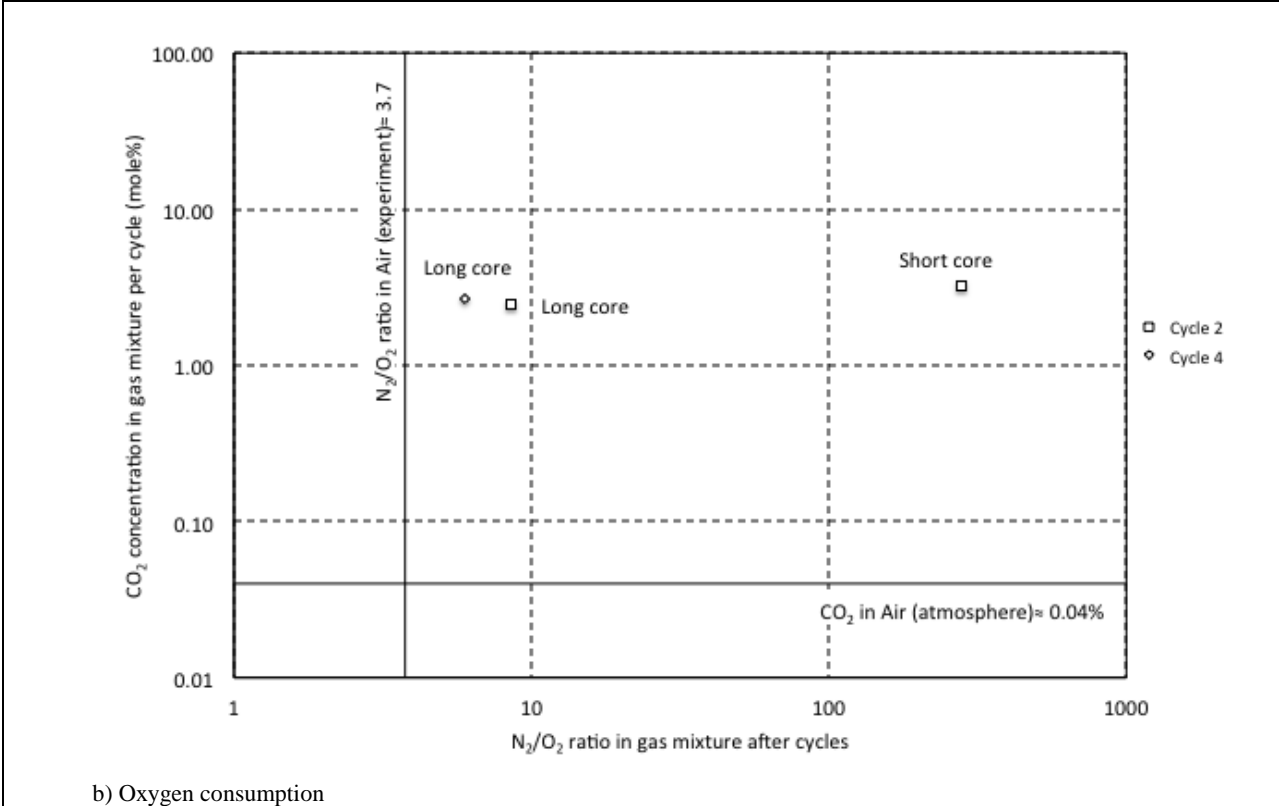
b) Oxygen consumption

Figure 3-8 Experimental results. Core size effect: $C_3/Air/C_3$ sequence.

Gas sequence: C_3/Air/C_3

Due to lower recovery than the shorter one (Exp. 22), five cycles were applied in the case of long core experiment (Exp. 30). Oil recovery in Cycle 1 (C_3) of Exp. 22 was higher than that of Exp. 30, which can be explained by longer diffusion time in the longer (or larger) core. The difference in the initial oil viscosity was trivial.

Mayorquin and Babadagli (2012) numerically analyzed the effect of matrix size on recovery factor for three cylindrical-shaped matrix blocks of different sizes surrounded by annular fracture filled with Air+C_3 mixture. They showed that the shorter matrix size (similar to that of our Exp. 22) yielded the highest recovery factor followed by the longer matrix size (similar to that of our Exp. 30), confirming our experimental results for Cycle 1 of Exp. 22 and 30.

Based on the lab results in Cycle 1, it can be stated that C_3 diffuses deeper into the matrix core having the higher A/V ratio; i.e. the Short core (A/V ratio for Short and Long cores were 2.35 and 1.45, respectively). This means that air would also diffuse deeper into the matrix in Cycle 2, which means that generated oxygenated compounds would cover a larger area of the core and the rate of oil expelled from the matrix would decrease as well as its oil recovery in a given time. In fact, this is what was observed in Cycle 2 of Exp. 22 (a null recovery was obtained in the Short core case). Conversely, the oil recovery in Cycle 2 of the Long core (Exp. 30), or lower A/V ratio, was greater than the shorter one (Exp. 22) because O_2 diffused less deep into the matrix and hence a greater area with less restriction (less oxygenated compounds) existed for the oil to flow down the matrix. Mayorquin and Babadagli (2015) numerically showed the distribution of oxygenated compounds in matrix blocks for two models indicating that the oxygenated compounds covered larger portions in small blocks than in large blocks.

Suggested oil production mechanism is reinforced based on consumed O_2. This can be observed in Figure 3-8b in which the highest N_2/O_2 ratio (maximum O_2 consumption) was observed in the Cycle 2 of the short core, while the lowest N_2/O_2 ratio (minimum O_2 consumption) was obtained in the Cycles 2 and 4 of the longer core. It should be noted that oil viscosity after Cycle 1 of Exp. 30 (87.8 cp) was very similar to the one before Cycle 1 (75.9 cp).

Gas sequence: Air/C$_3$/Air

Figure 3-9 shows the results for the corresponding cases. Long core experiment (Exp. 27) had six cycles (oil recovery was null in Cycles 5 and 6), while there were only three cycles in the case of short core experiment (Exp. 21). As in previous gas sequence, the oil recovery in Cycle 1 (Air) of Exp. 21 was higher than Exp. 27, which can be attributed to slower diffusion due to lower area/volume ratio (A/V) of the longer core.
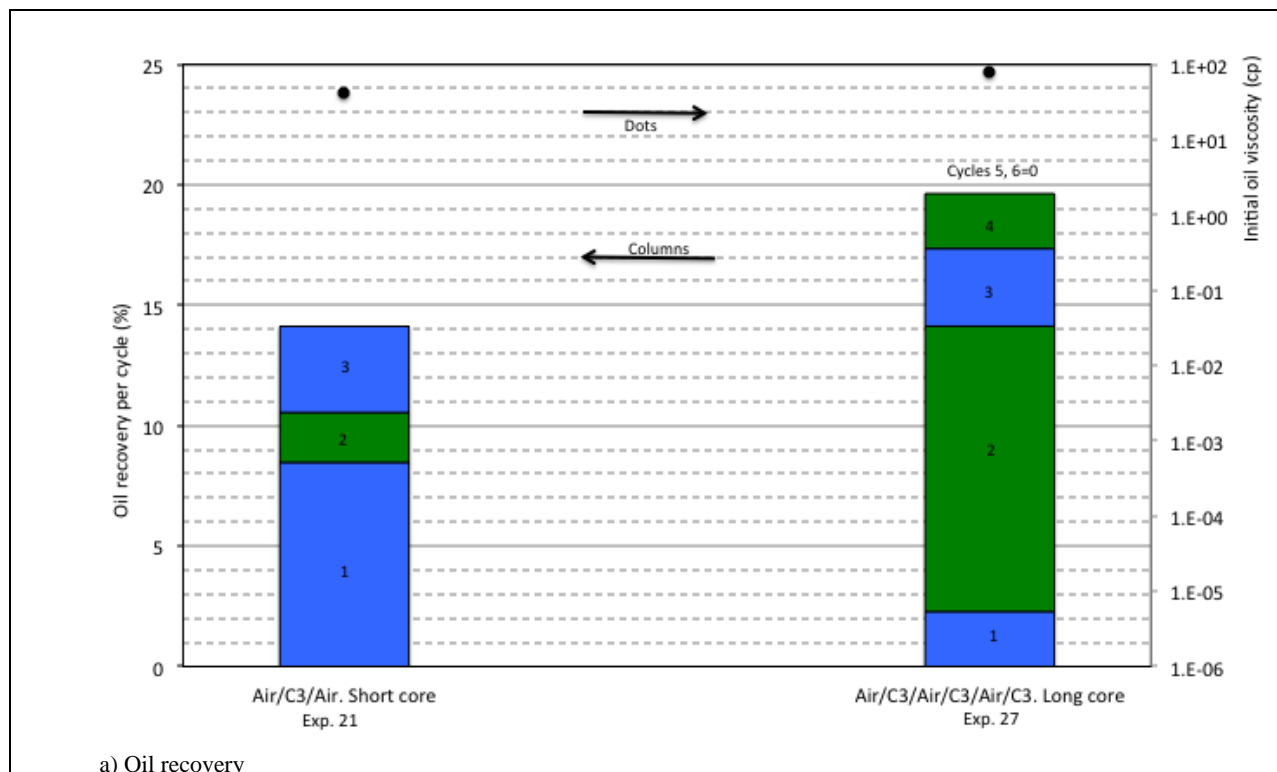
a) Oil recovery
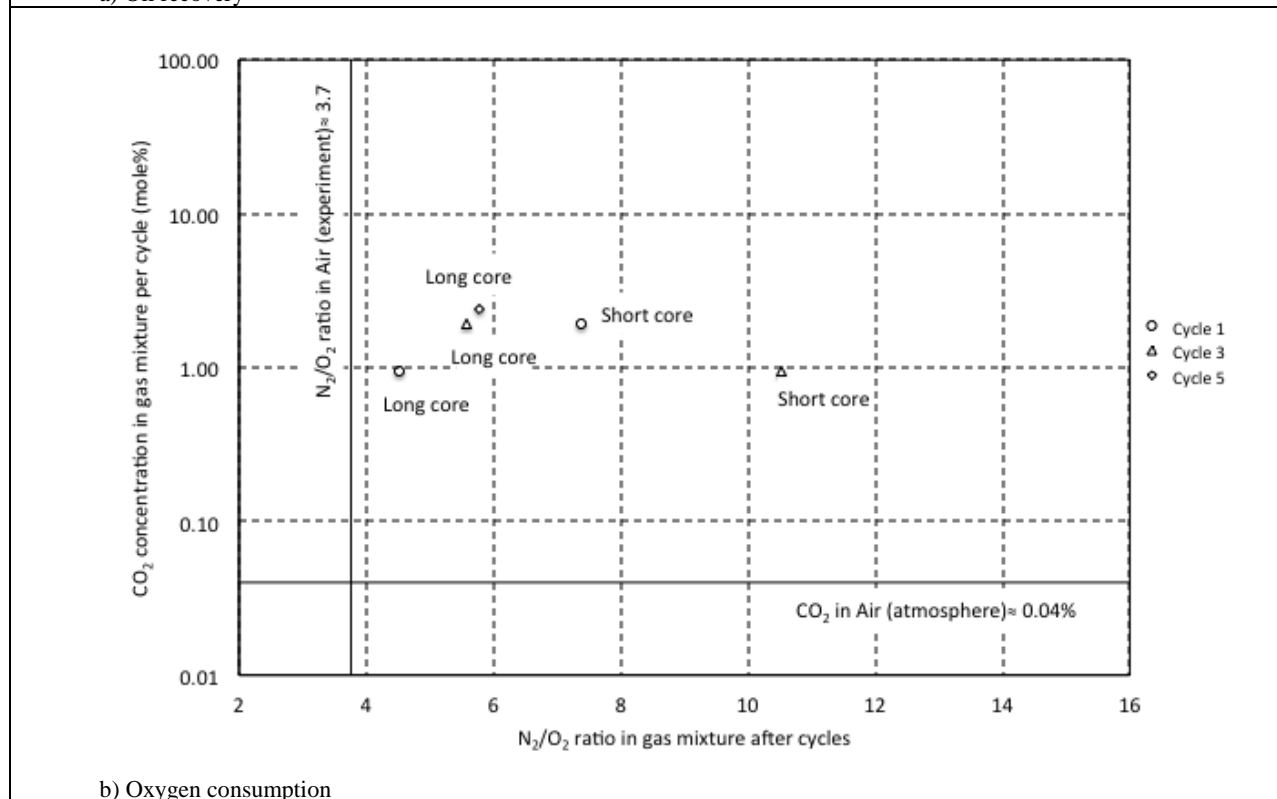
b) Oxygen consumption

Figure 3-9 Experimental results. Core size effect: Air/C$_3$/Air sequence.

Unlike the C_3/Air/C_3 sequence, the total oil recovery was higher for the long core (Exp. 27) even though it started with air. As explained previously, the short core (Exp. 21) had a higher A/V ratio than the longer one (Exp. 27). Thus, O_2 diffused deeper into the core and oxygenated compounds (high viscosity) were formed in a larger portion of the core. Certainly, the use of C_3 gas in Cycle 2 reduced oil viscosity but a low oil recovery was obtained from this cycle. However, in the larger core, C_3 was more effective and this can be explained by the fact that because the oxygenated compounds in the core were lower, most likely more matrix oil volume was not contacted or partially contacted by O_2. Hence, the easiness for the matrix oil to flow out of the cores was higher in the larger core. From the gas composition (Figure 3-9b) side, it is also observed that the highest O_2 consumption (highest N_2/O_2 ratio) occurred in the short core experiment, meaning that O_2 reacted with more matrix oil as suggested earlier.

From the two gas sequences experiments, it was confirmed experimentally that block size played a factor in the oil recovery, not only form the block height but from its A/V ratio perspective. Additionally, it can be concluded that the selection of the gas type (air or solvent) to be used in Cycle 1 was a crucial step for the oil recovery and was highly dependent on the A/V ratio of the matrix.

Effect of co-injection of Air and C_3

Up to this point, alternate injection of air and C_3 was analyzed. A more effective option could be to inject them together. This section provides the experimental results of injection of Air+C_3 mixtures. Different gas sequence experiments were conducted at similar conditions (rock and solvent type) in order to compare them. Results are shown in **Figure 3-10**. The analyzed gas sequences are:

Exp. 4 (Air+C_3 mixture)   vs. Exp. 10 (Air/C_3/Air)   vs.   Exp. 9 (C_3/Air/Air)

Exp. 5 (Air+C_3 mixture/Air+C_3 mixture)   vs. Exp. 19 (Air/C_3/Air)   vs.   Exp. 18 (C_3/Air/C_3)

Exp. 31 (Air+C_3 mixture/Air+C_3 mixture/Air+C_3 mixture)   vs. Exp. 30 (C_3/Air/C_3/Air/C_3)   vs.
        Exp. 27 (Air/C_3/Air/C_3/Air/C_3)

Exp. 32 (Air+C_3 mixture/Air+C_3 mixture/Air+C_3 mixture)   vs. Exp. 21 (Air/C_3/Air)   vs.
Exp. 22 (C_3/Air/C_3).
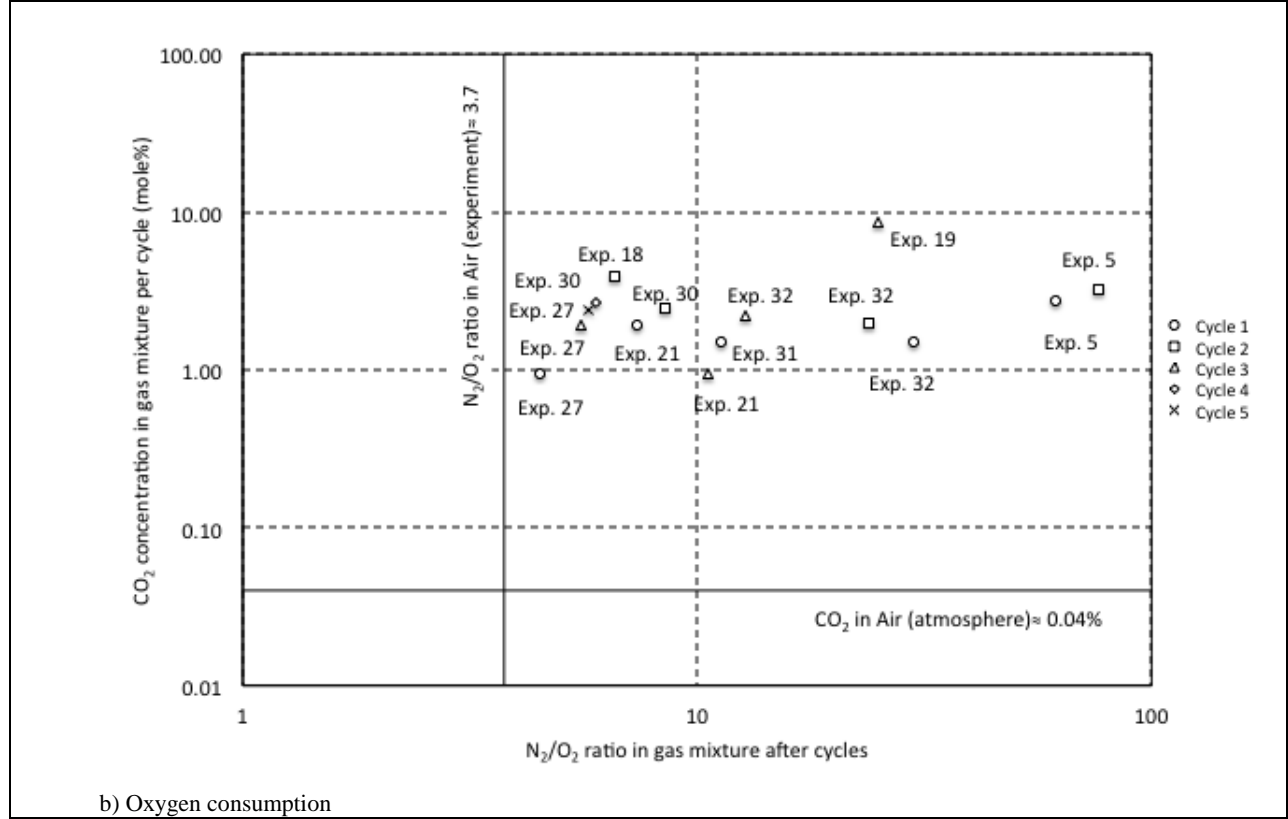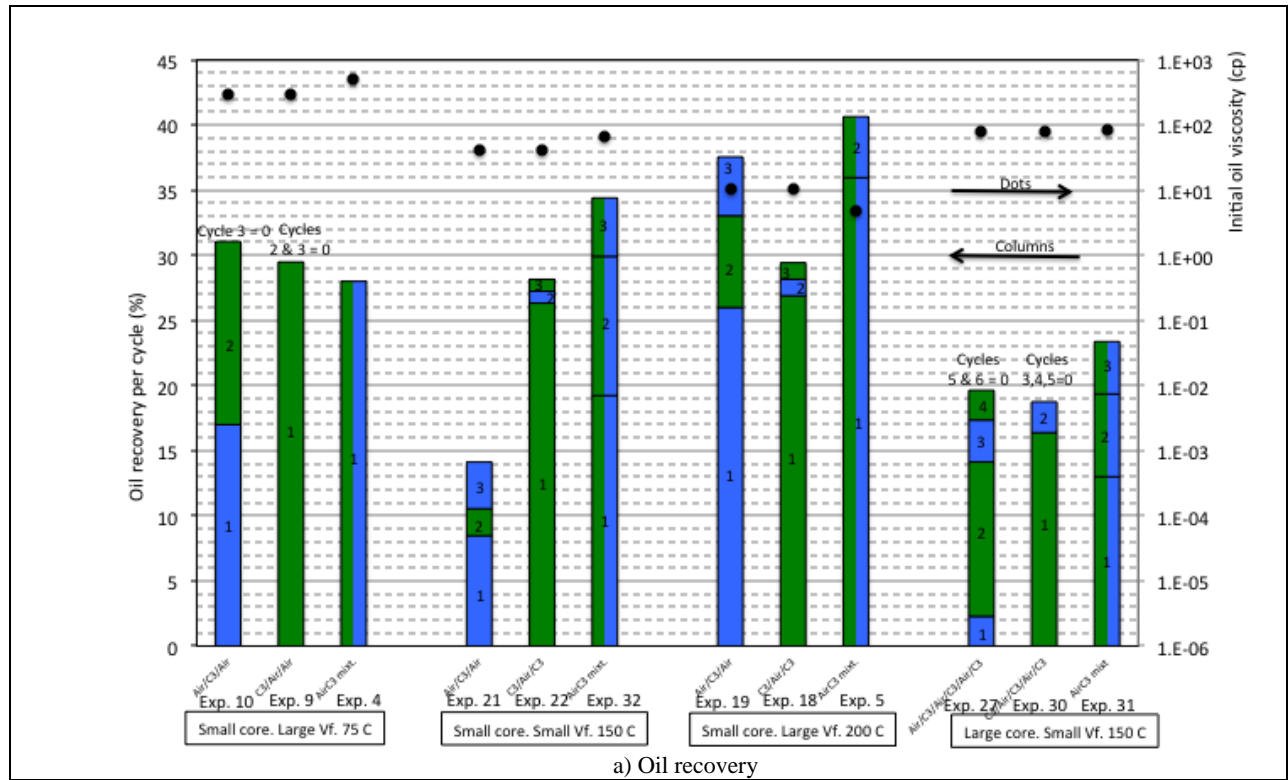
a) Oil recovery

b) Oxygen consumption

Figure 3-10 Experimental results. Effect of Air/C$_3$ mixtures.

Exp. 4 (Air+C$_3$ mixture) vs. Exp. 10 (Air/C$_3$/Air) vs. Exp. 9 (C$_3$/Air/Air)

These experiments were conducted at similar conditions: Small cores (2-in.-diameter, 6-in.-length), Large V_f/V_T ratio, sandstone cores, 75°C, and solvent (C$_3$). Gas mixture concentration for Exp. 4 was 53.1 C$_3$ mol% and 46.9 air mol%. Figure 3-10a shows that initial oil viscosity was the same in Exp. 9 and 10, and slightly higher in Exp. 4. The lowest, intermediate, and highest oil recoveries for Cycle 1 were obtained in Exp. 10 (Air), Exp. 4 (Air+C$_3$ mixture), and Exp. 9 (C$_3$), respectively. Differences existed in duration of Cycle 1 from these experiments, which were around 4.3 days in Exp. 9 and 10, and almost double (8.6 days) in Exp. 4. Certainly, duration had an effect in the highest oil recovery obtained in Cycle 1 of Exp. 4. However, we observed that duration of the first two cycles (Cycle 1+Cycle 2) in Exp. 9 and 10 was practically the same as the duration of Cycle 1 of Exp. 4 and oil recoveries were similar. Then, one may conclude that gas mixture (Air+C$_3$) is more efficient than alternating gases. It is worth mentioning that a second cycle was not conducted in Exp. 4 (total oil recovery could have been even higher). The benefits of using an Air+C$_3$ mixture are less O$_2$ concentration to react with heavy oil thus minimizing the amount of generated oxygenated compounds and quicker reduction of oil viscosity using the solvent from the initial stage of the process. Another benefit of using Air+C$_3$ mixture is a reduced O$_2$ concentration in produced gas; for instance, O$_2$ concentration in Exp. 4 was 13.5 mol%, while Exp. 10 was 19.1 and 18.8 mol% in Cycles 1 and 3, respectively (Appendix A).

Exp. 5 (Air+C$_3$ mixture/Air+C$_3$ mixture) vs. Exp. 19 (Air/C$_3$/Air) vs. Exp. 18 (C$_3$/Air/C$_3$)

These experiments were conducted at the following -similar- conditions: Small cores (2-in.-diameter, 6-in.-length), Large V_f/V_T ratio, sandstone cores, 200°C, and solvent (C$_3$). Gas mixture concentration for Exp. 5 was 51.5 C$_3$ mol% and 48.5 air mol%. Figure 3-10a shows that initial oil viscosity was the same in Exp. 18 and 19 and slightly lower in Exp. 5, which could be one of the reasons for a higher ultimate (total) oil recovery in Exp. 5. The other reason is cycle duration (soaking time); for instance, duration of Cycle 1 in Exp. 5, 18, and 19 were 8.1, 4.6, and 3.5 days. However, based on comparison of previous set of experiments, the same benefits would be expected when soaking a heavy oil saturated core into Air+C$_3$ mixture; i.e., a lower O$_2$

concentration (less amount of oxygenated compounds) and faster reduction of oil viscosity due to use of the solvent at the beginning of the process.

On the other hand, at high temperature (200ºC), the rate of oxidation reaction increased resulting in considerable O_2 consumption. What is critical to note is that O_2 consumption was higher in the Air+C_3 mixture cases (Exps. 5 and 31). Obviously, O_2 reaction with crude oil diluted by C_3 was more effective. O_2 concentration in Cycles 1 and 2 for Exp. 5 was 0.824 mol% and 0.62 mol%, respectively. O_2 concentration in Cycle 2 of Exp. 18 was 12.7 mol% and O_2 concentration in Cycle 3 of Exp. 19 was 3.5 mol% (O_2 concentration for Cycle 1 for Exp. 19 was not available). This is important as O_2 consumption is a critical element for this method proposed in this paper.

Exp. 31 (Air+C_3 mixture/Air+C_3 mixture/Air+C_3 mixture) vs. Exp. 27 (Air/C_3/Air/C_3/Air/C_3) vs. Exp. 30 (C_3/Air/C_3/Air/C_3)

Three gas sequences were conducted at these conditions: Long cores (3.25-in.-diameter, 9-in.-length), Low V_f/V_T ratio, sandstone core, 150°C, and solvent (C_3). Gas mixture concentration for Exp. 31 was 18.0 C_3 mol% and 82.0 Air mol% (Cycle 1); 6.5 C_3 mol% and 93.5 Air mol% (Cycle 2), and; 10.1 C_3 mol% and 89.9 Air mol% (Cycle 3). Figure 3-10a indicates that initial oil viscosities were similar. Thus, any changes in oil recovery should be attributed to other factors. As can be inferred from Figure 3-10b, using air in Cycle 1 (Exp. 27) delivered not only the smallest oil recovery but also the lowest O_2 consumption based on N_2/O_2 ratio (Figure 3-10b). On the other hand, when C_3 was used in Cycle 1 (Exp. 30), the highest oil recovery of Cycles 1 of the three cases was obtained. When air was used with C_3 as a mixture (82% mol% Air, 18 mol% C_3), the oil recovery was very close to the pure C_3 case, indicating a more economical application. Overall, the air/C_3 mixture experiment (Exp. 31) delivered the highest total oil recovery of all cases. This makes it economical not only from the number of cycles (only 3 cycles) but also in total duration (29.0, 28.8, and 12.3 days for Exps. 27, 30 and 31, respectively).

Cumulative oil recoveries after Cycle 2 (Cycle 1+Cycle 2) were similar in Exp. 30 and 31. However, after this cycle the oil expulsion mechanism in Exp. 31 was more effective than Exp. 30 as a lower amount of oxygenated compounds generated in the matrix oil (lower amount of O_2

is injected) and a reduction in the initial oil viscosity (or a reduced effect of increased oil viscosity related to the generated oxygenated compounds).

It is interesting to note that even when C_3 concentration in the injected $Air+C_3$ mixture in three cycles of Exp. 31 was low (less than 20 mol%), its benefits in oil recovery and O_2 consumption were highly prominent. In Exp. 4 and 5, C_3 concentration in the injected gas mixture was around 50 mol%, which means that C_3 concentration in the injected $Air+C_3$ mixture can be optimized in order to minimize its requirements and reduce related costs.

Exp. 32 ($Air+C_3$ mixture/$Air+C_3$ mixture/$Air+C_3$ mixture) vs. Exp. 21 ($Air/C_3/Air$) vs. Exp. 22 ($C_3/Air/C_3$).

Three gas sequences were conducted at the following conditions: Small -sandstone- cores (2-in.-diameter, 6-in.-length), Low V_f/V_T ratio, temperature=150°C, and C_3 as solvent.

Gas mixture concentration for Exp. 32 was 29.2 C_3 mole% and 70.8 Air mole% (Cycle 1), 21.4 C_3 mole% and 78.6 Air mole% (Cycle 2), and 20.0 C_3 mole% and 80.0 Air mole% (Cycle 3). Figure 3-10a indicates that initial oil viscosities were similar (slightly higher oil viscosity was observed in Exp. 32) and using air in Cycle 1 (Exp. 21) yielded the smallest oil recovery and the lowest O_2 consumption based on N_2/O_2 plot (Figure 3-10). When C_3 was used in Cycle 1 (Exp. 22), the highest oil recovery of Cycles 1 of the three experiments was obtained. Overall, the air/C_3 mixture experiment (Exp. 32) delivered the highest total oil recovery of all three experiments, even when its initial oil viscosity was the highest. Also, O_2 consumption (Figure 3-10b) in Exp. 32 is higher than that of Exp. 21.

Effect of C_3 concentration in co-injection of Air and C_3

Based on benefits observed in the use of Air/C_3 mixtures in cycles instead of alternate injection of C_3 and Air, the final step was set to assess the effect of the C_3 concentration in Air/C_3 mixtures. Minimization of expensive C_3 is a critical issue. This section provides the experimental results of injection of $Air+C_3$ mixtures at two different concentrations. The two experiments were conducted at similar conditions (rock type, temperature, V_f/V_T ratio, core size, and solvent type) in order to compare them. Results are shown in **Figure 3-11**. The analyzed gas sequences are:

Exp. 32 (Air+C_3 mixture/Air+C_3 mixture/Air+C_3 mixture)   vs   Exp. 33 (Air+C_3 mixture/Air+C_3 mixture/Air+C_3 mixture)

In experiments 32 and 33, the Air and C_3 were blended in the reactor by introducing C_3 first into it followed by Air addition. Once the scheduled injection pressure was reached, a gas sample was immediately taken from the reactor. Table 3-2 shows the Air and C_3 concentrations in the mixture for each cycle. Based on the data given in Table 3-2, the average C_3 concentration for cycles 1, 2, and 3 for experiments 32 and 33 was 23.5 mol% C_3 and 15.7 mol% C_3, respectively; i. e. higher C_3 concentration existed in experiment 32.

Total oil recovery (Table 3-4) for experiments 32 and 33 were 34.4 and 26.6%, respectively. Higher RF was measured when using more C_3 concentration. Mayorquin-Ruiz and Babadagli (2012) reported a sensitivity analysis to C_3 concentration in Air/C_3 mixture through numerical simulations and concluded that the process can be optimized by minimized hydrocarbon solvent for a given matrix size. That conclusion was experimentally confirmed in this work.

As a result of a lower Air concentration in Exp. 32 the N_2/O_2 ratio (Figure 3-11b) is higher than that of Exp. 33. In both experiments O_2 consumption occurred based not only on high N_2/O_2 ratios but also on CO_2 concentration present in the gas mixtures at the end of cycles.
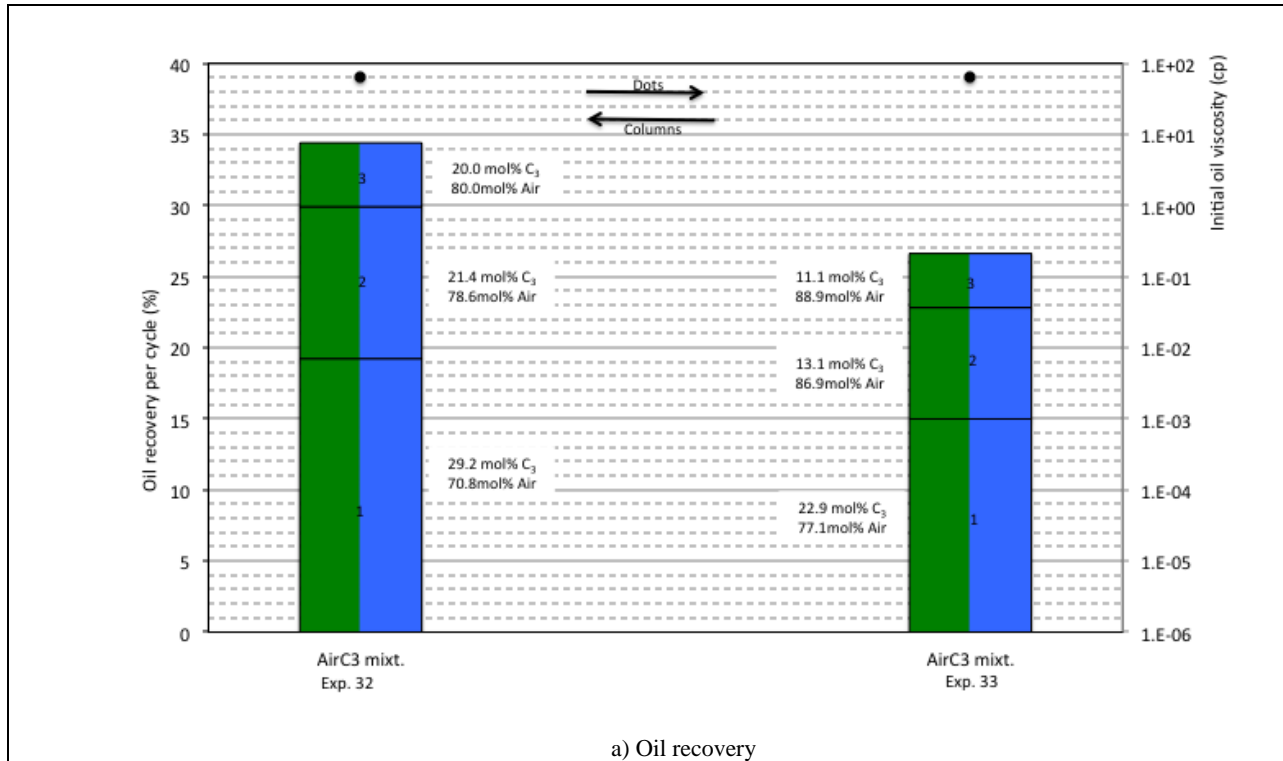
a) Oil recovery
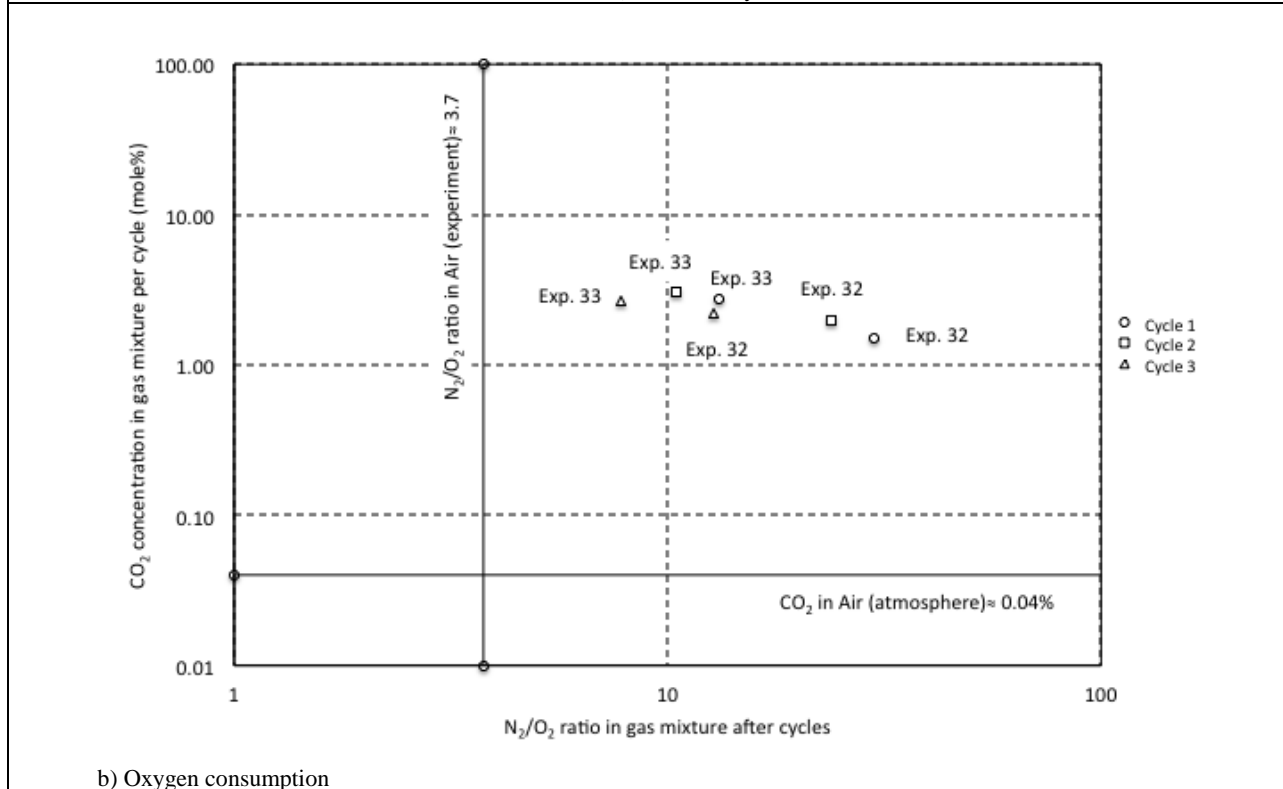
b) Oxygen consumption

Figure 3-11 Experimental results. Effect of C$_3$ concentration in co-injection of Air and C$_3$.

Based on the experimental results analyzed above, the benefits of injecting Air+C_3 mixture instead of alternate injection of air or solvent are as follows:

- Pressurizing gas

- Matrix oil dilution

- Maximum O_2 consumption

- Less solvent use

- Less amount of O_2 to be consumed in matrix, which means less amount of generated oxygenated compounds

- Oil viscosity increase due to generation of oxygenated compounds is reduced

- Oil recovery is higher and faster than both pure air and alternating air and C_3 injection

In the Air+C_3 mixture cases, the gases were introduced sequentially; i.e., C_3 was injected into the reactor followed by air. This was observed to be a safe way to use a flammable gas in the presence of oxygen and at high temperature conditions. A similar procedure can be recommended for the field applications when Air+C_3 mixture is injected jointly.

3.5 Conclusions

The main observations and conclusions are categorized based on our parametric analysis.

Fracture Volume Effect

• V_f/V_T ratio affects oil recovery. The larger the amount of available gas mass in fracture the larger the amount of gas diffuses into matrix oil and hence the greater the oil recovery.

• At 75ºC gas type selection for Cycle 1 is critical for oil recovery; C_3 delivers higher oil recovery than air.

• At 150ºC gas type selection for Cycle 1 is not critical for oil recovery in that cycle. However, in the alternate gas sequence, Cycle 1 gas type does affect oil recovery in Cycle 2. Higher total oil recovery is reached in C_3/Air/C_3 sequence.

• Detrimental effect of increased oil viscosity due to generated oxygenated compounds is more critical at 75ºC than at 150ºC.

Temperature Effect

• At 75ºC propane is required in order for the matrix oil to drain out from the core, being more effective in Cycle 1.

• At 75ºC gas sequence design affects oil recovery (being higher with alternating injection of C_3 and air, starting with C_3). Oxygen is practically unconsumed regardless of the gas sequence. Hence, air acts only as pressurizing agent.

• Oxygen consumption is higher in the experiments at 150°C than those at 75ºC.

• At 150ºC gas sequence affects oil recovery. A higher oil recovery was obtained when using C_3 in Cycle 1 due to a higher C_3 mass transfer from fracture gas into matrix oil reducing its viscosity and thus improving the gravity drainage mechanism. Also, in experiments at 150ºC oxygen consumption is higher in cycles followed by C_3 cycles.

Rock Type Effect

• At 75ºC, lower oil recovery was obtained from the limestone cores than sandstones due to lower permeability. It was not feasible to evaluate the effect of mineralogy in oil recovery at core scale or its effect on LTO reactions.

• At 150ºC experiments, it was observed that (1) higher oil recovery is obtained for the C_3/Air/C_3 sequence, (2) high O_2 consumption was observed in the sequences of Air/C_3/Air and C_3/Air/C_3, (3) the highest O_2 consumption is obtained when O_2 contacts a C_3/heavy oil liquid mixture instead of heavy oil.

Solvent Type Effect

• Oil recovery at 150 ℃ is higher using C_4 at any injection sequence (Air/Solvent/Air, Solvent/Air/Solvent) than using C_3. The dilution of C_4 in heavy oil is higher than that of C_3 in heavy oil, which means that a less viscous oil/solvent mixture is attained improving the conditions for matrix oil expulsion by means of reduced-viscosity gravity drainage.

• Oxygen consumption in air cycle is higher after core being previously soaked in C_4 rather than C_3.

Core Size Effect

• It was confirmed experimentally that core A/V ratio plays a critical role in oil recovery, showing an impact in the oxygenated compounds distribution in the core and thereby oil recovery.

• Gas type selection (air or solvent) for Cycle 1 is a critical step for oil recovery and is highly dependent on matrix A/V ratio.

Gas Sequence

• It was observed that gas sequence (assuming pure gas in cycles: air or solvent) depends not only in temperature and oil viscosity but also in timing. At early times (i.e. when core is fully oil saturated) (Cycle 1) oil recovery is more efficient with C_3.

Effect of co-injection of Air and C_3

• Benefits of soaking cores in Air+C_3 mixture rather than pure air or solvent are as follows: (1) pressurizing gas agent, (2) matrix oil dilution, (3) higher O_2 consumption, (4) less solvent usage, (5) smaller amount of O_2 to be consumed, which means lower amount of generated oxygenated compounds, (6) faster (and earlier) oil viscosity reduction due to reduced oxygenated compounds, (7) higher and faster oil recovery compared to alternate injection of air and C_3.

• It was observed that C_3 concentration in the injected gas mixture can be optimized in order to reduce its requirements and related costs. C_3 costs could be further minimized by means of retrieval at surface and re-injection.

Effect of C_3 concentration in co-injection of Air and C_3

• It was confirmed experimentally that C_3 concentration in Air/C_3 mixtures can be optimized for a given matrix size. Optimization studies are suggested.

3.6   Nomenclature

A   = total area of core

C_3 = propane, C_3H_8

C_4 = butane, C_4H_{10}

CO   = carbon monoxide

CO_2 = carbon dioxide

EOR   = enhanced oil recovery

HTO   = high temperature oxidation

ISC   = in-situ combustion

LTO   = low temperature oxidation

N_2 = nitrogen

O_2 = oxygen

RF   = recovery factor

V   = volume of core

V_f = fracture volume

V_m =   bulk matrix volume

V_T =   total reactor volume

References

Alvarez, J. M., Sawatzky, R. P., Forster, L. M. et al. 2008. Alberta's Bitumen Carbonate Reservoirs—Moving Forward with Advanced R&D. Presented at the World Heavy Oil Congress, Edmonton, Alberta, 10–12 March. Paper 2008-467.

Churcher, P. L., French, P. R., Shaw, J. C., and Schram, L. L. 1991. Rock properties of Berea sandstone, Baker dolomite, and Indiana limestone. Presented at the SPE International Symposium on Oilfield Chemistry, Anaheim, California, 20–22 February. SPE-21044-MS. http://dx.doi.org/10.2118/21044-MS.

Craig, F. F., Jr. and Parrish, D. R. 1974. A Multipilot Evaluation of the COFCAW Process. *J Pet Technol* **26** (06): 659–666. SPE-3778-PA. http://dx.doi.org/10.2118/3778-PA.

Drici, O. and Vossoughi, S. 1985. Study of the Surface Area Effect on Crude Oil Combustion by Thermal Analysis Techniques. *J Pet Technol* **37** (04): 731 – 735. SPE-13389-PA. http://dx.doi.org/10.2118/13389-PA.

Faure, P. and Landais, P. 2000. Evidence for clay minerals catalytic effects during low-temperature air oxidation of n-alkanes. *Fuel* **79** (14): 1751 – 1756. http://dx.doi.org/10.1016/S0016-2361(00)00039-9.

Greaves, M., Ren, S. R., Rathbone, R. R., et al. 2000. Improved Residual Light Oil Recovery by Air Injection (LTO Process). *J Can Pet Technol* **39** (01): 57–61. PETSOC-00-01-05. http://dx.doi.org/10.2118/00-01-05.

Kok, M. V. 2009. Influence of reservoir rock composition on the combustion kinetics of crude oil. *J. Therm. Anal. Cal.* **97** (2): 397–401.

Lacroix, S., Delaplace, P., Bourbiaux, B. et al. 2004. Simulation of Air Injection in Light-Oil Fractured Reservoirs: Setting-up a Predictive Dual Porosity Model. Presented at the SPE Annual

Technical Conference and Exhibition, Houston, 26–29 September. SPE-89931-MS. http://dx.doi.org/10.2118/89931-MS.

Lakatos, I., Lakatos-Szabo, J., Bauer, K. et al. 1998. Potential Application of Oxygen-Containing Gases in Heavy Oil Bearing Reservoirs. Presented at the European Petroleum Conference, The Hague, 20–22 October. SPE-50647-MS. http://dx.doi.org/10.2118/50647-MS.

Lee, D. G. and Noureldin, N. A. 1989. Effect of Water on the Low-Temperature Oxidation of Heavy Oil. *Energy and Fuels* **3** (06): 713–715.

Mayorquin-Ruiz, J. R. and Babadagli, T. 2012. Optimal Design of Low Temperature Air Injection for Efficient Recovery of Heavy Oil in Deep Naturally Fractured Reservoirs: Experimental and Numerical Approach. Presented at the SPE Heavy Oil Conference Canada, Calgary, 12–14 June. SPE-149896-MS. http://dx.doi.org/10.2118/149896-MS.

Mayorquin-Ruiz, J. R. and Babadagli, T. 2015. Low-Temperature Air/Solvent Injection for Heavy-Oil Recovery in Naturally Fractured Reservoirs. *J Can Pet Technol* **54** (03): 148–163. SPE-174542-PA. http://dx.doi.org/10.2118/174542-PA.

Mayorquin-Ruiz, J. R., Babadagli, T, and Rodriguez de la Garza, F. 2015. Low Temperature Air Injection at the Mature Stage of Deep Naturally Fractured Heavy-Oil Reservoirs: Field Scale Modeling. Presented at the Pan American Mature Fields Congress, Veracruz, 20–22 January. Paper PAMFC15-141.

Ruiz, J., Naccache, P., Priestley, A., et al. 2013. Modeling In-Situ Combustion in a Heavy Oil Field in Romania. Presented at the SPE Heavy Oil Conference Canada, Calgary, Alberta, 11–13 June. SPE-165490-MS. http://dx.doi.org/10.2118/165490-MS.

Schulte, W. M. and de Vries, A. S. 1985. In-Situ Combustion in Naturally Fractured Heavy Oil Reservoirs. *SPE J* **25** (01): 67–77. SPE-10723-PA. http://dx.doi.org/10.2118/10723- PA.

Stokka, S., Oesthus, A., and Frangeul, J. 2005. Evaluation of Air Injection as an IOR Method for the Giant Ekofisk Chalk Field. Presented at the SPE International Improved Oil Recovery Conference, Kuala Lumpur, 5–6 December. SPE-97481-MS. http://dx.doi.org/10.2118/97481-MS.

Appendix A. Oil properties and gas chromatography of produced fluids

Table 3-5 Properties of produced

		11				12				13			
		Cycle 1	Cycle 2	Cycle 3	Total	Cycle 1	Cycle 2	Cycle 3	Total	Cycle 1	Cycle 2	Cycle 3	Total
R. F. (%)		7.5	3.3	1.0	11.7	6.2	6.9	9.9	22.9	1.6	8.8	0.0	10.5
Asphaltene content (weight %)							48.1						
Temperature (°C)		75				75				75			
ρo @ temperature (gr/cm^3)													
μ_o @ temperature (cp)													
RI @ temperature													
Gas chromatography (mol %)	C_1												
	C_2												
	C_3							98.19		0.01	97.42	1.42	
	C_4							0.14			0.11		
	C_5												
	C_6	0.02	0.02	0.05									
	O_2	19.92	20.75	20.02		21.20	20.93	0.23		21.05	0.38	20.66	
	N_2	79.98	79.16	79.66		78.79	79.05	1.45		78.60	2.09	77.88	
	CO_2	0.04	0.03	0.11			0.02			0.06		0.03	
	CO						0.01			0.01	0.01	0.02	
	H_2S						0.0001			0.0002	0.0002	0.0002	

	14				17				18			
	Cycle 1	Cycle 2	Cycle 3	Total	Cycle 1	Cycle 2	Cycle 3	Total	Cycle 1	Cycle 2	Cycle 3	Total
R. F. (%)	16.0	0.2	5.6	21.8	57.6	0.0	8.8	66.4	26.9	1.3	1.3	29.4
Asphaltene content (weight %)												
Temperature (°C)	75				75				200			
ρ_o @ temperature (gr/cm^3)					0.9515							
μ_o @ temperature (cp)					1579.3		18.8		14.0			
RI @ temperature					1.54960		1.49690		1.52820			
Gas chromatography (mol %) — C_1									0.06			
C_2												
C_3	96.97	1.34			79.23	0.01	90.89		94.75	0.07	94.20	
C_4		0.08			0.05		0.09		0.22		0.16	
C_5									0.11		0.07	
C_6									0.08		0.02	
O_2	0.35	19.80			2.08	21.14	1.12		0.04	12.67		
N_2	2.60	78.83			18.64	78.84	7.90		4.43	83.37	5.34	
CO_2		0.04							0.15	3.88	0.21	
CO	0.01											
H_2S	0.00											

		19				20		21				22			
		Cycle 1	Cycle 2	Cycle 3	Total	Cycle 1	Total	Cycle 1	Cycle 2	Cycle 3	Total	Cycle 1	Cycle 2	Cycle 3	Total
R. F. (%)		26.0	7.0	4.5	37.5	12.4	12.4	8.5	2.1	3.6	14.1	26.3	0.0	0.0	26.3
Asphaltene content (weight %)															
Temperature (°C)		200				150		150				150			
ρ_o @ temperature (gr/cm^3)															
μ_o @ temperature (cp)			12.0												
RI @ temperature															
Gas chromatography (mol %)	C_1		0.05	0.58											
	C_2		0.01												
	C_3		95.35	0.07					97.14	0.12		75.96	0.42	95.70	
	C_4		0.12						0.15	0.01		0.12		0.13	
	C_5		0.02												
	C_6							0.06				0.02	0.05		
	O_2			3.49				11.64	0.12	1.75		0.12	0.34	0.17	
	N_2		4.28	87.25				85.90	2.51	18.41		1.79	95.49	3.89	
	CO_2		0.16	8.61				1.92	0.06	0.95		0.02	3.19	0.11	
	CO	>0.04						>0.07		0.15			>0.09		
	H_2S														

	23				24				25			
	Cycle 1	Cycle 2	Cycle 3	Total	Cycle 1	Cycle 2	Cycle 3	Total	Cycle 1	Cycle 2	Cycle 3	Total
R. F. (%)	24.7	0.0	0.0	24.7	13.0	0.0	2.8	15.8	33.0	2.9	0.5	36.4
Asphaltene content (weight %)	23.2				26.0				24.5			
Temperature (°C)	150				75				150			
ρ_o @ temperature (gr/cm^3)												
μ_o @ temperature (cp)												
RI @ temperature												
Gas chromatography (mol %) — C_1		0.29										
C_2												
C_3	97.92	0.45	98.33		98.15	0.96	92.70			0.18	0.04	
C_4	0.15	0.02	0.15		0.13		0.13			90.65	0.57	
C_5		0.02										
C_6		0.02										
O_2	0.11	0.19	0.07		0.24	20.06	1.18		7.40	0.22	8.95	
N_2	1.78	94.71	1.41		1.48	78.88	5.98			8.69	87.46	
CO_2	0.04	4.07	0.04			0.10	0.02			0.26	2.98	
CO		0.15				0.01			0.15		0.15	
H_2S												

		26				27							28			
		Cycle 1	Cycle 2	Cycle 3	Total	Cycle 1	Cycle 2	Cycle 3	Cycle 4	Cycle 5	Cycle 6	Total	Cycle 1	Cycle 2	Cycle 3	Total
R. F. (%)		29.5	0.0	0.0	29.5	2.3	11.8	3.2	2.3	0.0	0.0	19.6	6.2	1.8	0.0	8.0
Asphaltene content (weight %)								34.9	33.1							
Temperature (°C)		150				150							150			
ρ_o @ temperature (gr/cm^3)																
μ_o @ temperature (cp)						108.1		282.0	251.5				246.1			
RI @ temperature																
Gas chromatography (mol %)	C_1		0.43			14.13		0.18	0.03	0.25				0.64	0.32	
	C_2					2.74				0.02				0.05		
	C_3	0.15		0.04		1.36	97.31	0.18	92.67	0.25	97.82		0.15	91.96	0.89	
	C_4	91.70	1.02	88.62		0.58	0.16		0.20		0.25			0.14		
	C_5		0.02			0.12										
	C_6		0.02			0.02							0.02			
	O_2	0.35	0.17	0.46		14.52	0.14	14.88	0.56	14.33	0.23		6.60	0.10	8.48	
	N_2	7.66	94.75	10.55		65.56	2.34	82.83	6.25	82.73	1.62		89.22	6.64	86.22	
	CO_2	0.13	3.39	0.31		0.94	0.05	1.91	0.28	2.42			3.81	0.36	4.08	
	CO		0.15					0.15		0.15			0.15			
	H_2S															

		29				30						31			
		Cycle 1	Cycle 2	Cycle 3	Total	Cycle 1	Cycle 2	Cycle 3	Cycle 4	Cycle 5	Total	Cycle 1	Cycle 2	Cycle 3	Total
R. F. (%)		0.0	8.2	1.0	9.2	16.4	2.4	0.0	0.0	0.0	18.7	13.0	6.3	4.0	23.4
Asphaltene content (weight %)			26.5			44.2						36.0	37.3		
Temperature (°C)		75				150						150			
ρ_o @ temperature (gr/cm^3)															
μ_o @ temperature (cp)			7123.6			87.8						169.6	94.2	205.3	
RI @ temperature												1.54390	1.54870		
Gas chromatography (mol %)	C_1					0.07	0.21		0.28				0.01	0.00	
	C_2		0.03			0.05							0.01	0.00	
	C_3		97.77	0.97		91.27	0.54	92.06	0.31	97.75		37.76	34.44	32.16	
	C_4		0.23			0.19		0.13		0.18		0.07	0.09	0.07	
	C_5														
	C_6					0.03									
	O_2	21.12	0.35	20.45		0.09	10.16	0.67	13.89	0.14		4.91	2.56	5.21	
	N_2	78.83	1.61	78.52		7.85	86.64	6.88	82.86	1.81		55.72	62.91	62.56	
	CO_2	0.05		0.05		0.19	2.43	0.26	2.67	0.12		1.51	N/A	N/A	
	CO														
	H_2S														

		32				33			
		Cycle 1	Cycle 2	Cycle 3	Total	Cycle 1	Cycle 2	Cycle 3	Total
R. F. (%)		19.2	10.7	4.5	34.4	15.0	7.8	3.8	26.6
Asphaltene content (weight %)		27.18	57.5	54.25					
Temperature (°C)		150				150			
ρ_o @ temperature (gr/cm^3)									
μ_o @ temperature (cp)		86.2				118.7			
RI @ temperature		1.5364							
Gas chromatography (mol %)	C_1	0.15	0.1	0.2		0.26	0.3	0.3	
	C_2								
	C_3	52.7	50.0	48.72		24.7	24.0	23.92	
	C_4	0.10	0.09	0.1		0.05	0.11	0.0	
	C_5								
	C_6	0.05				0.05	0.03		
	O_2	1.5	1.9	3.5		5.1	6.3	8.3	
	N_2	43.8	45.8	45.2		66.8	65.9	64.7	
	CO_2	1.51	2.0	2.22		2.77	3.1	2.67	
	CO								
	H_2S								

Appendix B. Calculation of Experimental Uncertainties

Most of the experiments were conducted under different conditions: either different initial oil viscosity, rock type, gas type, temperature, fracture volume, or pressure. Just a few of them were carried out keeping most of these variables constant. For example, Cycle 1 of experiments 11 and 12 were done at 75°C, using sandstone rock, the same initial oil viscosity, the same fracture volume and air. Also, Cycle 1 of experiments 20 and 21 were conducted at the same experimental conditions.

Then, oil recovery obtained in Cycle 1 of two different sets of experiments were used to calculate the standard deviation, which is considered in this work as the value of the experimental error in oil recovery. Two standard deviations were obtained; one for Cycle 1 of experiments at 75 °C (Exp. 11 and 12) and another for Cycle 1 of experiments at 150 °C (Exp. 20 and 21).

For average values (x_{AV}) and standard deviation (s_x) equations used are:

$$x_{AV} = \frac{1}{n}(x_1 + x_2 + x_3 + \cdots + x_n)$$

(1)

(2)
$$s_x = \sqrt{\frac{1}{n-1}[(x_1 - x_{AV})^2 + (x_2 - x_{AV})^2 + \ldots + (x_n - x_{AV})^2]}$$

The standard deviation of the mean value (σ_m) of a set of experiments is given by:

(3)
$$\sigma_m = \sqrt{\frac{1}{n(n-1)}[(x_1 - x_{AV})^2 + (x_2 - x_{AV})^2 + \ldots + (x_n - x_{AV})^2]} = \frac{s}{\sqrt{n}}$$

where n is the number of repeated measurements (n=2 for both set of experiments) and x_1, x_2, x_3,..., x_n is the oil recovery for corresponding Cycle (1, 2, 3, ..., n).

Oil recovery standard deviation for Cycle 1 of experiments at 75 ºC (Exp. 11 and 12)

Oil recovery (%) for Cycle 1: 7.5 (Exp.11); 6.2 (Exp. 12)

Average value:

$$x_{AV} = \frac{1}{2}(7.5 + 6.2) = 6.85\% \tag{4}$$

Standard deviation:

$$s_x = \sqrt{\frac{1}{2-1}[(7.5 - 6.85)^2 + (6.2 - 6.85)^2]} = 0.9\% \tag{5}$$

Oil recovery standard deviation for Cycle 1 of experiments at 150 ºC (Exp. 20 and 21)

Oil recovery (%) for Cycle 1: 12.4 (Exp.20); 8.5 (Exp. 21)

Average value:

$$x_{AV} = \frac{1}{2}(12.4 + 8.5) = 10.45\% \tag{6}$$

Standard deviation:

$$s_x = \sqrt{\frac{1}{2-1}[(12.4 - 10.45)^2 + (8.5 - 10.45)^2]} = 2.8\% \tag{7}$$

Then, experimental oil recovery with experimental errors from previous experiments:

Exp. 11: (7.5 ± 0.9) % or 7.5 % with an uncertainty of 12%

Exp. 12: (6.2 ± 0.9) % or 6.2 % with an uncertainty of 14%

Exp. 20: (12.4 ± 2.8) % or 12.4 % with an uncertainty of 22%

Exp. 21: (8.5 ± 2.8) % or 8.5 % with an uncertainty of 33%

Finally, the standard deviation for the oil recovery mean value of Cycle 1 for set of experiments 11 and 12:

$$\sigma_m = \frac{0.9\%}{\sqrt{2}} = 0.6\% \tag{8}$$

i. e. (6.85 ± 0.6) %.

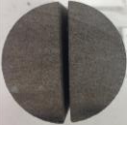The standard deviation for oil recovery of Cycle 1 for set of experiments 20 and 21:
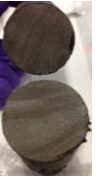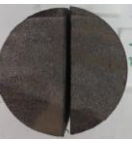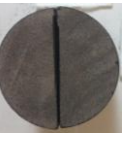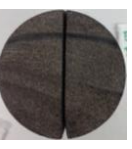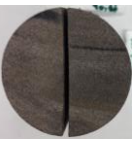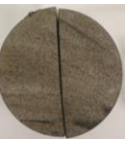
$$\sigma_m = \frac{2.8\%}{\sqrt{2}} = 2.0\% \tag{9}$$
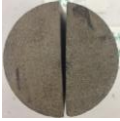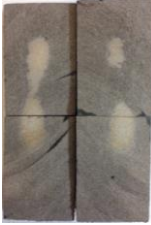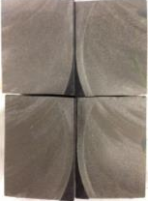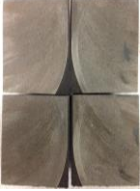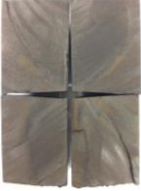
i. e. (10.45 ± 2.0) %.

It was only possible to calculate the experimental uncertainties for two pairs of experiments. In order to estimate experimental uncertainties for the whole set of experiments, repetition of experiments would be needed, which was highly time consuming. Instead, a broader set of conditions (gas types, rock types, temperatures, gas sequences, and cycle duration) were considered as presented in this work (Table 3-2 summarizes the conditions).

Appendix C. Photos from cores after experimentation

Figure 3-12 Cores after experimentation.

Experiment	Photo		Experiment	Photo	
11			18		
12			19		
13			20		
14			21		
17			22		

Experiment	Photo		Experiment	Photo	
23			29		
24			30		
25			31		
26			32		
27			33		
28					

Chapter 4 : Optimal Design of Low Temperature Air Injection with Propane for Efficient Recovery of Heavy Oil in Deep Naturally Fractured Reservoirs: Experimental and Numerical Approach

4.1 Summary

Low temperature air injection (LTAI) can be a possibility if injected air diffuses into matrix effectively to oxidize oil in it. However, early breakthrough of air with partial consumption of oxygen due to the highly conductive nature of the reservoirs is a concern. Once it is controlled by proper injection scheme and consumption of air injected through efficient diffusion into matrix, LTAI can be an alternative technique for heavy-oil recovery from deep NFR.

Limited number of studies on light oils showed that this process was highly dependent on oxygen diffusion coefficient and matrix permeability. In this process, oil production is governed by drainage and stripping of light oil components, which have a greater effect on recovery than the swelling of oil.

In the present study, static laboratory tests were performed by immersing heavy-oil saturated porous media into air filled reactors to determine critical parameters on recovery such as diffusion coefficient. A data acquisition system was established for continuous monitoring of pressure at different temperatures. Also analyzed was the possibility of hydrocarbon gas additive to air minimizing the oil viscosity increase created by oxidation reactions. Based on core scale experimental results, a numerical simulation model of air diffusion into a single matrix was created to obtain diffusion coefficient through matching of laboratory results. Then, sensitivity runs were performed for different matrix sizes and composition of injected gas (air and hydrocarbon). Additionally, a scaling-up study was performed in order to obtain an approximate production time for different matrix block sizes and temperatures.

It is imperative that enough timing is required for diffusion process before injected air filling to fracture network breakthrough. This implies that huff and puff type injection is an option as opposed to continuous injection of air. The optimal design and duration of the cycles were also tested experimentally and numerically for a single matrix case.

4.2 Introduction

A very limited number of studies on the numerical simulation of air injection into fractured reservoir were reported in the literature.   Schulte and De Vries (1985) conducted experimental and numerical simulations of in-situ combustion process in fractured reservoirs for heavy-oil recovery. They showed that diffusion of oxygen from the fracture into the matrix governed the burning process and also that injection rate should be minimized to prevent oxygen breakthrough. Based on numerical simulation runs, Tabasinejad et al. (2006) concluded that preferential passage of air through the fractures exists and combustion front in the fracture moves faster than in the matrix. Fatemi et al. (2008) studied in-situ combustion in a fractured reservoir using a thermal simulator and reported that the air injection rate should be optimized for a specific system in order to minimize the air breakthrough.

As seen in these limited number of published works, controlling the air injection rate is critical in in-situ combustion processes in fractured reservoirs.   The air injection rate should be synchronized with matrix diffusion rate to prevent early breakthrough of air from process efficiency and safety points of view. Also, note that high temperature air injection, i.e., combustion, may be difficult to achieve due to heterogeneous nature of the fractured reservoirs. An alternative is low temperature air injection, i.e., at low temperature oxidation conditions. Mayorquin-Ruiz and Babadagli (2015b) tested low temperature air-solvent injection (LTASI) on a single matrix block surrounded by fractures experimentally and observed that addition of hydrocarbon solvent can improve the diffusion process and yield higher recovery.

On the basis of above observations, this work was designed to conduct numerical simulation study for a single matrix block and test the applicability of low temperature air injection in fractured reservoirs. The numerical model was validated using data provided by Mayorquin and Babadagli (2015b), and then a sensitivity analysis was performed for matrix size and the ratios of air/propane mixtures.   Also, a scaling-up study was performed to obtain an approximate production time for different matrix block sizes and soaking times.

4.3 Experimental studies

4.3.1 Type of experiments

Ten experiments were designed in such a way to mimic a representative gas-saturated region (a secondary gas cap) in a dual-porosity medium, in which the fracture network essentially provides the reservoir-flow channels (Cinco-Ley 1996). Different -pure- gases (N_2, Air, and C_3) and gas mixtures (O_2-enriched air, Air/C_3 mixture) were injected in the fracture network and left there soaking the oil-saturated matrix at static conditions for several days. Gas was then released. The chromatographic analysis of the produced oil and gas were performed as well as the measurement of oil properties.

4.3.2 Setup

In the experiments, a dual-porosity medium was thought as a 100% heavy oil-saturated Berea sandstone core (rock matrix) inside a reactor, and the fracture system was represented by the region existing between the matrix and the interior wall of the reactor (**Figure 4-1**). The core was placed into a funnel inside a flask, which is located in the reactor (10-in.-length and 6.2-in.-diameter), which in turn was put inside an oven. Details of these four experiments are given in Chapter 2.
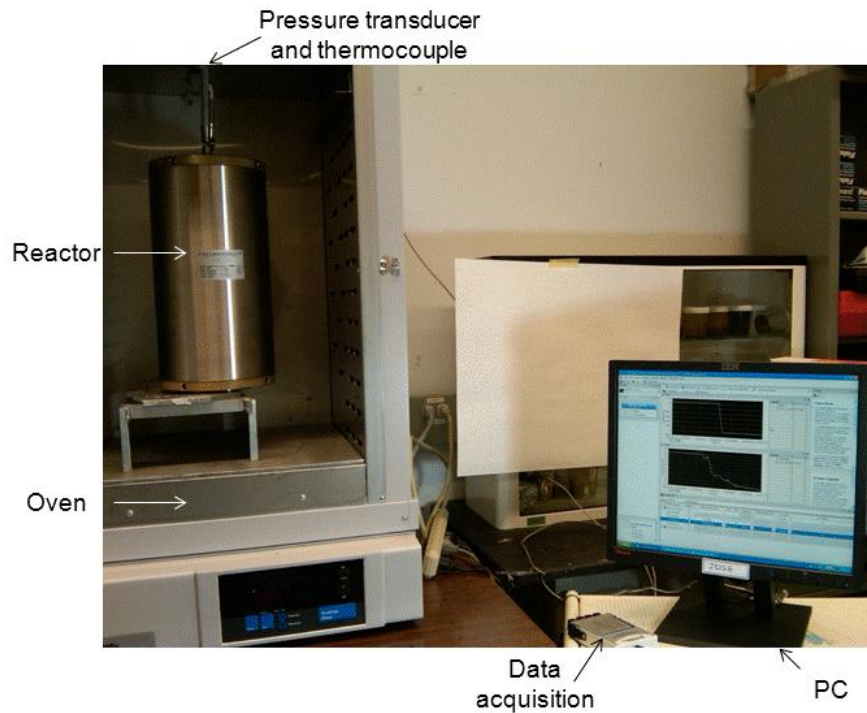
Figure 4-1 Setup for experiments (from Mayorquin-Ruiz and Babadagli 2015b).

The reactor was filled with gas at certain pressure and temperature. Reactor temperature was kept constant during a pre-established period; oil expelled from the matrix was collected in the flask where the core was placed. Once the time period ended, the gas was released from the reactor and the produced oil volume was measured. Gas pressure and oven temperature were continuously recorded over the whole period. The following analyses were performed on the produced fluids: (1) gas chromatography, (2) density, viscosity, and refractive index of oil, and (3) asphaltene content. We call this procedure (from the filling of reactor with gas to the gas release) a "cycle". Oil properties were also measured before the start of experiment.

4.3.3 Core and fluid properties

Sandstone cores were cleaned up and dried and then fully saturated with dead heavy oil (no gas in solution nor interstitial water) at vacuum pressure and laboratory temperature. Core dimensions and oil properties (density and asphaltene content) are shown in **Table 4-1**. Measurements of dead-oil viscosity (at atmospheric pressure) before the experiments were conducted with a Brookfield Viscometer model LVDV-II+P CP.

Table 4-1 Experimental fluid and core properties.

Experiment	Core				Crude-Oil Properties at Atmospheric Pressure					
	Porosity (%)	Length (in.)	Diameter (in.)	Pore volume (cm^3)	Density (°API)	Asphaltene Content (wt%)	Temperature (°C)	Density at Temperature (g/cm^3)	Viscosity at Temperature (cp)	Refractive Index at Temperature
1	19.0	6.022	1.972	57.3	10.8	28.0	75	0.9586	758.4	1.54513
2	16.5	6.000	1.978	49.9	11.6	22.5	150	0.9099	24.4	1.51722
3	15.5	5.760	1.977	44.9	12.5	26.0	75	0.9432	548.8	1.54339
4	14.6	5.495	1.979	40.4	10.9	20.4	75	0.9553	501.1	1.54366
5	16.4	5.811	1.979	48.0	12.5	34.5	200	0.8623	4.7	1.48699
6	17.0	6.054	1.978	51.8	12.5	34.5	75	0.9469	174.3	1.53443
7	18.2	6.033	1.980	55.4	12.5	30.8	75	0.9468	217.9	1.54706
8	18.5	5.701	1.979	53.3	12.3	27.2	75	0.9479	246.0	1.53673
9	17.4	6.010	1.978	52.8	12.1	29.3	75	0.9495	291.5	1.53792
10	17.7	5.843	1.976	52.1	12.1	29.3	75	0.9490	290.9	1.53767

(Table from Mayorquin-Ruiz and Babadagli 2015b)

Thermal analysis (Thermogravimetric Analysis, TGA, and Differential Scanning Calorimetry, DSC) was also done at atmospheric pressure in oil samples for experiments 1 and 2. TGA and DSC runs were done using air as oxidizing agent; two heating rates (10 and 15 °C/min) were applied in order to compare the effect of this variable. Temperature range used in TGA and DSC experiments were 25-800°C and 26-600°C, respectively. Additionally, DSC runs in similar oil samples were done at four different pressures using another DSC instrument: HP DSC 1 STAR System Mettler Toledo.

To measure the composition of gas released at the end of cycles, two instruments were used: (1) Lumidor MicroMax Pro Gas Detector (detection of peak concentration of oxygen, carbon monoxide, hydrogen sulfide and methane) and (2) Agilent Technologies 7090A GC (gas chromatography).

The asphaltene content was measured based on the weight of asphaltene deposited after being mixed in heptane and filtered in filter paper

4.3.4 Experimental results

Based on the thermal analysis four reactions were identified:

(1) Low Temperature Oxidation (LTO) and distillation: 25-280°C (not exothermic peaks in DSC).

(2) Low Temperature Combustion: 280 – 380°C. Razzaghi et al. (2008) reported low temperature combustion reaction in the range of temperature from 275 to 375ºC.

(3) HTC (High Temperature Combustion): 380 to 510°C (exothermic peaks in DSC)

(4) A second HTC (cracking reaction): 510 to 800°C.

Ten experiments were conducted as listed below; operating conditions and soaking time are shown in **Table 4-2**:

Experiment 1: Air at 75°C - Two cycles

Experiment 2: Air at 150°C - Two cycles

Experiment 3: C_3 at 75°C - One cycle

Experiment 4: Gas mixture (53.1 mol% C_3 and 46.9 mol% air) at 75°C - One cycle

Experiment 5: Gas mixture (51.5 mol% C_3 and 48.5 mol% air) at 200°C - Two cycles

Experiment 6: N_2 (vertical core) at 75 °C - Two cycles

Experiment 7: O_2-enriched air (62.7 mol% N_2 and 37.3 mol% O_2) at 75°C - Two cycles

Experiment 8: N_2 at 75°C - Two cycles (horizontal core)

Experiment 9: C_3 (cycle 1) / Air (cycle 2) / Air (cycle 3) at 75°C - Three cycles

Experiment 10: Air (cycle 1) / C_3 (cycle 2) / Air (cycle 3) at 75°C - Three cycles

Table 4-2 Experimental operating conditions.

Experiment	Cycle	Gas	Temperature (°C)	Maximum Pressure (psia)	Soaking Time (days)
1	1	Air	75	281.6	8.1
1	2	Air	75	277.8	22.1
2	1	Air	150	320	8.4
2	2	Air	150	320	21.2
3	1	C_3	75	200	9.4
4	1	C_3 (53.1 mol%) + Air (46.9 mol%)	75	197.7	8.6
5	1	C_3 (51.5 mol%) + Air (48.5 mol%)	200	281.1	8.1
5	2	C_3 (51.5 mol%) + Air (48.5 mol%)	200	283.8	8.2
6	1	N_2	75	252.4	8.0
6	2	N_2	75	256.2	8.1
7	1	N_2 (62.7 mol%) + O_2 (37.3 mol%)	75	244.3	7.1
7	2	N_2 (62.7 mol%) + O_2 (37.3 mol%)	75	243.5	8.0
8	1	N_2 (horizontal core)	75	249.5	8.1
8	2	N_2 (horizontal core)	75	244.5	8.5
9	1	C_3	75	195.6	4.5
9	2	Air	75	202.6	4.2
9	3	Air	75	176.5	3.9
10	1	Air	75	209.3	4.1
10	2	C_3	75	187.1	4.0
10	3	Air	75	187.4	4.0

(Table from Mayorquin-Ruiz and Babadagli 2015b)

Based on experimental conditions and thermal analysis results, it is concluded that the reactions that took place in experiments 1 and 2 are LTO type and distillation. The oil used in four experiments is essentially the same hence same reactions are expected to occur in all experiments. The DSC runs in heavy oil with air as oxidizing gas were carried out at different pressures (atmospheric, 300, 700 and 1000 psi) over the temperature range of 25-550 °C keeping the heating rate constant at 15°C/min. It was observed that exothermic activity shift from high temperature region to low temperature region as pressure is increased. Similar oxidation behavior with variations in pressure was reported by Li et al. (2006).

4.4 Numerical simulation

4.4.1 Numerical simulation model

A 2-D (r-z) numerical simulation model (13 x 26) was created representing the core (matrix) and the reactor void space (annular fracture) as depicted in **Figure 4-2**. Matrix is represented with 20 layers in z-direction of same thickness and the ten innermost cells in r-direction. The annular fracture is represented with 26 layers in z-direction and the three outermost cells in r-direction. Approximate cell width in r-direction is 0.25 and 1.79 cm for matrix and fracture, respectively; while approximate cell thickness is 0.75 cm for the matrix gridblocks and 1.7 cm for the fracture

gridblocks above and below the matrix gridblocks. Each numerical simulation model consists of 338 cells (200 cells for matrix, and 138 for fracture). Porosity and permeability of fracture were 99.9% and 50,000 md, respectively. Matrix permeability and diffusion coefficient were used to match the experimental data: produced oil volume and gas pressure in the reactor. A commercial thermal simulator (CMG STARS) was used to analyze and understand the mechanisms involved in the oil recovery from matrix when it is immersed in an oxidizing-solvent environment and LTO reactions occur.
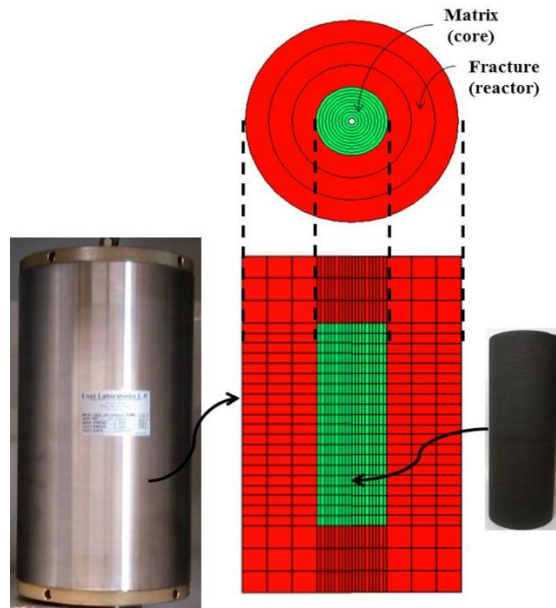
Figure 4-2 Schematics of cylindrical (r-Z) numerical model.

In general, the PVT fluid model consists of one pseudo-component for oil and, depending on the experiment, one, two or three components for gas, i.e., one component (C_3) in experiment 3; two components (N_2 and O_2) in experiments 1 and 2; and three components (N_2, O_2, and C_3) in experiment 4. PVT fluid models were created using Peng-Robinson equation of state (EOS), which was tuned to oil density and oil viscosity measurements conducted at atmospheric pressure and different temperatures. The Pedersen Corresponding States model was used to match oil viscosity data measured at atmospheric pressure and different temperatures.

125

4.4.2 Modeling of kinetic reaction

Two approaches can be followed in the numerical simulation modeling of the laboratory experiments reported by Mayorquin and Babadagli (2015b), either assuming that the process is governed solely by thermodynamics or both thermodynamics and chemical (kinetic) reactions take place in the process. As a first step, and only for some of the experiments, thermodynamics is assumed in the history matching. The second approach is more suitable if oxidation reactions occur when oxygen contacts hydrocarbons and oxygenated compounds are produced.

Reaction scheme. In this work, the numerical modeling of kinetic reactions, particularly the LTO reactions, is based on oxygenated compounds (aldehydes, alcohols, ketones) as proposed earlier by different researchers (Phillips and Hsieh 1985; Yoshiki and Phillips 1985; Clara et al. 1999; Sakthikumar and Berson 2001; Gutierrez et al. 2009; Khansari et al. 2013). In fact, two of the reaction models proposed by Khansari et al. (2013) were used in the modeling of the oxygenated compounds generated at two different ranges of temperatures. However, the stoichiometric coefficients were modified in order to get balanced the stoichiometric equations according to the characteristics of heavy oil used in experiments.

Temperature range: 50-150°C:

$$Heavy\ oil + 6\ Oxygen \xrightarrow{yields} 3.96\ Aldehydes + Coke + Water + CO + CO_2 \tag{1}$$
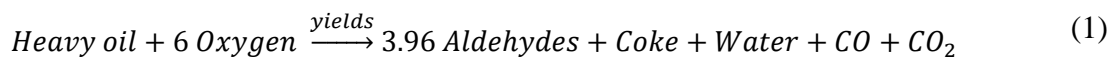
Temperature range: 150 -200°C:

$$Aldehydes\ + 4.33\ Oxygen \xrightarrow{yields} Alcohols\ + Ketones + Water \tag{2}$$
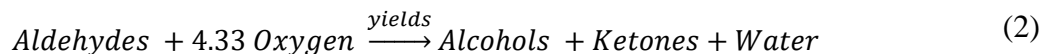
Recall that experimental studies were conducted at 75, 150 and 200°C, then reaction models for higher temperatures are not considered (the proposed approach in this work is not high temperature oxidation reactions).

Calculation of kinetic parameters. According to Bousaid and Ramey (1968), Burger and Sahuquet (1972), Fassihi et al. (1984), and Stokka et al. (2005), the oxidation rate of the crude in the LTO region or the rate of oxygen consumption can be calculated by:

$$-\frac{dC_m}{dt} = k p_{O_2}^m C_m^n \tag{3}$$

The Arrhenius equation (Brady et al. 2000) relates temperature and activation energy through the rate constant (k) defined as follows:

$$k = A exp(-E/RT) \tag{4}$$

The calculation of activation energy (E) and frequency factor (A) was done by using the method suggested by Coats and Redfern (1964) and the data reported for experiment 2 by Mayorquin and Babadagli (2015b). The resulting values were 10.1 1/s for the frequency factor and 10887.73 BTU/mole-lb for the activation energy. In the history matching of experimental data, the activation energy was used as the matching parameter. The matched value was 14500 BTU/mole-lb.

Additionally, the enthalpy was required to be introduced for the numerical calculations. This value was obtained in the laboratory from thermal analysis studies. For the LTO region the enthalpy was in the range -31.71 BTU/lb and -77.86 BTU/lb. In the numerical simulation model the enthalpy used was -31.75 BTU/lb-mole.

The same kinetic models and kinetic parameters as used by Mayorquin-Ruiz and Babadagli (2015a) obtained through their experimental measurement were applied. As mentioned earlier, some of the laboratory experiments were modeled considering thermodynamic processes (experiments 1, 2, 3, 4, 6, 7, and 8) and some others assuming thermodynamics and kinetic reactions (experiments 5, 9 and 10). **Figure 4-3** shows the comparison of oil recoveries obtained from experimental and numerical results after Cycle 1 for all experiments (Table 4-2).
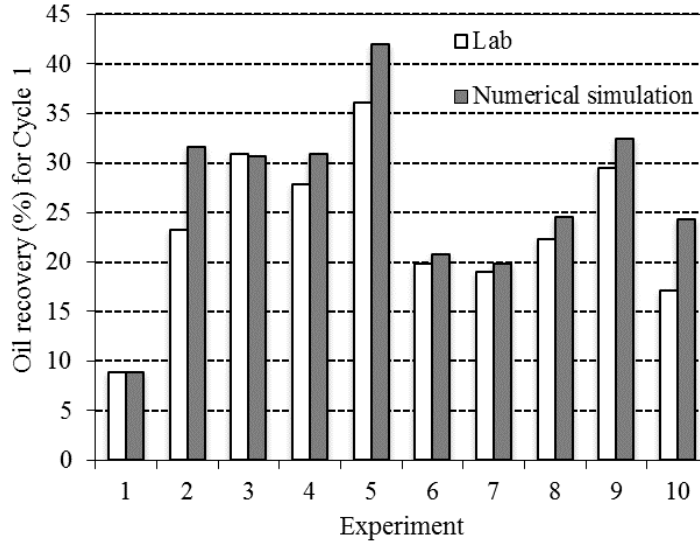
Figure 4-3 Oil recovery after Cycle 1: lab and numerical simulation matching results.

4.4.3 History matching: kinetic reactions not modeled

In general, the history matching of experiments was reasonably good. **Table 4-3** shows the range of diffusion coefficient that results from the history matching of laboratory data. For sake of simplicity, only a few comments were made for some experiments:

Table 4-3 Match results of numerical simulation models.

Diffusion coefficient (ft^2/hr)					
N_2		O_2		C_3	
Gas phase	Oil phase	Gas phase	Oil phase	Gas phase	Oil phase
$8x10^{-5}$	$1x10^{-5}$ - $5x10^{-5}$	$8x10^{-6}$	$8x10^{-8}$	$3x10^{-4}$ - $5x10^{-4}$	$1x10^{-6}$ - $3x10^{-6}$

Experiment 1: Air at 75°C - Two cycles

The history matching was acceptable: the peak point was captured as well as the early trend. Late times showed only 1-2 psi difference, which is negligible compared to the absolute pressure change in the order of 300 psi. In regards to the produced oil volume at the end of cycle 1, the match is perfect (numerical simulation and measured values are 5.15 cm^3 and 5.1 cm^3, respectively). The oxygen concentration measured in the gas mixture (in fracture) at the end of cycle 1 was 20.7 mol%, the same as in the numerical simulation model.

Experiment 2: Air at 150°C - Two cycles

A similar matching quality was observed as in Experiment 1. Additionally, the produced oil volume at the end of first cycle lies above the measured oil volume.

Experiment 3: C_3 at 75°C - One cycle

The matching of pressure as well as produced oil volume was reasonably good. On the other hand, at the end of the experiment, the measured propane concentration was 98.907 mol%, showing an agreement with the numerical simulation model value of 97.43 mol%.

Experiment 4: Gas mixture (53.1 mol% C_3 and 46.9 mol% air) at 75°C - One cycle

The gas pressure matching (**Figure 4-4**) for this experiment is also reasonable, especially at early times (first 48 hours). After this period, a slight disagreement between the simulated and measured data, but the error percentage involved is negligible (the difference between them is about 1 psi). **Figure 4-5** shows the oil distribution at the end of the experiment in the matrix transversal section at the middle of core.
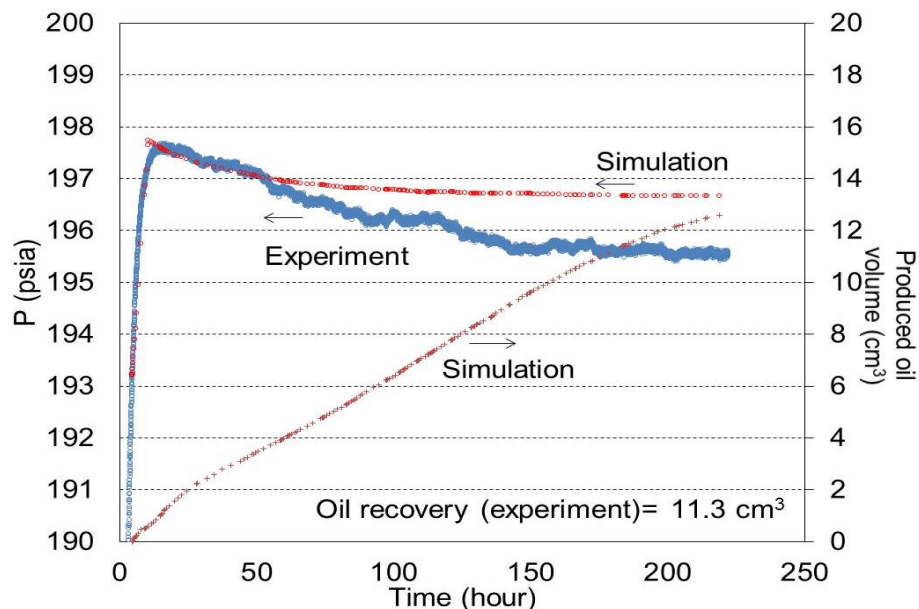
Figure 4-4 Pressure match for experiment 4 (Air/C_3@75°C).

Experiment 6: N$_2$ at 75 °C - Two cycles

In general, the history matching was good both in pressure and expelled oil volume.

Transversal section in the middle of the core
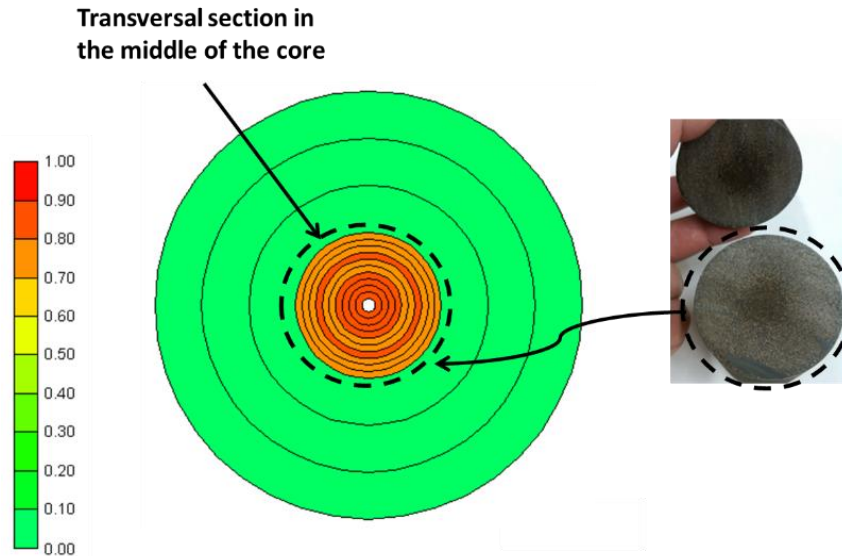
Figure 4-5 Oil saturation in core 4 at the end experiment 4 (Air/C$_3$@75°C).

4.4.4 Sensitivity analysis

After ensuring an acceptable match to experimental data the validated numerical model was used for further sensitivity analysis. In this exercise, two variables were considered: (1) gas mixture concentration, and (2) matrix size. In both sensitivity analyses, the rock properties were kept constant: horizontal matrix permeability (250 md), matrix vertical permeability (150 md), fracture permeability (50 darcies), matrix porosity (0.124), and fracture porosity (0.999). The PVT model used is the one used for the matching of experiment 4 and it was not changed at all. The diffusion coefficients used are the same as those obtained in the match of experiment 4. A gas mixture of propane (53.1 mol%), nitrogen (36.9 mol%) and oxygen (10.0 mol%) was considered as base case. The design of the runs included the same steps followed in the experimental work, i.e., a heavy-oil saturated core was soaked into a gas mixture at static conditions for nine days. It is assumed that matrix is inside a chamber or reactor of same dimensions of that used in experimental setup.

The sensitivity analysis results are shown in terms of oil recovery with time. For this particular study, the oil recovery is defined as the cumulative oil at the bottom fracture (no producer well was modeled in order to mimic the experimental conditions).

Concentration in the gas mixture. An optimal design of low temperature (LTO) air injection was the main interest of this study. Hence, minimizing the expensive hydrocarbon concentration is the critical task in this sensitivity analysis study. Five cases of Air/C_3 mixture concentrations were analyzed at 75°C as given below.

Case 1. C_3 (100 mol%)

Case 2. C_3 (75 mol%) + N_2 (19.7 mol%) + O_2 (5.3 mol%)

Case 3. C_3 (53.1 mol%) + N_2 (36.9 mol%) + O_2 (9.9 mol%)

Case 4. C_3 (25 mol%) + N_2 (59.1 mol%) + O_2 (15.9 mol%)

Case 5. N_2 (78.8 mol%) + O_2 (21.2 mol%), i. e. air

Figure 4-6 shows the results of numerical simulation for the above cases. It can be observed that the air case produces the lowest oil recovery while C_3 case produces the highest amount. Also, the addition of solvent to air enhances oil recovery. An optimum Air/C_3 ratio should be defined for particular reservoir conditions.
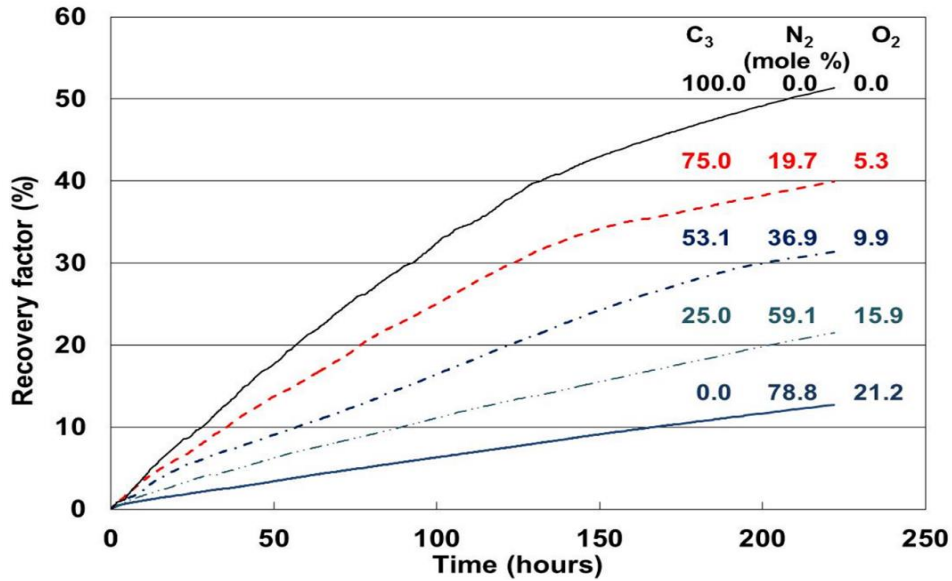
Figure 4-6 Effect of Air/C$_3$ mixture concentration in oil recovery.

Matrix size. Matrix size is a critical parameter controlling the diffusion and gravity drainage processes. Thus, the following scenarios were considered to scrutinize the effect of this parameter considering a cylindrical shape of the matrix:

Case 1. Diameter = 1.9790-in., length = 5.495-in.

Case 2. Diameter = 3.5795-in., length = 9.000-in.

Case 3. Diameter = 4.1333-in., length = 9.000-in.

The result of numerical simulation runs changing the size of the matrix is shown in **Figure 4-7**. As seen, the oil recovery is extremely sensitive to the vertical length of the matrix indicating the importance of diffusion augmented gravity drainage.
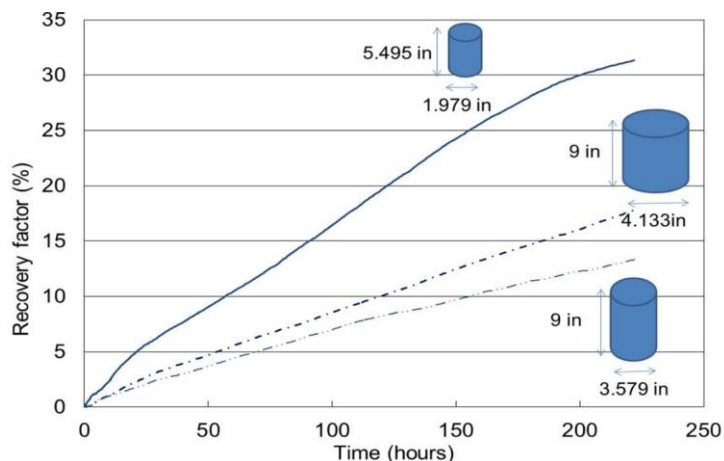
Figure 4-7 Effect of matrix size in oil recovery.

4.4.5 History matching: kinetic reactions modeled

Experiment 10: Air/C_3/Air gas at 75°C - Three cycles.

Chemical reactions were modeled in this case. In general, the history matched-pressure is good (**Figure 4-8**); less than 1% pressure difference between experimental data and numerical simulation model exists at the end of each cycle. It is also important to notice that the declining pressure trend is reproduced in all cycles due to effective diffusion and oxidation reactions. An analysis of the distribution of fluid components in the matrix at different depths and radial positions (centre, middle, edge) at the end of cycles was performed. **Figure 4-9** shows a schematic of the analyzed regions. **Figure 4-10** displays the distribution of oil, C_3, and oxygenated compounds (aldehydes, alcohols, ketones) in the matrix at the end of cycles 1, 2 and 3.
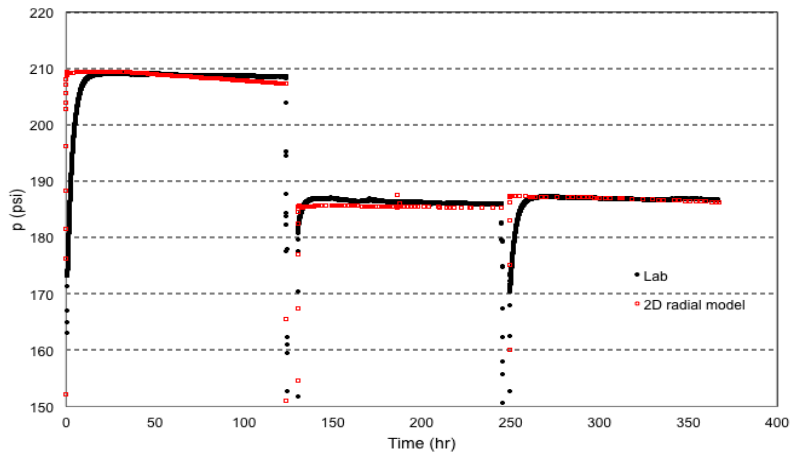
Figure 4-8 Pressure match for experiment 10 (Air/C₃/Air@75°C).
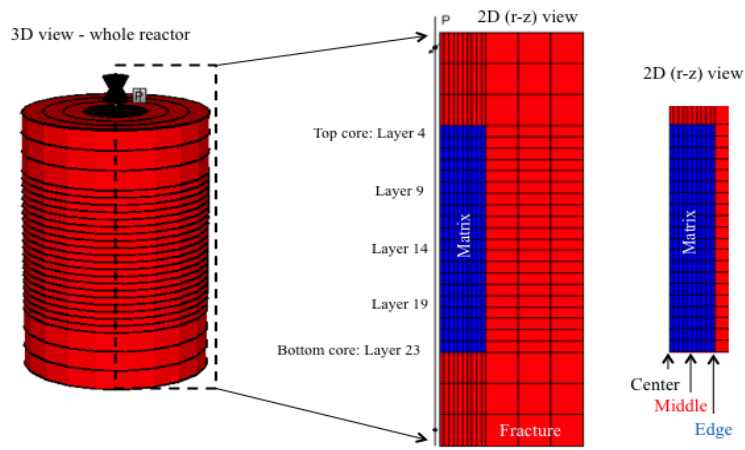
Figure 4-9 Numerical simulation model: experiment 10 (Air/C₃/Air@75°C).

Component saturation

	End of cycle 1	End of cycle 2	End of cycle 3
Compone			

Oil

C3

Center — Half — Edge

Aldehyde

Alcohol

Ketone

Figure 4-10 Component saturation in matrix liquid for experiment 10 (Air/C₃/Air@75°C).
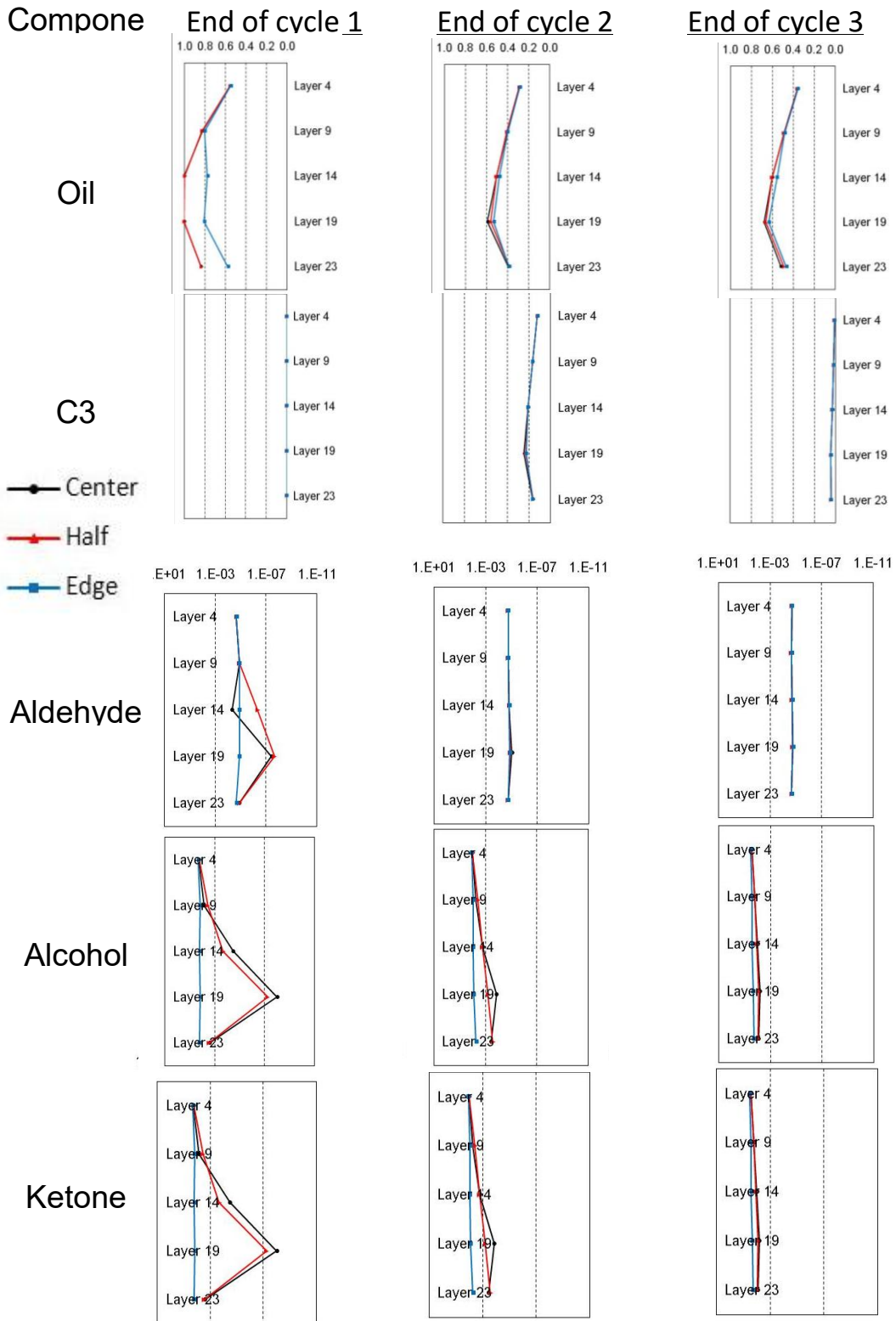
$$\text{Figure 4-10 Component saturation in matrix liquid for experiment 10 (Air/C}_3\text{/Air@75°C).}$$

Critical observations can be listed as follows:

(1) The oil is drained out from the matrix by means of voidage replacement of oil by fracture gas (Air, C_3) and gas diffusion into matrix (Rodriguez et al. 2004 observed a similar mechanism in presence of N_2).

(2) Oxygenated compounds are generated in the matrix and their saturations are higher at top and edge of the core.

(3) In general, the oxygenated compounds saturation increases smoothly with time.

(4) The lack of oil expulsion from the matrix in cycle 3 (compared with cycle 2) can be attributed to relatively high saturation of oxygenated compounds along the core.

Additionally, an analysis of the liquid volume change with time was implemented and observed that matrix liquid volume decreases as it is expelled from the matrix while the fracture fluid volume (fluid volume accumulated at the bottom horizontal fracture) increases. It was observed that fracture liquid volume increases more rapidly than the decrease of the matrix fluid volume, which can be attributed to the oxygenated compounds that are generated in the fracture; i. e. the oxidation reactions occur faster in fracture oil than in matrix oil. Also, fracture porosity is 1.0, hence, the diffusion is higher (molecular diffusion) than effective diffusion in the matrix.

4.4.6 Upscaling study

The objective of the up-scaling study was to obtain an approximate production time for different matrix block sizes. This study was done based on a 3D (x-y-z) homogeneous single-porosity single-matrix explicit-fracture numerical simulation models depicting a fractured medium: one matrix cubic-shaped model block surrounded by fractures (**Figure 4-11**). A huff-and-puff process was modeled by means of a vertical injector/producer well completed in the corner of the fracture system; the injector well completed in the upper half of the block height while producer well completed in the lower half of the block height. Gas (Air, C_3, Air/C_3) injection was carried out until the shut in pressure (210 psi) and left soaking the oil saturated matrix block for a period (soaking time) and then put into production until RF was practically unchanged. Three soaking times were modeled: 1, 2, and 3 months. Also, two temperatures were analyzed: 75 and 150°C.

The same PVT model was used in all numerical simulation models and LTO reactions were also included in the model.
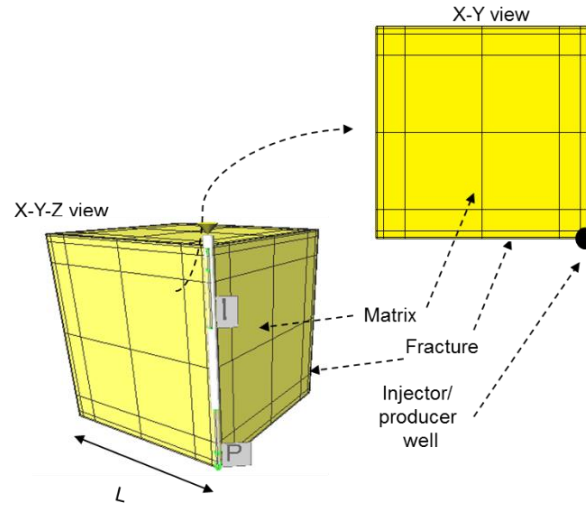
Figure 4-11 Schematics of numerical simulation model for up-scaling study.

Six matrix block-sizes were considered in the up-scaling study: 100, 180, 333, 500, 750 and 1000 cm; fracture width for each of these cases was 0.78, 1.4, 2.6, 5.55, 5.9, and 7.83 cm, respectively. The fracture width varied depending on matrix-block size but, in all cases, the fracture pore volume/matrix pore volume ratio was 0.3. The numerical simulation models took into account the information obtained in the history matching of the data of experiment 10.

At initial conditions the matrix block is 100% heavy oil-saturated (no free gas, no solution gas, no water saturation) and fracture system is saturated with gas. Reservoir properties are shown in **Table 4-4**.

Table 4-4 Numerical simulation model properties for up-scaling study.

Matrix porosity	0.1589
Fracture porosity	0.999
Matrix permeability (kx, ky)	320 md
Matrix permeability (kz)	192 md
Fracture permeability	50,000 md
Reservoir temperature	75, 150°C
Solvent type	Propane

Prior to the up-scaling a study of matrix block gridding resolution was done in order to analyze the degree of numerical dispersion. Different uniform matrix block grids were assessed for each matrix block size: 1x1x1, 3x3x3, 5x5x5, 7x7x7, and 9x9x9 being the total gridding (matrix and fractures): 3x3x3, 5x5x5, 7x7x7, 9x9x9, and 11x11x11. Some numerical simulation runs did not converge. Additional runs were done changing the time step: 1, 3, 5, 10 and 30 days.

Even after reducing the grid size and time steps, numerical instabilities were observed which were likely due to a large contrast in the grid cell size used in the discretization of neighboring matrix block and fracture cells. To solve this problem, non-uniform cells were used in the modeling: matrix block grids used were 6x6x6 and 8x8x8; numerical simulation performed better with 6x6x6; time step used was 3 days. It should be emphasized that numerical simulation instabilities were greatly reduced with the use of non-uniform grids. However, certain cases still showed instabilities but available results allowed to obtain well defined trends.

Results of upscaling study. The outcome from the up-scaling exercise is presented as recovery factor (RF) change against the matrix size and time (log-log scale). For each temperature cases (75 and 150°C), an explanation is given about the time (logarithmic value) required to reach RFs of 2, 6 and 10% for different matrix block sizes for different type of injection gases.

Up-scaling at 75°C:

Figure 4-12 shows the plots log (L) vs. log (t) for different soaking times, type of gas, and recovery factors. For the air case and RFs from 2 to 10% (Figure 4-12a,b,c), it is observed that time systematically increases as the block size (log L) gets larger regardless of the soaking time. Air does not provide any gain in terms of production through viscosity reduction as it does cause any viscosity reduction by diffusing into oil. It acts as a pressurizing agent but its effects on oil viscosity increase due to oxygenation are expected. The effect of all these processes are reflected in a systematic manner as the matrix size gets larger and this is represented as a linear trend in the log-log plots given in Figure 4-12a,b,c.
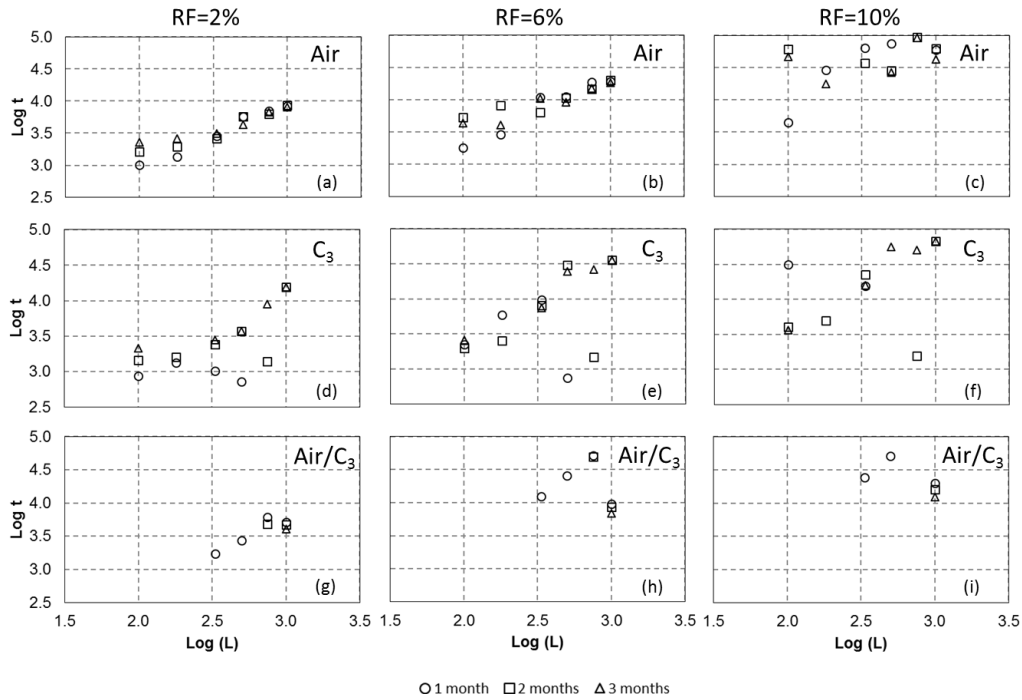
Figure 4-12 Log t (time) vs. Log L (matrix size) at 75°C.

When pure C_3 (propane) is injected (Figure 4-12d,e,f), similar -linear- trends were captured. The soaking time effect is more obvious in this case compared to the previous air injection process. As the soaking time increases, less time is needed to reach a particular RF (2, 6 and 10%). This observation was true for any block size. It is clear that diffusion plays a role in the oil production mechanism when C_3 is injected and its effect is larger for the smaller block sizes (Figure 4-12b). C_3 diffuses into matrix oil reducing its viscosity and enhances the gravity drainage process.

On the other hand, when air/C_3 mixture is injected, benefits from C_3 can be observed compared to the air case. As mentioned before, a certain degree of numerical instabilities were detected mainly in air/C_3 mixture runs but meaningful trends were captured especially at the early stages of the process (Figure 4-12g and Figure 4-12h). As the soaking time increases (block size 1000 cm or Log=3, Figure 4-12g,h,i), the time needed to reach a certain RF is reduced. This time is lower than the air case (Figure 4-12a,b,c) meaning that oil recovery is produced faster in air/C_3 mixture case compared to the air case.

139

The results at this high temperature condition are plotted similarly as in low temperature case. **Figure 4-13** shows the (Log L) vs. (Log t) plots for different injected gases at different recovery factors. Interestingly, temperature controls the process and the viscosity reduction due to higher temperature results in a similar recovery times for all the blocks at the earlier stages (RF=2% and 6%) for the air and C_3 cases (Figure 4-13a,b,d,e,g, and h). At later times (RF=10%), the matrix size effect became critical and larger matrix sizes caused faster recovery (Figure 4-13c,f,l). This is systematically seen in all three gases injected (even though they represent different slopes) and can be attributed to enhanced gravity due to increasing matrix height also assisted by reduced viscosity due to diffusion of C_3.
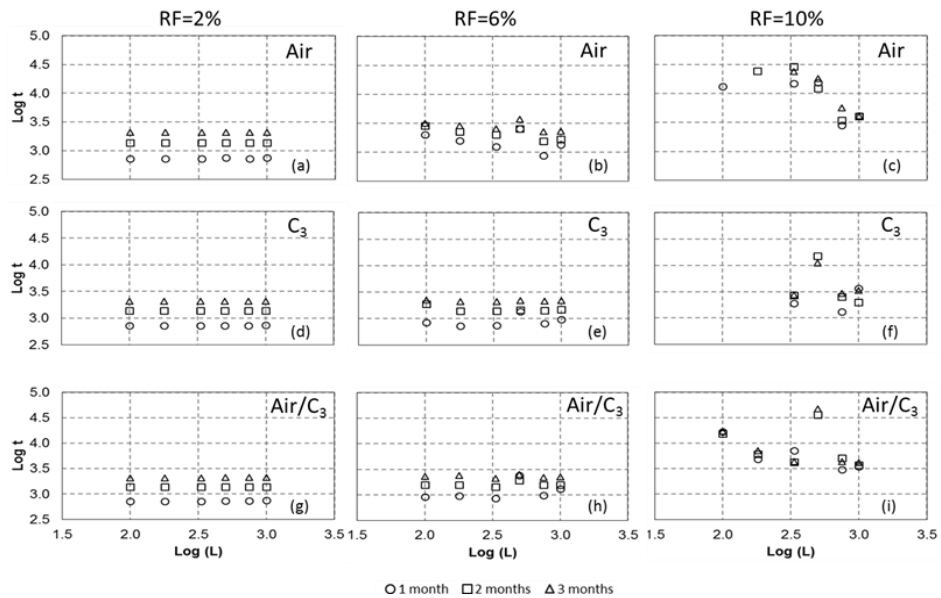
Figure 4-13 Log t (time) vs. Log L (matrix size) at 150°C.

Based on the systematic and linear behavior on the log-log scale (Figure 4-12 and Figure 4-13), one may come up with scaling correlations. **Figure 4-14** shows the relationships for each gas injected (air, C_3, air/C_3 mixture) for a RF value of 10% (almost end of the process) at 75 and 150°C.
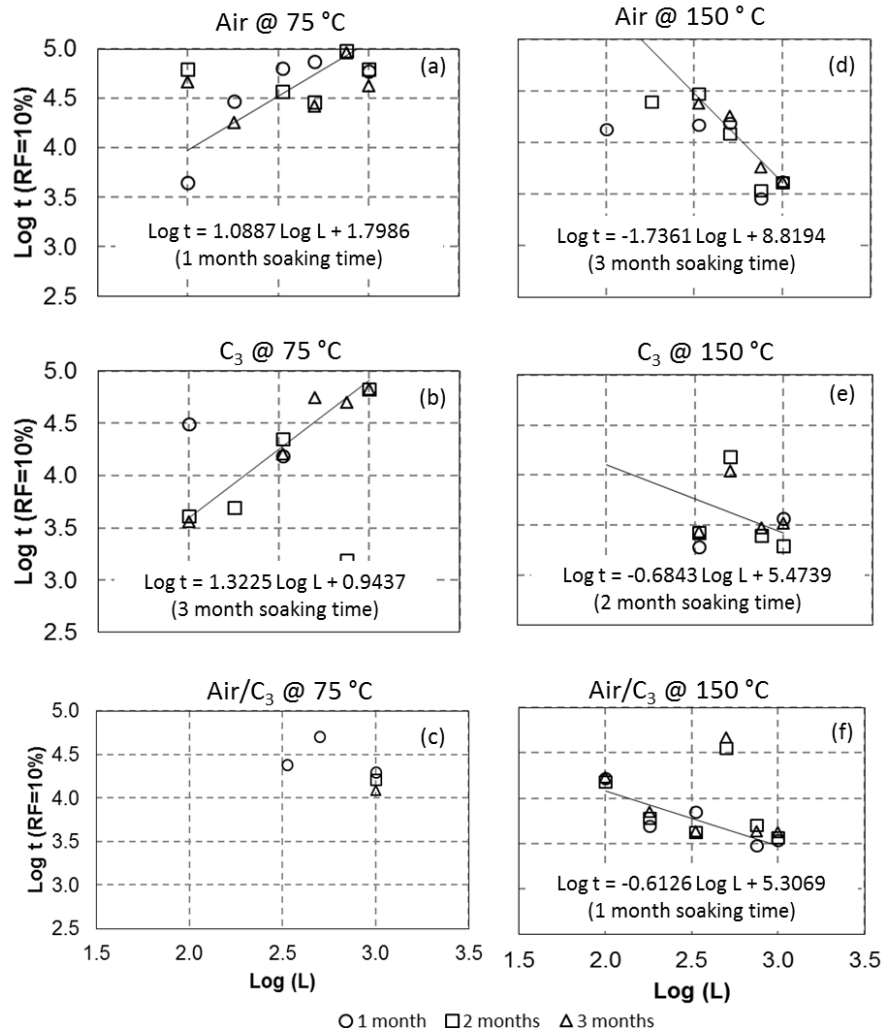
Figure 4-14 Log t (time) vs. Log L (matrix size) at RF=10% at 75 and 150°C.

Based on the best curve fitting results, the following relationships are proposed for each gas type:

At 75°C :　　　Air: t ~ $L^{1.0887}$　　　C_3: t ~ $L^{1.3225}$

At 150°C:　　　Air: t ~ $L^{(-1.7361)}$　　　C3: t ~ $L^{(-0.6843)}$　　　Air/C_3: t ~ $L^{(-0.6126)}$

Note that the air/C_3 case at 75°C did not show a trend due to lack of data caused by numerical instability problems, especially for smaller matrix sizes.

4.5 Conclusions

1.   Using previously published experimental data, a numerical model to simulate matrix behavior during air and hydrocarbon gas injection in fractured reservoirs was validated. Sensitivity runs were performed to analyze the effect of the ratio of Air/C_3 mixture and matrix size. The process is extremely sensitive to matrix size, especially the vertical length.

2.   With the given simulation scheme, the optimization of air injection (assisted by hydrocarbon solvents) can be achieved based on the minimized hydrocarbon solvent for a given matrix size.

3.   The oil production mechanisms acting in a matrix block surrounded by gas (air, air/C_3 mixture) filling the fractures are: 1) gas-oil gravity drainage, 2) effective diffusion, 3) voidage replacement of oil by gas. Viscous forces also play a role once the producer well is open to production.

4.   Oxygenated compounds produced in matrix oil due to LTO reactions lessen the effect of gravity drainage. This negative effect is reduced when C_3 is injected.

5.   The degree of participation of different oil production mechanisms depends on oil viscosity, temperature, soaking time, block size, type of gas (air, C_3, air/C_3).

6.   Air (oxygen) reacts with both matrix oil and fracture oil; oxygen in the fracture is diffused freely to fracture oil in the absence of matrix.

7.   From the up-scaling study based on different matrix sizes, a non-integer exponent is obtained from the logarithmic relationship between the time to reach RF=10% and matrix size. These exponents are defined for different temperatures and type of gases.

4.6 Nomenclature

A   = Arrhenius constant (also known as frequency factor or pre-exponential factor)

C_m = instantaneous concentration of fuel

C_3 = Propane

CMG   = Computer Modelling Group

CO   = Carbon monoxide

CO_2 = Carbon dioxide

DSC   = Differential Scanning Calorimetry

E   = Activation energy

EOS   = Equation of state

HPDSC = High Pressure Differential Scanning Calorimetry

k   = rate constant

L   = Matrix block side length

LTAI   = Low-temperature air injection

LTASI = Low-temperature air-solvent injection

LTO   = Low Temperature Oxidation

m, n   = reaction orders

N_2 = Nitrogen

NFR   = Naturally fractured reservoir

O_2 = Oxygen

p^m_{O2} = partial pressure of oxygen

PVT   = Pressure-Volume-Temperature

R   = Universal gas constant

RF   = Recovery factor

SARA = Saturates- Aromatics-Resins-Asphaltenes

T   = Temperature

TGA   = Thermogravimetric Analysis

References

Belgrave, J.D. M., Moore, R.G., Ursenbach, M. G. et al. 1990. A Comprehensive Approach to In-Situ Combustion Modeling. *SPE Advanced Technology Series* **1** (1): 98–107. SPE-20250-PA. http://dx.doi.org/10.2118/20250-PA.

Bousaid, I.S. and Ramey Jr., H.J. 1986. Oxidation of Crude Oil in Porous Media. *SPE J* **8** (02): 137–148. SPE-1937-PA. http://dx.doi.org/10.2118/1937-PA.

Brady, J.E., Russell, J.W., and Holum, J. R. 2000. *Chemistry. Matter and its changes*, third edition. John Wiley & Sons, Inc., p. 599.

Burger J.G. and Sahuquet, B.C. 1972. Chemical Aspects of In-Situ Combustion–Heat of Combustion   and   Kinetics.   *SPE   J*   **12**   (05):   410–422.   SPE-3599-PA. http://dx.doi.org/10.2118/3599-PA.

Cinco-Ley, H. 1996. Well Test Analysis for Naturally Fractured Reservoirs. *J Pet Technol* **48** (01): 51–54. SPE-31162-JPT. http://dx.doi.org/10.2118/31162-JPT.

Clara, C., Durandeau, M., Queanault, G., and Nguyen, T-H. 1999. Laboratory Studies for Light Oil Air Injection Projects: Potential Application in Handil Field. Presented at the SPE Asia

Pacific Oil and Gas Conference and Exhibition, Jakarta, 20–22 April. SPE-54377-MS. http://dx.doi.org/10.2118/54377-MS.

Coats, A.W. and Redfern, J.P. 1964. Kinetic Parameters from Thermogravimetric Data. *Nature* **201**: 68–69. doi:10.1038/201068a0.

Fassihi, M.R., Brigham, W.E., and Ramey Jr., H. J. 1984. Reaction Kinetics of In-Situ Combustion: Part 1-Observations. *SPE J* **24** (04): 399–407. SPE-8907-PA. http://dx.doi.org/10.2118/8907-PA.

Fatemi, S.M., Kharrat, R. and Vossoughi, S. 2008. Feasibility Study of In-Situ Combustion (ISC) in a 2-D Laboratory-Scale Fractured System Using a Thermal Simulator. Presented at the World Heavy Oil Congress 2008, Edmonton, 10–12 March. Paper 2008-449.

Gutierrez, D., Moore, R.G., Mehta, S. A. et al. 2009. The Challenge of Predicting Field Performance of Air Injection Projects Based on Laboratory and Numerical Modelling. *J Can Pet Technol* **48** (04): 23–34, PETSOC-09-04-23-DA. http://dx.doi.org/10.2118/09-04-23-DA.

Khansari, Z., Kapadia, P., Mahinpey, N. et al. 2013. Kinetic Models for Low Temperature Oxidation Subranges based on Reaction Products. Presented at the SPE Heavy Oil Conference, Calgary, 11–13 June. SPE-165527-MS. http://dx.doi.org/10.2118/165527-MS.

Li, J., Mehta, S.A., Moore, R.G. et al. 2006. Investigation of the Oxidation Behaviour of Pure Hydrocarbon Components and Crude Oils Utilizing PDSC Thermal Technique. *J Can Pet Technol* **45** (01): 48–53, PETSOC-06-01-04. http://dx.doi.org/10.2118/06-01-04.

Mayorquin-Ruiz, J.R. and Babadagli, T. 2015a. Low Temperature Air Injection at the Mature Stage of Deep Naturally Fractured Heavy-Oil Reservoirs: Field Scale Modeling. Presented at the Pan American Mature Fields Congress, Veracruz, 20–22 January. Paper PAMFC15-141.

Mayorquin-Ruiz, J.R. and Babadagli, T. 2015b. Low-Temperature Air/Solvent Injection for Heavy-Oil Recovery in Naturally Fractured Reservoirs. *J Can Pet Technol* **54** (03): 148–163. SPE-174542-PA. http://dx.doi.org/10.2118/174542-PA.

Peaceman, D.W. 1977. *Fundamentals of Numerical Reservoir Simulation*. Elsevier Scientific Publishing Company, p. 164

Phillips, C.R. and Hsieh, I. 1985. Oxidation Reaction Kinetics of Athabasca Bitumen. *FUEL* **64** (7): 985–989. http://dx.doi.org/10.1016/0016-2361(85)90155-3.

Razzaghi, S., Kharrat, R., and Vossoughi, S. 2008. Design of In Situ Combustion Process by Using Experimental Data. Presented at the World Heavy Oil Congress, Edmonton, 10–12 March. Paper 2008-349.

Rodríguez, F. Sanchez, J.L., Galindo-Nava, A. 2004. Mechanisms and Main Parameters Affecting Nitrogen Distribution in the Gas Cap of the Supergiant Akal Reservoir in the Cantarell Complex. Presented at the SPE Annual Technical Conference and Exhibition, Houston, 26 – 29 September. SPE-90288-MS. http://dx.doi.org/10.2118/90288-MS.

Sakthikumar, S. and Berson, F. 2001. Air Injection into Light and Medium-Heavy Oil, Carbonate Reservoirs. Presented at the EXITEP 2001, Mexico, 4–7 February.

Sequera, B., Moore, R. G., Mehta, S.A. et al. 2010. Numerical Simulation of In-Situ Combustion Experiments Operated Under Low Temperature Conditions. *J Can Pet Technol* **49** (01): 55-64. SPE-132486-PA. http://dx.doi.org/10.2118/132486-PA.

Shulte, W.M., and De Vries, A.S. 1985. In-Situ Combustion in Naturally Fractured Heavy Oil Reservoirs. *SPE J* **25** (01): 67–77. SPE-10723-PA. http://dx.doi.org/10.2118/10723-PA.

Stokka, S., Oesthus, A. and Frangeul, J. 2005. Evaluation of Air Injection as an IOR Method for the Giant Ekofisk Chalk Field. Presented at the SPE International Improved Oil Recovery Conference, Kuala Lumpur, 5–6 December. SPE-97481-MS. http://dx.doi.org/10.2118/97481-MS.

Tabasinejad, F., Karrat, R., and Vossoughi, S. 2006. Feasibility Study of In-Situ Combustion in Naturally Fractured Heavy Oil Reservoirs. Presented at the International Oil Conference and Exhibition in Mexico, Cancun, 31 August – 2 September. SPE-103969-MS. http://dx.doi.org/10.2118/103969-MS.

Yang, X. and Gates, I. D. 2008. History Match of an Athabasca Bitumen Combustion Tube Experiment. Presented at the World Heavy Oil Congress, Edmonton, 10 – 12 March. Paper 2008-441.

Yoshiki, K.S. and Phillips, C.R. 1985. Kinetics of the Thermo-Oxidative and Thermal Cracking Reactions of Athabasca Bitumen. *FUEL* **64** (11): 1591–1598. http://dx.doi.org/10.1016/0016-2361(85)90377-1.

Chapter 5 : Field Scale Numerical Modeling of Low Temperature Air Injection with Propane for Heavy-Oil Recovery from Naturally Fractured Reservoirs

5.1 Summary

The alternatives for EOR in heavy oil deep fractured reservoirs are limited. Air injection is one of the options but running it in the high temperature mode, namely in-situ combustion, has technical limitations (poor areal distribution of injected air) because of highly heterogeneous characteristics of fractured reservoirs. This may also create a problem from safety point of view, i.e., there is a risk that oxygen is not completely consumed in reservoir reaching production wells quickly without fully consumed. Air, however, can be used as a pressurizing agent to recover matrix oil in the low temperature oxidation mode (LTO) even though it may result in oxidation of oil that forms asphaltenes. Our recent lab results showed that injecting a mixture of air–propane instead of pure air might reduce these negative effects. This enhanced diffusion of air and propane into matrix may also add to recovery. Hence, those lab results opened the window to think of air injection (LTO mode) as a way to produce some of the oil left in the matrix in addition to its pressurizing effect.

In the present study, a single porosity numerical simulation model, with explicit representation of fractures, was developed to analyze the injection of a mixture of gases in a naturally fractured reservoir, involving the use of air in the LTO mode. A sector model of a hypothetical fractured heavy oil reservoir was created and several air-gas injection cases such as pure air, propane-air-propane and air-propane-air cycles were analyzed. The runs were performed using the diffusion data obtained from our previous experimental studies. Different scenarios of huff-and-puff options (cycle type and duration) were tested.

Attention was paid to oxygen consumption in the matrix, while fracture to matrix oxygen transfer was mainly due to voidage replacement of oil by air, and some through diffusion of air into matrix during the injection and shut off periods of each cycle.

The results obtained considering various shut in times and injection rates scenarios as well as safety aspects, showed benefits in the use of air in the LTO mode mixed with propane. This optimized air injection scheme could be considered as an alternative to develop naturally fractured heavy oil fields.

5.2 Introduction

5.2.1 Problem description

Air injection in light and medium oil reservoirs has been implemented and analyzed for decades in non-fractured reservoirs in two modes: low temperature oxidation (LTO) and high temperature oxidation (HTO). In addition, a limited number of laboratory studies on in-situ combustion in naturally fractured heavy oil reservoirs were documented. For example, Shulte and de Vries (1985) showed that diffusion of fracture oxygen into matrix oil governed the burning process; Fatemi et al. (2011) reported experimental results of ISC obtained from a model of crushed rock. Awoleke et al. (2010) presented experimental results investigating the effects of different scales of porous medium heterogeneity on ISC and concluded that the ISC process was challenged by relatively fast transport of air through high-permeability zones.

The numerical model study performed by the same authors showed that oxygen breakthrough occurred when a critical value in air-injection rate, which was determined by fracture spacing, was exceeded. Experimental studies are needed in the LTO mode for fractured heavy oil reservoirs in order to understand different aspects of the oil production mechanisms involved in this oxidation mode.

When air injection is considered for enhanced oil recovery in naturally fractured heavy oil reservoirs, it is commonly thought to be a thermal EOR process, referring to air injection at high temperature oxidation conditions, namely in-situ combustion. However, frontal heat displacement may not be possible in naturally fractured reservoirs (NFR) even if the combustion conditions are met. Therefore, the question is whether air at LTO conditions can be injected relying only on oxidation reactions with fracture oil and oil in the matrix after air is transferred into it.

Drawbacks in the use of air at LTO conditions could explain its lack of use in heavy oil reservoirs. For example, air is not an inert, non-reactive, gas; oxygen addition reactions occur when oxygen contacts hydrocarbons from which oxygenated compounds, such as asphaltenes (Gutierrez et al. 2009) are generated increasing the oil viscosity. However, important benefits are usually disregarded, such as the unlimited availability of air and less cost compared to other

fluids (nitrogen); the use of existing gas injection facilities; pressure maintenance; and the substitution for gas produced from the gas cap. Hence, if one can consume all the oxygen through kinetic reactions with oil in the fractures and in the matrix, after oxygen is transferred into it, this process may be a success. At this point, one has to make sure that the negative outcome of the reaction of oxygen in the air with oil (viscosity increase through polymerization) is minimized. Thus, one has to find out under what condition this is overcome and what is the minimal temperature to avoid this outcome. In other words, one need to determine how to minimize the drawbacks of the LTO air injection and determine conditions required for a successful application; conditions under which LTO air injection is not beneficial at all need also be determined.

5.2.2 Proposed solution

Mayorquin-Ruiz and Babadagli (2012a) reported the results of experimental studies conducted on heavy oil-saturated sandstone cores (surrounded by an annular fracture) soaked into air-solvent mixtures, also comparing the observations with the extreme cases, i.e., 100% air and 100% solvent. They concluded that a higher recovery factor was obtained by soaking the matrix cores into an air-solvent chamber at static conditions than in pure air. Note that gas was injected into annular fracture up to a certain pressure and the system was shut down for soaking. Thus, this mimics a huff&puff process (cyclic gas injection) and diffusion and gravity drainage are the controlling production mechanism rather than fluid drive. They also observed a lower asphaltene deposition in an air-solvent mixture than in 100% air. Later, Mayorquin-Ruiz and Babadagli (2012b) matched experimental results by means of one-matrix numerical simulations models which were then used for performing sensitivity analysis to parameters such as air - propane ratio and matrix block size.   They found that the lower recovery factor was obtained when using pure air, and the higher when using pure propane, all this at lab size matrix. They concluded that the process is extremely sensitive to matrix block size, especially the vertical length. The numerical simulation model was limited to a one-matrix core and further analysis is required for larger scales in order to capture all the phenomenology of the field scale recovery process.

5.2.3 Description of the process

The analyzed approach in this paper is a huff-and-puff process on a single matrix block at the field scale. The recovery process consisting of three phases:

Phase-1: Gas (air or solvent) is injected to fill-up the fracture system (i. e. fracture gas saturation=100%) so that matrix blocks are soaked in gas.

Phase-2: This is a soaking period at static conditions (no fluid production nor fluid injection) during which gas components diffuse into matrix oil and oxygen reacts with it. This is a critical phase for two reasons: 1) proper oxygen consumption is intended to occur thus enough soaking time must elapse in order to reach the lowest oxygen concentration in fluids to be produced in phase-3; and 2) solvent is intended to diffuse in matrix oil and reduce its viscosity.

Phase-3: Both injected gases and gases generated from kinetic reactions are produced back as well as oil expelled from the matrix to the fracture system. Oxygen concentration in produced fluids must comply with safety regulations, to minimize the risk of explosion. Fassihi et al. (2014) stated that if oxygen is found in the producers, the flammability limit needs to be compared against its concentration and the flammability limits need to be established experimentally at the pressures experienced in the production well. If found close to the limit, the producer needs to be shut in.

In this work a numerical simulation model with explicit fractures is created and used to study the effect of gas type and production-soaking schemes on recovery factor and oxygen consumption. These studies are intended to clarify the conditions for oxygen to be completely consumed in the reservoir so that it does not reach the producer well unconsumed.

5.3   Background data

Static diffusion experiments were performed on sandstone heavy oil – saturated cores (2-in.-diameter, 6-in.-length) soaked in gas; different gas types such as air, propane, and air/propane mixture were analyzed. Core and gas are contained in a reactor (**Figure 5-1**) at given pressure (between 175 and 320 psi) and temperature (75, 150, 200°C) conditions for a certain period of time (for example 4, 8 and 20 days), after which the gas is released, and the volume of oil

expelled from the matrix is measured. This process is called a "cycle". One to three cycles were applied using the same or different type of gases at each cycle. The tested gases were nitrogen, air, oxygen-enriched air, propane, and a mixture of air-propane. Experimental setup details as well as lab results are reported by Mayorquin and Babadagli (2012a).
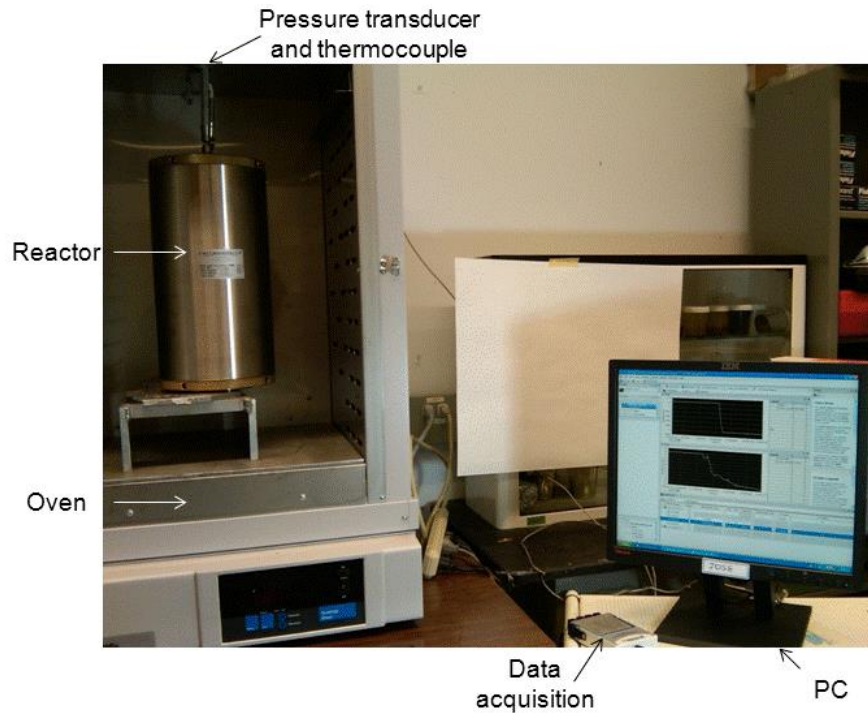
Figure 5-1 Experimental setup (from Mayorquin and Babadagli 2012a).

Later, a numerical simulation study was conducted in which the previous experimental studies were history-matched using a 2D (r-z) numerical simulation model. Then, using the matched numerical simulation model, a sensitivity study to matrix size was performed from which it was found that the process is extremely sensitive to matrix size. Mayorquin and Babadagli (2012b), reported details from this study in which three matrix block sizes were analyzed: 1) 1.9790-in.-diameter, 5.495-in.-length; 2) 3.5795-in.-diameter, 9.0-in.-length; and 4.1333-in.-diameter, 9.0-in.-length. Figure 4-7 shows results for these three cases. At 225 hr of simulation time, the highest oil recovery was observed in shorter matrix block (i. e. case 1, having the highest area/volume ratio), and the lowest oil recovery corresponded to case 3 (i. e. case 3, having the lowest are/volume ratio). It should be emphasized that this sensitivity analysis was done up to 225 hours. At longer times, higher recovery factor is expected from the blocks having longer height.

5.4   Modeling study

5.4.1 Numerical model

3-D (Cartesian), multi-component, thermal, single-porosity (explicit fracture) numerical simulation models were created. Model 1 (**Figure 5-2a**) represents one-matrix 10-m-cubic-shaped block surrounded by fractures whereas Model 2 **(Figure 5-2b)** contains eight-matrix 5-m-cubic-shaped blocks, each of them surrounded by fractures. These were homogeneous models in which fracture and matrix grids have different properties (Golf-Racht 1982; Narr et al. 2006). Fracture gridblocks (Figure 5-2b) have their own properties such as porosity, permeability, relative permeability curves, being different from the matrix gridblocks. Numerical simulation modeling of fractured reservoirs using explicit fractures has been widely used (Reza et al., 2008, Talukdar et al., 2000 and Yanze and Clemens, 2011). Grid refinement (non-uniform gridding) was done in the matrix blocks (the reason for this was the large gridblock size contrast between neighboring matrix gridblocks and fracture gridblocks). Details of non-uniform gridding is explained below. Both models have same total matrix-oil volume as well as same fracture/matrix pore volume ratio being equal to 0.3. Fracture widths are 7.86 cm and 5.2 cm for Models 1 and 2, respectively. Matrix blocks are initially saturated with "dead" heavy oil (no free gas nor interstitial water) and fractures with gas. Reservoir properties are shown in **Table 5-1**.
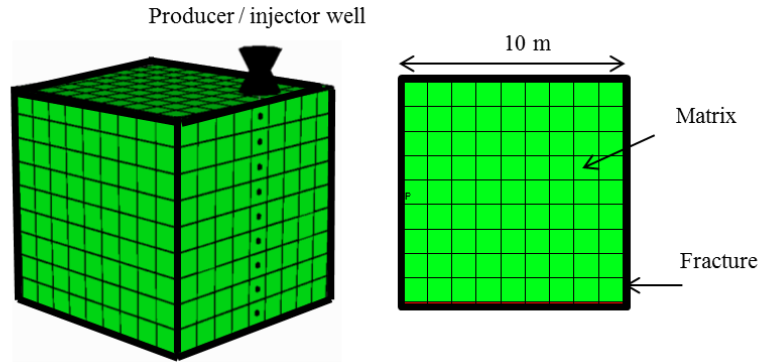
Fig. 5-2a Model 1. One-matrix block surrounded by fractures.
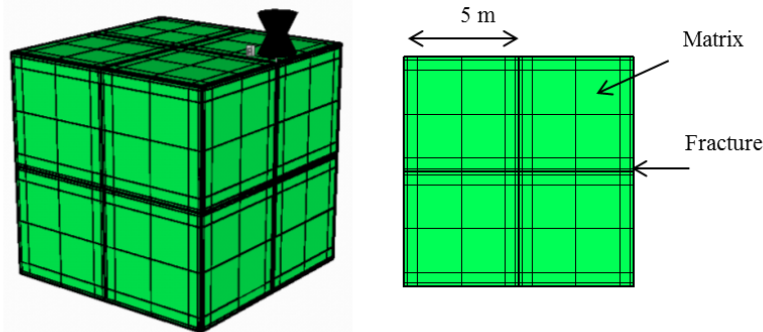
Fig. 5-2b Model 2. Multiple (eight) matrix blocks separated by fractures.

Figure 5-2 Numerical simulation models.

Table 5-1 Reservoir properties used in Models 1 and 2

Matrix porosity	0.1589
Fracture porosity	0.999
Matrix permeability (kx, ky)	320 md
Matrix permeability (kz)	192 md
Fracture permeability	50,000 md
Reservoir temperature	75, 150°C
Solvent type	Propane

Gridding used in Model 1 (75 and 150ºC) was 11x11x11. A uniform grid 9x9x9 was used for modeling the matrix block. On the other hand, due to numerical convergence problems, a non-uniform grid was used in Model 2 (75 and 150ºC); the discretization algorithm is based on a geometric distribution of gridblock sizes, see Figure 5-2, that allows for proper representation of the fracture thickness and matrix-fracture flow using less gridblocks than otherwise required by the uniform grid. Gridding used in Model 2 at 150ºC (eight matrix blocks surrounded by

155

fractures) was 15x15x15. For each of the eight matrix blocks a 6x6x6 grid was used. Also, in Model 2 at 75 ºC, one-quarter (two matrix blocks surrounded by fractures) of the full model was applied in order to reduce simulation times. The gridding for this model was 12x12x23 (for each of the two matrix blocks the number of gridblocks were 10x10x10).

The producer/injector well was completed in the fractures system along the block thickness. The production of fluids was controlled by well bottom hole pressure at 30 psi. The gas injection was carried out at a constant rate of $6x10^6$ cm^3/h and $12x10^6$ cm^3/h for air and C$_3$, respectively, until the shut in pressure (210 psi) was reached.

5.4.2 Fluid model

PVT model was created based on the property measurements conducted with the oil used in experiments reported by Mayorquin and Babadagli (2012a). Oil viscosity is 235 cp at 75ºC and atmospheric pressure. The PVT fluid model includes two components: oil and propane and was generated using the Peng-Robinson equation of state matching oil density conducted at different temperatures and atmospheric pressure.

In order to model kinetic reactions, it was necessary to include other components in the fluid model: nitrogen (N$_2$), oxygen (O$_2$), carbon monoxide (CO), carbon dioxide (CO$_2$), as well as oxygenated compounds such as alcohol, aldehyde, ketone, and coke. A total of eleven components were set in the numerical simulation model: heavy oil, C$_3$, N$_2$, O$_2$, CO, CO$_2$, alcohol, ketones, aldehydes, coke, and water. This amount of components was manageable for our study purpose; for larger numerical simulation models another fluid modeling strategy (for example lumping of components, different reaction models, etc.) should be followed in order to have reasonable numerical simulation times.

The viscosity of the oil was modeled by means of the Pedersen Corresponding States model, matching lab data measured at different temperatures and atmospheric pressure. The viscosity of oxygenated compounds was determined by history matching of measured viscosity of produced oil. After different trials, it was concluded that the best match was obtained when modeling the viscosity of oxygenated compounds in one order of magnitude higher than oil viscosity.

Effective diffusion coefficients used in the models were obtained from the history matching of experimental data reported by Mayorquin and Babadagli (2012b): 5×10^{-4} ft^2/h, 8×10^{-5} ft^2/h, and 8×10^{-6} ft^2/h for propane, nitrogen and oxygen, respectively. After this, negligible discrepancies were observed.

5.4.3 Kinetic reaction

It is well known that oxidation reactions occur when air (oxygen) contacts oil in the form of low temperature oxidation reactions (LTO) and/or high temperature oxidation reactions (HTO; i.e. in-situ combustion conditions). The first one occurs at temperatures below 350ºC and the last one at temperatures above 350ºC. Based on the thermal analysis conducted on experimental oil samples (Mayorquin and Babadagli 2012a) it was concluded that low temperature oxidation reactions occur at 75ºC and 150ºC.

Different approaches for LTO reaction modeling such as SARA fractions (Belgrave et al. 1990; Yang and Gates 2008; Sequera et al. 2010) and oxygenated compounds (Phillips and Hsieh 1985; Yoshiki and Phillips 1985; Clara et al. 1999; Sakthikumar and Berson 2001; Gutierrez et al. 2009; Khansari et al. 2013) were reported. The LTO reaction model proposed in this work is based on oxygenated compounds and taken from Khansari et al. (2013) even though the stoichiometric coefficients are not the same due to differences in oil characteristics. Based on experimental conditions (Mayorquin and Babadagli 2012a), temperature range 75–200°C, the following two reaction models were used:

Sub-range: 50 -150°C:

Oil + 6 O_2 → 3.96 Aldehydes + Coke + Water + CO + CO_2

Sub-range: 150 -200°C:

Aldehydes + 4.33 O_2 → Alcohols + Ketones + Water
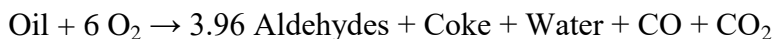
Kinetic parameters

The rate of oxygen consumption or oxidation rate of the crude in the low-temperature zone can be modeled as (Fassihi et al. 1984; Burger and Sahuquet 1972; Bousaid and Ramey 1968; Stokka et al. 2005):

$$- d(C_m)/dt = k * (p_{O2})^m * (C_m)^n \qquad (1)$$

where

C_m = instantaneous concentration of fuel,

k = rate constant,

p_{O2} = oxygen partial pressure,

m, n = reaction orders

The rate constant, *k*, may be related to temperature and activation energy by the Arrhenius equation (Brady et al. 2000):

$$k = A * \exp(-E/RT) \qquad (2)$$

where

A = Arrhenius constant, frequency factor or pre-exponential factor

E = Activation energy

R = Universal gas constant

T = Temperature

The values for frequency factor and activation energy are 10.1 1/s and 10887.73 BTU/mole-lb, respectively, which were evaluated from TGA data reported by Mayorquin and Babadagli (2012a) based on the method proposed by Coats and Redfern (1964). Activation energy was used as a history match parameter and it was obtained as 14500 BTU/mole-lb.

On the other hand, from DSC (differential scanning calorimetry) data by Mayorquin and Babadagli (2012a), the enthalpy ranged from -31.71 BTU/lb to -77.86 BTU/lb in the LTO region. A value of -31.75 BTU/lb-mole was used in the models.

The software used for numerical simulations was CMG STARS. No asphaltene precipitation is modeled.

5.4.4 Pressure effect in LTO reaction

Thermal analysis at different pressures was conducted in oil samples in order to assess the effect of pressure in LTO reactions. Instrument HP DSC 1 STAR System Mettler Toledo was used for DSC study. DSC was done at four different gauge pressures: 0, 300, 700, 1000 psi (the results were reported by Mayorquin and Babadagli (2015) –a paper under review). Results showed that pressure had a greater effect in the HTO region than in the LTO regions (**Figure 5-3**). In the HTO regions, a decrease in the peak temperature of exothermic activities was observed. Similar observations were reported by Li et al (2006) in their own DSC studies. Based on DSC results and operation conditions in this numerical simulation study (temperature range: 75 – 150°C, pressure 210 psi), pressure seems to have a minor effect in LTO reaction. At higher pressures its effect in LTO reaction modeling should be considered.
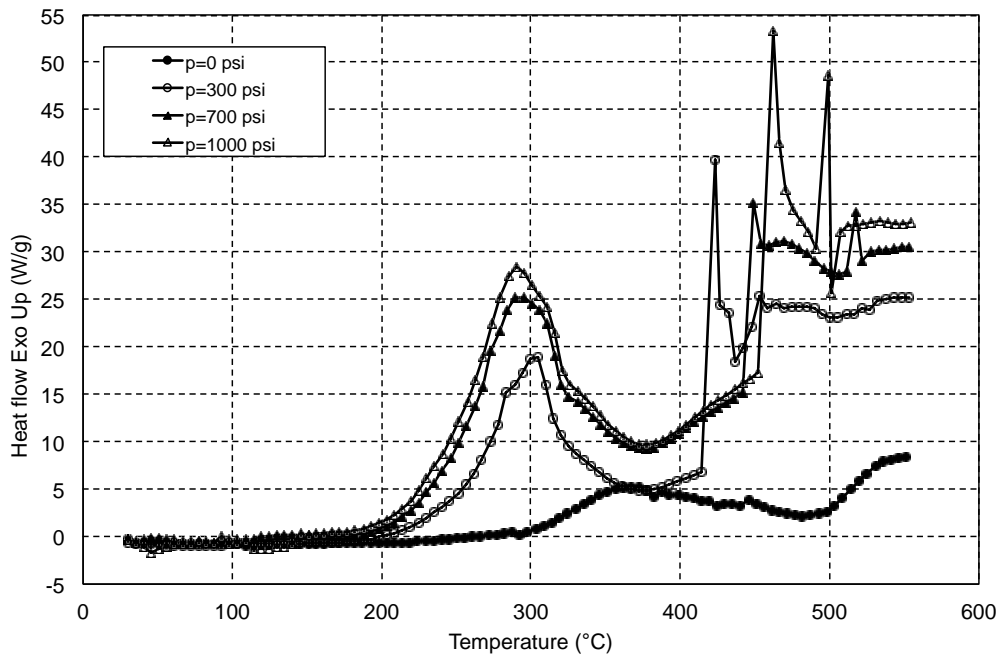
Figure 5-3 DSC analysis at different pressures.

5.4.5 Study of matrix grid resolution

After doing a matrix block grid resolution study, it was concluded that the optimal grid resolutions were 9x9x9 for Model 1 (75 and 150°C), 10x10x10 for Model 2 at 75°C and 6x6x6 for Model 2 at 150°C. No grid resolution study was conducted on fracture blocks. The reservoir model grids are: 11x11x11 (1331 cells) for Model 1; 12x12x23 (3312 cells) for Model 2 at 75°C, and 15x15x15 (3375 cells) for Model 2 at 150°C.

5.4.6 Simulation procedure

Three cycles with different gas sequences were tested in both numerical simulation models at two different temperatures: 75°C and 150°C (**Table 5-2**). For each of the two models six operational sequences, or cases, were tested (**Table 5-3**). Each cycle consisted of three phases.

160

Phase 1: Gas injection (air or solvent).

Phase 2: Soaking period at static conditions.

Phase 3: Fluid production

For example, one of the numerical simulation runs for Model 1 assumed a temperature of 75°C injecting air in the three cycles, i. e. Air-Air-Air (Table 5-2), and considering 1-month soaking time in each cycle and 1-month production time for Cycles 1 and 2, and 7.6 years for Cycle 3 (Case 1 of Table 5-2 and Table 5-3):

Table 5-2 Numerical simulation scenarios.

Model	Temperature	Gas sequence (Cycle 1 - Cycle 2 - Cycle 3)	Cases	Time (month) Soaking	Time (month) Production
Model 1	75 °C	Air - Air - Air	1	1	1
			2	2	1
		Air - C3 - Air	3	3	1
		C3 - Air - C3	4	1	2
Model 2	150 °C	C3 - C3 - C3	5	2	2
			6	3	2

Table 5-3 Duration of operations in each cycle for different cases

	Phase	Case 1	Case 2	Case 3	Case 4	Case 5	Case 6
		Duration (m = months; y = years)					
Cycle 1	Gas injection	---	---	---	---	---	---
	Soaking time	1 mo.	2 mo.	3 mo.	1 mo.	2 mo.	3 mo.
	Production time	1 mo.	1 mo.	1 mo.	2 mo.	2 mo.	2 mo.
Cycle 2	Gas injection	---	---	---	---	---	---
	Soaking time	1 mo.	2 mo.	3 mo.	1 mo.	2 mo.	3 mo.
	Production time	1 mo.	1 mo.	1 mo.	2 mo.	2 mo.	2 mo.
Cycle 3	Gas injection	---	---	---	---	---	---
	Soaking time	1 mo.	2 mo.	3 mo.	1 mo.	2 mo.	3 m
	Production time	7.6 yr	7.3 yr	7.1 yr	7.6 yr	7.3 yr	7.1 yr

Duration of gas injection for different cycles is around 4 days for air injection and around 9 days for propane injection.

5.4.7 Results

Simulations at low temperature: 75°C

Model 1. **Figure 5-4** shows the RF obtained for different production time/soaking time ratios. These results include the four gas sequences and the six cases mentioned earlier (Table 5-2 and Table 5-3). In both models the lowest RF's correspond to the Air/Air/Air sequence at any production time/soaking time ratio, this result was also observed experimentally at the core scale. Similarly, the highest RF's are obtained in the $C_3/C_3/C_3$ sequence, again regardless of the injection/production time's ratio. Results of these extreme cases, Air and C_3, can be thought of lower and upper RF's limits, respectively, at specified duration of operations (Table 5-3). Thus, it is expected that RF for any combination of gas sequences should fall in between those limits as seen in Figure 5-4.
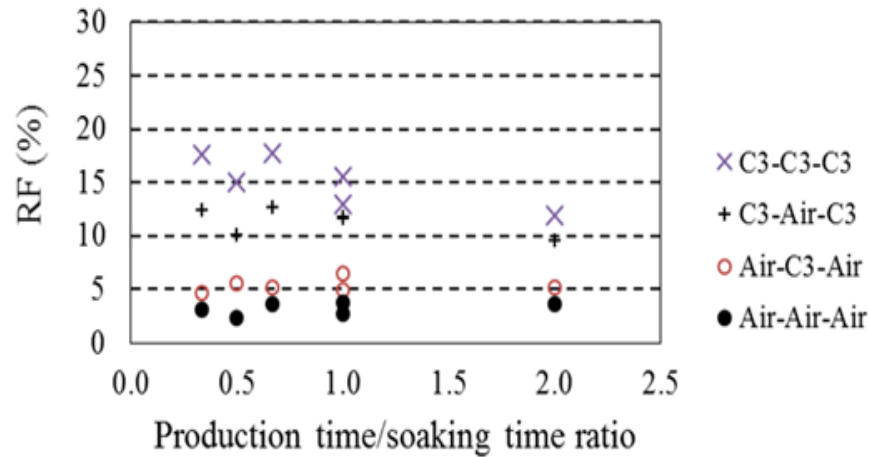
Figure 5-4 RF for Model 1 at 75 °C: four gas sequences.

RFs for Air/Air/Air sequence show relatively slight differences at different production/soaking times; however, it is noticeable that two different trends depend on production times. When the production time is one month (three lowest RFs) the RF remains practically unchanged, but when it is increased to 2 months (three highest RFs), a maximum RF was obtained. From these results, it can be concluded that an optimum soaking time exists to deliver a maximum RF.

If RFs are compared in terms of increasing production time for a particular soaking time, one can observe that higher RFs are obtained when production time is increased. What is interesting is that higher increments in the RF are obtained when soaking times are three months.

For Air/Air/Air gas sequence the oxygen concentration in the produced gas (**Table 5-4**) shows high values (11.6 mol%) when air is used in Cycle 1 and soaking time is 1 month. However, this concentration decreases as soaking times increase, regardless of production time: at 2 and 3 months soaking time the maximum O_2 concentration is 7.2 mol% and 3.7 mol%, respectively. For any particular soaking/production time ratio it is also observed that in general oxygen concentration in produced gas decreases sharply from Cycle 1 to Cycle 2, and increases slightly from Cycle 2 to Cycle 3.

Table 5-4 Maximum oxygen concentration in produced gas.

| | Time (mo.) | | | Maximum O$_2$ concentration (mol%) | | | |
| | | | | Temperature= 75 °C | | Temperature= 150 °C | |
	Soaking	Production	Cycle	Model 1	Model 2	Model 1	Model 2
Air-Air-Air	1	1	1	11.6	1.1	2.3	8.4
			2	0.1	0.3	16.3	4.0
			3	0.3	1.3	13.9	3.9
	2	1	1	7.2	0.2	4.4	4.7
			2	0.1	1.1	12.3	3.6
			3	0.7	2.9	16.0	3.7
	3	1	1	3.7	0.1	2.1	3.0
			2	0.1	1.0	9.9	3.4
			3	0.8	2.3	12.6	3.0
	1	2	1	11.6	1.1	2.3	8.4
			2	4.9	2.7	15.2	4.5
			3	4.9	5.7	15.2	4.2
	2	2	1	7.2	0.2	4.3	4.7
			2	1.5	3.0	14.0	3.6
			3	2.6	5.5	10.2	4.2
	3	2	1	3.7	0.1	2.1	3.0
			2	0.4	2.0	13.6	3.4
			3	2.1	3.8	7.6	3.5
Air-C3-Air	1	1	1	11.6	1.1	2.3	8.4
			2	9.E-10	9.E-04	9.E-10	0
			3	1.8	1.4	14.6	2.4
	2	1	1	7.2	0.2	4.4	4.7
			2	5.E-08	5.E-04	1.E-08	0
			3	2.5	2.7	10.3	2.1
	3	1	1	3.7	0.1	2.1	3.0
			2	1.E-07	9.E-05	4.E-09	0
			3	3.9	2.1	6.4	0.8
	1	2	1	11.6	1.1	2.3	8.4
			2	8.E-08	4.E-04	5.E-10	0
			3	9.0	7.8	13.6	3.0
	2	2	1	7.2	0.2	4.3	4.7
			2	4.E-08	2.E-04	1.E-08	0
			3	6.9	4.6	9.0	2.0
	3	2	1	3.7	0.1	2.1	3.0
			2	8.E-08	3.E-03	4.E-09	0
			3	7.1	2.9	7.1	1.3
C3-Air-C3	1	1	1	0	0	0	0
			2	0.5	1.3	13.6	3.0
			3	1.E-08	2.E-03	6.E-05	0
	2	1	1	0	0	0	0
			2	1.1	2.2	8.1	1.6
			3	1.E-07	4.E-03	7.E-06	0
	3	1	1	0	0	0	0
			2	0.9	1.4	6.8	1.5
			3	1.E-08	2.E-03	2.E-05	0
	1	2	1	0	0	0	0
			2	3.6	5.2	12.3	3.4
			3	3.E-06	2.E-03	3.E-05	0
	2	2	1	0	0	0	0
			2	2.5	4.0	8.3	2.0
			3	2.E-07	2.E-03	4.E-05	0
	3	2	1	0	0	0	0
			2	3.6	2.7	7.1	1.5
			3	7.E-08	2.E-03	3.E-05	0.0

164

On the other hand, when C_3 is used in Cycle 2 (Air/C_3/Air), an increase in RF is obtained expectedly. The optimum production/soaking time ratio is equal to 1 (soaking and production time equal are 2 months). In regard to the oxygen concentration in gas sequences of Air/C_3/Air, negligible O_2 concentration exists during production in Cycle 2, which corresponds to C_3 soaking period. This results from unreacted oxygen left after Cycle 1 (Air). In Cycle 3 (Air), after C_3 was used in cycle 2, a lower oxygen concentration was obtained compared to Cycle 1. In the C_3/Air/C_3 sequence, higher RFs were obtained for production time/soaking time ratios lower than 1. In terms of O_2 concentration in produced gas, a relatively low value was observed in Cycle 2 (Air), which was much lower than Cycle 1 of Air/Air/Air sequence. The maximum O_2 concentration was lower than 4.0 mol% in the C_3/Air/C_3 sequence case and 11.6 mol% in the Air/Air/Air sequence.

Model 2. **Figure 5-5** shows the RF obtained for different production time/soaking time ratios. Results include four gas sequences and the six cases mentioned (Table 5-2 and Table 5-3 Duration of operations in each cycle for different cases). In general, RF behavior in models 1 and 2 are alike. However, slightly higher RF's are obtained in Model-2.
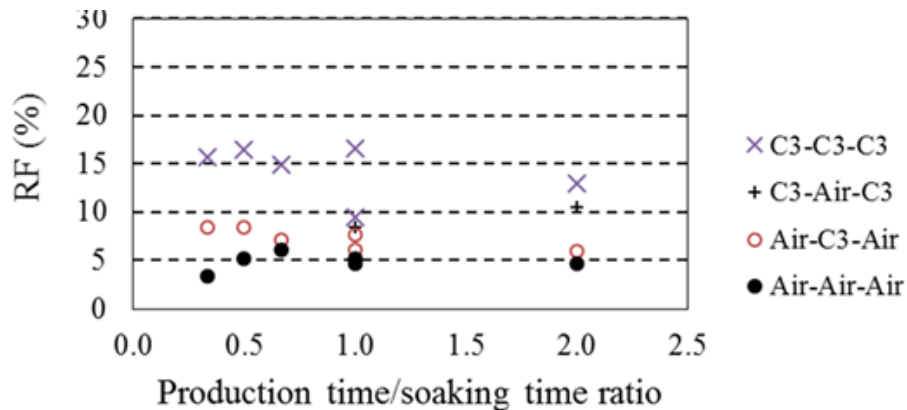

Figure 5-5 RF for Model 2 at 75 °C: four gas sequences.

O_2 concentration in each of the cycles in Air/Air/Air sequence is in general lower compared to that of same sequence in the cycles of Model 1 at 75°C.

Discussion on low temperature (75°C) simulations

The distribution of the gas saturation in the middle vertical plane of the matrix block at the end of the soaking period (**Figure 5-6**), which is previous to the production phase, gives insight into the oil mechanisms acting in the air injection process in a NFR. Due to the fact that matrix blocks in models 1 and 2 are surrounded by fractures, the gas from the fractures is transferred from top, bottom and the vertical lateral sides. Gas saturation is more prominent at the top followed by the vertical sides of matrix blocks; lower gas saturation is observed at the bottom. Certainly, diffusion occurs between the fracture gas and matrix oil due to the existence of a fluid compositional gradient. On the other hand, the oil drained from the matrix at the bottom by means of gravitational effects is replaced by surrounding gas in the top fracture. At the bottom of the matrix block a counter- current diffusion occurs aiming to lower gas saturation while co-current diffusion exists at the top of matrix blocks. Based on these observations, it can be concluded that a replacement mechanism is acting and it is more effective than diffusion. Similar observations were made by Rodríguez et al. (2004) for the case in which fractures are filled with nitrogen.
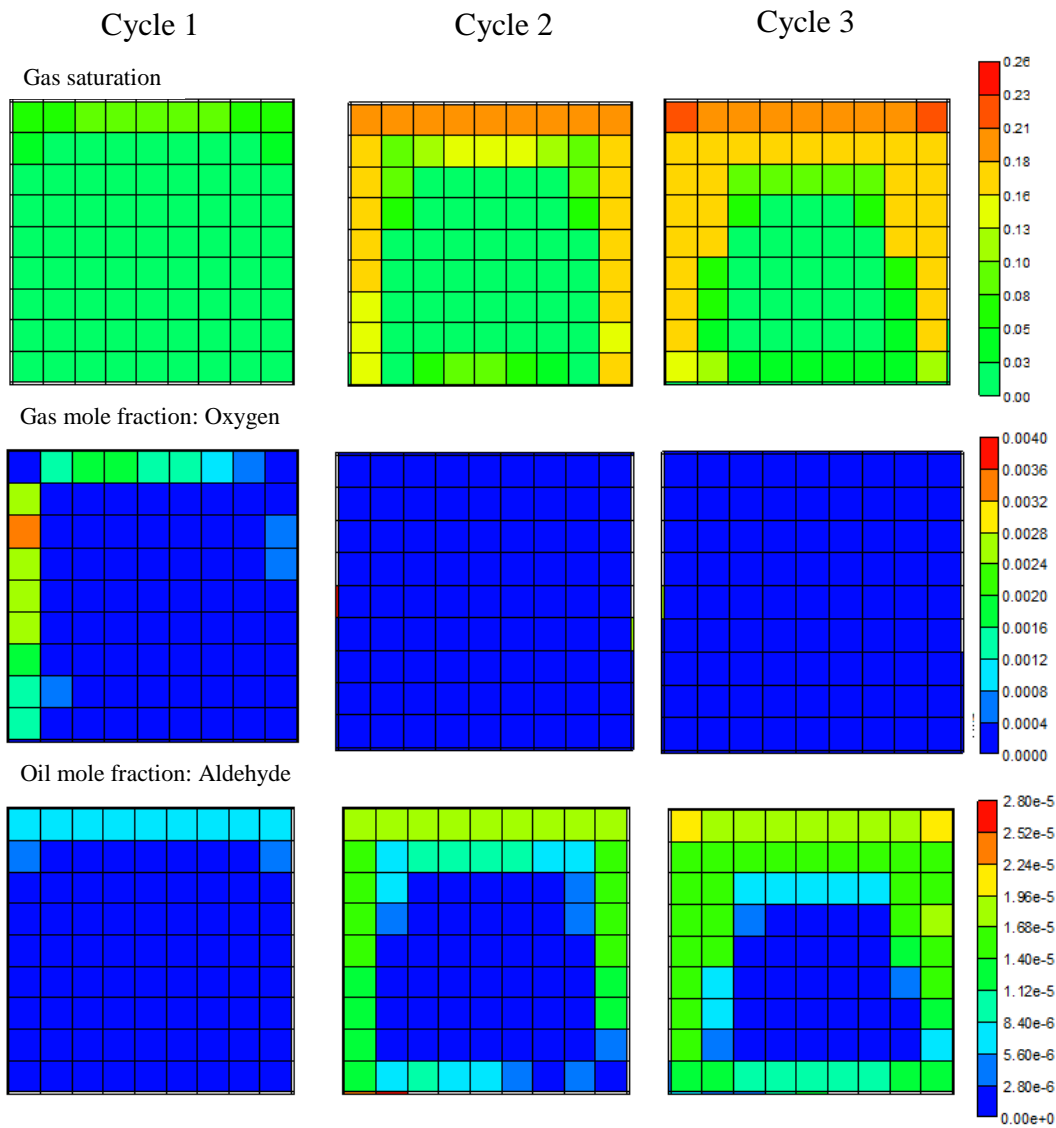
Figure 5-6 Fluids distribution for Model 1 at 75 °C: Air-Air-Air (case 4).

During the soaking time, when air exists in the fracture, oxygen diffuses and reacts with both fracture oil and matrix oil at LTO conditions. Reactions at LTO conditions produce oxygenated compounds as well as carbon oxides in the matrix near the fracture. As time elapses, the oxygen from the fracture gas continues reacting near the fracture with the previously generated oxygenated compounds but also some oxygen is transferred deeper into the matrix oil. Due to the replacement mechanism oxygenated compounds and carbon oxides are generated mainly at the top of the matrix block of Model-1, these products are also generated at the bottom of the matrix block but in a lesser extent due to less effective (counter- current) diffusion of oxygen. In Model-2, a replacement mechanism also occurs in the upper and lower matrix blocks (**Figure 5-7**). However gas saturation at the top of lower blocks is lower than that in upper blocks. This can be

attributed to the oil drained from the bottom of upper blocks flows downward into the horizontal fractures. From this point towards the lower matrix blocks, re-infiltration occurs under these conditions.
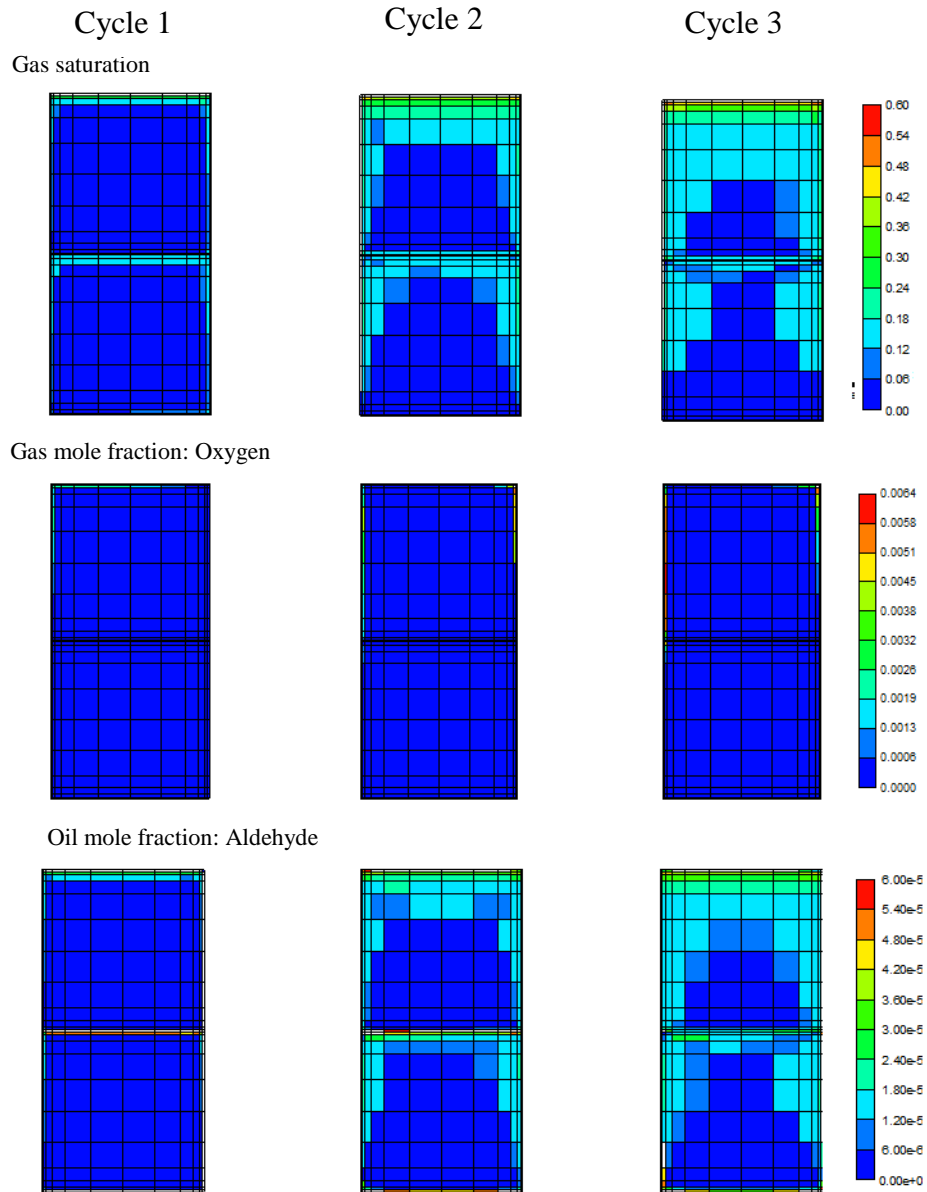
Figure 5-7 Fluids distribution for Model 2 at 75 °C: Air-Air-Air (case 4).

Additionally, it was also found that products resulting from LTO reactions fill out a larger matrix pore volume in Model-2 (Figure 5-7) compared to that of Model-1 (Figure 5-6); this could be explained in terms of the area/volume ratio of the matrix blocks: the area/volume ratio of each matrix block in Model-2 is higher than the area/volume ratio of the matrix block in Model-1.

In regards to oil viscosity, it is well known that it increases when oxygenated compounds are formed and this is the reason for proposing the alternate injection of a solvent (propane) with air. **Figure 5-8** shows how the oil viscosity behaves in the innermost matrix cells throughout the matrix height of Model 1 at 75°C, case 4 at the end of soaking time of Cycles 1, 2 and 3, (just before the well is opened to production,) for two gas sequences: Air/Air/Air and Air/C$_3$/Air. In the three cycles of the Air/Air/Air gas sequence, an increase can be observed in oil viscosity mainly at top of matrix block due to the effect of oxygenated compounds; a slight increase in oil viscosity is also seen at bottom. The opposite (oil viscosity reduction) was observed when C$_3$ was used in Cycle 2 of the gas sequence Air/C$_3$/Air. In fact, in Cycle 3 (i.e. air) a lower oil viscosity than original was also observed, mainly at the top of matrix.
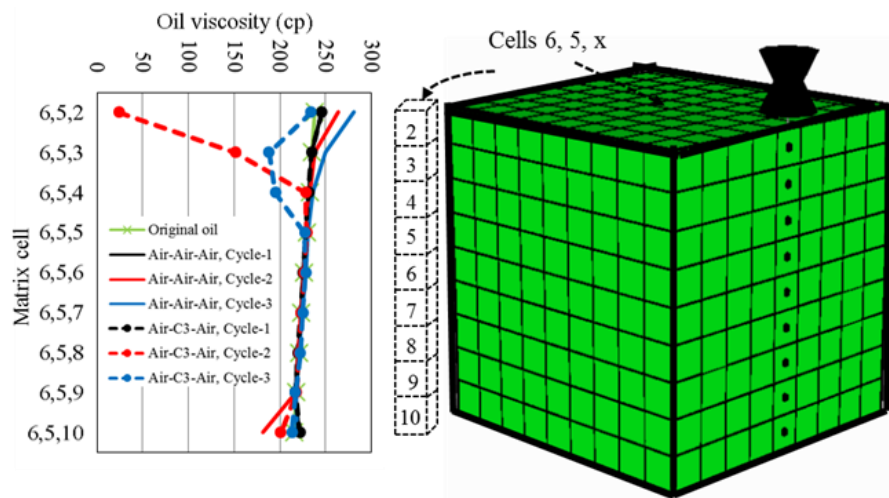
Figure 5-8 Oil viscosity for Model 1 at 75°C for sequences: Air-Air-Air and Air-C$_3$-Air.

Figure 5-9 shows the oil viscosity in the innermost matrix cells along one-quarter of Model 2 at 75°C, case 4, at Cycles 1, 2 and 3 for Air/Air/Air and Air/C$_3$/Air sequences. It can be observed that, unlike Model 1, oil viscosity increases not only in the top of the matrix but practically along the upper and lower matrix blocks, again due to a higher area/volume ratio, compared to Model 1. But also due to this condition, a lower oil viscosity is observed in both blocks, upper and lower, compared to Model-1.
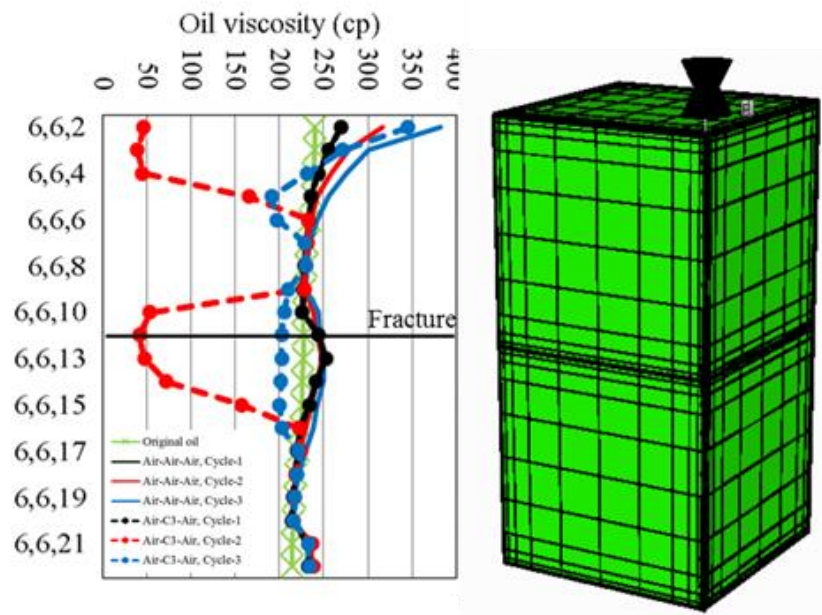
Figure 5-9 Oil viscosity for Model 2 at 75°C for sequences: Air-Air-Air and Air-C₃-Air.

On the other hand, a low production time (1 month) means less oil volume is removed from the reservoir and consequently air (oxygen) at every new cycle reacts with remaining oil in the matrix-fracture system and then oxygen can be consumed resulting in a low oxygen concentration in produced gas. On the contrary, at high production times (2 months) more oil volume is removed from the system and a lower amount of oil is available for reacting with oxygen, then more oxygen is left unreacted in which case a higher oxygen concentration exists in produced gas.

Models 1 and 2 have the same matrix/facture pore volume ratio but fracture density (lower matrix block sizes) is higher in Model 2, and then a larger amount of oxygen reacts with more matrix oil (scattered in eight blocks) due to the higher area/volume ratio.

Simulations at high temperature: 150°C

Model 1. **Figure 5-10** shows the RF for same production time/soaking time ratio, gas sequences and cases analyzed in Models 1 and 2 at 75°C. Higher RF's are observed at 150°C compared to that at 75°C due to an enhanced gravity drainage induced by lower oil viscosity. Again, the Air/Air/Air gas sequence represents the lowest RF while $C_3/C_3/C_3$ shows the highest RF; in between are the RF's of gas sequences involving the interchange of Air and C_3. At 150°C it is

observed that in general the highest RFs occur at production time/soaking time ratios lower or equal to 1.
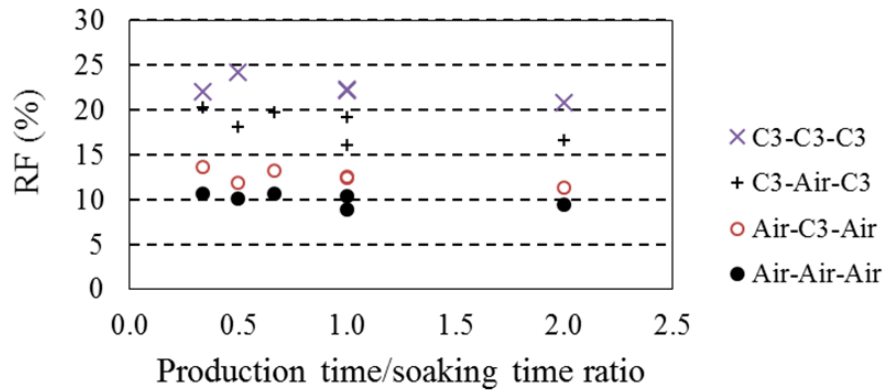
Figure 5-10 RF for Model 1 at 150°C: four gas sequences.

Model 2. **Figure 5-** shows results for this case. As in previous model (model 1), higher RFs are obtained in cases in which production time/soaking time ratio is less than 1.0.
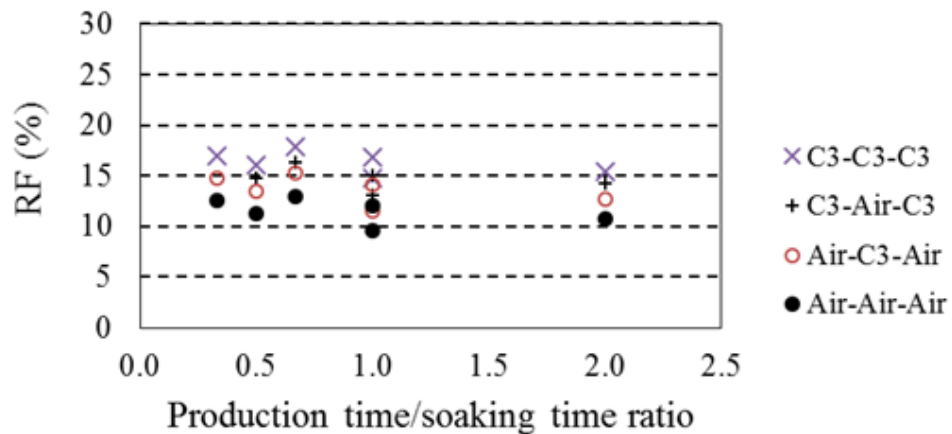
Figure 5-11 RF for Model 2 at 150 °C: four gas sequences.

Discussion on high temperature (150°C) simulations

As in models 1 and 2 at 75°C, a replacement mechanism is also acting at 150°C being more effective at this high temperature due to reduced oil viscosity. More gas volume enters the matrix block and hence more oxygen (in air cycles) is available to react with heavy oil and thus more oxygenated compounds are produced due to LTO reactions. **Figure 5-** and **Figure 5-** show the distribution of oxygen and aldehydes for Models 1 and 2, respectively, at 150°C.
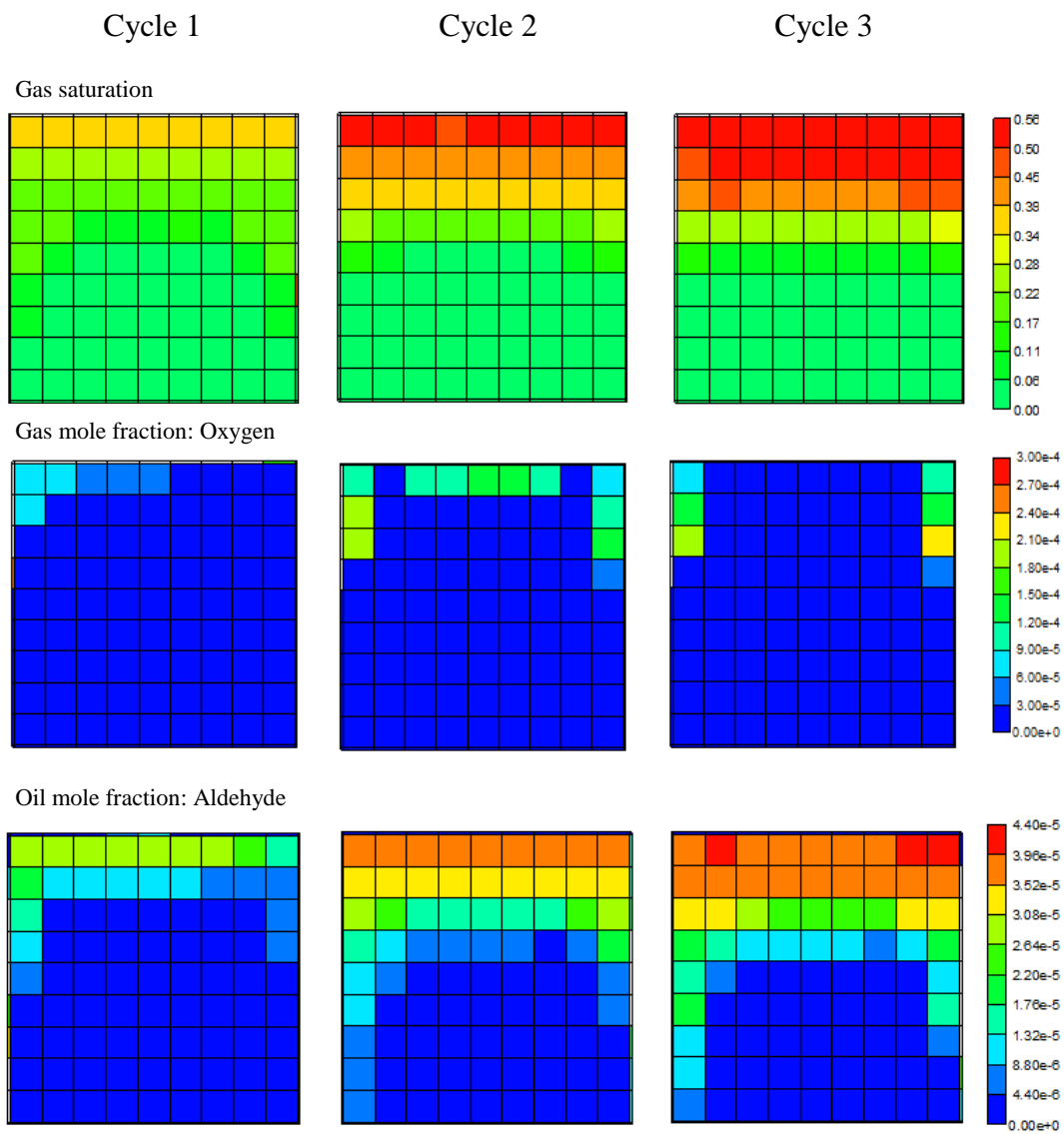
Figure 5-12 Fluids distribution for Model 1 at 150°C: Air-Air-Air (case 4).
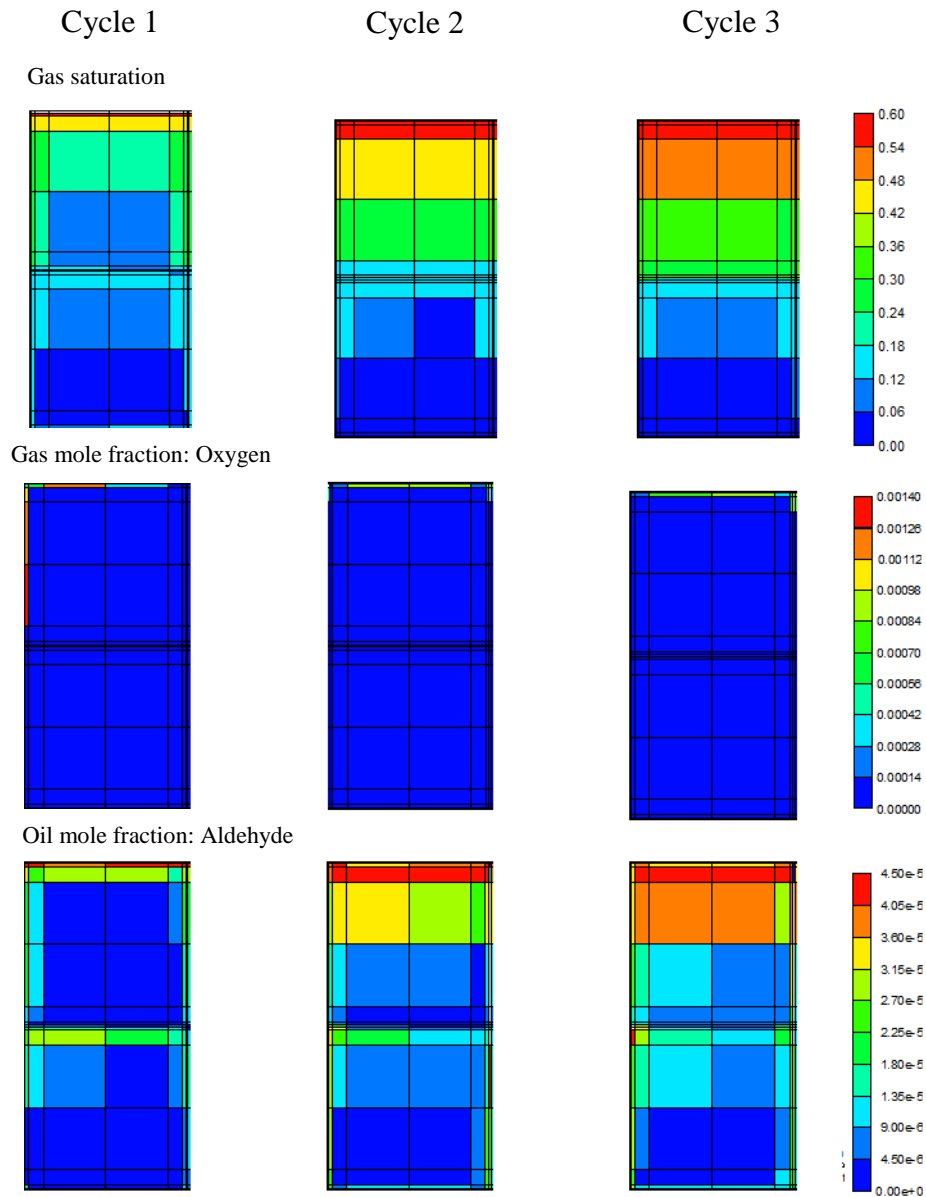
Figure 5-13 Fluids distribution for Model 2 at 150°C: Air-Air-Air (case 4).

Even when oxygenated compounds results in an oil viscosity increase, its impact is reduced due to a high temperature (150°C), **Figure 5-** and **Figure 5-**). On the other hand, the injection of C_3 to reduce the increased oil viscosity is not as effective as it is at lower temperature (75°C) due to pre-existing temperature-associated low oil viscosity.
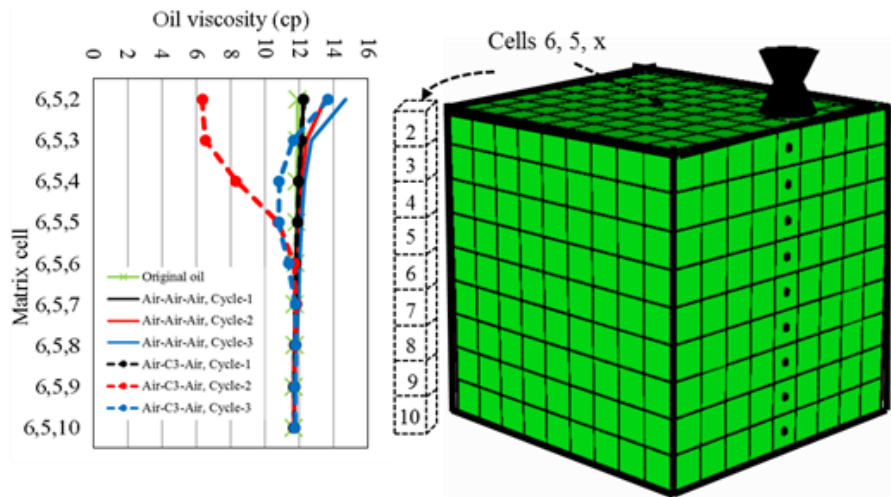
Figure 5-14 Oil viscosity for Model 1 at 150°C for sequences: Air-Air-Air and Air-C$_3$-Air.
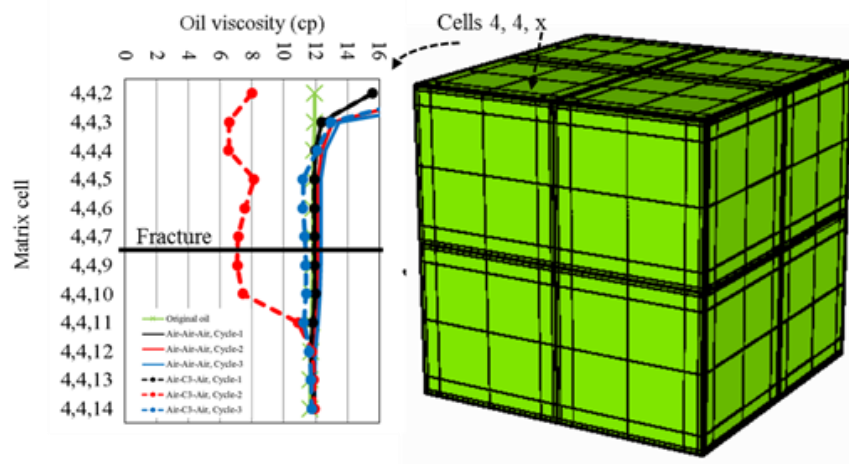
Figure 5-15 Oil viscosity for Model 2 at 150°C for sequences: Air-Air-Air and Air-C$_3$-Air.

In Air/Air/Air sequence high oxygen consumption occurs in Cycle 1 (Table 5-4) and it drops from 21.0 mol% to less than 5 mol%, regardless of soaking time. However, in Cycles 2 and 3, oxygen consumption is low. More oxygen is left unreacted in pore volume matrix, either more soaking time is needed and/or less oil exists in the system; the explanation for this second statement is that at high temperature the RF is high which means that less oil remains in the system. The first statement is confirmed as shown by the O$_2$ concentration results, as soaking time increases the O$_2$ concentration in produced gas reduces (for any production time); this was also confirmed for Model 2.

In Air/C$_3$/Air sequence (Table 5-4), the oxygen concentration in Cycle 3 is slightly lower than that of Air/Air/Air sequence, which means that oil remaining in matrix after soaking of C$_3$ in Cycle 2 has a positive effect in the consumption of oxygen.

Finally, it should be emphasized that CO$_2$ is produced in the LTO reaction but its effect in oil recovery might be not as important due to small produced quantities (less than 0.02 mol% in produced gas).

5.5 Reservoir heterogeneity

The ultimate goal of the study was to clarify the effect of operational conditions (gas sequences, production and soaking times) in the oil recovery and oxygen consumption. Therefore, models used in this work represent idealized fracture media rather than complex fracture structure to avoid excessive computational times. What is critical in this type model is the volume of fracture (how much gas needs to be injected) and matrix/fracture interaction area (diffusion process). For further research, these properties can be changed (different matrix sizes generating different matrix/fracture interaction area and fracture volume) to include the effect of heterogeneity to some extent.

5.6 Conclusions

1. Injection of air (at LTO conditions) and propane represents an alternative for NFR – heavy oil at field scale.

2. An optimum production time/soaking time ratio exists for different gas sequences, temperatures, and block sizes (fracture density).

3. Propane minimizes the effects of increased oil viscosity due to oxygenated compounds.

4. At high reservoir temperature (150°C), the oxygen consumption is high; oxygen concentration in produced gas drops to more safe limits [an average produced oxygen range of 0.8 - 7.0% was reported by Emery (1962) for the wells under thermal-recovery tests]. Also the oil viscosity increase due to produced oxygenated compounds is not

critical at 150°C meaning that C_3 injection might not be required (less cost). This conclusion needs to be verified with other types of heavy oils.

5.   Matrix block area/volume ratio has an impact in the oxygen consumption and distribution of oxygenated compounds in the matrix block.

6.   Technical results reported in this work must be complemented with both economic analysis and an optimization study.

5.7   Nomenclature

A   = Arrhenius constant, frequency factor or pre-exponential factor

yr   = year

mo   = month

C_3 = Propane

C_m = instantaneous concentration of fuel

CO   = Carbon monoxide

CO_2 = Carbon dioxide

E   = Activation energy

HPDSC= High Pressure Differential Scanning Calorimetry

HTO   = High Temperature Oxidation

k   = rate constant

LTO   = Low Temperature Oxidation

m, n   = reaction orders

NFR   = Naturally fractured reservoir

N_2 = Nitrogen

O_2 = Oxygen

p_{O2} = oxygen partial pressure

R   = Universal gas constant

RF   = Recovery Factor

T   = Temperature

TGA   = Thermogravimetric Analysis

References

Belgrave, J.D. M., Moore, R.G., Ursenbach, M. G. et al. 1990. A Comprehensive Approach to In-Situ Combustion Modeling. *SPE Advanced Technology Series* **1** (1): 98-107. SPE-20250-PA. http://dx.doi.org/10.2118/20250-PA.

Bousaid, I.S. and Ramey Jr., H.J. 1968. Oxidation of Crude Oil in Porous Media. *SPE J* **8** (02): 137-148. SPE-1937-PA. http://dx.doi.org/10.2118/1937-PA.

Brady, J.E., Russell, J.W., and Holum, J.R. 2000. *Chemistry: Matter and its changes*. 3rd Ed., p. 599, John Wiley & Sons, Inc., New York.

Burger J.G. and Sahuquet, B.C. 1972. Chemical Aspects of In-Situ Combustion–Heat of Combustion and Kinetics. *SPE J* **12** (05): 410-422. SPE-3599-PA. http://dx.doi.org/10.2118/3599-PA.

Clara, C., Durandeau, M., Queanault, G., Nguyen, T-H. 1999. Laboratory Studies for Light Oil Air Injection Projects: Potential Application in Handil Field. Presented at the SPE Asia Pacific Oil and Gas Conference and Exhibition, Jakarta, 20-22 April 20-22. SPE 54377-MS. http://dx.doi.org/10.2118/54377-MS.

Coats, A. W. and Redfern, J. P. 1964. Kinetic Parameters from Thermogravimetric Data. *Nature* **201**: 68-69; doi:10.1038/201068a0.

Emery, L. W. 1962. Results from a Multi-Well Thermal-Recovery Test in Southeastern Kansas. *J Pet Technol* **14** (06): 671 – 678. SPE-140-PA. http://dx.doi.org/10.2118/140-PA.

Fassihi, M.R., Brigham, W.E., and Ramey Jr., H.J. 1984. Reaction Kinetics of In-Situ Combustion: Part 1- Observations. *SPE J* **24** (04): 399-407. SPE-8907-PA. http://dx.doi.org/10.2118/8907-PA.

Fatemi, S. M., Kharrat, R., and Vossoughi, S. 2011. Investigation of Top-Down In-Situ Combustion Process in Complex Fractured Carbonate Models: Effects of Fractures' Geometrical Properties. Presented at the Canadian Unconventional Resources in Calgary, 15 – 17 November. SPE-149314-MS. http://dx.doi.org/10.2118/149314-MS.

Golf-Racht, T. D. van. 1982. *Fundamentals of fractured reservoir engineering*. Elsevier Scientific Publishing Company. Page 608.

Gutierrez, D., Moore, R.G., Mehta, S.A. et al. 2009. The Challenge of Predicting Field Performance of Air Injection Projects Based on Laboratory and Numerical Modelling. *J Can Pet Technol* **48** (04): 23-34. PETSOC-09-04-23-DA. http://dx.doi.org/10.2118/09-04-23-DA.

Khansari, Z., Kapadia, P., Mahinpey, N. et al. 2013. Kinetic Models for Low Temperature Oxidation Subranges based on Reaction Products. Presented at the SPE Heavy Oil Conference, Calgary, 11-13 June. SPE-165527-MS. http://dx.doi.org/10.2118/165527-MS.

Li, J., Mehta, R. G., Moore, E., et al. 2006. Investigation of the Oxidation Behaviour of Pure Hydrocarbon Components and Crude Oils Utilizing PDSC Thermal Technique. *J Can Pet Technol* **45** (01): 48-53. http://dx.doi.org/10.2118/06-01-04.

Mayorquin-Ruiz, J.R. and Babadagli, T. 2012a. Can Injection of Low Temperature Air-Solvent (LTASI) Be a Solution for Heavy Oil Recovery in Deep Naturally Fractured Reservoirs? Presented at the SPE EOR Conference at Oil and Gas West Asia, Muscat, Oman, 16–18 April. SPE-153997-MS. http://dx.doi.org/10.2118/153997-MS.

Mayorquin-Ruiz, J.R. and Babadagli, T. 2012b. Optimal Design of Low Temperature Air Injection for Efficient Recovery of Heavy Oil in Deep Naturally Fractured Reservoirs: Experimental and Numerical Approach. Presented at the SPE Heavy Oil Conference Canada, Calgary, 12–14 June. SPE-149896-MS. http://dx.doi.org/10.2118/149896-MS.

Mayorquin-Ruiz, J. R. and Babadagli, T. 2015. Optimal Design of Low Temperature Air Injection with Propane for Efficient Recovery of Heavy Oil in Deep Naturally Fractured Reservoirs: Experimental and Numerical Approach. Paper submitted to *SPE Reservoir Evaluation & Engineering Journal* (under review)

Narr, W., Schechter, D. W., and Thompson, L. B. 2006. *Naturally fractured reservoir characterization*. Society of Petroleum Engineers. USA. Page 67

Phillips, C.R. and Hsieh, I. 1985. Oxidation Reaction Kinetics of Athabasca Bitumen. *FUEL* **64** (7) 985-989. http://dx.doi.org/10.1016/0016-2361(85)90155-3.

Reza, A., Kharrat, R., Ghotbi, C., et al. 2008. Simulation study of the VAPEX process in fractured heavy oil system at reservoir conditions. *Journal of Petroleum Science and Engineering* **60** 51 – 66. http://dx.doi.org/10.1016/j.petrol.2007.05.011.

Rodríguez, F., Sanchez, J.L., and Galindo-Nava, A. 2004. Mechanisms and Main Parameters Affecting Nitrogen Distribution in the Gas Cap of the Supergiant Akal Reservoir in the Cantarell Complex. Presented at the SPE Annual Technical Conference and Exhibition, Houston, 26–29 September. SPE 90288-MS. http://dx.doi.org/10.2118/90288-MS.

Sakthikumar, S. and Berson, F. 2001. Air Injection Into Light and Medium-Heavy Oil, Carbonate Reservoirs. Presented at the EXITEP 2001, Mexico, 4-7 February.

Sequera, B., Moore, R.G., Mehta, S.A. et al. 2010. Numerical Simulation of In-Situ Combustion Experiments Operated Under Low Temperature Conditions. *J Can Pet Technol* **49** (01): 55-64. SPE-132486-PA. http://dx.doi.org/10.2118/132486-PA.

Shulte, W.M., and De Vries, A.S. 1985. In-Situ Combustion in Naturally Fractured Heavy Oil Reservoirs. *SPE J* **25** (01): 67–77. SPE-10723-PA. http://dx.doi.org/10.2118/10723-PA.

Stokka, S., Oesthus, A. and Frangeul, J. 2005. Evaluation of Air Injection as an IOR Method for the Giant Ekofisk Chalk Field. Presented at the SPE International Improved Oil Recovery Conference, Kuala Lumpur, 5–6 December. SPE-97481-MS. http://dx.doi.org/10.2118/97481-MS.

Talukdar, M. S., Banu, H. A., Torsæter, O., et al. 2000. Applicability and Rate Sensitivity of Several Up Scaling Techniques in Fractured Reservoir Simulation. Presented at SPE International Petroleum Conference and Exhibition, Mexico, 1-3 February. Paper SPE-59048-MS. http://dx.doi.org/10.2118/59048-MS.

Yang, X. and Gates, I. D. 2008. History Match of an Athabasca Bitumen Combustion Tube Experiment. Presented at the World Heavy Oil Congress, Edmonton, 10-12 March. Paper 2008-441.

Yanze, Y. and Clemens, T. 2011. The Role of Diffusion for Non-Miscible Gas Injection in a Fractured Reservoir. *SPE Res Eval & Eng* **15** (01): 60 – 71. SPE-142724-PA. http://dx.doi.org/10.2118/142724-PA.

Yoshiki, K.S. and Phillips, C.R.. 1985. Kinetics of the Thermo-Oxidative and Thermal Cracking Reactions of Athabasca Bitumen. *FUEL* **64** (11): 1591-1598. http://dx.doi.org/10.1016/0016-2361(85)90377-1.

Chapter 6 : Summary and Limitations of the Method Proposed and Contributions

6.1 Summary of the research

In this research, a new approach for air injection at non-thermal conditions, i.e. in the low temperature oxidation region, was assessed for a dual porosity medium. Inherent drawbacks of the methods caused by generated products (oxygenated compounds) in this temperature region were minimized by adding hydrocarbon solvent to air. The proposed approach was investigated through laboratory experiments and numerical simulation studies. Static diffusion experiments were conducted by soaking heavy oil saturated cores into different types of gases mimicking a cyclic injection gas into dual porosity media and a wide set of conditions were tested. Numerical simulation studies were performed both at cores and field scale. Cores scale modeling emulated experimental conditions from which diffusion coefficients were obtained, while the larger scale modeling was oriented to evaluate oil recovery and oxygen consumption when air/solvent is injected in different matrix/fracture configurations.

6.2 Limitations and applicability of this research

The present research is the first attempt, both experimentally and numerically, devoted to analyze the effect of air injection at low temperature oxidation conditions and solvents in oil heavy recovery from a dual porosity medium.

Certain field conditions were properly incorporated in the experimental setup such as heavy oil (from a field) and temperature (75, 150 and 200°C). Pressure range (175 – 415 psi), on the other hand, represents depleted reservoirs and higher pressure conditions could be observed in more juvenile fields. This could be a limitation in the setup and further analysis would be required. Higher pressure implies higher oxygen partial pressure, which impacts the kinetic parameters. In this research, thermal analyses were conducted at different pressures observing changes in the temperature range at which exothermic reactions occur. But, LTO reactions did not show major effect when pressure changed. However, experiments at core scale would be desirable at higher pressures to confirm it.

Cores used in experimentation were cut from homogeneous rocks (Berea sandstone and Indiana limestone). Reservoir matrix blocks are generally heterogeneous having sealed/open fractures at different scales and/or vugs. Experimentation with these rock characteristics is needed and

improved gas diffusion would be expected at these conditions. Cores were fully saturated with heavy oil, i.e. water saturation was null but in reality there exists certain amount of interstitial water. It is expected that water also has an effect in the development of oxygenated compounds generated in the low temperature oxidation region.

In the numerical simulations, the fluid model consists of 11 components (heavy oil, nitrogen, oxygen, propane, aldehydes, ketones, alcohols, carbon monoxide, carbon dioxide, coke, and water), which include the compounds generated from oxidation reactions. However, these approach is useful to analyze the chemical/thermodynamic processes involved. Such amount of components may not be practical when modeling a field scale case. For this type of modeling, the components should be grouped in order for simulation times not to be time-consuming but still capable of representing the process. Similarly, reactions models were assumed to be same as those available in the literature (although stoichiometric coefficients were modified to represent our oil properties) that proved to be valid since concentration of carbon oxides (CO, CO_2) in produced gas obtained by means of numerical modeling were same as those obtained experimentally. On the other hand, modeling of oil viscosity increase due to oxygenated compounds was done by increasing the viscosity of those compounds one order of magnitude higher than oil viscosity to match the history. Modeling of asphaltene was not included.

6.3   Scientific and practical contributions to the literature and industry

Chapter 2:

The experiments showed encouraging results at 75°C when a heavy-oil-saturated core was immersed into an air/propane (C_3) gas mixture rather than pure air or pure propane. Hence, a certain amount of C_3 added to air may yield a highly attractive recovery (an optimum C_3/air ratio should be investigated). However, an important issue prevails at 75°C; high oxygen (O_2) concentration is present in the gas mixture at the end of the experiments.

High temperatures (150 and 200°C) showed a more promising condition compared with 75°C because of high O_2 consumption. At high temperatures, the impact of oxygenated compounds is minor and the recovery factors for both pure-air and air/C_3-gas mixture is similar. However, for this gas mixture, the operating conditions near C_3-saturation temperature show better results.

Critical parameters in oil recovery are soaking time, operation conditions (pressure and temperature), and fluid-injection sequence. The effects of these parameters on oil recovery are clarified to a greater extent, and the margins of the optimal conditions are defined.

Chapter 3:

The main observations and conclusions are categorized based on our parametric analysis.

Fracture volume effect

- V_f/V_T ratio affects oil recovery. The larger the amount of available gas (solvent) mass in fracture the larger the amount of gas diffuses into matrix oil and hence the greater the oil recovery.

Temperature effect

- At 75ºC, gas type selection for Cycle 1 is critical for oil recovery (C_3 delivers higher oil recovery than air). At 150ºC, gas type selection for Cycle 1 is not critical for oil recovery. However, in the alternating gas sequence, Cycle 1 gas type does affect oil recovery in Cycle 2. Higher total oil recovery is obtained for the $C_3/Air/C_3$ sequence.
- Detrimental effect of increased oil viscosity due to generated oxygenated compounds is more critical at 75ºC than at 150ºC.
- At 75ºC propane is required in order for the matrix oil to drain out from the core, being more effective in Cycle 1.
- At 75ºC gas sequence design affects oil recovery (being higher with alternating injection of C_3 and air, starting with C_3). Oxygen is practically unconsumed regardless of the gas sequence. Hence, air acts only as pressurizing agent.
- Oxygen consumption is higher in the experiments at 150°C than those at 75ºC.
- At 150ºC gas sequence affects oil recovery. A higher oil recovery was obtained when using C3 in Cycle 1 due to a higher C3 mass transfer from fracture gas into matrix oil reducing its viscosity and thus improving the gravity drainage mechanism. Also, in experiments at 150ºC oxygen consumption is higher in cycles followed by C3 cycles.

Rock type effect

- At 75ºC, lower oil recovery was obtained from the limestone cores than sandstones due to lower permeability. It was not feasible to evaluate the effect of mineralogy in oil recovery at core scale or its effect on LTO reactions.

- At 150 ºC experiments, it was observed that (1) higher oil recovery is obtained for the C_3/Air/C_3 sequence, (2) high O_2 consumption was observed in the sequences of Air/C_3/Air and C_3/Air/C_3, (3) the highest O_2 consumption is obtained when O_2 contacts a C_3/heavy oil liquid mixture instead of heavy oil.

Solvent type effect

- Oil recovery at 150ºC is higher using C_4 at any injection sequence (Air/Solvent/Air, Solvent/Air/Solvent) than using C_3. The dilution of C_4 in heavy oil is higher than that of C_3 in heavy oil, which means that a less viscous oil/solvent mixture is attained improving the conditions for matrix oil expulsion by means of reduced-viscosity gravity drainage.

- Oxygen consumption in air cycle is higher after core being previously soaked in C_4 rather than C_3.

Core size effect

- It was confirmed experimentally that core A/V ratio plays a critical role in oil recovery, showing an impact in the oxygenated compounds distribution in the core and thereby oil recovery.

- Gas type selection (air or solvent) for Cycle 1 is a critical step for oil recovery and is highly dependent on matrix A/V ratio.

Gas sequence

- It was observed that gas sequence (assuming pure gas in cycles: air or solvent) depends not only in temperature and oil viscosity but also on timing. At early times, i.e. when core is fully oil saturated (Cycle 1), oil recovery is more efficient with C_3.

Effect of co-injection of air and C_3

- Benefits of soaking cores in Air+C_3 mixture rather than pure air or solvent are as follows: (1) Pressurizing gas agent, (2) matrix oil dilution, (3) higher O_2 consumption, (4) less solvent usage, (5) smaller amount of O_2 to be consumed, which means lower amount of generated oxygenated compounds, (6) faster (and earlier) oil viscosity reduction due to reduced oxygenated compounds, and (7) higher and faster oil recovery compared to alternate injection of air and C_3.

- It was observed that C_3 concentration in the injected gas mixture can be optimized in order to reduce its requirements and related costs. C_3 costs could be further minimized by means of retrieval at surface and re-injection

Effect of C_3 concentration in co-injection of air and C_3

- It was confirmed experimentally that C_3 concentration in Air/C_3 mixtures can be optimized for a given matrix size. Optimization studies are suggested.

<u>Chapter 4</u>:

- Sensitivity runs were performed by numerical simulation to analyze the effect of the ratio of Air/C_3 mixture and matrix size. The process is extremely sensitive to matrix size, especially the vertical length.

- With the given simulation scheme, the optimization of air injection (assisted by hydrocarbon solvents) can be achieved based on the minimized hydrocarbon solvent for a given matrix size.

- The oil production mechanisms acting in a matrix block surrounded by gas (air, air/C_3 mixture) filling the fractures are (1) gas-oil gravity drainage, (2) effective diffusion, and (3) voidage replacement of oil by gas.

- Oxygenated compounds produced in matrix oil due to LTO reactions lessen the effect of gravity drainage. This negative effect is reduced when C_3 is injected.

- The degree of participation of different oil production mechanisms depends on oil viscosity, temperature, soaking time, block size, and type of gas (air, C_3, air/C_3).

- Air (oxygen) reacts with both matrix oil and fracture oil; oxygen in the fracture is diffused freely to fracture oil in the absence of matrix.
- From the up-scaling study based on different matrix sizes, a non-integer exponent is obtained from the logarithmic relationship between the time to reach RF=10% and matrix size. These exponents are defined for different temperatures and type of gases.

Chapter 5:

- Injection of air (at LTO conditions) and propane represents an alternative for NFR – heavy oil at field scale.
- An optimum production time/soaking time ratio exists for different gas sequences, temperatures, and block sizes (fracture density).
- Propane minimizes the effects of increased oil viscosity due to oxygenated compounds.
- At high reservoir temperature (150 °C), the oxygen consumption is high; oxygen concentration in produced gas drops to more safe limits. Also, the oil viscosity increase due to produced oxygenated compounds is not critical at 150 °C meaning that C_3 injection might not be required (less cost). This conclusion needs to be verified with other types of heavy oils.
- Matrix block area/volume ratio has an impact in the oxygen consumption and distribution of oxygenated compounds in the matrix block.

6.4 Suggested future work

Experimental studies (static diffusion experiments) can be extended to include:

- Cores saturated with heavy oil and water.
- High pressure conditions.

Numerical simulation modeling can be extended to include:

- Modeling LTO reactions in terms of SARA fractions (Saturates-Aromatics-Resins-Asphaltenes).
- Modeling air/solvent injection in a dual porosity model. This kind of models is usually the one used in the oil industry (a reduced simulation time is expected).

- Further efforts toward the optimization of the methodology (air/C_3 injection) for different matrix sizes and fracture volumes (i.e., reservoir properties).

Bibliography

Alvarez, J.M., Sawatzky, R.P., Forster, L.M. et al. 2008. Alberta's Bitumen Carbonate Reservoirs—Moving Forward with Advanced R&D. Presented at the World Heavy Oil Congress, Edmonton, Alberta, Canada, 10–12 March. Paper 2008-467.

Bashkirov, A.N., Kamzolkin, V.V., Sokova, K.M. et al. 1965. The Mechanism of the Liquid-Phase Oxidation of Paraffinic Hydrocarbons. In The Oxidation of Hydrocarbons in the Liquid Phase, first edition. Ed. Emanuel N.M. 183–193. New York: Elsevier. http://dx.doi.org/10.1016/B978-0-08-010491-1.50018-5.

Belgrave, J.D.M., Moore, R.G., Ursenbach, M.G. et al. 1990. A Comprehensive Approach to In-Situ Combustion Modeling. *SPE Advanced Technology Series* **1** (1): 98–107. SPE-20250-PA. http://dx.doi.org/10.2118/20250-PA.

Bousaid, I.S. and Ramey Jr., H.J. 1986. Oxidation of Crude Oil in Porous Media. *SPE J* **8** (02): 137 – 148. SPE-1937-PA. http://dx.doi.org/10.2118/1937-PA.

Brady, J.E., Russell, J.W., and Holum, J.R. 2000. *Chemistry: Matter and Its Changes*, third edition. New York: John Wiley & Sons, Inc.

Burger J. G. and Sahuquet, B. C. 1972. Chemical Aspects of In-Situ Combustion–Heat of Combustion and Kinetics. *SPE J* **12** (05): 410–422. SPE-3599-PA. http://dx.doi.org/10.2118/3599-PA.

Chávez, E. and González, J.A. 2013. Implantación de la Prueba Tecnológica de Inyección de Aire en Cárdenas JSK. Presented at Congreso Mexicano del Petróleo, Cancún-Riviera Maya, México, 5–8 June.

Churcher, P.L., French, P.R., Shaw, J. C., and Schram, L. L. 1991. Rock properties of Berea sandstone, Baker dolomite, and Indiana limestone. Presented at the SPE International Symposium on Oilfield Chemistry, Anaheim, California, 20–22 February. SPE-21044-MS. http://dx.doi.org/10.2118/21044-MS.

Cinco-Ley, H. 1996. Well Test Analysis for Naturally Fractured Reservoirs. *J Pet Technol* **48** (01): 51–54. SPE-31162-JPT. http://dx.doi.org/10.2118/31162-JPT.

Clara, C., Durandeau, M., Queanault, G. et al. 1999. Laboratory Studies for Light Oil Air Injection Projects: Potential Application in Handil Field. Presented at the SPE Asia Pacific Oil and Gas Conference and Exhibition, Jakarta, 20 – 22 April. SPE-54377-MS. http://dx.doi.org/10.2118/54377-MS.

Coats, A.W. and Redfern, J.P. 1964. Kinetic Parameters from Thermogravimetric Data. *Nature* **201**: 68 – 69. doi:10.1038/201068a0.

Craig, F.F., Jr. and Parrish, D. R. 1974. A Multipilot Evaluation of the COFCAW Process. *J Pet Technol* **26** (06): 659–666. SPE-3778-PA. http://dx.doi.org/10.2118/3778-PA.

Cruz, L., Sheridan, J., Aguirre, E. et al. 2009. Relative Contribution to Fluid Flow from Natural Fractures in the Cantarell Field, Mexico. Presented at the Latin American and Caribbean Petroleum Engineering Conference, Cartagena de Indias, Colombia, 31 May–3 June. SPE-122182-MS. http://dx.doi.org/10.2118/122182-MS.

Drici, O. and Vossoughi, S. 1985. Study of the Surface Area Effect on Crude Oil Combustion by Thermal Analysis Techniques. *J Pet Technol* **37** (04): 731–735. SPE-13389-PA. http://dx.doi.org/10.2118/13389-PA.

Emery, L. W. 1962. Results from a Multi-Well Thermal-Recovery Test in Southeastern Kansas. *J Pet Technol* **14** (06): 671 – 678. SPE-140-PA. http://dx.doi.org/10.2118/140-PA.

Fadaei, H., Debenest, G., Kamp, A.M. et al. 2010. How the in-Situ Combustion Process Works in a Fractured System: 2D Core- and Block-Scale Simulation. *SPE Res Eval & Eng* **13** (01): 118–130. SPE-117645-PA. http://dx.doi.org/10.2118/117645-PA.

Fassihi, M.R., Brigham, W.E., and Ramey Jr., H. J. 1984. Reaction Kinetics of In-Situ Combustion: Part 1-Observations. *SPE J* **24** (04): 399 – 407. SPE-8907-PA. http://dx.doi.org/10.2118/8907-PA.

Fatemi, S.M., Kharrat, R. and Vossoughi, S. 2008. Feasibility Study of In-Situ Combustion (ISC) in a 2-D Laboratory-Scale Fractured System Using a Thermal Simulator. Presented at the World Heavy Oil Congress 2008, Edmonton, 10 – 12 March. Paper 2008-449.

Fatemi, S. M., Kharrat, R., and Vossoughi, S. 2011. Investigation of Top-Down In-Situ Combustion Process in Complex Fractured Carbonate Models: Effects of Fractures' Geometrical Properties. Presented at the Canadian Unconventional Resources in Calgary, 15 – 17 November. SPE-149314-MS. http://dx.doi.org/10.2118/149314-MS.

Faure, P. and Landais, P. 2000. Evidence for clay minerals catalytic effects during low-temperature air oxidation of n-alkanes. *Fuel* **79** (14): 1751 – 1756. http://dx.doi.org/10.1016/S0016-2361(00)00039-9.

Golf-Racht, T. D. van. 1982. *Fundamentals of fractured reservoir engineering*. Elsevier Scientific Publishing Company. Page 608.

Greaves, M., Ren, S.R., Rathbone, R.R., et al. 2000. Improved Residual Light Oil Recovery by Air Injection (LTO Process). *J Can Pet Technol* **39** (01): 57–61. PETSOC-00-01-05. http://dx.doi.org/10.2118/00-01-05.

Guo, P., Wang, Z., Shen, P. et al. 2009. Molecular Diffusion Coefficients of the Multicomponent Gas-Crude Oil Systems under High Temperature and Pressure. *Ind Eng Chem Res* **48** (19): 9023–9027. http://dx.doi.org/10.1021/ie801671u.

Gutierrez, D., Moore, R.G., Mehta, S.A. et al. 2009. The Challenge of Predicting Field Performance of Air Injection Projects Based on Laboratory and Numerical Modelling. *J Can Pet Technol* **48** (04): 23 – 34, PETSOC-09-04-23-DA. http://dx.doi.org/10.2118/09-04-23-DA.

Gutierrez, D., Skoreyko, F., Moore, R.G. et al. 2009. The Challenge of Predicting Field Performance of Air Injection Projects Based on Laboratory and Numerical Modelling. *J Can Pet Technol* **48** (04): 23–34. PETSOC-09-04-23-DA. http://dx.doi.org/10.2118/09-04-23-DA.

Islas-Juárez, R., Samaniego V, F., Luna, E. et al. 2004. Experimental Study of Effective Diffusion in Porous Media. Presented at the SPE International Petroleum Conference in Mexico, Puebla, Mexico, 8–9 November. SPE-92196-MS. http://dx.doi.org/10.2118/92196-MS.

Jamaluddin, A.K.M., Joshi, N., Iwere, F. et al. 2002. An Investigation of Asphaltene Instability under Nitrogen Injection. Presented at the SPE International Petroleum Conference and Exhibition in Mexico, Villahermosa, Mexico, 10–12 February. SPE-74393-MS. http://dx.doi.org/10.2118/74393-MS.

Kapadia, P., Gates, I.D., Mahinpey, N. et al. 2013. Kinetic Models for Low Temperature Oxidation Subranges Based on Reaction Products. Presented at the SPE Heavy Oil Conference—Canada, Calgary, 11–13 June. SPE-165527-MS. http://dx.doi.org/10.2118/165527-MS.

Khansari, Z., Kapadia, P., Mahinpey, N. et al. 2013. Kinetic Models for Low Temperature Oxidation Subranges based on Reaction Products. Presented at the SPE Heavy Oil Conference, Calgary, 11 – 13 June. SPE-165527-MS. http://dx.doi.org/10.2118/165527-MS.

Kok, M. V. 2009. Influence of reservoir rock composition on the combustion kinetics of crude oil. *J. Therm. Anal. Cal.* **97** (2): 397–401.

Lacroix, S., Delaplace, P., Bourbiaux, B. et al. 2004. Simulation of Air Injection in Light-Oil Fractured Reservoirs: Setting-up a Predictive Dual Porosity Model. Presented at the SPE Annual Technical Conference and Exhibition, Houston, 26–29 September. SPE-89931-MS. http://dx.doi.org/10.2118/89931-MS.

Lakatos, I., Lakatos-Szabo, J., Bauer, K. et al. 1998. Potential Application of Oxygen-Containing Gases in Heavy Oil Bearing Reservoirs. Presented at the European Petroleum Conference, The Hague, 20–22 October. SPE-50647-MS. http://dx.doi.org/10.2118/50647-MS.

Lee, D.G. and Noureldin, N.A. 1989. Effect of Water on the Low-Temperature Oxidation of Heavy Oil. *Energy and Fuels* **3** (06): 713–715.

Leyva, H. and Babadagli, T. 2011. Optimal Application Conditions for Heavy-Oil/Bitumen Recovery by Solvent Injection at Elevated Temperatures. Presented at the SPE Heavy Oil Conference and Exhibition, Kuwait City, Kuwait, 12–14 December. SPE-150315-MS. http://dx.doi.org/10.2118/150315-MS.

Li, J., Mehta, S.A., Moore, R.G. et al. 2006. Investigation of the Oxidation Behaviour of Pure Hydrocarbon Components and Crude Oils Utilizing PDSC Thermal Technique. *J Can Pet Technol* **45** (01): 48 – 53, PETSOC-06-01-04. http://dx.doi.org/10.2118/06-01-04.

Limón-Hernández, T., De-la-Fuente, G., Garza-Ponce, G. et al. 1999. Overview of the Cantarell Field Development Program. Presented at the Offshore Technology Conference, Houston, 3–6 May. OTC-10860-MS. http://dx.doi.org/10.4043/10860-MS.

Luo, P. and Gu, Y. 2007. Effects of Asphaltene Content on the Heavy Oil Viscosity at Different Temperatures. Fuel 86 (7–8): 1069–1078. http://dx.doi.org/10.1016/j.fuel.2006.10.017.

Mayorquin-Ruiz, J.R. and Babadagli, T. 2012a. Can Injection of Low Temperature Air-Solvent (LTASI) Be a Solution for Heavy Oil Recovery in Deep Naturally Fractured Reservoirs? Presented at the SPE EOR Conference at Oil and Gas West Asia, Muscat, Oman, 16–18 April. SPE-153997-MS. http://dx.doi.org/10.2118/153997-MS.

Mayorquin-Ruiz, J.R. and Babadagli, T. 2012b. Optimal Design of Low Temperature Air Injection for Efficient Recovery of Heavy Oil in Deep Naturally Fractured Reservoirs: Experimental and Numerical Approach. Presented at the SPE Heavy Oil Conference Canada, Calgary, 12–14 June. SPE-149896-MS. http://dx.doi.org/10.2118/149896-MS.

Mayorquin-Ruiz, J.R. and Babadagli, T. 2015. Low-Temperature Air/Solvent Injection for Heavy-Oil Recovery in Naturally Fractured Reservoirs. *J Can Pet Technol* **54** (03): 148–163. SPE-174542-PA. http://dx.doi.org/10.2118/174542-PA.

Mayorquin-Ruiz, J.R., Babadagli, T, and Rodriguez de la Garza, F. 2015. Low Temperature Air Injection at the Mature Stage of Deep Naturally Fractured Heavy-Oil Reservoirs: Field Scale Modeling. Presented at the Pan American Mature Fields Congress, Veracruz, 20–22 January. Paper PAMFC15-141.

Mayorquin-Ruiz, J.R., Babadagli, T, and Rodriguez de la Garza, F. 2015. Field Scale Numerical Modeling of Low Temperature Air Injection with Propane for Heavy-oil Recovery from Naturally Fractured Reservoirs. *Fuel* **160** (2015) 140 – 152.

Mayorquin-Ruiz, J. R. and Babadagli, T. 2015. Optimal Design of Low Temperature Air Injection with Propane for Efficient Recovery of Heavy Oil in Deep Naturally Fractured Reservoirs: Experimental and Numerical Approach. Paper submitted to *SPE Reservoir Evaluation & Engineering Journal* (under review)

Narr, W., Schechter, D. W., and Thompson, L. B. 2006. *Naturally fractured reservoir characterization*. Society of Petroleum Engineers. USA. Page 67

Pathak, V. 2011. Heavy Oil and Bitumen Recovery by Hot Solvent Injection: An Experimental and Computational Investigation. Presented at the SPE International Student Paper Contest at SPE Annual Technical Conference and Exhibition, Denver, 30 October–November 2. SPE-152374-STU. http://dx.doi.org/10.2118/152374-STU.

Pathak, V., Babadagli, T., and Edmunds, N.R. 2010. Hot Solvent Injection for Heavy Oil/Bitumen Recovery: An Experimental Investigation. Presented at the Canadian Unconventional Resources and International Petroleum Conference, Calgary, 19–21 October. SPE-137440-MS. http://dx.doi.org/10.2118/137440-MS.

Peaceman, D.W. 1977. *Fundamentals of Numerical Reservoir Simulation*. Elsevier Scientific Publishing Company, p. 164

Phillips, C.R. and Hsieh, I. 1985. Oxidation Reaction Kinetics of Athabasca Bitumen. *FUEL* **64** (7): 985–989. http://dx.doi.org/10.1016/0016-2361(85)90155-3.

Razzaghi, S., Kharrat, R., and Vossoughi, S. 2008. Design of in Situ Combustion Process by Using Experimental Data. Presented at the World Heavy Oil Congress, Edmonton, Canada, 10–12 March. Paper 2008-349.

Ren, S.R., Greaves, M., and Rathbone, R.R. 2002. Air Injection LTO to Process: An IOR Technique for Light-Oil Reservoirs. *SPE J* **7** (01): 90–99. SPE-57005-PA. http://dx.doi.org/10.2118/57005-PA.

Reza, A., Kharrat, R., Ghotbi, C., et al. 2008. Simulation study of the VAPEX process in fractured heavy oil system at reservoir conditions. *Journal of Petroleum Science and Engineering* **60** 51 – 66. http://dx.doi.org/10.1016/j.petrol.2007.05.011.

Riazi, M.R., Whitson, C.H., and da Silva, F. 1994. Modelling of Diffusional Mass Transfer in Naturally Fractured Reservoirs. *J Pet Sci Eng* **10** (3): 239–253. http://dx.doi.org/10.1016/0920-4105(94)90084-1.

Rodriguez, F. and Christopher, C.A. 2004. Overview of Air Injection Potential for Pemex. Presented at the AAPG International Conference, Cancún, México, 24–27 October. Paper #89612.

Rodríguez, F., Ortega, G., Sánchez, J.L. et al. 2001. Reservoir Management Issues in the Cantarell Nitrogen Injection Project. Presented at the Offshore Technology Conference, Houston, 30 April–3 May. OTC-13178-MS. http://dx.doi.org/10.4043/13178-MS.

Rodriguez, F., Sanchez, J.L., and Galindo-Nava, A. 2004. Mechanisms and Main Parameters Affecting Nitrogen Distribution in the Gas Cap of the Supergiant Akal Reservoir in the Cantarell Complex. Presented at the SPE Annual Technical Conference and Exhibition, Houston, 26–29 September. SPE-90288-MS. http://dx.doi.org/10.2118/90288-MS.

Ruiz, J., Naccache, P., Priestley, A., et al. 2013. Modeling In-Situ Combustion in a Heavy Oil Field in Romania. Presented at the SPE Heavy Oil Conference Canada, Calgary, Alberta, 11–13 June. SPE-165490-MS. http://dx.doi.org/10.2118/165490-MS.

Sakthikumar, S. and Berson, F. 2001. Air Injection into Light and Medium-Heavy Oil, Carbonate Reservoirs. Presented at the EXITEP 2001, Mexico, 4–7 February.

Schulte, W.M. and de Vries, A.S. 1985. In-Situ Combustion in Naturally Fractured Heavy Oil Reservoirs. *Society of Petroleum Engineers Journal* **25** (01): 67–77. SPE-10723-PA. http://dx.doi.org/10.2118/10723-PA.

Sequera, B., Moore, R.G., Mehta, S.A. et al. 2010. Numerical Simulation of In-Situ Combustion Experiments Operated Under Low Temperature Conditions. *J Can Pet Technol* **49** (01): 55-64. SPE-132486-PA. http://dx.doi.org/10.2118/132486-PA.

Sheu, E.Y. and Mullins, O.C. 1995. Asphaltenes: Fundamentals and Applications, first edition. New York: Springer. http://dx.doi.org/10.1007/978-1-4757-9293-5.

Shulte, W.M., and De Vries, A.S. 1985. In-Situ Combustion in Naturally Fractured Heavy Oil Reservoirs. *SPE J* **25** (01): 67–77. SPE-10723-PA. http://dx.doi.org/10.2118/10723-PA.

Stokka, S., Oesthus, A., and Frangeul, J. 2005. Evaluation of Air Injection as an Ior Method for the Giant Ekofisk Chalk Field. Presented at the SPE International Improved Oil Recovery Conference, Kuala Lumpur, 5–6 December. SPE-97481-MS. http://dx.doi.org/10.2118/97481-MS.

Tabasinejad, F., Karrat, R., and Vossoughi, S. 2006. Feasibility Study of In-Situ Combustion in Naturally Fractured Heavy Oil Reservoirs. Presented at the International Oil Conference and Exhibition in Mexico, Cancun, 31 August – 2 September. SPE-103969-MS. http://dx.doi.org/10.2118/103969-MS.

Talukdar, M. S., Banu, H. A., Torsæter, O., et al. 2000. Applicability and Rate Sensitivity of Several Up Scaling Techniques in Fractured Reservoir Simulation. Presented at SPE International Petroleum Conference and Exhibition, Mexico, 1-3 February. Paper SPE-59048-MS. http://dx.doi.org/10.2118/59048-MS.

Vaughan, W.E. and Rust, F.F. 1995. Low Temperature Oxidation of Paraffin Hydrocarbons: Oxidation of Paraffin Wax. *In The Chemistry of Petroleum Hydrocarbons*, first edition. Ed. Brooks B.T. and Boord C.E. and Kurtz J. S. S. Jr., et al., Vol. II. 309–323. New York: Reinhold Publishing Corporation.

Wattana, P., Wojciechowski, D.J., Bolaños, G. et al. 2003. Study of Asphaltene Precipitation Using Refractive Index Measurement. Petroleum Science and Technology 21 (3–4): 591–613. http://dx.doi.org/10.1081/lft-120018541.

Whitfield, R. C. 1966. *A Guide to Understanding Basic Organic Reactions*, first edition. London: Concepts in Chemistry, Longmans.

Yang, X. and Gates, I.D. 2008. History Match of an Athabasca Bitumen Combustion Tube Experiment. Presented at the World Heavy Oil Congress, Edmonton, 10–12 March. Paper 2008-441.

Yanze, Y. and Clemens, T. 2011. The Role of Diffusion for Non-Miscible Gas Injection in a Fractured Reservoir. Presented at the SPE EUROPEC/EAGE Annual Conference and Exhibition, Vienna, Austria, 23–26 May. SPE-142724-MS. http://dx.doi.org/10.2118/142724-MS.

Yoshiki, K.S. and Phillips, C.R. 1985. Kinetics of the Thermo-Oxidative and Thermal Cracking Reactions of Athabasca Bitumen. *FUEL* **64** (11): 1591–1598. http://dx.doi.org/10.1016/0016-2361(85)90377-1.